Library
13/7/89

सी.एस.आई.आर. क्षेत्रीय केन्द्र
C.F.T.R.I. REGIONAL CENTRE
330
डायरी सं./DIARY NO.
दिनांक/DATE 13/7/89
लुधियाना/LUDHIANA-141 006

Indian J Chem
FEBRUARY 1989
CODEN:IJOCAP 28A(2) 95-186 (1989)
ISSN: 0019-5103

Indian Journal of

CHEMISTRY

SECTION A

(Inorganic, Physical, Theoretical & Analytical)

वैज्ञानिक तथा औद्योगिक अनुसंधान पुस्तकालय
SCIENTIFIC & RESEARCH LIBRARY
Accession No.
17 JUL 1989
सी.एफ.टी.आर.आई. क्षेत्रीय केन्द्र
C.F.T.R.I. REGIONAL CENTRE, LUDHIANA

Published by
PUBLICATIONS & INFORMATION DIRECTORATE, CSIR, NEW DELHI
in association with
THE INDIAN NATIONAL SCIENCE ACADEMY, NEW DELHI

A RANGE OF HIGH PRECISION, HIGH QUALITY RECORDING INSTRUMENTS FOR THE DISCRIMINATING RESEARCH SCIENTIST

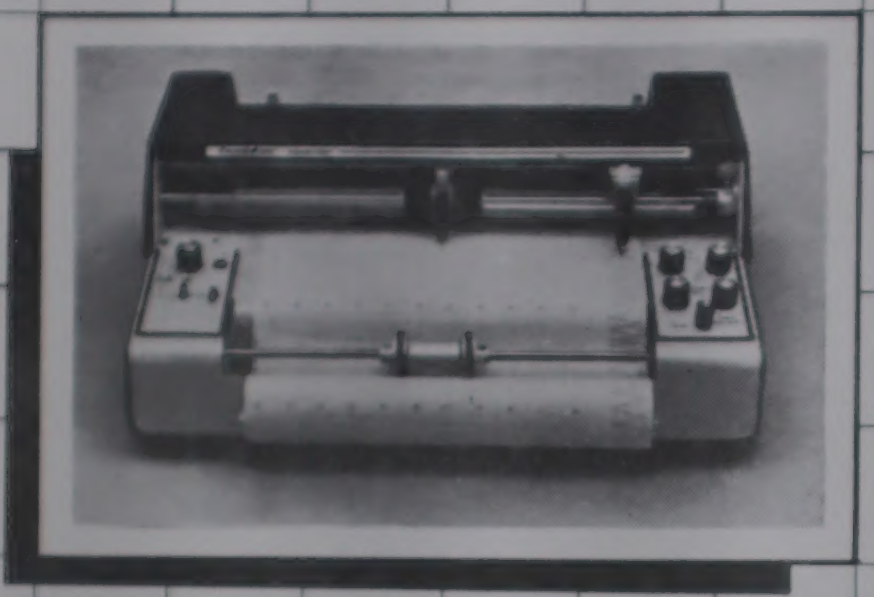

Series 5000 Strip Chart Recorder

The series 5000 Strip Chart Recorder and the series 2000 XY Recorder are well proven instruments incorporating State of the Art Circuitry. A wide range of models offer tremendous flexibility to the user. With over 5000 installations, these instruments are the preferred choice of discriminating users all over India.

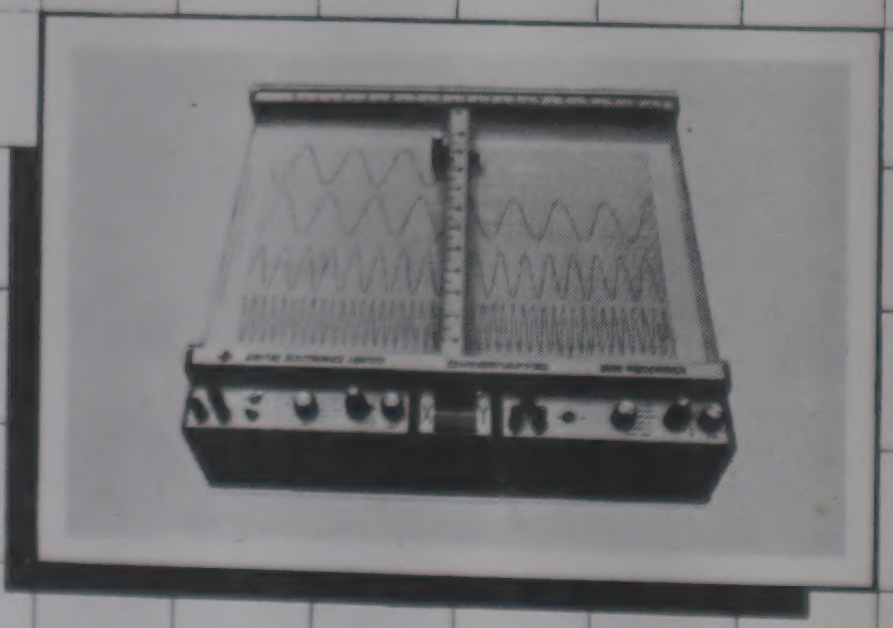

Series 2000 XY Recorder

Another quality product from

DIGITAL ELECTRONICS LIMITED

Reliability in Recording Instruments.

Digilog House 74/1, Marol Industrial Area MIDC, Andheri (East), Bombay- 400 093 Tel: 634 09 01, 632 86 76 Grams: 'DIGILOG'

A Company in collaboration with houston instrument

Special Effects/DE/25/86

INDIAN JOURNAL OF CHEMISTRY

Section A: Inorganic, Physical, Theoretical & Analytical Chemistry

Editorial Board

Prof. C N R Rao
Director
Indian Institute of Science
Bangalore 560 012

Prof. R C Mehrotra
Chemistry Department
Rajasthan University
Jaipur

Prof. D V S Jain
Chemistry Department
Panjab University
Chandigarh 160 014

Prof. U C Agarwala
Department of Chemistry
Indian Institute of Technology
Kanpur 208 016

Prof. S. Mitra
Tata Institute of Fundamental Research
Homi Bhabha Road
Bombay 400 005

Prof. P Natarajan
Department of Inorganic Chemistry
University of Madras
Madras 600 025

Dr R M Iyer
Director, Chemical Group
Bhabha Atomic Research Centre
Trombay, Bombay 400 085

Dr N Venkatasubramanian
IDL-NNB Research Institute
Post Bag No. 397
Sankey Road, Bangalore 560 012

Prof. N K Ray
Department of Chemistry
Delhi University
Delhi 110 007

Prof. J.C. Ahluwalia
Department of Chemistry
Indian Institute of Technology
Delhi 110 016

Prof. S L Khetrapal
National NMR Facility
Indian Institute of Science
Bangalore 560 012

Prof. S S Krishnamurthy
Department of Inorganic & Physical Chemistry
Indian Institute of Science
Bangalore 560 012

Prof. K K Kundu
Department of Chemistry
Jadavpur University
Calcutta 700 032

Prof. M V Kaulgud
Department of Chemistry
Nagpur University
Nagpur 440 010

Shri S.S. Saksena, Editor-in-Chief
(*Ex-officio*)

Editors

S.S. Saksena **B.C. Sharma** **S. Sivakamasundari**

Assistant Editor: S.K. Bhain

Sr. Scientific Assistant: Geeta Mahadevan

Published by the Publications & Information Directorate (CSIR), Hillside Road, New Delhi 110012

Copyright, 1989, by the Council of Scientific & Industrial Research, New Delhi 110012

The Indian Journal of Chemistry is issued monthly in two sections: A and B. Communications regarding contributions for publication in the journal should be addressed to the Editor, Indian Journal of Chemistry, Publications & Information Directorate, Hillside Road, New Delhi 110012.

Correspondence regarding subscriptions and advertisements should be addressed to the Sales & Distribution Officer, Publications & Information Directorate, hillside Road, New Delhi 110012.

The Publications & Information Directorate (CSIR) assumes no responsibility for the statements and opinions advanced by contributors. The Editorial Board in its work of examining papers received for publication is assisted, in an honorary capacity by a large number of distinguished scientists, working in various parts of India.

Annual Subscription: Rs. 300.00 £ 70.00 $ 100.00; 50% discount admissible to research workers and students and 25% discount to non-research individuals on annual subscription.

Single Copy: Rs. 30.00 £ 7.00 $ 10.00

Payments in respect of subscriptions and advertisements may be sent by cheque, bank draft, money order or postal order marked payable to Publications & Information Directorate, Hillside Road, New Delhi 110012.

Claims for missing numbers will be allowed only if received within 3 months of the date of issue of the journal plus the time normally required for postal delivery of the journal and the claim.

वैज्ञानिक तथा अनुसं... पुस्तकालय
SCIENTIFIC & RESEARCH LIBRARY
Accession No .....
11 JUL 1989
R.L. REGIONAL CENTRE LUDHIANA

Indian Journal of Chemistry

Sect. A: Inorganic, Physical, Theoretical & Analytical

VOLUME 28A NUMBER 2 FEBRUARY 1989

CONTENTS

Estimation of Inductive Effect PMO Parameters of Methyl & Ethyl Groups from Charge-Transfer Bands of Some π-Molecular Complexes 95
R Ghosh, K K Dutta & A K Mukherjee*

Flow through Porous Media: Part X—Permeability Studies of Ethylene Glycol, Diethylene Glycol & Their Aqueous Mixtures through Titanium Oxide Membrane 98
R L Blokhra* & Chander Prakash

Ion-Pair Association Constants of Alkali & Alkaline Earth Metal Formates in Formic Acid-Acetonitrile Mixtures at 30°C—A Conductance Study 102
K Chowdoji Rao, (Mrs) M C S Subha* & S Brahmaji Rao

Ion-Solvent Interactions in Alcohol Rich Binary Mixtures: Densities & Viscosities of Alkali Metal Propionates in Propionic Acid + 1-Propanol Mixtures 106
(Mrs) M C S Subha*, K Chowdoji Rao & S Brahmaji Rao

Electronic Spectrum of 5,6-Dimethyl-2-aminobenzimidazole: Effect of Solvents & *p*H on Spectral Bheaviour 111
Sanjay Srivastava & Sneh K Dogra*

Influence of *Ortho* Substituents on UV Spectra of Aryl Methyl Sulphoxides 116
V Baliah* & R Varadachari

Kinetics of Chlorination of Aniline by Dichloramine-T in Aqueous Acetic Acid Medium 120
B Thimme Gowda* & B S Sherigara

Kinetics & Mechanism of Chlorination of Aniline by Trichloromelamine in Aqueous Acetic Acid-Perchloric Acid Medium: A Novel Dependence of Chlorinating Agent on Nature of Solvent System (Part I) 124
P S Radhakrishnamurti* & J C Panigrahi

Metal Complexes of S-Acetyl(β-N-acetyl)dithiocarbazate 129
M T H Tarafder

Derivatives of Cobalt(III) & Nickel(II) Dithiophosphinates with Polydentate Nitrogen Donors 132
R N Mukherjee*, B B S Shastri, S Shankar & D L Mascarenhas

Coordination Compounds of Rare Earth Cyanoacetates 135
(Kum) M A Vaidya & S C Jain*

Synthesis & Characterisation of Co(II), Ni(II), Cu(II), Zn(II), Ru(II), Pd(II) & Pt(II) Complexes with Substituted Quinazoline (3H)-4-ones 140
B Prabhakar, K Laxma Reddy & P Lingaiah*

Continued overleaf

CONTENTS

Trace Determination of Iron(III) by a Kinetic Method Based on Catalase like Activity of $[(Trien)Fe(OH)_2]^+$ Complex on Decomposition Rate of Hydrogen Peroxide . . 145
Nishi Gupta & P C Nigam*

Selective Separation of Uranium(VI) on a Chelating Styrene-DVB Based Resin Containing Quinaldinic Acid Amide Group 150
(Miss) Niyati Das & Jyotirmoy Das*

Notes

Stabilities of Quinarene Hydrocarbons 154
Dilip K Deb, Pratip R Ray & Nirad G Mukherjee*

Characterization of Tin Oxide Supported Vanadia & Molybdena Catalysts by Low Temperature Oxygen Chemisorption Technique 157
K Narsimha, Ch Sivaraj, B Mahipal Reddy & P Kanta Rao*

Photolysis of Alkali Hexa(formato)ferrates(III) in Solution 159
A S Brar*, S Brar & S Sandhu

Excess Viscosities of Binary Mixtures of Water with Tetrahydrofuran & Dioxane at 303.15K 160
R Venkateswarlu, Pallagolla Rajasekhar & K S Reddy*

Kinetics of Oxidation of Lactic, Mandelic & Glycollic Acids by Diperiodatonickelate(IV) in Alkaline Media 162
U Chandraiah, C P Murthy & Sushama Kandlikar*

Molybdenum Carbonyl Complexes Containing 2-Thienylphosphines 164
V K Jain*, V S Sagoria & M S Gill

Synthesis & Characterization of a Ten-coordinated Uranium(VI) Complex 167
I S Ahuja*, G L Yadava & Shailendra Tripathi

Stability Constants of the Binary Complexes of Co(II), Ni(II), Cu(II) & Zn(II) with Thiamine & Ternary Complexes with Thiamine as Primary Ligand & Thymine or Uracil as Secondary Ligand 169
S Satyanarayana* & K Venugopal Reddy

Formation of Binary & Ternary Chelates of Calmagite with Lanthanides in Presence of Some Amino Polycarboxylic Acids 172
B Satyanarayana, K L Omprakash, M L N Reddy & A V Chandra Pal*

Formation Constants of Binary & Ternary Chelates of Ln(III) with Maltol & Kojic Acid in Presence of Aminocarboxylic Acids 174
M Narasimha Rao, K L Omprakash, A V Chandra Pal* & M L N Reddy

A Novel Precipitate-based Manganese(II) Sensor 176
Naheed Faizan & M C Chattopadhyaya*

Electrochemical & Thermodynamic Behaviour of Palladium-Palladium Sulphide Electrode in Presence of Sulphide Ions 177
Pravin Chandra Katiyar & Mukhtar Singh*

Rapid Spectrophotometric Determination of Thallium with Mepazine Hydrochloride . 179
H Sanke Gowda* & G K Rekha

CONTENTS

Extractive Spectrophotometric Determination of Palladium(II) Using Mixed Ligand Complex Formation with Pyridine/α-Picoline/β-Picoline/γ-Picoline/2,4,6-Collidine & Iodide 181
T K Thokdar, A Sarkar, P K Paria* & S K Majumdar

Book Reviews

Secondary Ion Mass Spectroscopy of Solid Surfaces (Author: V T Cherepin) 183
B Viswanathan

Future Directions in Polymer Colloids (Editors: M S El-Aasser & R M Fitch) 183
Asit Baran Mandal & K S V Srinivasan*

Announcements 185

Authors for correspondence are indicated by (*)

Author Index

Ahuja I S 167

Baliah V 116
Blokhra R L 98
Brahmaji Rao S 102,106
Brar A S 159
Brar S 159

Chander Prakash 98
Chandra Pal A V 172,174
Chandraiah U 162
Chattopadhyaya M C 176
Chowdoji Rao K 102,106

Das Jyotirmoy 150
Das Niyati 150
Deb Dilip K 154
Dogra Sneh K 111
Dutta K K 95

Faizan Naheed 176

Ghosh R 95
Gill M S 164
Gupta Nishi 145

Jain S C 135
Jain V K 164

Kandlikar Sushama 162
Kanta Rao P 157
Katiyar Pravin Chandra 177

Laxma Reddy K 140
Lingaiah P 140

Mahipal Reddy B 157
Majumdar S K 181
Mandal Asit Baran 185
Mascarenhas D L 132
Mukherjee A K 95
Mukherjee Nirad G 154
Mukherjee R N 132
Murthy C P 162

Narsimha K 159
Narasimha Rao M 174
Nigam P C 145

Omprakash K L 172,174

Panigrahi J C 124
Paria P K 181
Prabhakar B 140

Radhakrishnamurti P S 124
Rajasekhar Pallagolla 160
Ray Pratip R 154
Reddy K S 160
Reddy M L N 172,174
Rekha G K 179

Sagoria V S 164
Sandhu S 159
Sanke Gowda H 179
Sarkar A 181
Satyanarayana B 172
Satyanarayana S 169
Shankar S 132
Shastri B B S 132
Sherigara B S 120
Singh Mukhtar 177
Sivaraj Ch 157
Srinivasan K S V 185
Srivastava Sanjay 111
Subha M C S 102,106

Tarafder M T H 129
Thimme Gowda B 120
Thokdar T K 181
Tripathi Shailendra 167

Vaidya M A 135
Varadachari R 116
Venkateswarlu R 160
Venugopal Reddy K 169
Viswanathan B 183

Yadava G L 167

Indian Journal of Chemistry
Vol. 28A, February 1989, pp. 95-97

Estimation of Inductive Effect PMO Parameters of Methyl & Ethyl Groups from Charge-Transfer Bands of Some π-Molecular Complexes

R GHOSH, K K DUTTA & A K MUKHERJEE*
Burdwan Raj College, Chemistry Department, Burdwan 713 104

Received 30 *December* 1987; *revised and accepted* 28 *March* 1988

The inductive effect PMO parameters of methyl and ethyl groups have been calculated from the trends in the charge-transfer bands of two series of π-molecular complexes; (i) of methyl- and ethyl-benzenes with iodine monochloride and (ii) of methylated thiophenes with tetracyanoethylene. Coulson-Longuet-Higgins perturbation technique has been applied to obtain expressions for the energies of the donor-MO's in terms of the Hückel parameters of alkyl groups, and by correlating such expressions linearly with the longest wavelength CT-absorption bands of the molecular complexes, values of the Hückel parameters of the alkyl groups have been determined. The calculated value for the methyl group is approximately the same for the two series studied and is close to the ones obtained by previous workers. The PMO parameter for ethyl group is found to be less than that for methyl group as expected, since inductive effect decreases with increase in chain-length of the alkyl group.

The energy ($h\nu_{CT}$) of electronic charge-transfer (CT) transition observed in molecular complexes is expressed by the well-known equation[1,2],

$$h\nu_{CT} = I_D - E_A - C \quad \ldots (1)$$

where I_D is the vertical ionisation potential of the donor, E_A is the vertical electron-affinity of the acceptor and C is a term summing the contributions from non-bonding species, polarisation and solvation. The main part of C comes from the electrostatic attraction between the negatively charged acceptor and the positively charged donor in the excited state[3]. Working with a common acceptor and a series of structurally similar donors in a given solvent, one may use equation (1) in the form,

$$h\nu_{CT} = -E_D + \text{constant} \quad \ldots (2)$$

where E_D is the energy of the highest occupied molecular orbital (HOMO) of the donor. A correlation of this type has been extensively used to obtain various heteroatom Hückel parameters and inductive effect parameters of alkyl groups[4-8].

Principles and Methods

According to Coulson-Longuet-Higgins perturbation method[9], as applied to Hückel theory, the π-energy of the HOMO of any alkyl-benzene is given by[4,6],

$$E_{HOMO} = E^0 + h_R\beta \cdot \frac{1}{n}\sum_n\sum_r C_{rj}^2 \quad \ldots (3)$$

where E^0 is the energy of the HOMO of benzene, the unperturbed system, n is the number of equivalent structures of the alkylbenzene and C_{rj} is the atomic orbital coefficient of the rth conjugated C-atom of benzene (to which R is attached) in the LCAO wavefunction of the HOMO of benzene. In Eq. (3), β is the standard C – C resonance integral in benzene, the coulomb integral of benzene carbon being taken as of zero energy. Combining equations (2) and (3) one obtains a linear correlation

$$h\nu_{CT} = -h_R\beta \cdot \frac{1}{n}\sum_n\sum_r C_{rj}^2 + \text{constant} \quad \ldots (4)$$

from the slope of which one can get the inductive effect PMO parameters h_R for R. The method of computation of the perturbational coefficient $\frac{1}{n}\sum_n\sum_r$

Table 1—CT Absorption Bands and Perturbational Coefficients of Molecular Complexes of Methyl- and Ethyl-benzenes with Iodine Monochloride

Location of substituents	$h\nu_{CT}$ (eV)		$\frac{1}{n}\sum_n\sum_r C_{rj}^2$
	Methyl-benzenes	Ethyl-benzenes	
1,4	4.25	—	0.667
1,3	—	4.1505	0.500
1,2,4	4.1505	4.1093	0.777
1,3,5	—	4.0032	0.667
1,2,3,5	3.9776	3.9272	0.917
1,2,3,4	3.9776	—	1.000
1-5	3.8540	—	1.133
1-6	3.7156	—	1.333
1,2,4,5	—	3.9904	1.000

Table 2—Eigenvalues and Wavefunctions of Thiophene MO's with SALC's as Basic Set

Symmetry	Eigenvalue (β)	Wavefunction*		
		Coeff. of ψ_1	Coeff. of ψ_2	Coeff. of ψ_3
	−1	0.7808688	0	−0.624695
A_2	0.8747727	0.3523588	0.825741	0.4404486
	−1.8747727	−0.5158363	0.5640494	−0.6447954
	1	0.7808688	0	0.624695
B_2	1.8747727	0.5158362	0.5640494	0.6447954
	−0.8747727	−0.3523588	0.825741	−0.4404486

*$\psi_1 = (\phi_1 \pm \phi_6)/\sqrt{2}$, $\psi_2 = (\phi_2 \pm \phi_5)/\sqrt{2}$ and $\psi_3 = (\phi_3 \pm \phi_4)/\sqrt{2}$ depending on symmetry.

C_{rj}^2, taking into consideration the degeneracy of the HOMO of benzene, can be found in ref. 6. The computed values are given in Table 1 together with the experimental CT transition energies of the two series of methyl- and ethyl-benzenes with iodine monochloride in carbon tetrachloride medium. The experimental data have been taken from the work of Farrel and Newton[10].

In the case of methylated thiophenes, thiophene has been regarded as the unperturbed system. For construction of its π-molecular orbitals, the sulphur atom has been treated in a manner suggested by Longuet-Higgins[11]; in his method Longuet-Higgins considered the contributions of the 3*d* orbitals of S and showed that a particular hybridisation gave two pd^2 hybrid orbitals, not mutually orthogonal, having symmetry and energy appropriate for conjugation with carbon ^2p_z-orbitals. In such calculations, a LCAO method does not require the AO's to be centered on separate atoms[12]—the two sulphur orbitals are symbolised S′ and S″ and the calculation of thiophene becomes equivalent to that of benzene with two adjacent orbitals replaced by S′ and S″. Using this model, the symmetry (C_{2v})-adapted linear combinations (SALC) are $(\phi_1 \pm \phi_6)/\sqrt{2}$, $(\phi_2 \pm \phi_5)/\sqrt{2}$ and $(\phi_3 \pm \phi_4)/\sqrt{2}$ where the '+' and '−' signs refer to B_2 and A_2 symmetries respectively and the numbering of AO's (1 to 6) is in accordance with Fig. 1. Eigenvalues and eigenvectors have been calculated with these SALC's as basis set and with the heteroatom sulphur parameters as suggested by Longuet-Higgins[11,12], e.g., $h_{S'} = h_{S''} = 0$, $k_{C-S'} = k_{C-S''} = 0.8$ and $k_{S'-S''} = 1$. The results are shown in Table 2.

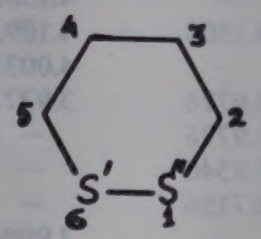

Fig. 1—Enumeration of AO's of thiophene

Table 3—CT Transition Energies of Complexes of Thiophene and Methylthiophenes with TCNE and Calculated Perturbation Coefficient

Donor*	$\sum_r C_r^2$	$h\nu_{CT}$ (eV)
Thiophene	0	2.770
3-Methylthiophene	0.0969974	2.596
2-Methylthiophene	0.340924	2.497
2,5-Dimethylthiophene	0.681848	2.256
2,3,4,5-Tetramethylthiophene	0.8758429	2.050

The energy of the HOMO of a methylated thiophene is given by Eq. 5,

$$E_{HOMO} = E^0 + h_{Me}\beta \sum_r C_r^2 \quad \ldots (5)$$

where E^0 is the energy of the HOMO of thiophene, r denotes the location of the Me-group and C_r is the coefficient of the rth conjugated AO in the HOMO wavefunction of thiophene. Equation (5) is somewhat simpler than equation (3) since the thiophene HOMO is non-degenerate. Combination of (2) and (5) gives,

$$h\nu_{CT} = -h_{Me}\beta \sum_r C_r^2 + \text{constant} \quad \ldots (6)$$

The calculated perturbational coefficients of a series of methylthiophenes and the CT transition energies of their complexes with tetracyanoethylene (TCNE) in dichloromethane medium are shown in Table 3. The experimental transition energies have been taken from the works of Aloisi *et al.*[13].

Results and Discussion

The linear plots in Figs 2 and 3 clearly show the validity of the Eqs (4) and (6). From the slopes of these lines, h_{Me} is found to be −0.27 for both methylbenzenes and methylthiophenes, and h_{Et} is

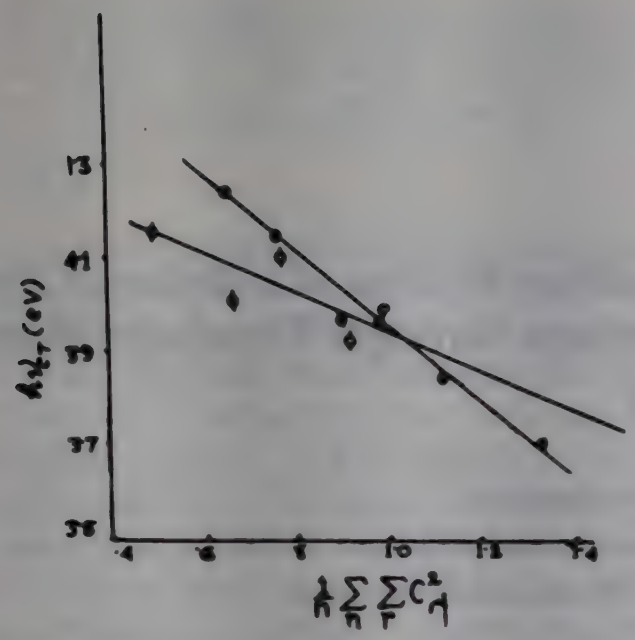

Fig. 2—Plots of transition energies against perturbational coefficients for complexes of methyl- and ethyl-benzenes with ICI [Dark circles-methyl; open circles-ethyl]

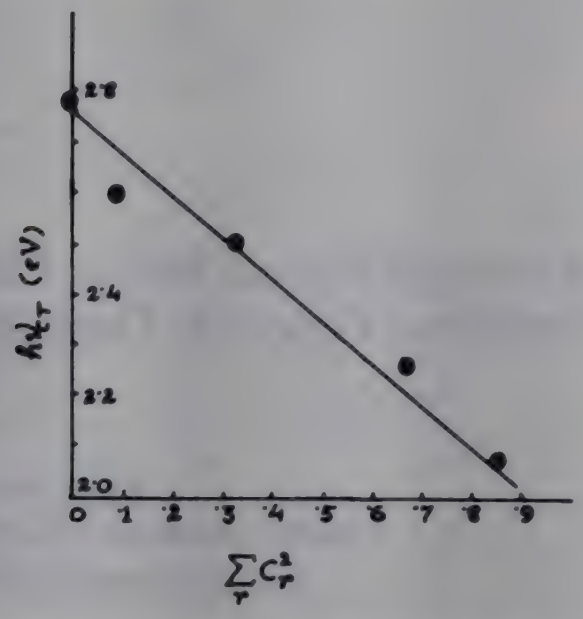

Fig. 3—Plots of transition energies against perturbational coefficients for complexes of methylthiophenes with TCNE

found to be -0.14, with $\beta = -3.1$ eV as obtained from the first four singlet-singlet transitions of benzene. The correlation coefficient (r) between CT-transition energy and perturbation coefficient as plotted in Fig. 2 is 0.99 for methylbenzenes and 0.74 for ethylbenzenes. For Fig. 3, $r = 0.988$. So, for two cases the correlation is excellent as $P_N(|r| \geq 0.9)$, the probability that N sets of two variables with $r \geq 0.9$ are uncorrelated linearly[14] is only 3.7% for $N = 5$ (methylthiophenes) and 1.4% for $N = 6$ (methylbenzenes). For ethylbenzenes $P_N(|r| \geq 0.74) \simeq 15\%$ indicating that the correlation is moderate. The value of h_{Me} obtained in this way is in close agreement with the values -0.21 and -0.3 obtained by Lepley[4] and Keysel[5] respectively using similar method for other systems. Lepley's work involved complexes of methylbenzenes with TCNE and ethylbenzenes were not investigated by him. In Kysel's work the donors were methylnaphthalenes. The treatment of methylthiophenes reported in this paper is new. Thiophene MO's have heitherto been calculated by two different models other than the two-centre model suggested by Longuet-Higgins. In one, used by Kreevoy[15], thiophene has been regarded as a five-membered heterocycle with S as a 'normal heteroatom' with $h_S = 0$ and $h_{C-S} = 1$. In the other, the 5-membered skeleton has been retained by h_S has been taken to be equal to $h_{\tilde{N}}$ since ammonia and hydrogen sulphide have close ionisation potentials (10.52 and 10.47 eV respectively)[12,16]. We have tried both the methods and applied the perturbation technique reported in this paper but failed to obtain any good parallelism between the HOMO energies and the observed CT bands of the methylthiophene complexes. The two-centre model of Longuet-Higgins works well, as illustrated in Fig. 3, not only enabling interpretation of trends in CT bands but also yielding a good estimate of the inductive effect PMO parameter of the methyl group. It is found that $h_{Me} > h_{Et}$, which is consistent with the fact that CH_3-CH_2- group with a longer chain must have lower inductive effect than that of CH_3-. The same order of inductive effects was found by Baker and Nathan[17] in the relative reaction rates of *p*-alkylbenzyl bromides with pyridine and by Mulliken *et al.*[18,19] in models of hyperconjugation.

References

1 Mc Connell H, Ham J & Platt J, *J chem Phys*, **21** (1953) 66.
2 Mulliken R S & Person W B, *Ann rev phys Chem*, **13** (1961) 107.
3 Mulliken R S & Person W B, *Molecular complexes* (Wiley Interscience) 1969, 120.
4 Lepley A R, *J Am chem Soc*, **86** (1964) 2545.
5 Kysel O, *Z phys Chem* (*Neue Folge*), **89** (1974) 62.
6 Seal B K & Mukherjee A K, *Indian J Chem*, **23A** (1984) 797.
7 Mukherjee A K & Seal B L, *Indian J Chem*, **25A** (1986) 531.
8 Mukherjee A K & Seal B K, *Indian J Chem*, **26A** (1987) 367.
9 Coulson C A & Longuet-Higgins H C, *Proc r Soc* (*London*), **A191** (1947) 39.
10 Farrell P G & Newton J, *J phys Chem*, **69** (1965) 3506.
11 Longuet-Higgins H C, *Trans Faraday Soc*, **45** (1949) 173.
12 Streitwieser (Jr) A, *Molecular orbital theory for organic chemists* (John Wiley, NY) 1961, 127.
13 Aloisi G G, Santini S & Savelli G, *Faraday Trans I*, **71** (1975) 2045.
14 Taylor J R, *An introduction to error analysis* (Univ. Science Books, California) 1982, 249.
15 Kreevoy M M, *J Am chem Soc*, **80** (1958) 5543.
16 Field F H & Franklin J L, *Electron impact phenomena* (Academic Press, NY) 1951, Appendix.
17 Baker J W & Nathan W S, *J chem Soc*, (1939) 1144.
18 Mulliken R S, Rieke C A & Brown W G, *J Am chem Soc*, **63** (1941) 41.
19 Mulliken R S & Rieke C A, *J Am chem Soc*, **63** (1941) 1770.

Indian Journal of Chemistry
Vol. 28A, February 1989, pp. 98-101

Flow through Porous Media: Part X-Permeability Studies of Ethylene Glycol, Diethylene Glycol & Their Aqueous Mixtures through Titanium Oxide Membrane

R L BLOKHRA* & CHANDER PRAKASH

Chemistry Department, Himachal Pradesh University, Summer Hill, Shimla 171 005

Received 1 *February* 1988; *revised* 21 *April* 1988; *accepted* 12 *May* 1988

The flow of water, ethylene glycol, diethylene glycol and their aqueous mixtures through a titanium oxide plug has been measured at different temperatures. The results are discussed in terms of frictional coefficient, which measures the interaction between water and the walls of the membrane. The results are further interpreted in terms of a unit rate process. The values of enthalpy of activation (ΔH^*), entropy of activation (ΔS^*) and free energy of activation (ΔG^*) are determined. The molecular exchange rate $A_{\alpha\beta}$ between the two phases α and β across the membrane has been reported.

Flow studies involving electrolyte and non-electrolyte solutions have been made by different investigators[1-8] using different types of membranes and diaphragms, both theoretically and experimentally on the basis of thermodynamics of irreversible processes[9]. These flows not only characterise[10] the membrane in terms of its effective cross-sectional area, radius and number of pores, but also characterise the system in terms of a set of experimentally accessible phenomenological co-efficients. Moreover, these processes help us to elucidate qualitatively the structural effect[11] of solute on solvent by allowing determination of permeant-permeant and membrane-permeant interactions from the excess values of the phenomenological co-efficients[12]. Since the flow process through the membrane and plug involves the activated unit rate process[13], the activation enthalpies (ΔH^*) and entropies (ΔS^*) as well as free energy of activation (ΔG^*) can be determined. These parameters are likely to throw more light on the mechanism of transport through the membrane. Studies on membranes of inorganic materials are rare, inspite of the fact that inorganic ion-exchangers are more stable than organic resins under certain conditions[14] and have important potential applications in the conversion of sea or brackish water to fresh water[15], and in the fuel cells[16]. In continuation of our earlier studies, we report here the results of our studies on the flow of ethylene glycol, diethyl glycol and their aqueous mixtures through titanium oxide plug as the membrane.

Materials and Methods

Water of specific conductivity of the order of 10^{-6} ohm^{-1} cm^{-1} was used. Ethylene glycol and diethylene glycol were purified before use by the method described elsewhere[17,18]. All the solutions were made by weight.

Membrane

The titanium oxide sample used was thoroughly washed with water to remove soluble impurities. It was then kept in conductivity water for 48 hr for allowing the particles to be completely swollen. A known amount (12 g) of the swollen particles was placed in the middle of a glass tube having a narrower part in the middle. Titanium oxide was mixed with 5% araldite adhesive and was then compressed with the help of a mechanical device consisting of wooden rods having diameter slightly less than that of the narrower part of the tube. The assembly was kept as such for 24 hr. In this manner, a compact plug of titanium oxide was obtained. The experimental liquid was streamed through the membrane, so as to remove the air contained in the pores and avoid blocking of the pores.

Apparatus

The apparatus used for the measurements in the present investigations was similar to that used earlier[19]. All the experiments were carried out in a thermostat allowing control of temperature within ±0.05°C.

Results and Discussion

In the present study, the liquid on both sides of the membrane has the same composition and hence the volume flux, J_v, will be given by[20],

$$J_v = L_p \Delta P \qquad \ldots (1)$$

where L_p is the permeability of the membrane for the fluid. L_p has the character of mobility and represents the velocity of fluid per unit pressure difference for the unit cross-sectional area of the membrane. The permeability for water and different aqueous mixtures of EG and DEG has been measured and Eq. (1) is found to be obeyed in all the cases. The values of L_p have been estimated from the linear plots of J_v and ΔP. The values of L_p so obtained at different temperatures are reported in Table 1.

Evaluation of frictional coefficients

On translating the thermodynamic coefficients into frictional coefficients, it has been found that, L_p can be related to the coefficient of friction[21] between water and the membrane, F_{wm}, by the equation,

$$L_p = \frac{\phi_w \bar{V}_w}{F_{wm} \delta} \qquad \ldots (2)$$

where ϕ_w is the volume fraction of water in the membrane, $\bar{V}_w$ is the molar volume of water and δ is the thickness of the membrane. ϕ_w has been determined by the method described by Ginzburg and Katchalsky[22]. The value of ϕ_w in the present case has come out to be 0.279; substituting the values of various parameters in Eq. (2), we estimated F_{wm} for various solutions (Table 2).

It is clear from Table 2 that the frictional coefficient, F_{wm}, increases with the increase in the composition of both the glycols meaning thereby that water-membrane interaction increases with increase in [glycol] and the viscosity of the medium. In the case of titanium oxide membrane, oxygen atoms lie at the matrix of the membrane[23] and make it negatively charged. In glycols the hydroxyl proton is likely to undergo intermolecular exchange as a result of autoprotolysis and lead to the formation of more positively charged particles; hence, the interaction of the permeant with the negatively charged membrane increases.

Different separators/membranes used in alternate energy devices have been characterised in terms of parameters of activation[13,24]. Titanium oxide is very stable material and is a potential candidate for use in batteries. Therefore, the parameters of activation for flow through it were estimated as described earlier[13]. The values of ΔH^*, ΔS^*, and ΔG^*, are given in Table 3.

Table 3 shows that the entropy of activation decreases with increase in viscosity of the medium,

Table 1—Permeability Coefficient, L_p, of Titanium Oxide Membrane for Water and Aqueous Solutions of EG and DEG at Different Temperatures

Composition (w/w)	$L_p \times 10^9$ ($m^3 N^{-1} S^{-1}$)			
	303K	308K	313K	318K
Water	4.29	5.26	6.90	9.18
20% EG	2.35	2.81	3.86	4.90
40% EG	2.04	2.34	2.75	3.45
60% EG	1.55	1.69	2.04	2.80
80% EG	0.78	0.86	1.06	1.20
100% EG	0.64	0.68	0.79	0.86
20% DEG	2.06	2.45	3.07	3.93
40% DEG	1.77	2.09	2.55	2.95
60% DEG	0.85	0.97	1.12	1.31
80% DEG	0.64	0.70	0.83	0.89
100% DEG	0.60	0.64	0.72	0.76

Table 2—Frictional Coefficient for Different Compositions of EG–H_2O and DEG–H_2O Mixtures at Different Temperatures

Composition (w/w)	$F_{wm} \times 10^{-5}$ (m^{-1} mol^{-1} NS)	
	EG	DEG
Temperature 303K		
0% (water)	0.78	
20%	1.43	1.63
40%	1.65	1.90
60%	2.17	3.96
80%	4.31	5.25
100%	5.26	5.64
Temperature 308K		
% (water)	0.64	
20%	1.20	1.38
40%	1.44	1.61
60%	1.65	3.45
80%	2.90	4.78
100%	4.96	5.26
Temperature 313K		
/% (water)	0.49	
20%	0.87	1.10
40%	1.22	1.32
60%	1.99	3.00
80%	3.19	4.07
100%	4.26	4.67
Temperature 318K		
0% (water)	0.37	
20%	0.69	0.86
40%	0.98	1.15
60%	1.21	2.57
80%	2.81	3.81
100%	3.93	4.46

Table 3—Activation Energy Parameters for Flow Through Titanium Oxide Membrane at 303K

Composition (w/w)	$E_\eta \times 10^{-4}$ (J mol^{-1})		ΔS^* (JK^{-1} mol^{-1})		$\Delta G^* \times 10^{-3}$ (J mol^{-1})	
	EG-H_2O	DEG-H_2O	EG-H_2O	DEG-H_2O	EG-H_2O	DEG-H_2O
0% (water)	1.71	—	43.47	—	3.93	—
20%	1.69	1.45	31.71	22.65	7.19	7.60
40%	1.16	1.15	12.32	10.79	7.87	8.22
60%	1.04	0.97	5.35	1.87	8.78	9.13
80%	1.01	0.76	1.38	7.95	9.69	10.07
100%	0.70	0.57	−12.33	−18.91	10.74	11.39

and the decrease is more rapid in the case of diethylene glycol (DEG). This may be attributed to the greater interactions of the medium containing DEG with the membrane.

The positive values of ΔG^* in all the cases show that the flow is not favoured across the porous medium.

Evaluation of molecular exchange rate

The statistical theory of transport processes[25] gives the following expression for the flow rate,

$$J_v = 2\, K_{\beta\alpha}(\mu^\beta - \mu^\alpha)/kT \qquad \ldots (3)$$

where J_v is the volume flow, $K_{\beta\alpha}$ is the molecular exchange rate between phases α and β on two sides of the membrane, k is Blotzmann's constant and T is temperature in Kelvin. The factor $\mu^\beta - \mu^\alpha$ across the membrane is given by[26],

$$\Delta\mu_{\beta\alpha} = \bar{V}_w(\Delta P - \Delta\pi) \qquad \ldots (4)$$

where $\bar{V}_w$ is the molar volume of water, ΔP is the pressure across the membrane and $\Delta\pi$ is the osmotic pressure. If there is no concentration difference across the membrane then expression (4) reduces to,

$$\Delta\mu^\alpha_\beta = \bar{V}_w \Delta P \qquad \ldots (5)$$

Use of (5) reduces Eq. (3) to,

$$J_v = 2\, K_{\beta\alpha} \frac{\bar{V}_w \Delta P}{kT} \qquad \ldots (6)$$

The molecular exchange rate can be calculated from Eq. (6) using the values of T, ΔP and J_v for different aqueous solutions of EG and DEG. The values of molecular exchange rate thus obtained have been reported in Table 4.

The molecular exchange rate has been defined[25] as the transition probability of the distribution from the liquid phase on the side of membrane where pressure is higher to the phase within the membrane. The small values of the molecular exchange rate may be attributed to the same distribution function in the bulk and the membrnae phases. The increase in $K_{\beta\alpha}$ with temperature and decrease with glycol content show that the transport through the membrane follows the activated unit rate process.

Table 4—Molecular Exchange Rate of Water and Different Aqueous Mixtures of EG and DEG at Different Temperatures

Composition (w/w)	$K_{\beta\alpha} \times 10^{25}$ (mS^{-1})			
	303K	308K	313K	318K
0% (water)	4.96	6.17	8.21	11.08
20% EG	2.72	3.30	4.49	5.91
40% EG	2.36	2.75	3.27	4.16
60% EG	1.79	2.01	2.39	3.38
80% EG	0.90	1.02	1.26	1.45
100% EG	0.74	0.80	0.94	1.04
20% DEG	2.38	2.87	3.65	4.74
40% DEG	2.05	2.45	3.03	3.56
60% DEG	0.98	1.14	1.33	1.58
80% DEG	0.74	0.82	0.99	1.07
100% DEG	0.69	0.75	0.86	0.92

Acknowledgement

One of the authors (C.P.) is thankful to the UGC, New Delhi for the award of a Research Fellowship.

References

1 Rastogi R P, Singh K & Singh J, *J phys Chem*, **79** (1975) 2574.
2 Srivastava R C & Jain A K, *J polym Sci*, **13** (1975) 1603.
3 Srivastava M L & Lal S N, *J Colloid polym Sci*, **257** (1979) 427.
4 Blokhra R L & Kohli S, *J electronal Chem*, **124** (1981) 285.
5 Blokhra R L, Chauhan S C & Mahajan S, *J Indian chem Soc*, **LIX** (1982) 63.
6 Blokhra R L, Parmar M L & Thakur S S, *J memb Sci*, **21** (1984) 123.
7 Singh K & Kumar Vijai, *Indian J Chem*, **23A** (1984) 551.
8 Ruoque H A, Francisco J D & Nieves P G, *J chem Soc Faraday Trans I*, **81** (1985) 609.

9 Degroot S R, *Thermodynamics of irreversible processes*, 3rd Edn. (Interscience, New York) 1952, 187.
10 Singh K, Kumar R & Srivastava V N, *J Indian chem Soc*, **LVII** (1980) 203.
11 Blokhra R L & Singal T C, *Proc Nat Acad Sci*, **45A** IV (1975) 287.
12 Srivastava M L & Lal S N, *Kolloid-Zuz Polymer*, **1** (1980) 71.
13 Blokhra R L, *J electrochem Soc (India)*, **36** (1987) 245.
14 Amphlett C M, *Inorganic ion-exchangers* (Elsevier Amsterdam) 1964, VII.
15 Lakshminarayaniah N, *Transport phenomena in membranes* (Academic Press, New York) 1969, 30.
16 Lakshminarayaniah N, *Transport phenomena in membranes* (Academic Press, New York) 1969, 46.
17 Blokhra R L, Sehgal Y P & Kuthiala V P, *Electrochim Acta*, **21** (1976) 1079.
18 Blokhra R L & Sehgal Y P, *Indian J Chem*, **15A** (1977) 1035.
19 Blokhra R L, Parmar M L & Sidhu R, *J Non-equilib Thermodynamics*, **8** (1983) 183.
20 Lakshminarayaniah N, *Transport phenomena in membranes* (Academic Press, New York) 1969, 313.
21 Katchalsky A & Curran P F, *Non-equilibrium thermodynamics in bio-physics* (Harvard University Press, Cambridge) 1967, 128.
22 Ginzburg B Z & Kathalsky A, *J gen Physiol*, **47** (1963) 403.
23 Srivastava M L & Lal S N, *J memb Sci*, 7 (1980) 21.
24 Blokhra R L, NASA-TM (1983) No. 83371.
25 Ward C A, Findlay R D & Rizk M, *J chem Phys*, **76** (1982) 5590.
26 Lakshminarayaniah N, *Transport phenomena in membranes* (Academic Press, New York) 1969, 304.

Indian Journal of Chemistry
Vol. 28A, February 1989, pp. 102-105

Ion-Pair Association Constants of Alkali & Alkaline Earth Metal Formates in Formic Acid-Acetonitrile Mixtures at 30°C—A Conductance Study

K CHOWDOJI RAO †, (Mrs) M C S SUBHA* & S BRAHMAJI RAO
Department of Chemistry, Sri Krishnadevaraya University, Anantapur 515 003

Received 24 *November* 1987; *revised and accepted* 8 *March* 1988

Equivalent conductance values of solutions of lithium, sodium, potassium, calcium and barium formates in 20% formic acid + 80% acetonitrile and 80% formic acid + 20% acetonitrile mixtures have been determined at different concentrations. Fuoss-Kraus and Shedlovsky extrapolation methods are used to determine ion-pair association constants (K_a). Reasonable agreement is found between the K_a values obtained by the two methods. Experimentally obtained ion-pair association constants are compared with those calculated using Bjerrum (B), Fuoss (F), Denison & Ramsey (DR) and Ebeling-Kraeft-Yokoyama-Yamatera (EKYY) theories. The results are used to arrive at the type of the ion-pairs and to establish the nature of the ion-solvent interactions.

In continuation of our earlier work on physical properties[1,2] of formic acid (FA) + acetonitrile (AN) mixtures, we have now measured the equivalent conductances of the formates of lithium, sodium, potassium, calcium and barium in these mixtures at 30°C. The results are used to determine the association constants of the ion-pairs using Fuoss-Kraus and Shedlovsky extrapolation methods and to get an insight into possible ion-solvent interactions and the nature of the ion-pairs.

Materials and Methods

Formic acid (Riedel, 98-100%) and acetonitrile (E. Merck) were purified by the standard procedures[3]. The specific conductances of formic acid and acetonitrile were les than 0.61×10^{-5} ohm^{-1} cm^{-1}. Alkali and alkaline earth metal formates were prepared and purified as reported earlier[1]. Formic acid + acetonitrile mixtures were prepared by weight percent. The dielectric constants of solvent mixtures at 30°C were measured with DK meter 60 GK (Franz Kustner Nacf. K.G. Dresden); the values were found to be 50.65 for 80% formic acid + 20% acetonitrile and 38.75 for 20% formic acid + 80% acetonitrile mixtures. A Biochem Digital Conductivity meter (model 808), capable of measuring conductance with an accuracy of ±0.2% in the range of 2 micromhos to 2 mhos, and a dip type conductance cell[4] with smooth electrodes (since formic acid is oxidized at platinized electrodes) were used in the studies. The measurements were made at 30 ± 0.01°C. The instrument was standardized with a standard aqueous KCl solution of a known concentration thermostated at the same temperature. The reproducibility of the measurement was checked at frequent intervals for half an hour and the final equilibrium value noted.

Results and Discussion

The measured molar conductance values of the salts were used to evaluate Λ_0 graphically. A typical graph between Λ and $\sqrt{C}$ is presented in Fig. 1. The measured data have been used to calculate, by Fuoss-Kraus[5] and Shedlovsky[6] equations, the three parameters; the limiting equivalence conductance (Λ_0), the ion-pair association constant

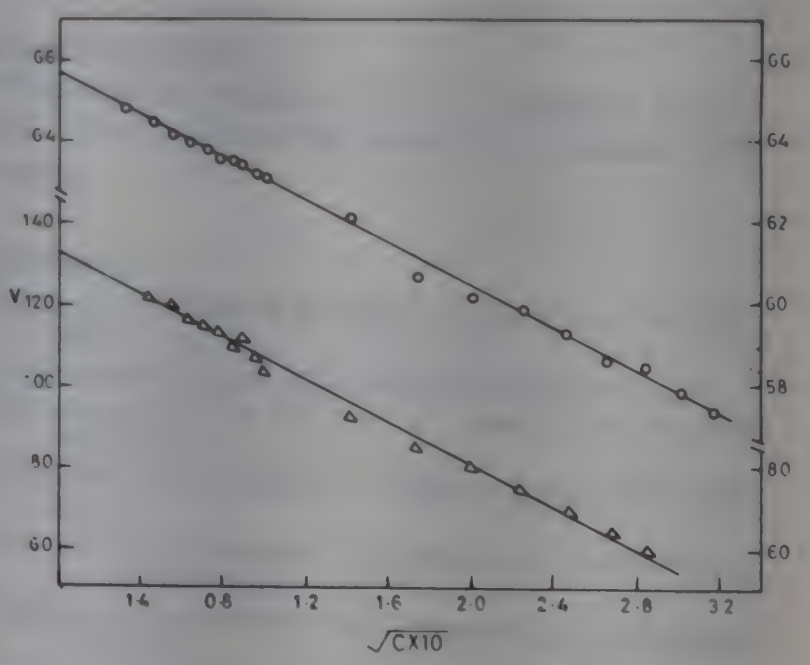

Fig. 1—Plots of Λ versus $\sqrt{C}$ for sodium formate in 80% formic acid + 20% acetonitrile (○) and in 20% formic acid + 80% acetonitrile (Δ) mixtures at 30°C

†Department of Polymer Science, Sri Krishnadevaraya University, Anantapur 515 003

Table 1—Λ_0 and K_a Values Obtained from Fuoss-Kraus and Shedlovsky Extrapolation Techniques for Alkali and Alkaline Earth Metal Formates in Formic Acid + Acetonitrile Mixtures at 30°C

Formate	Fuoss-Kraus		Shedlovsky	
	Λ_0 (ohm^{-1} cm^2 mol^{-1})	K_a (dm^3 mol^{-1})	Λ_0 (ohm^{-1} cm^2 mol^{-1})	K_a (dm^3 mol^{-1})
80% Formic Acid + 20% Acetonitrile				
HCOOLi	47.2	1.0	47.6	1.3
HCOONa	66.9	1.1	66.9	1.1
HCOOK	93.9	3.6	94.3	5.3
$(HCOO)_2Ca$	107.1	1.5	107.0	1.7
$(HCOO)_2Ba$	115.8	8.9	115.7	8.8
20% Formic Acid + 80% Acetonitrile				
HCOOLi	95.2	48.6	94.8	47.1
HCOONa	143.9	69.6	142.9	69.2
HCOOK	183.5	99.3	183.5	100.7
$(HCOO)_2Ca$	—	—	—	—
$(HCOO)_2Ba$	—	—	—	—

(K_a, the equilibrium constant of $M^+ + A^- \rightleftharpoons M^+A^-$ existing between the free ions and ion-pairs) and the ion-size parameter (a, the distance from the centre of the cation of an ion-pair within which a unique parameter can be found for a paired ion). The results are presented in Table 1. The results show that there is an increase in Λ_0 and K_a as the solvent is changed from 80% formic acid + 20% acetonitrile to 20% formic acid + 80% acetonitrile (with decrease in dielectric constant of the medium).

Values of a and K_a were also calculated by the different expressions (Eqs 1-4) reported in the literature. The results are presented in Tables 2 and 3 respectively.

Bjerrum expression[7]:

$$K_B = \frac{4\pi N}{1000}\left[\frac{|Z_+Z_-|e^2}{DKT}\right]^3 Q(b) \quad \ldots (1)$$

Fuoss expression[8]:

$$K_F = \frac{4\pi Na^3}{3000}.e^b \quad \ldots (2)$$

Denison and Ramsey expression[9]:

$$K_{DR} = e^b \quad \ldots (3)$$

EKYY expression[10,11]:

$$K_{EKYY} = \frac{8\pi Na^3}{1000}\cdot\sum_{n=1}^{\infty}\frac{b^{n+2}}{[(2n+2)!(2n-1)]} \quad \ldots (4)$$

Table 2—Ion-Size Parameter Values (a) Calculated from Different Theories for Alkali and Alkaline Earth Metal Formates in Formic Acid + Acetonitrile Mixtures at 30°C

Formate	a(Å)			
	B	F	DR	EKYY
80% Formic Acid + 20% Acetonitrile				
HCOOLi	4.63	V. low value	43.54	0.24
HCOONa	4.73	V. low value	91.03	0.81
HCOOK	3.18	V. low value	6.50	0.99
$(HCOO)_2Ca$	4.41	V. low value	20.40	1.12
$(HCOO)_2Ba$	4.96	V. low value	5.01	1.09
20% Formic Acid + 80% Acetonitrile				
HCOOLi	1.74	2.09	3.69	6.20
HCOONa	1.55	2.92	3.33	5.40
HCOOK	1.42	3.10	3.08	4.24
$(HCOO)_2Ca$	—	—	—	—
$(HCOO)_2Ba$	—	—	—	—

where

$b = |Z_+Z_-|e^2/aDKT$

and n = number of a particular type of ions (cation or anion) in V cm^3 of the solution.

The ion-size parameter a was calculated from the crystallographic radii of the cations[12] ($Li^+ = 0.60$, $Na^+ = 0.95$, $K^+ = 1.33$, $Ca^{2+} = 0.99$ and $Ba^{2+} = 1.35$ Å) and that for the formate ion[13] (1.27 Å) was calculated from the available bond length data of the carboxylate ion.

The a values were employed to calculate K_a values from the theoretical expressions. The results are included in Tables 2 and 3. These results show that none of the theories predicts correctly the

Table 3—Experimental and Theoretical Values of Association Constants (K_a) of Alkali and Alkaline Earth Metal Formates in Formic acid + Acetonitrile Mixtures at 30°C

Formate	K_a (Exp.) ($dm^3\ mol^{-1}$)	Theoret. ($dm^3\ mol^{-1}$)			
		K_B	K_F	K_{DR}	K_{EKYY}
	80% Formic Acid + 20% Acetonitrile				
HCOOLi	1.3	9.8	5.6	336.9	7.3
HCOONA	1.1	7.3	3.7	134.6	5.4
HCOOK	5.4	5.9	2.9	65.8	4.3
$(HCOO)_2Ca$	1.7	39.0	443.5	15230.0	252.0
$(HCOO)_2Ba$	8.8	22.0	18.4	4055.0	145.7
	20% Formic Acid + 80% Acetonitrile				
HCOOLi	47.1	36.1	33.2	2012.0	30.3
HCOONa	69.2	25.1	16.7	606.6	20.1
HCOOK	100.7	19.6	10.5	237.8	14.7
$(HCOO)_2Ca$	—	—	—	—	—
$(HCOO)_2BA$	—	—	—	—	—

K_a = Experimental association constant, K_B = Bjerrum association constant, K_F = Fuoss association constant, K_{DR} = Denison-Ramsey association constant, and K_{EKYY} = Ebeling-Kraeft-Yokoyama-Yamatera association constant.

state of the salts in these solvent systems. This may be attributed to the inadequacy of the theories.

An examination of K_a values indicates that the experimental values in 80% FA+20% AN mixture are lower, while those in 20% FA+80% AN mixture are higher than the theoretical values. This suggests that in 80% FA+20% AN mixture ion-solvent interactions are quite strong and that solvent separated ion-pairs (SSIP) are formed in this mixture as reported by Kay *et al.*[14] in such systems. The results in 20% FA+80% AN mixture suggest the existence of contact ion-pairs as well as solvent separated ion-pairs.

The Walden product and hydrodynamic factor

The product $\Lambda_0\eta$ is known as Walden product and is generally constant for a given electrolyte in a series of pure solvents or solvent mixtures in which ion-solvent interactions are uniform. For uni-univalent electrolytes ($Z_+ = Z_- = 1$),

$$\Lambda_0\eta = 0.8201 \left(\frac{1}{r_s^+} + \frac{1}{r_s^-}\right) \quad \ldots (5)$$

or

$$\left[\frac{1}{r_s^+} + \frac{1}{r_s^-}\right]^{-1} = \frac{0.8201}{\Lambda_0\eta} \quad \ldots (6)$$

The factor $\left(\frac{1}{r_s^+} + \frac{1}{r_s^-}\right)^{-1}$ is a measure of the hydrodynamic radii of ions and it indicates ion-solvent interactions. The values of the Walden product ($\Lambda_0\eta$) and the factor $\left(\frac{1}{r_s^+} + \frac{1}{r_s^-}\right)^{-1}$ for lithium, sodium, potassium, calcium and barium formates in 80% formic acid + 20% acetonitrile and 20% formic acid + 80% acetonitrile mixtures are presented in Table 4. The results show that with the decrease in the formic acid content in the mixtures, the magnitude of the Walden product decreases while that of the hydrodynamic factor increases. These observations suggest that the ions are less solvated in mixtures containing low formic acid content. The low positive *B*-coefficients[2] in this medium substantiates the results. It may, therefore, be concluded that increase in acetonitrile content reduces the solvation of the ions, due to the decrease in dielectric constant of the mixture.

Table 4—Walden Product ($\Lambda_0\eta$) and Hydrodynamic Radii $[(1/r_s^+)+(1/r_s^-)]^{-1}$ of Alkali Metal Formates in Formic Acid + Acetonitrile Mixtures at 30°C

Formate	$\Lambda_0\eta$	$[(1/r_s^+)+(1/r_s^-)]^-$
80% Formic Acid + 20% Acetonitrile		
HCOOLi	46.20	1.7749×10^{-2}
HCOONa	64.92	1.2631×10^{-2}
HCOOK	91.48	0.8964×10^{-2}
20% Formic Acid + 80% Acetonitrile		
HCOOLi	40.18	2.0408×10^{-2}
HCOONa	60.55	1.3543×10^{-2}
HCOOK	77.77	1.0544×10^{-2}

References

1 Chowdoji Rao K & Brahmaji Rao S, *Indian J Chem*, **21A** (1982) 69; **21A** (1982) 71.

2 Chowdoji Rao K, Ph D Thesis, Sri Krishnadevaraya University, Anantapur, 1984.
3 Weissberger A, *Techniques of organic chemistry*, Vol 3, 2nd Edn (Interscience, New York), 1967.
4 Wehman T C & Popov A I, *J phys Chem*, **72** (1968) 4031.
5 Fuoss R M & Kraus C A, *J Am chem Soc*, **55**(1933) 476.
6 Shedlovsky T, *J Fraklin Inst*, 225 (1938) 739.
7 Bjerrum B, *Z Electrochem*, **24** (1918) 32.
8 Fuoss R M, *J Am chem Soc*, **80** (1958) 5059.
9 Denison J T & Ramsey J B, *J Am chem Soc*, **77** (1915) 2615.
10 Ebeling W & Kraeft W D, *Z phys Chem* (*Liepzig*), **240** (1969) 41.
11 Yokoyama H & Yamatera H, *Bull chem Soc Japan*, **48** (1975) 1770.
12 Robinson R A & Stokes R H, *Electrolyte solutions* (Butterworths, London) 1965, 230.
13 Masterton W L, Bolocafsky D & Lee T P, *J phys Chem*, **75** (1971) 2809.
14 Kay R L, Evans D F & Mateskh M A, *Solute-solvent interactions*, edited by J F Coetzee & C D Ritchie, (Marcel Dekkar Inc, New York), 1976 Ch. 10.

Indian Journal of Chemistry
Vol. 28A, February 1989, pp. 106-110

Ion-Solvent Interactions in Alcohol Rich Binary Mixtures: Densities & Viscosities of Alkali Metal Propionates in Propionic Acid + 1-Propanol Mixtures

(Mrs) M C S SUBHA*, K CHOWDOJI RAO† & S BRAHMAJI RAO
Department of Chemistry, Sri Krishnadevaraya University, Anantapur 515 003

Received 12 January 1988; revised 21 March 1988; accepted 4 April 1988

Viscosities and densities of propionates of lithium, sodium and potassium have been measured at 308.15 K in propionic acid (PA) + 1-propanol mixtures containing 5, 15 and 30 wt% of propionic acid. The viscosity data have been analysed using the Jones-Dole equation. The activation parameters of viscous flow have been obtained to throw light on the mechanism of viscous flow. The apparent molar volumes (ϕ_v) of these electrolytes at different concentrations have been estimated and the results indicate that these electrolytes behave as structure promoters.

Even though studies on ion-solvent interactions in mixed solvents are quite extensive[1-6], such studies in binary solvents containing 1-propanol + nonaqueous ionizing cosolvent, specially where the anion of the ionizing cosolvent is the same as the anion of the salt, are limited. This led the authors to undertake the title investigations, the results of which are presented in this paper.

Materials and Methods

Sodium propionate (Riedel, AR) was used as received. Lithium and potassium propionates were prepared and purified by procedures described by Franzosini *et al.*[7] The salts were dried and stored in a vacuum desiccator.

Propionic acid (Fluka, purity > 99.5%) was dried over anhydrous sodium sulphate, fractionally distilled and the fraction distilling between 412.15 K and 414.15 K was collected and redistilled in the presence of potassium permanganate, b.p. 413.85 K/760 mm. 1-Propanol (AR) was refluxed over calcium oxide for several hours, fractionally distilled and the middle cuts collected and stored in bottles having Linda-type 5A molecular sieves.

Solvent mixtures of propionic acid (PA) + 1-propanol (1-PrOH) and the solutions of electrolytes in these solvent mixtures were made by weight. Densities were measured using a double capillary pycnometer described earlier[8]. The precision in density determinations was within ± 2 parts in 10^4 which introduce an uncertainty of 0.1 to 1.0 cm^{-3} mol^{-1} in ϕ_v values. Viscosities were measured using an Ubbelohde suspended level viscometer with a flow time of 302 sec for water at 308.15 K. The time of efflux through the capillary was measured correct to ± 0.1 sec. The viscometer was held in a water thermostat capable of controlling the temperature within ± 0.02 K. Kinetic energy corrections were not applied since the flow times were sufficiently large.

Results and Discussion

Viscosities (η) and the densities (d) of salt solutions in PA + 1-PrOH mixtures containing 5, 15 and 30 wt% PA at 308.15 K and at different concentrations (C) are given in Table 1.

The apparent molar volume (ϕ_V) was calculated from density data using Eq. (1)

$$\phi_V = \frac{M_2}{d_0} - \frac{1000\,(d - d_0)}{C d_0} \qquad \ldots (1)$$

where C is the molar concentration of the electrolyte, d is the density of the solution, d_0 is the density of the appropriate solvent mixture and M_2 is the molecular weight of the electrolyte. The ϕ_V values are also included in Table 1.

The relative viscosities (η_r) of electrolytes in PA + 1-PrOH mixtures containing 5, 15, 30 wt % PA were determined and are also listed in Table 1. The viscosity data were analysed by means of the well known Jones-Dole equation[9], (2)

$$\eta_r = \frac{\eta}{\eta_0} = 1 + AC^{1/2} + BC \qquad \ldots (2)$$

The values of the parameters A and B were calculated by the method of least squares and are given in Table 2.

The A-values are negative for C_2H_5COONa in the PA + 1-PrOH mixture containing 15% PA and

† Department of Polymer Science, Sri Krishnadevaraya University, Anantapur 515 003.

Table 1—Densities (d), Viscosities (η), Relative Viscosities (η_r) and Apparent Molar Volumes (ϕ_V) of Alkali Propionates in Propionic Acid (PA) + 1-propanol Mixtures at 308.15 K

Wt % PA in solvent mixture	C (mol dm^{-3})	d (kg m^{-3})	$\eta \times 10^4$ (kg m^{-1} s^{-1})	η_r	ϕ_V (cm^3 mol^{-1})
		Lithium propionate			
5	0.0000	801.0	14.4		
	0.0102	801.4	14.6	1.014	47.6
	0.0204	801.8	14.8	1.023	49.6
	0.0300	802.2	14.9	1.031	50.8
	0.0402	802.5	15.0	1.039	52.0
	0.0504	802.9	15.1	1.048	53.6
	0.0600	803.2	15.2	1.056	53.6
	0.0702	803.5	15.3	1.060	54.0
	0.0804	803.9	15.4	1.066	54.8
	0.0900	804.2	15.5	1.074	55.4
	0.1002	804.5	15.7	1.085	56.8
15	0.0000	818.2	14.2		
	0.0102	818.6	14.3	1.010	51.1
	0.0204	819.0	14.4	1.015	52.4
	0.0300	819.3	14.5	1.023	54.2
	0.0402	819.6	14.6	1.031	54.9
	0.0504	819.9	14.8	1.041	57.2
	0.0600	820.2	14.9	1.050	57.0
	0.0702	820.5	15.0	1.057	57.8
	0.0804	820.9	15.1	1.063	56.3
	0.0900	821.1	15.2	1.073	58.4
	0.1002	821.4	15.3	1.080	59.3
30	0.0000	844.8	13.7		
	0.0102	845.2	13.9	1.005	51.4
	0.0204	845.5	13.9	1.012	52.2
	0.0300	845.8	14.0	1.018	53.5
	0.0402	846.2	14.1	1.026	53.9
	0.0504	846.6	14.2	1.033	55.1
	0.0600	846.8	14.5	1.037	55.2
	0.0702	847.1	14.4	1.047	56.4
	0.0804	847.3	14.4	1.055	57.6
	0.0900	847.6	14.6	1.062	57.3
	0.1002	847.0	14.7	1.070	57.1
		Sodium propionate			
5	0.0000	801.0	14.4		
	0.0099	807.3	15.0	1.006	59.7
	0.0198	807.7	15.1	1.012	60.8
	0.0301	808.2	15.2	1.019	62.7
	0.0400	808.5	15.4	1.024	64.8
	0.0499	808.9	15.3	1.028	65.7
	0.0602	809.4	15.5	1.036	65.8
	0.0701	809.8	15.6	1.043	65.8
	0.0800	810.1	15.7	1.048	68.1
	0.0900	810.5	15.9	1.053	68.3
	0.1002	818.9	16.1	1.059	68.4
15	0.0000	818.2	14.2		
	0.0102	824.2	14.8	1.004	59.0
	0.0204	824.6	14.9	1.010	61.6
	0.0300	825.1	15.1	1.016	62.4
	0.0402	825.5	15.1	1.021	63.7
	0.0504	825.9	15.2	1.024	64.4
	0.0600	826.2	15.3	1.036	66.5
	0.0702	826.6	15.4	1.041	67.5

(*Contd.*)

Table 1—Densities (d), Viscosities (η), Relative Viscosities (η_r) and Apparent Molar Volumes (ϕ_V) of Alkali Propionates in Propionic Acid (PA) + 1-propanol Mixtures at 308.15 K—*Cont.*

Wt % PA in solvent mixture	C (mol dm^{-3})	d (kg m^{-3})	$\eta \times 10^4$ (kg m^{-1} s^{-1})	η_r	ϕ_V (cm^3 mol^{-1})
	0.0804	827.1	15.5	1.045	66.3
	0.0900	827.5	15.6	1.057	66.1
	0.1002	827.8	15.6	1.056	67.7
30	0.0000	844.8	13.7		
	0.0102	849.8	14.6	1.010	59.5
	0.0204	850.2	14.7	1.016	62.1
	0.0300	850.6	14.8	1.024	63.1
	0.0402	851.0	14.8	1.032	63.6
	0.0504	851.4	15.0	1.040	64.1
	0.0600	851.8	15.2	1.049	64.6
	0.0702	852.3	15.2	1.054	63.7
	0.0804	852.6	15.3	1.060	66.1
	0.0900	852.9	15.3	1.066	66.2
	0.1002	853.3	15.4	1.074	66.4
		Potassium propionate			
5	0.0000	801.0	14.4		
	0.0102	801.0	14.5	1.009	62.5
	0.0204	801.6	14.7	1.015	64.5
	0.0300	802.1	14.7	1.020	66.4
	0.0402	802.7	14.8	1.028	67.2
	0.0504	803.2	14.9	1.032	68.3
	0.0600	803.9	14.9	1.039	68.2
	0.0702	804.3	15.1	1.043	70.1
	0.0804	804.8	15.2	1.050	70.4
	0.0900	805.3	15.2	1.057	71.6
	0.1002	805.8	15.3	1.062	72.4
15	0.0000	818.2	14.2		
	0.0102	819.3	14.2	1.007	64.0
	0.0204	819.9	14.2	1.014	65.4
	0.0300	820.4	14.4	1.019	66.5
	0.0402	821.0	14.5	1.025	67.3
	0.0504	821.5	14.7	1.034	68.2
	0.0600	822.0	14.7	1.038	69.6
	0.0702	822.6	14.8	1.045	69.1
	0.0804	823.1	14.9	1.051	70.4
	0.0900	823.5	14.9	1.056	71.6
	0.1002	824.1	15.0	1.063	71.7
30	0.0000	844.8	13.7		
	0.0102	844.5	14.0	1.009	63.6
	0.0204	845.1	14.1	1.017	64.7
	0.0300	845.7	14.1	1.022	65.4
	0.0402	846.2	14.3	1.031	65.4
	0.0504	846.8	14.3	1.033	66.4
	0.0600	847.3	14.5	1.045	67.3
	0.0702	847.8	14.4	1.049	67.8
	0.0804	848.3	14.6	1.055	68.7
	0.0900	848.8	14.6	1.057	69.0
	0.1002	849.4	14.7	1.069	68.6

C_2H_5COOLi in PA + 1-PrOH mixture containing 30% PA. Such negative values are not expected on the basis of Falkenhagen theory[10] and hence no significance is attached to these negative values as has been done by the other workers[11-13]. The small *A*-values may however indicate that they contribute very little to absolute viscosities.

The *B*-values are positive and large indicating

Table 2—*A* and *B* Coefficients of Jones-Dole equation for Alkali Propionates in Propionic Acid (PA) + 1-Propanol Mixtures at 308.15 K

Wt % PA in solvent mixture	*A* ($dm^{3/2}\ mol^{-1/2}$)	*B* ($dm^3\ mol^{-1}$)
	Lithium propionate	
5	0.077	0.60
15	0.024	0.72
30	−0.032	0.79
	Sodium propionate	
5	0.010	0.56
15	−0.021	0.65
30	0.015	0.69
	Potassium propionate	
5	0.031	0.53
15	0.009	0.60
30	0.022	0.61

Standard deviations in *A*-coefficients and *B*-coefficients are ±0.002-0.005 and ±0.02-0.05, respectively.

that alkali metal propionates act as structure makers in these solvent mixtures. The structure making tendencies of the salts are in the order: Li-salt > Na-salt > K-salt. The *B*-values increase with increase in acid concentration in the solvent medium indicating that propionic acid in the solvent mixtures behaves as a structure breaker.

The viscosity data have also been analysed on the basis of a transition state treatment of the relative viscosity of electrolytic solutions as suggested by Feakins *et al.*[1] The *B*-parameter in terms of this theory is given by Eq. (3)

$$B = \frac{\bar{V}_1^0 - \bar{V}_2^0}{1000} + \frac{\bar{V}_1^0}{1000}\left[\frac{\Delta\mu_2^{0\neq} - \Delta\mu_1^{0\neq}}{RT}\right] \quad \ldots (3)$$

where $\bar{V}_1^0$ and $\bar{V}_2^0$ are the partial molar volumes of solvent and solute (at infinite dilution) respectively, $\Delta\mu_2^{0\neq}$ is the contribution per mol of solute to the free energy of activation of viscous flow of the solution and $\Delta\mu_1^{0\neq}$ the free energy of activation per mol of the pure solvent and is given by[14] Eq. (4)

$$\Delta\mu_1^{0\neq} = \Delta G_1^{0\neq} = RT \ln(\eta_0 \bar{V}_1^0/hN) \quad \ldots (4)$$

In Eq. (4) h is the Planck's constant, N the Avogadro's number and η_0 is the viscosity of the solvent. Equation (3) is rewritten as

$$\Delta\mu_2^{0\neq} = \Delta\mu_1^{0\neq} + \frac{RT}{\bar{V}_1^0}[1000B - (\bar{V}_1^0 - \bar{V}_2^0)] \quad \ldots (5)$$

Table 3—Values of $\Delta\mu_2^{0\neq}$ for Alkali Propionates in Propionic Acid (PA) + 1-Propanol Mixtures at 308.15 K

Wt% PA in solvent mixture	$\Delta\mu_2^{0\neq}$ ($kJ\ mol^{-1}$)	Wt % PA in solvent mixture	$\Delta\mu_2^{0\neq}$ ($kJ\ mol^{-1}$)
Lithium propionate		*Potassium propionate*	
5	21.56	5	20.68
15	22.59	15	21.74
30	23.15	30	21.82
Sodium propionate			
5	21.37		
15	22.12		
30	22.43		

$\Delta\mu^{0\neq}$ ($kJ\ mol^{-1}$) values are 17.00, 16.98, 16.97 for mixtures containing 5, 15, and 30% propionic acid.

Table 4—Values of ϕ_V^0 and S_V^* of Masson's Equation for Alkali Propionates in Propionic Acid (PA) + 1-Propanol Mixtures at 308.15 K

Wt % PA in solvent mixture	ϕ_V^0 ($cm^3\ mol^{-1}$)	S_V^* ($cm^3\ l^{1/2}\ mol^{-3/2}$)
	Lithium propionate	
5	43.6	42.1
15	55.4	41.5
30	57.8	40.0
	Sodium propionate	
5	47.2	38.6
15	56.3	36.3
30	60.0	35.0
	Potassium propionate	
5	48.8	27.6
15	58.4	26.0
30	61.8	20.7

and $\Delta\mu_2^{0\neq}$ values have been calculated from Eq. (5). The values of $\Delta\mu_1^{0\neq}$ and $\Delta\mu_2^{0\neq}$, presented in Table 3, indicate that $\Delta\mu_1^{0\neq}$ is practically constnat at all solvent compositions. This implies that $\Delta\mu_2^{0\neq}$ is dependent mainly on *B*-coefficient and $(\bar{V}_1^0 - \bar{V}_2^0)$ term. The $\Delta\mu_2^{0\neq}$ values are positive and larger than $\Delta\mu_1^{0\neq}$ values suggesting that the formation of the transition state is less favoured in the presence of these salts. This means that formation of the transition state is probably accompanied by cleavage and distortion of intermolecular bonds.

The apparent molar volumes (ϕ_V), vary linearly with $\sqrt{C}$ in confirmity with the Masson's equation[15] (6)

$$\phi_V = \phi_V^0 + S_V^*\sqrt{C} \quad \ldots (6)$$

The apparent molar volumes at infinite dilution ($\phi_V^0 = \bar{V}_2^0$) and the slope S_V^* for the electrolytes are given in Table 4.

The ϕ_V^0 values are positive and large indicating the presence of positive solute-solvent interactions. It is also observed that ϕ_V^0 is higher in solvent mixture containing higher percentage of propionic acid for any salt under investigation. This may be explaned by (i) preferential solvation of the ions[16,17] by different species present in the solvent system, and (ii) interactions between molecules of 1-propanol and propionic acid. If the reduction in solvent dipoles of one solvent (1-propanol) due to the presence of the other solvent (propionic acid) molecules in solution is greater, the lesser is the extent of solvation of the electrolyte and greater is the molar volume. This explains the increase of ϕ_V^0 with the increase in propionic acid content of the solvent mixture.

The ϕ_V^0 values follow the order (at each solvent composition): K-salt > Na-salt > Li-salt. Similar trend was reported by Desnoyers *et al.*[18] in the case of partial molar volumes of alkali metal halides in water + *t*-butanol mixtures. Smaller the size of the cation, greater is the ionic association or electrostriction and the lesser is the ϕ_V^0 value. The S_V^* values are positive but the magnitude decreases with increase in the percentage of PA. S_v^* values follow the order: Li-Salt > Na-salt > K-salt. A similar trend was reported by Chowdoji Rao[19] in the case of viscosities of alkali formates in formic acid + dimethylformamide mixtures. This order in S_V^* values is opposite to that observed in the case of simple electrolytes in aqueous alcoholic mixtures[2,3].

References

1 Feakins D, Freemantle D J & Lawrence K G, *Jchem Soc Faraday Trans I*, **70** (1974) 795.
2 Palma M & Morel J P, *J sol Chem*, **8** (1979) 767.
3 El-Hammamy N H, Hasanein A A & El-Halin F M, *J Indian chem Soc*, **61** (1984) 512.
4 Singh H N, Swarup S & Singh R P, *Indian J Chem*, **23A** (1984) 175.
5 Gill D S & Cheema J S, *Z phys Chem (Nue Folge)*, **140** (1984) 149.
6 Gill D S & Chauhan M S, *Z phys Chem (Neue Folge)*, **134** (1982) 205.
7 Franzosini P & Edgar (Jr) F W, *J chem Thermodynamics*, **16** (1984) 81.
8 Subha M C S, Chowdoji Rao K & Brahmaji Rao S, *Indain J Chem*, **25A** (1986) 424.
9 Jones G & Dole M, *J Am chem Soc*, **51** (1929) 2950.
10 Falkenhagen H & Vernon E L, *Z Phys*, **33** (1932) 140.
11 Kay R L, Vituccio T, Zawoyski C & Evans D F, *J phys Chem*, **70** (1966) 2336.
12 Yao N P & Bennion D N, *J phys Chem*, **75** (1971) 1727.
13 Blokhra R L & Parmar M L, *Z phys Chem (Neue Folge)*, **95** (1975) 310.
14 Glasstone S, Laidler K J & Eyring H, *The theory of rate processes* (McGraw Hill, New York) 1941, pp 477.
15 Masson D O, *Phil Mag*, **8** (1929) 218.
16 Bateman R L, *J Am chem Soc*, **71** (1949) 2291; **74** (1952) 5516.
17 Butler J A V & Lees A D, *Proc roy Soc (London)*, **A131** (1931) 382.
18 Desnoyers J E, Avedikia L & Perron G, *J sol Chem*, **4** (1978) 331.
19 Chowdoji Rao K, Ph.D. Thesis, SK University, Anantapur (1984).

Indian Journal of Chemistry
Vol. 28A, February 1989, pp. 111-115

Electronic Spectrum of 5,6-Dimethyl-2-aminobenzimidazole:Effect of Solvents & *p*H on Spectral Behaviour

SANJAY SRIVASTAVA & SNEH K DOGRA*
Department of Chemistry, Indian Institute of Technology, Kanpur 208 016
Received 13 *January* 1988; *accepted* 13 *April* 1988

Effect of solvents on the electronic spectrum of 5,6-dimethyl-2-aminobenzimidazole indicates that the amino group acts as a proton donor to proton acceptor and proton acceptor to proton donor solvents in S_0 state but it acts as a proton donor in the S_1 state. The absorption and fluorescence spectra indicate that DMAB and its dication appear to behave like arylamine and arylammonium ion respectively in S_0 and S_1 states. The above studies along with the infrared spectra have shown that the monocation (protonated at tertiary nitrogen) of DMAB has cyclic amidine structure in S_0 and S_1 states. The studies at different *p*H values also support the above results and the values of pK_a have been explained on the basis of relative contributions of increase in acidic and basic character of respective species.

It is now well established[1-3] that benzimidazole exists in manifold of singlet states (i.e. $\pi \rightarrow \pi^*$; charge transfer, CT). These energy levels are either degenerate or the difference between these singlet states is not large. Which of the state is of low energy depends upon the nature and position of the substituent as well as on the nature of solvents. For example, electron donating groups (e.g. $-NH_2$) on the carbocyclic ring or electron withdrawing groups[1,3] at position-2 of the imidazole ring or both favour the CT state to be of low energy. On the other the lowest energy transition of the monocation of benzimidazole, formed by protonation of the tertiary nitrogen atom, is of CT in nature. The driving force behind this transition is the presence of positive charge on the tertiary nitrogen atom. Whereas the presence of conjugated system, like phenyl group[4-9] etc, at position-2 favours the $\pi \rightarrow \pi^*$ transition, whether the benzimidazole is present as a neutral molecule or a monocation, because the charge migration from benzene ring to imidazole ring is not localised on the tertiary nitrogen atom but completely distributed on the benzene ring. In some of the methyl substituted benzimidazoles, fluorescence is observed from both the states[2,10], indicating that the difference between these two states is not large.

The molecule under investigation, 5,6-dimethyl-2-aminobenzimidazole (DMAB) contains two electron donating groups in benzene ring and one in the imidazole ring. The absorption and fluorescence spectra in different solvents will indicate the effect of two charge clouds, acting in opposite direction, on the nature of energies of the states. Effect of *pH* on the spectral characteristics has also been investigated, pK_a values for the various prototropic reactions have been determined and discussed.

Materials and Methods

DMAB (Aldrich Chemicals) was purified by recrystallization from ethanol-water mixture. Spectrograde methanol (BDH), AR grade sulphuric acid, sodium hydroxide and orthophosphoric acid were used as such. Acetonitrile (AR, E. Merck), cyclohexane (SDS) and ether (Allembic) were purified by the methods described in the literature[13]. Triply distilled water was used for the preparation of aqueous solutions. *pH* in the range of 3-11 was adjusted by adding appropriate amounts of orthophosphoric acid and sodium hydroxide, as the small amount of phosphate buffers do not quench the fluorescence of the species and do not disturb the various prototropic equilibria[14]. Modified Hammett's acidity scale[15] (H_0) for H_2SO_4-H_2O mixtures and Yagil's[16] basicity scale for NaOH-H_2O mixture were used for solutions below *p*H 1 and above *p*H 13 respectively.

Absorption spectra were recorded on a Shimadzu 190 UV spectrophotometer, equipped with 135 U chart recorder. Fluorescence spectra were recorded on a scanning spectrofluorimeter, fabircated in our laboratory[17]. The band width of the excitation radiation was 8 nm. The concentration of the solutions was of the order of $\sim 5 \times 10^{-4}$ *M*. The fluorescence spectra were corrected according to the procedure described by Parker[18] and quantum yields were calculated using quinine sulphate-0.1*N* H_2SO_4 as a standard[19]. The excitation wavelength was 285 nm. In the fluorimetric titrations, isosbestic wavelengths were used for excitation of different species. The *p*H

values in the range of 1-13 were measured on a Toshniwal *pH* meter model CL-44A.

Results and Disussion

Effect of solvents

Absorption maxima, molar extinction coefficients, fluorescence maxima and fluorescence quantum yields of DMAB in solvents of different polarities and H-bond formation tendencies are compiled in Table 1. These data could not be obtained in cyclohexane because of the insolubility of DMAB in cyclohexane. The data in Table 1 clearly indicate that (i) absorption maximum of DMAB is at longer wavelength than those of 5,6-dimethylbenzimidazole (DMBI)[2] or 2-aminobenzimidazole (2ABI)[12] in any one particular solvent. Similar to benzimidazole (BI)[20], DMBI or 2ABI, a constant blue shift is noticed with increase in proton donor capacity of solvents and absorption maximum in water nearly resembles that of DMBI[2]. Like the absorption spectra, the fluorescence spectra are characterised by a broad band at longer wavelength than those of DMBI[2] or 2ABI[12] in any one solvent and unlike absorption spectra, a constant red shift is noticed in fluorescence maxima. The fluorescence quantum yield decreases while Stoke's Shift increases with increase in proton donor capacity of the solvents.

It is well established that the long wavelength band (278 nm) arises by the localisation of charge in benzene ring whereas 240 nm band arises by charge localisation in imidazole ring of BI[20]. The 278 nm band is long axis polarised transition (^1L_b) and the 240 nm band is short axis polarised transition and both the bands belong to $\pi \rightarrow \pi^*$ transition. The data in Table 1 further support this because the two methyl groups are present in benzene moiety and amino group is present in imidazole ring, i.e. both these band systemsare perturbed by the presence of these two groups more than the effect of individual groups on the specific band system but the effect is more on the long axis polarised transition as these groups are localised along this axis. (e.g. in 2ABI, the band maxima in acetonitrile appear at 283 and 247 nm, whereas in DMBI these occur at 286 and 247 nm). The data in Table 1 further prove that the presence of electron donating amino group at position-2 decreases the energy of the first singlet state.

The absorption and fluorescence spectra are not much affected by the change in polarities and H-bond forming tendencies of the solvents. Thus it can be concluded that the emitting and absorbing state in DMAB is of $\pi \rightarrow \pi^*$ character. The spectral shift observed in the absorption and fluorescence spectra of DMAB in different solvents is consistent with the results of the individual group i.e. H-bonding with both the sites (with the lone pair of tertiary nitrogen atom and the lone pair of the amino group) leads to the blue shift in the absorption spectrum. In case of former, since the long wavelength band is localised on the benzene ring, the lone pair on the tertiary nitrogen atom can perturb this transition like the lone pair of the amino groups, but this effect will be much less than the amino group as the lone pair is perpendicular to the π cloud and the perturbation effect will be through inductive effect only. Similar effect has also been observed in phenanthro[9,10-*d*]imidazole[21]. On excitation, the charge migration takes place from benzene ring to heterocyclic ring, as well as from amino group to imidazole ring. Both will lead to red shift in fluorescence spectra indicating that amino group acts as a proton donor and tertiary nitrogen atom as a proton acceptor in proton acceptor/donor solvents. Increase in the Stokes' shift indicates that the interaction of DMAB increases with solvents and the moelcule becomes more polar in S_1 state. This is further manifested by decrease in fluorescence quantum yield in water as a solvent.

Table 1—Absorption and Fluorescence Maxima ε_{max} and Quantum Yield (ϕ_f) of DMAB in Different Solvents and at Different *p*H Values at 298K

Solvent	λ_{max}(abs) (nm)	log ε_{max}	λ_{max}(flu) (nm)	ϕ_f
Dioxane	292	4.03	314	0.10
	252	4.03		
	247	4.04		
	223	4.19		
Acetonitrile	291	4.02	315	0.12
	250	—		
	222	4.24		
Methanol	290	4.01	319	0.16
	247	sh		
	242	3.90		
	216	3.93		
Water				
*p*H = 9	287	—	320	—
	241	—		
	209	—		
Monocation				
*p*H 3	286	4.34		
	282	4.38	307	0.03
	226	4.46		
	204	5.07		
Dication				
H_0-7	286	—	343	—
	280	—		
	223	—		
	204	—		
Monoanion				
H_--14	296	—	—	—
	250	—		
	225	—		

Effect of pH

The absorption and fluorescence spectral data of various prototropic species are listed in Table 1. The long wavelength band maximum in the absorption spectrum is not affected much with decrease of *pH* ~ 7, but it becomes structured, whereas the 241 nm band system disappears and probably is blue shifted to 226 nm, appearing as a shoulder to very strong band at 204 nm. On further increase of proton concentration, H_0-7, not much change is observed in the absorption spectrum of monocation except the intensity of the 286 nm peak of long wavelength band becomes more than that of 272 nm peak. At high *pH* the absorption specrum gets red shifted as compared to the neutral molecule, and unlike the monocation and dication, all the three band systems are observed. Thus the species formed under these conditions are the monocation, dication and monoanion respectively. Under similar proton concentrations, the fluorescence spectrum of monocation (307 nm) is blue shifted as compared to that of the neutral (320 nm), and that of dication (343 nm) is largely red shifted both in comparison to those of the monocation and neutral molecule. The monoanion is found to be nonfluorescent. The various prototropic reactions occurring in the S_0 and S_1 states are listed in Scheme 1.

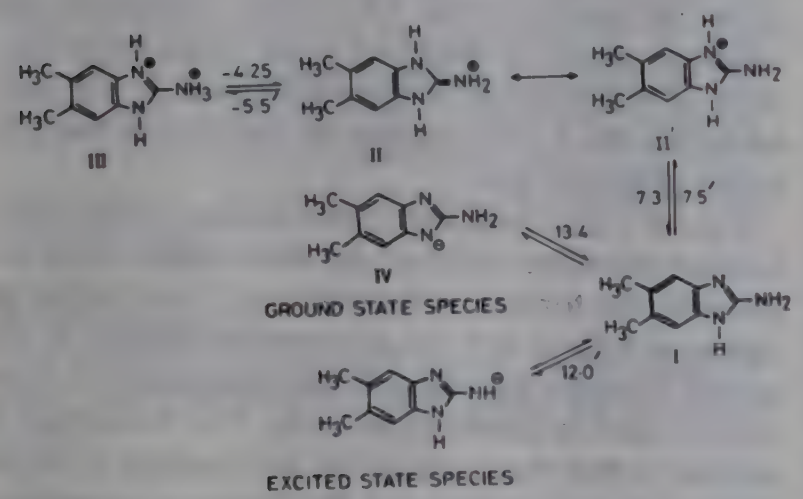

Scheme 1—Prototropic reactions taking place in S_0 and S_1 states. (Prime refers to excited state pK_a)

It is clear from Scheme 1 that DMAB(I) possesses two sites where the protonation can take place (i.e. tertiary nitrogen atom and amino group) and two sites where deprotonation can occur (i.e. imino group and amino group). It is well established that if $\pi \rightarrow \pi^*$ is the lowest singlet state, then (i) tertiary nitrogen atom becomes more basic[22], (ii) aryl amines group become less basic[7] and (iii) imino and amino groups become more acidic on excitation[22]. These changes lead to red shift, blue shift and red shift in the spectral characteristics in (i), (ii) and (iii) respectively. Data in Table 1 indicate that the long wavelength absorption band of the monocation is not affected but the fluorescence spectrum is blue shifted by 10 to 14 nm, i.e. no well-defined criterion is established. A similar behaviour is also observed in the case of 2- and 4- aminoquinolines[11], where it has been shown that the first protonation at the tertiary nitrogen atom is followed by a change in hybridisation at amino nitrogen, thus forming a cyclic amidine structure. It is proposed that similar behaviour is also observed in the case of first protonation of DMAB. These results are based on the following facts:

(i) CNDO/S calculations carried on 2-aminobenzimidazole ($BINH_2$)[23], have shown that the charge densities on imino nitrogen atom, tertiary nitrogen and amino nitrogen in the ground and excited states are 5.127, 5.362 and 5.203 and 5.134, 5.496 and 5.185 respectively. These data clearly show that tertiary nitrogen atom gets protonated first, followed by amino group. Further since the imino nitrogen gives both its electron pair to the aromatic ring, so it will not be accessible to protonation. Although no CNDO/S calculations have been carried out on DMAB, it can be assumed that the trend will be the same because the two methyl groups are symmetrically placed to long axis.

(ii) The ground state pK_a(II) value observed (see later) spectrophotometrically is higher as compared to that of 5-aminobenzimidazole, but similar to those of 2- and 4-aminoquinolines[11].

(iii) The absorption and fluorescence spectra of the hydrochloride of DMAB are relatively insensitive to the polarities of the solvents as compared to other arylammonium salts, thereby indicating that $DMABH^+Cl^-$ is less polar in S_1 state as compared to S_0 state. This can also be visualised from the structure II and II′, because structure II is more symmetrical than structure II′ (Scheme 1).

(iv) Absorption spectrum of species (II) is similar to that of 2(3*H*)-benzimidazolone[24]. The blue shift observed in the short wavelength band (241 nm) on protonation of DMAB is due to loss of aromatic character of the imidazole ring and the long wavelength transition (287 nm) which is localised on the benzene ring remains nearly unaffected because of the presence of two amino group nitrogen atoms, *ortho* to each other.

(v) The infrared spectrum of hydrochloride of $BINH_2$ is similar to that of 2-benzimidazolone[24], but different from those of other arylamines. The absorption, ~ 3450 cm^{-1} in neutral amines and their hydrochlorides has been assigned to $\bar{\nu}_{as}$ N-H (exco-

cyclic)[25]. In the IR spectrum of $DMAB^+Cl^-$ this mode appears at ~ 3260 cm^{-1}, a phenomenon which has been interpreted as characteristic of imine formation[25,26]. With further increase in proton concentration, the species present is a dication, formed by the protonation of tertiary and amino nitrogens. This has been further manifested by the fact that the spectral characteristics of DMAB dication resemble those of the monocation of 5,6-dimethylbenzimidazole, as the lone pair of the amino group is not free to perturb the BI system.

Under high basic conditions, the absorption studies have shown the formation of monoanion, whereas the fluorescence intensity of neutral DMAB is decreased without the appearance of any new band. Further, data in Table 1 have clearly shown that the structure of benzimidazole moiety is kept intact during monoanion formation. Actually monoanion can be formed by the deprotonation of either imino or amino group. The pK_a for deprotonation of >NH group in benzimidazole[20] is 13.2 and increases to some extent if electron donating group is present. On the other hand, pK_a for similar reaction of $-NH_2$ group is >16[26] and decreases little when electron withdrawing group is present. Our data indicate that in S_0 state deprotonation occurs from the >NH group, but in S_1 state the deprotonation takes place from the amino group. This is because the monoanion formed by deprotonation of $-NH_2$ is non-fluorescent with few exceptions[27] and that formed by deprotonation of >NH group is fluorescent[28]. This is further confirmed by the fluorescence spectrum of DMAB at *p*H 12 and 77K. At this low temperature only the ground state species, i.e. DMAB monoanion (IV) can exist, as confirmed by its fluorescent spectrum. This is further manifested by the CNDO/S charge density calculations. As mentioned earlier, it is clear that the charge density in the ground state is more at $-NH_2$ nitrogen atom than that at >NH nitrogen. But on excitation to S_1 state, the charge density increases at the latter and decreases at the former group. Similar behaviour has also been observed in case of 5-[22], 6-[29] and 7-amino-indazoles[30], 2-(2′-aminophenyl)[7]-, 2-(3′-aminophenyl)[5]-and 2-(4′-aminophenyl)-benzimidazoles[6]. Thus it is clear and in agreement with the earlier results that the amino group becomes more acidic on excitation and relative increase in the acidity of amino group is more than that of imino group upon excitation.

Acidity constants

The pK_a values in the S_0 state for various prototropic reactions have been determined spectrophotometrically and the values are listed in Table 2. pK_a (II) is higher than the similar prototropic reaction with the tertiary amine (5.4 for BI) or with the amino group (~ 4-5). The reasons have already been discussed earlier. pK_a (III) is slightly higher than that of benzimidazole, due to the presence of amino group in the imidazole ring and two methyl groups in the benzene ring.

Table 2—pK_a and pK^*_a Values for Various Prototropic Equilibria of DMAB

Equilibrium	pK_a	pK^*_a
Dication-Monocation (I)	−4.25	−5.5
Monocation-Neutral (II)	7.3	b
Neutral-Monoanion (III)	13.4	12.0

b = Ground state pK_a is obtained from fluorimetric titrations

Förster cycle method[31] cannot be used to calculate the respective pK_a values in the S_1 state, since the structure of the molecule is changed in the equilibria dication-monocation and monocation-neutral, whereas in case of neutral-monoanion, equilibrium reactions involved in the S_0 and S_1 states are different. pK_a values in S_1 state have been calculated using fluorimetric titration method as shown in Fig. 1. All pK_a values have been compiled in Table 2. Figure 1 clearly shows that the $-NH_2$ group becomes stronger acid on excitation and relative increase in the acidity of $-NH_2$ group is more than that of the >NH group. Fluorimetric titrations carried out in the case of monocation-neutral equilibrium have given the ground state pK_a value, indicating that either no change is observed in the dissociation constant of monocation or the equilibrium is not established in the S_1 state during the lifetimes of the conjugate acid-base pair.

Figure 1 also indicates that decrease in the fluorescence intensity curve of the monocation does not intersect the formation fluorescence curve of the dication at $I/I_0 = 0.5$, i.e. no correspondence is observed between the removal and formation of monocation and dication respectively. This behaviour is similar to that observed for the protonation of arylamines (i.e. proton-induced fluorescence quenching is observed for neutral arylamine prior to protonation). This confirms our earlier conclusion that dication has a benzimidazole structure rather than a cyclic amidine one. So the pK_a (I) value in S_1 is calculated from the formation curve of dication, rather than from the decrease in the fluorescence intensity of monocation. It is found to be −5.5, which is less than the ground state value. Although this behaviour is similar to that observed for normal arylamine, i.e. arylammonium ion is stronger acid in S_1 state as compared to S_0, but the decrease in pK_a is

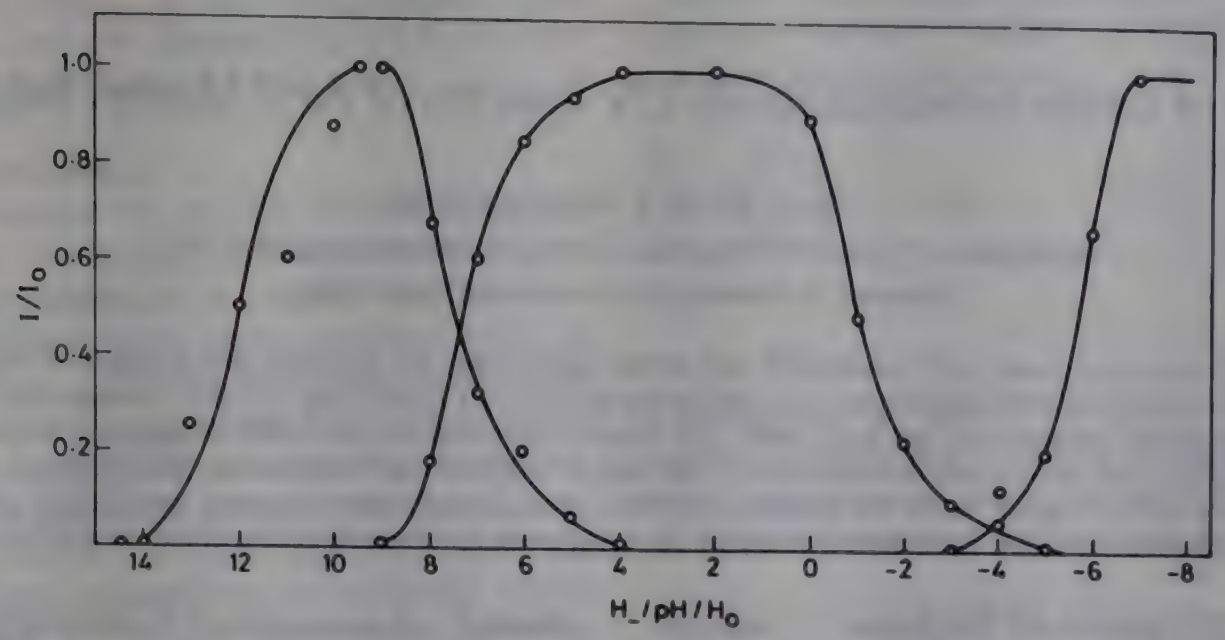

Fig. 1—Plot of I/I_0 vs $H_0/pH/H_-$.

very small. This can be explained as follows. It is well known that arylammonium ions are stronger acids, as said earlier, in S_1 states, whereas ketones[32] and carboxylic acids[33] become stronger bases upon excitation. If it is assumed that the monocation derived from DMAB is isosteric with the monocations derived from ketones or carboxylic acids, it is possible that the monocation becomes stronger base in the excited singlet state. Now the gain in basicity of monocation of DMAB upon excitation could be greater than, equal to or less than the gain in the acidity of the doubly protonated cation upon excitation. The data in Table 2 indicate that the gain in the acidity of arylammonium ion is more than the gain in the basicity of cyclic amidine and thus the net effect is small. A similar trend is also observed in the case of 2- and 4-amino-quinolines[11] and 2(3*H*)-benzimidazolone[24], where the former effect clearly over weighs the latter.

Acknowledgement

The authors are thankful to the Department of Science and Technology, New Delhi for financial support.

References

1 Tway P C & Clinelove L J, *J phys Chem*, **86** (1982) 5223, 5227.
2 Krishnamurthy M, Phaniraj P & Dogra S K, *J chem Soc Perkin Trans*, **2** (1986) 1917.
3 Sinha H K & Dogra S K, *J chem Soc Perkin Trans*, **2** (1987) 1465.
4 Mishra A K & Dogra S K, *Spectrochim Acta*, **39A** (1983) 609.
5 Mishra A K & Dogra S K, *Indian J Phys*, **58B** (1984) 480; *Indian J Chem*, **24A** (1985) 364.
6 Mishra A K & Dogra S K, *Bull chem Soc Jpn*, **58** (1985) 3587.
7 Mishra A K & Dogra S K, *J Photochem*, **31** (1985) 333.
8 Sinha H K & Dogra S K, *Chem Phys*, **103** (1986) 325.
9 Sinha H K & Dogra S K, *J Photochem*, **36** (1987) 149.
10 Kondo M & Kuwano H, *Bull chem Soc Jpn*, **42** (1969) 1433.
11 Kovi P J, Capomacchia A C & Schulman S G, *Analyt Chem*, **44** (1972) 1611.
12 Mishra A K & Dogra S K, *Indian J Chem*, **24A** (1985) 815.
13 Riddick J A & Bunger W B, *Organic solvents* (Wiley Interscience, New York) 1970, 592, 644, 695.
14 Mishra A K, Swaminathan M & Dogra S K, *J Photochem*, **26** (1984) 49.
15 Jorgenson M J & Hartter D R, *J Am chem Soc*, **85** (1963) 878.
16 Yagil G, *J phys Chem*, **71** (1967) 1034.
17 Swaminathan M & Dogra S K, *Indian J Chem*, **22A** (1983) 853.
18 Parker C A, *Photoluminescence of solutions with applications to photochemistry and analytical chemistry* (Elsevier, Amsterdam) 1968, 261.
19 Guilbault G G, *Practical fluorescence* (Marcel Dekker, New York) 1971, 13.
20 Preston P N, *Benzimidazoles and congeneric tricyclic compounds*, Part I (Wiley, New York) 1981, 64.
21 Swaminathan M & Dogra S K, *J chem Soc Perkin Trans*, **2** (1983) 1641.
22 Swaminathan M & Dogra S K, *J Am chem Soc*, **105** (1983) 6223.
23 Mishra H P, M Phil Theses, Department of Chemistry, Sambalpur University, Jyoti Vihar, 1986.
24 Mishra A K & Dogra S K, *J Photochem*, **29** (1985) 435.
25 Mason S F, *J chem Soc*, (1959) 1281.
26a Angyal F A & Werner R, *J chem Soc*, (1952) 2911.
b Ireland J F & Wyatt J A H, *Adv phys-org Chem*, **12** (1976).
27 Förster Th, *Z Elektrochem*, **54** (1950) 531.
28 Swaminathan M & Dogra S K, *Indian J Chem*, **22A** (1983) 278, 407; *J Photochem*, **21** (1983) 245.
29 Mishra A K & Dogra S K, *Indian J Chem*, **24A** (1985) 285.
30 Phaniraj P, Mishra A K & Dogra S K, *Indian J Chem*, **24A** (1985) 913.
31 Förster Th, *Z Elektrochem*, **54** (1950) 577.
32 Ireland J F & Wyatt J A H, *Adv phys-org Chem*, **12** (1976) 185.
33 Manoharan R & Dogra S K, *Spectrochim Acta*, **43A** (1987) 91.

Indian Journal of Chemistry
Vol. 28A, February 1989, pp. 116-119

Influence of *Ortho* Substituents on UV Spectra of Aryl Methyl Sulphoxides

V BALIAH*[+] & R VARADACHARI
Department of Chemistry, Annamalai University, Annamalainagar 608 002

Received 24 *February* 1988; *accepted* 27 *April* 1988

The UV spectra of some *ortho* substituted aryl methyl sulphoxides are recorded and analysed. A comparison of the steric effects of *ortho* substituents on conjugation of CH_3S-, CH_3SO- and CH_3SO_2- groups with the *para* substituents in the benzene ring has been made. The *ortho* substituents do not inhibit conjugation in the case of sulphones while they cause a marked inhibition in the case of sulphides and sulphoxides. The inhibition of conjugation of the CH_3SO- group under the influence of *ortho* substituents is observed when the CH_3SO- group acts both as an electron donor and as an electron acceptor. An explanation is offered for the observed steric effects.

Though the UV spectra of sulphides[1-5] and sulphones[6-12] have been extensively studied, available spectral data on sulphoxides[13-17] are not much. The sulphoxide group can be compared with either the sulphonyl or the sulphide group. Price and Hydock[13] as well as Bordwell and Boutan[14] found that methyl phenyl sulphoxide behaves more like methyl phenyl sulphide, the sulphinyl group entering into electron-donor type of conjugation. The possibility of the sulphoxide group, when present *para* to a hydroxyl group, entering into electron-acceptor type of conjugation, was also suggested by Bordwell and Boutan[14]. The main objective of the present study is to know whether bulky *ortho* substituents inhibit the conjugation of the CH_3SO- group with benzene nucleus.

Materials and Methods

UV spectra were recorded in purified ethanol (95%), cyclohexane and dioxane on a Beckmann spectrophotometer, model DU.

Methyl 2,6-dimethyl-4-nitrophenyl sulphoxide was prepared by the H_2O_2 oxidation of methyl 2,6-dimethyl-4-nitrophenyl sulphide[19]. It was recrystallised from methanol, m.p. 165-66° (Found: C, 50.4; H, 5.1. $C_9H_{11}O_3NS$ requires C, 50.7; H, 5.2%).

Methyl 4-amino-2,6-dimethylphenyl sulphide was prepared by the Sn(IV)/HCl reduction of methyl 2,6-dimethyl-4-nitrophenyl sulphide under H_2S atmosphere. The desired compound, which separated out as an oil, solidified after keeping for two days in the refrigerator. It was crystallised from methanol, m.p. 68-69° (Found: C, 64.5; H, 7.9. $C_9H_{13}NS$ requires C, 64.6; H, 7.8%).

Methyl 4-acetamido-2,6-dimethylphenyl sulphide was prepared by the acetylation (acetyl chloride/pyridine; 1 hr) of the corresponding amino derivative. It was recrystallised from ethanol-water, m.p. 149-50° (Found: C, 63.0; H, 7.0. $C_{11}H_{15}ONS$ requires C, 63.2; H, 7.2%).

Methyl 4-acetamido-2,6-dimethylphenyl sulphoxide was prepared by the H_2O_2 oxidation of the above sulphide and recrystallised from benzene, m.p. 69-70° (Found: C, 58.4; H, 6.7. $C_{11}H_{15}O_2NS$ requires C, 58.7; H, 6.7%).

Methyl 2,6-dibromo-4-nitrophenyl sulphide was prepared as follows: A solution of 2,6-dibromo-4-nitroaniline (23.4 g) in hot glacial acetic acid (270 ml) was rapidly cooled to room temperature and gradually added to a solution of sodium nitrite (5.5g) in conc. sulphuric acid (40 ml), keeping the temperature at 20°. The temperature was raised to 70° until the nitrite dissolved, the solution cooled to room temperature, filtered and added to a paste of cuprous cyanate (21.6g) and potassium thiocyanate (10g). The mixture was stirred for 6 hr and heated on a water-bath for 30 min. After cooling, it was diluted with water, the separated solid filtered off (7g), treated with a solution of potassium hydroxide (7g) in water (15 ml) and dimethyl sulphate (18g) and refluxed for 1 hr. The excess of dimethyl sulphate was destroyed by adding aq. sodium hydroxide and the mixture poured into water. An oil separated, which solidified after cooling in ice; yield 5.5g. It was crystallised from ethanol, m.p. 85-86° (Found: C, 25.9; H, 1.6. $C_7H_5O_2NSBr_2$ requires C, 25.7; H, 1.5%).

Methyl 2,6-dibromo-4-nitrophenyl sulphoxide was prepared by the H_2O_2 oxidation of the above sulphide and crystallised from methanol, m.p. 128-29° (Found: C, 24.7; H, 1.4. $C_7H_5O_3NSBr_2$ requires C, 24.5; H, 1.5%).

[+] Present address: 79, 3rd Cross Road, Venkatanagar, Pondicherry 605 011

Methyl 2,6-dibromo-4-nitrophenyl sulphone was prepared by oxidising the above sulphoxide with excess of H_2O_2. It was recrystallised from ethanol, m.p. 118-19° (Found: C, 23.7; H, 1.6. $C_7H_5O_4NSBr_2$ requires C, 23.4; H 1.4%).

Results and Discussion

The UV spectra of methyl phenyl, methyl *o*-tolyl, methyl *o*-*t*-butylphenyl and methyl 2,6-dimethylphenylsulphones in ethanol exhibit maximum absorptions (only most intense band is given) at 217 (ε_{max}, 7100), 219(7200), 222(7200) and 219 nm(7400), respectively. The data indicate that no steric inhibition of resonance is observable with the sulphonyl group. Even in a compound like methyl 2,6-dimethylphenyl sulphone, the *ortho* methyl groups do not sterically inhibit the conjugation of the sulphonyl group with the benzene nucleus. Structure I chiefly

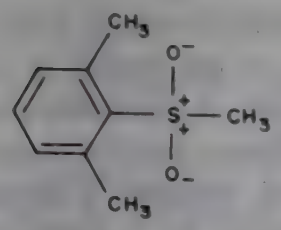

I

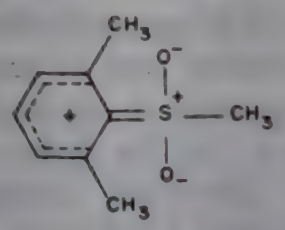

II

contributes to the ground state of the molecule. The four valence bonds of sulphur in I result from $3s3p^3$, i.e. from sp^3 hybridisation and they may be taken as essentially tetrahedral. Structure II makes a contribution to the excited state. The four σ-bonds of sulphur in II are still tetrahedral. The electron that moves from the benzene ring to the sulphur atom goes into one of the vacant *d*-orbitals of sulphur and the double bond is formed by the overlapping of 2*p*-orbital of carbon with the 3*d*-orbital of sulphur, i.e. it is a $p\pi$-$d\pi$ bond. In that case planarity of the atoms of the sulphonyl group with the benzene ring is not necessary for conjugation. So there is no steric inhibition of resonance in the exicited state of methyl 2,6-dimethylphenyl sulphone.

When we consider steric inhibition of resonance in sulphoxides, we will have to examine two different cases: (i) when the sulphoxide group behaves as an electron donor and (ii) when it behaves as an electron acceptor. Methyl *p*-nitrophenyl sulphoxide (III) is an example of the former type. If there is to be effective conjugation between the CH_3SO- and $-NO_2$ groups (as in structure IV) the atoms C, S and O of the CH_3SO- group should be in the plane of the benzene ring. So bulky substituents *ortho* to the CH_3SO- group are expected to cause steric inhibition of resonance.

Methyl *p*-acetamidophenyl sulphoxide (V) provides an example in which the sulphoxide group acts as an electron acceptor.

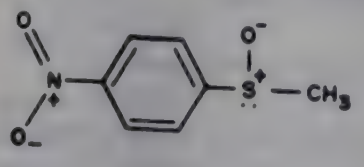

III

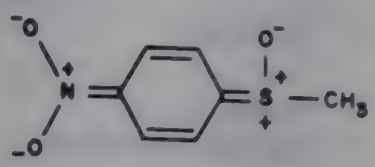

IV

If in structure VI one of the vacant 3*d*-orbitals of sulphur is filled and is used in π-bond formation, bulky substituents *ortho* to the CH_3SO- group should not inhibit conjugation.

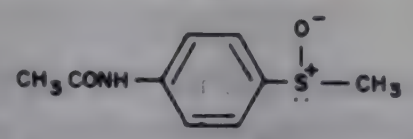

V

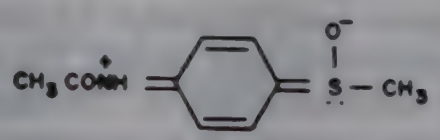

VI

With a view to testing the above predictions, several sulphoxides with the requisite substituents were prepared and their spectra were recorded. The data are given in Table 1. When the -SO- group is electron releasing, its conjugation is inhibited by bulky *ortho* substituents. In order to see clearly the steric influence on the specra, it is necessary to know first the electronic origin of the various bands observed. Comparing the spectra of methyl phenyl sulphoxide and methyl *p*-nitrophenyl sulphoxide, it is seen that the 296 nm band arises from conjugation between -SO- and $-NO_2$ groups. The band at 244 nm is due to the $-C_6H_4.NO_2$ partial chromophore (for nitrobenzene in cyclohexane[18]; λ_{max} 253 nm; ε_{max} 9,900). By the same consideration the 311 nm band of methyl 2,6-dimethyl-4-nitrophenyl sulphoxide must be due to conjugation between -SO- and $-NO_2$ groups through the benzene nucleus and the 256 nm band must be due to 2,6-dimethyl-4-nitrophenyl chromophore. This view gains support from an examination of the spectrum of 3,5-dimethylnitrobenzene in cyclohexane (λ_{max} 264 nm; ε_{max} 7,700).

The 319 nm band of methyl 2,6-dibromo-4-nitrophenyl sulphoxide is weaker than the 296 nm band of methyl 4-nitrophenyl sulphoxide. It is

Table 1 — UV Spectra of Sulphoxides

[Spectra in cyclohexane for Nos.1-4 and in dioxane for Nos.5 and 6]

No.	Sulphoxide	λ_{max} (nm)	ε_{max}
1.	Methyl phenyl	253	4,000
2.	Methyl *p*-nitrophenyl	296	5,600
		244	8,700
3.	Methyl 2,6-dimethyl-4-nitrophenyl	311	2,200
		256	9,600
4.	Methyl 2,6-dibromo-4-nitrophenyl	319	2,800
		261	6,400
5.	Methyl 4-acetamidophenyl	263	18,500
6.	Methyl 2,6-dimethyl-4-acetamidophenyl	256	12,600
		275(sh)	11,000

the conjugation band, and the 261 nm band must be due to 2,6-dibromo-4-nitrophenyl group (for 3,5-dibromonitrobenzene in cyclohexane: λ_{max} 260 nm; ε_{max} 6300). Thus we observe weakening of the conjugation band in methyl 2,6-dimethyl-4-nitrophenyl sulphoxide and methyl 2,6-dibromo-4-nitrophenyl sulphoxide due to the steric influence of the *ortho* groups. It is important to note that the ε_{max} of the bands has considerably decreased, though there is some bathochromic shift of the absorption maxima. A considerable decrease in ε_{max} is the true index of steric inhibition of resonance. The UV spectra (not given) clearly reveal the steric influence. Hence there seems to be no doubt that the sulphinyl-aryl conjugation undergoes steric inhibition. In this respect the sulphoxide function is comparable to the sulphide function. The UV spectral data of sulphides in cyclohexane support this view: Methyl phenyl, methyl *p*-nitrophenyl, methyl 2,6-dimethyl and methyl 2,6-dibromo-4-nitrophenyl sulphides exhibit UV λ_{max} (ε_{max} values in parentheses) at 255 (6900); 326 (16000); 320 (4700), 265 (8000); and 340 (2800), 268 nm (7400) respectively.

The influence of substituents *ortho* to the sulphoxide group, when they are electron attracting, may be seen by comparing the spectra of methyl 4-acetamidophenyl sulphoxide and methyl 4-acetamido-2,6-dimethylphenyl sulphoxide. The former exhibits λ_{max} at 263 nm (ε_{max}, 18500). Relative to the spectra of methyl phenyl sulphoxide (λ_{max} 249 nm; ε_{max} 3500 in dioxane) and acetanilide (λ_{max} 242 nm; ε_{max} 14400), there is a bathochromic shift of absorption maximum and a considerable increase in ε_{max}. This is to be expected if there is conjugation between CH_3CONH- and $-SOCH_3$ groups through benzene nucleus. The two methyl groups in methyl 4-acetamido-2,6-dimethylphenyl sulphoxide have very much affected the 263 nm band, the ε_{max} being significantly reduced (which is the criterion for steric inhibition of resonance); only a shoulder appears at 275 nm (ε_{max} 11,000). There is an absorption maximum at 256 nm (ε_{max} 12,600) which is presumably due to the partial 4-acetamido-2,6-dimethylphenyl chromophore. Such a view gets support from the spectrum of 3,5-dimethylacetanilide (λ_{max} 248 nm; ε_{max} 13,200 in dioxane). The behaviour of 4-acetamido-2,6-dimethylphenyl sulphoxide is in contrast to that of methyl 4-acetamido-2,6-dimethylphenyl sulphone (λ_{max} 263 nm; ε_{max} 24,000 in dioxane) in which no steric inhibition of conjugation is observable.

The lack of steric effect in sulphones was explained[11] as due to *d*-orbital π-bonding which does not demand coplanarity of the atoms. The fact that there is steric effect in sulphoxides (when the -SO- group is electron withdrawing) indicates a different type of geometry of the bonds in these compounds in the excited state. A plausible explanation can be given as follows: Let us suppose that electronic excitation of methyl 4-acetamidophenyl sulphoxide (V) leads to a significsant contribution of structure VI to the excited state. In V, $3p^3$ electrons of sulphur are involved in bond formation, the bonds being pyramidal. In VI, if the excited electron occupies 4*s*-orbital and not the 3*d*-orbital of sulphur, there will be four valence electrons available for bond formation. These are $3p^34s$ electrons. Of these one *p* electron will be involved in π-bond formation with the carbon atom of the benzene ring. The remaining three electrons ($3p^24s$) hybridize to give three equivalent sp^2 hybridized orbitals for the formation of σ-bonds; sp^2 hybridization leads to planarity of the atoms and they cannot be coplanar with the benzene ring having two *ortho* methyl groups. Thus the observed steric effect of the *ortho* methyl groups becomes understandable.

Why should the excited electron enter the 3*d*-orbital in the case of sulphones and 4*s*-orbital in the case of sulphoxides? This question can be answered if we take into account the valence electrons in sulphones. As in the previous examples, we can consider the structures of sulphones VII and VIII. In VII the valence electrons of sulphur

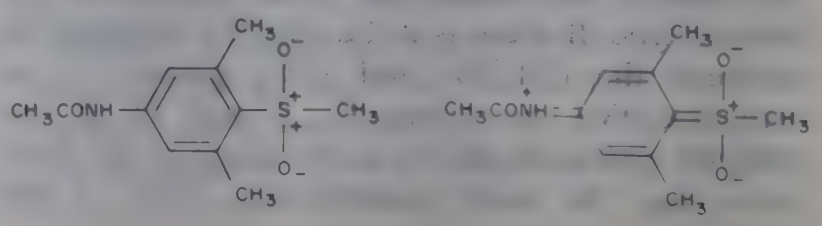

VII VIII

which are involved in bond formation are $3s3p_x3p_y3p_z$. They are hybridized to give four equivalent orbitals. The bonds are therefore tetrahedral. In VIII if the excited electron enters the $4s$-orbital of sulphur, the electrons available for bond formation are $3s3p_x3p_y3p_z4s$. Of these one of the p-electrons must be used for π-bond formation. The electrons left for the four σ-bonds are $3s3p^24s$. This means s^2p^2 hybridization which is not possible for bond arrangement[20]. Hence in the case of sulphones, the excited electron enters the $3d$-orbital and this itself may be involved in π-bond formation. The σ-bonds still retain their tetrahedral character and no planarity of the atoms is required for conjugation with the benzene ring.

References

1 Fehnel E A & Carmack M, *J Am chem Soc*, **71** (1949) 84, 2891.

2 Koch H P, *J chem Soc*, (1949) 387.

3 Mangini A & Passerini R, *J chem Soc*, (1952) 1168.

4 Leandri G, Mangini A & Passernini R, *Gazz chim ital*, **84** (1954) 3.

5 Mangini A, Passerini R & Serra S, *Gazz chim ital*, **84** (1954) 47.

6 Fehnel A & Carmack M, *J Am chem Soc*, **71** (1949) 231.

7 Koch H P, *J chem Soc*, (1949) 408.

8 Leandri G, Mangini A & Passerini R, *Gazz chim ital*, **84** (1954) 73.

9 Baliah V & Shanmuganathan Sp, *J Indian Chem Soc*, **35** (1958) 31.

10 Baliah V & Ramakrishnan V, *J Indian chem Soc*, **35** (1958) 151.

11 Baliah V & Rangarajan T, *J Indian chem Soc*, **38** (1961) 33.

12 Fehnel E A & Carmack M, *J Am chem Soc*, **72** (1950) 1292.

13 Price C C & Hydock J J, *J Am chem Soc*, **74** (1952) 1943.

14 Bordwell G & Boutan P J, *J Am chem Soc*, **79** (1957) 717.

15 Koch H P, *J chem Soc*, (1950) 2892.

16 Szmant H H & McIntosh J J, *J Am chem Soc*, **73** (1951) 4356.

17 Leandri G, Mangini A & Passerini R, *J chem Soc*, (1957) 1386.

18 Bayliss N S & McRae E G, *J phys Chem*, **58** (1954) 1006.

19 Bolsens J, Brouwers J A C Th, Choufoer J H, Kats A, Verkade P E & Wepster B M *Rec trav chim*, **73** (1954) 819.

20 Eyring H, Walter J E & Kimbal G E, *Quantum chemistry* (John Wiley, New York) 1954, 231.

Indian Journal of Chemistry
Vol. 28A, February 1989, pp. 120-123

Kinetics of Chlorination of Aniline by Dichloramine-T in Aqueous Acetic Acid Medium

B THIMME GOWDA* & B S SHERIGARA

Department of Post-Graduate Studies and Research in Chemistry, Mangalore University, Mangalagangothri, Mangalore 574 199

Received 18 *September* 1987; *revised* 26 *February* 1988; *accepted* 21 *March* 1988

Chlorination of aniline by dichloramine-T in 1:1 aqueous acetic acid medium, in the presence and absence of acetate ions is first order in [oxidant], nearly first order in [aniline], inverse fractional order in $[H^+]$ and fractional order in added [acetate ion] at constant ionic strength. Effects of added reaction products and variations in ionic strength and solvent composition of the reaction medium have also been investigated. Mechanisms consistent with the observed results are discussed and the related rate laws deduced.

The present investigation is a part of our mechanistic studies with positive halogens in general and N,N-dihalosulphonamides in particular[1-4]. We report herein the kinetics of chlorination of aniline by N,N-dichloro-*p*-toluenesulphonamide (dichloramine-T, DCT) in 1:1 (v/v) water-acetic acid medium under varying conditions.

Materials and Methods

N,N-Dichloro-*p*-toluenesulphonamide (dichloramine-T or DCT) was prepared in the laboratory and its purity checked by elemental analyses, spectral data (IR and PMR) and iodometric estimation of active halogen present in it. Stock solution (~0.1 mol dm^{-3}) of DCT was prepared in purified dry acetic acid and standardised by iodometric method.

Aniline was redistilled before use. All other reagents used were of AR grade. The ionic strength of the medium was kept at 0.2 or 0.4 mol dm^{-3} by adding concentrated aqueous solution of sodium acetate or sodium perchlorate.

Kinetic measurements

The kinetic studies were carried out in 50% (v/v) aqueous acetic acid under pseudo-first order conditions ([aniline] > > [CAT]; 5-10 times). The reactions were initiated by quick addition of a measured quantity of DCT solution in acetic acid, thermally equilibrated at a desired temperature, to a mixture containing known amounts of aniline, sodium acetate (and sodium perchlorate), $HClO_4$, acetic acid and water [to maintain 50% (v/v) solvent composition], pre-equilibrated at the same temperature. The progress of the reaction was monitored for nearly two half-lives by iodometric method. The pseudo-first order rate constants computed by the method of least squares were reproducible within ±4%.

Stoichiometry

The stoichiometry of DCT-aniline reaction was determined by equilibrating (at 303 K) reaction mixtures containing slight excess of DCT and different $[HClO_4]$ in solvent mixtures of different compositions, both in the presence and absence of sodium acetate. Analysis of reaction mixtures showed that two moles of aniline reacted with one mole of DCT in accordance with Eq. (1).

$$2C_6H_5NH_2 + RNCl_2 \rightarrow 2C_6H_4ClNH_2 + RNH_2 \quad \ldots (1)$$

where $R = CH_3C_6H_4SO_2$.

Results

Plots of log [DCT] versus time were linear for two half-lives (Fig. 1). Pseudo-first order rate constants (k_{obs}) remained unaffected by changes in $[DCT]_0$, both in the presence and absence of NaOAc (Table 1), establishing first order dependence in $[DCT]_0$. Rate increased with increase in [aniline] with almost first order dependence in [aniline] both in the presence and absence of NaOAc. Plot of k_{obs} versus [aniline] was linear without any intercept. Variation in $[H^+]$ by adding $HClO_4$ decreased the rate of oxidation both in the presence of NaOAc and in the absence (twenty-fold variation in $HClO_4$ changed *p*H by 0.5 unit only) (Table 2). Plot of log k_{obs} versus log $[H^+]$ showed inverse fractional order dependence in $[H^+]$ both in the absence and presence of NaOAc. Increase in ionic strength of the medium by adding $NaClO_4$ solution had negligible effect. Further the rate increased with increase in [NaOAc] at constant ionic strength. Plot of k_{obs} versus [NaOAc] was linear with a finite intercept, indicating participation of acetate ion in the reaction (Fig. 2). Addition of the reaction product, *p*-toluenesulphonamide had no ef-

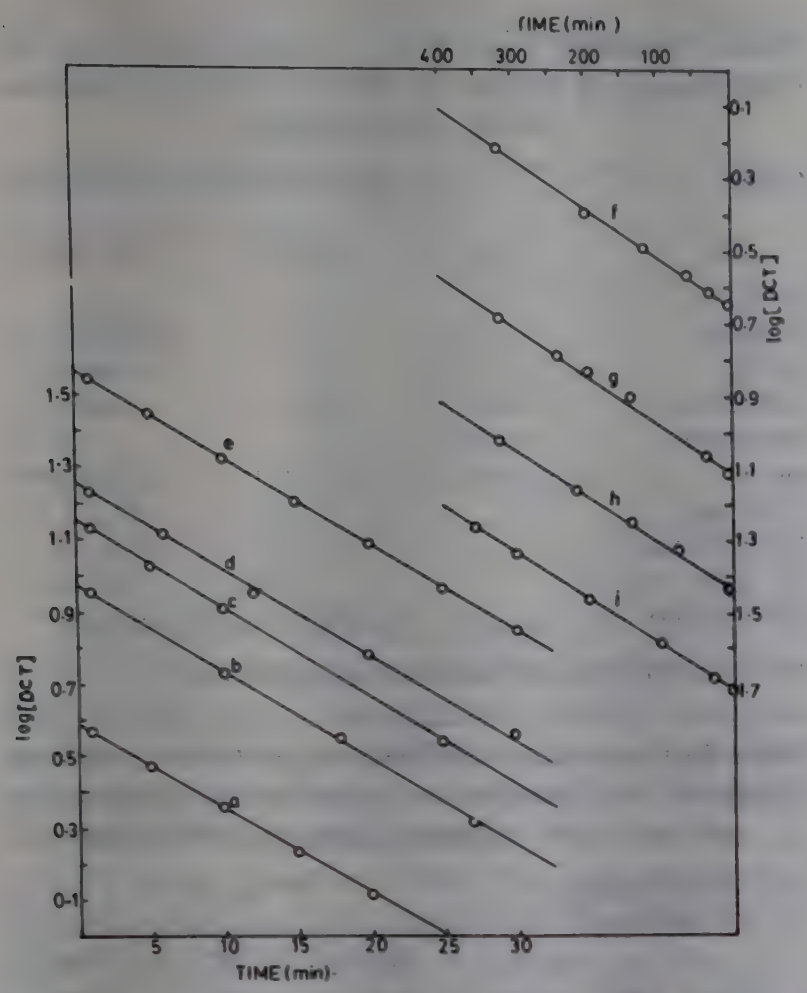

Fig. 1—Plot of log[DCT] versus time ($10^3[S]_0 = 5.0$ mol dm^{-3}, medium: 1:1 (v/v) water-acetic acid temp: 303 K. $10^4[DCT]_0$ (mol dm^{-3}) = (a) 2.0, (b) 5.0 (c) 7.5, (d) 10.0 and (e) 20 at $\mu = 0.2$ mol dm^{-3} (NaOAc) and (f) 2.0, (g) 5.0, (h) 10.0 and (i) 20 at $\mu = 0.4$ mol dm^{-3} ($NaClO_4$))

Table 1—Effect of Varying $[DCT]_0$, $[Aniline]_0$, Ionic Strength, Solvent Composition, and Addition of Reaction Product on Rate of Chlorination of Aniline by Dichloramine-T (DCT) in 1:1 (v/v) Aqueous Acetic Acid at 303 K

$10^4[DCT]_0$ (mol dm^{-3})	$10^3[Aniline]_0$ (mol dm^{-3})	$10^4 k_{obs}$ (s^{-1}) at μ (mol dm^{-3})	
		0.4 ($NaClO_4$)	0.2 (NaOAc)
2.0	5.0	0.55	9.1
5.0	5.0	0.52	9.1
10.0	5.0	0.48	8.9
5.0	1.0	—	1.9
5.0	2.0	0.25	3.8 (1.8[b], 5.6[c])
5.0	3.0	—	5.6
5.0	5.0	0.52	9.1 (4.8[b], 15.0[c])
5.0	7.0	0.78	13.9 (7.4[b], 21.3[c])
5.0	10.0	1.10	19.5
5.0	5.0	0.60[a1]	25.6[d1]
5.0	5.0	0.52[a2]	15.6[d2]
5.0	5.0	0.49[a3]	6.0[d3]
5.0	5.0	—	8.9[c1]
5.0	5.0	—	8.6[c2]
5.0	5.0	—	8.5[c3]

[a] μ (mol dm^{-3}) = (1) 0.2, (2) 0.4, (3) 0.5
[b,c] Values at 293 and 313 K respectively
[d] HOAc (%, v/v) = (1) 30, (2) 40, (3) 60.
[e] In the presence of PTS, $10^3[PTS]$ (mol dm^{-3}) = (1) 2.0, (2) 5.0, (3) 10.0

Table 2—Effect of Variation in $[H^+]$ (by the Addition of $HClO_4$) or [NaOAc] on Rate of Chlorination of Aniline by Dichloramine-T in 1:1 (v/v) Water-Acetic Acid Medium at 303 K

($10^4[DCT]_0 = 10^3[Aniline]_0 = 5.0$ mol dm^{-3})

$[HClO_4]$ (mol dm^{-3})	*p*H at μ (mol dm^{-3})		$10^4 k_{obs}$ at μ (mol dm^{-3})	
	0.4 ($NaClO_4$)	0.2 (NaOAc[a])	0.4 ($NaClO_4$)	0.2 (NaOAc[a])
0.0	1.14	2.71	0.52	9.1
0.005	—	2.67	—	8.4
0.01	0.99	2.60	0.40	8.2
0.02	0.70	2.52	0.31	6.8
0.05	0.49	2.42	0.29	5.9
0.10	—	2.18	—	4.4
10[NaOAc]				
0.5	1.86	2.05	0.16	3.9
1.0	2.14	2.40	0.30	6.4
2.0	2.50	2.71	0.66	9.1
3.0	2.74	2.84	0.95	13.6

[a]While varying $[HClO_4]$

fect on the rate. But the increase in HOAc content of the solvent medium decreased the rate (Table 1). Activation parameters were calculated by studying the reaction at 293, 303 and 313 K (Table 3).

Discussion

Mechanism of chlorination

The probable reactive oxidant species in aqueous acetic acid medium are $RNCl_2$, $(RNCl_2H)^+$ and

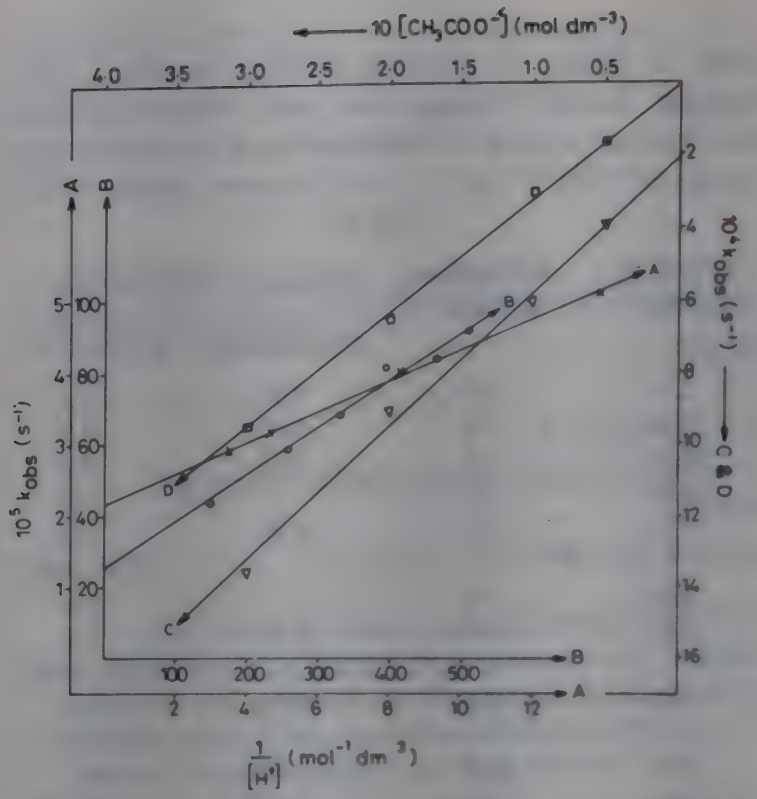

Fig. 2—(i) Plot of k_{obs} versus $1/[H^+]$ at varying $[HClO_4]$ ($10^4[DCT]_0 = 10^3[S]_0 = 5.0$ mol dm^{-3}, medium: 1:1 (v/v) water-acetic acid, temp: 303 K (A) $\mu = 0.4$ mol dm^{-3} with $NaClO_4$, (B) $\mu = 0.2$ mol dm^{-3} with NaOAc)

(ii) Plot of k_{obs} versus $[CH_3COO^-]$ ($10^4[DCT]_0 = 10^3[S]_0 = 5.0$ mol dm^{-3}, medium 1:1 (v/v) water-acetic acid, temp.: 303 K. (C) in the absence of $NaClO_4$ and (D) $\mu = 0.4$ mol dm^{-3} with $NaClO_4$)

CH_3COOCl. First order dependence in [DCT], nearly first order dependence in [aniline], fractional order in [acetate] and inverse fractional order dependence in $[H^+]$ may be explained by a two-pathway mechanism, one via the formation of acyl hypochlorite intermediate (Eq. 2) and the other through the direct pathway (Eq. 3). This is supported by the fact that the plots of k_{obs} versus [acetate], and k_{obs} versus $1/[H^+]$ are linear with finite intercepts (Fig. 2) and the corresponding reciprocal plots are nonlinear (figure not shown), attaining the limiting values. Increase in rate with increase in [acetate] at constant ionic strength also indicates participation of CH_3COO^- in the reaction.

$$RNCl_2 + CH_3COO^- + S \xrightarrow{k_1} \text{Products} \qquad \ldots (2)$$

and

$$RNCl_2 + S \xrightarrow{k_2} \text{Products} \qquad \ldots (3)$$

(S refers to substrate)
Related rate laws are given by Eqs (4) and (5).

$$-\frac{d[DCT]}{dt} = k_1[DCT][S][CH_3COO^-] + k_2[DCT][S] \qquad \ldots (4)$$

Table 3—Kinetic Data and Activation Parameters for Chlorination of Aniline by DCT in 1:1 (v/v) Aqueous Acetic Acid Medium

Order	Order of reaction at constant μ	
	$NaClO_4$	NaOAc
[DCT]	1.0	1.0
[Aniline]	0.9	1.0
$[H^+]_{eff}$	−0.4	−0.6
$[CH_3COO^-]$	0.9	0.7
Parameter		
log A	6.2 ± 0.1	4.4 ± 0.1
E_a (kJ mol^{-1})	61 ± 2	45 ± 1
$\Delta H^{\neq}$ (kJ mol^{-1})	59 ± 2	43 ± 1.5
$\Delta S^{\neq}$ (JK^{-1} mol^{-1})	−133 ± 4	−166 ± 5
$\Delta G^{\neq}$ (kJ mol^{-1})	99 ± 2	94 ± 2

[a]Calculated from the *p*H values at varying $[HClO_4]$.

Table 4—Comparison of Predicted and Observed Rate Constants for Chlorination of Aniline by Dichloramine-T in 1:1 (v/v) Aqueous Acetic Acid Medium

$10^3[Aniline]_0$ (mol dm^{-3})	$10^4 k_{obs}$ (s^{-1})		
	Calc[a]	Calc[b]	Obs
1.0	1.9	1.9	1.9
2.0	3.8	3.9	3.8
3.0	5.8	5.8	5.6
5.0	9.6	9.8	9.1
7.0	13.4	13.6	13.9
10.0	19.2	19.5	19.3

Calculated from k_1 and k_2 values computed from the plot of
[a] k_{obs} versus $[CH_3COO^-]$ (Eq. 5)
[b] k_{obs} versus $1/[H^+]$ (Eq. 6)

and

$$k_{obs} = k_1[S][CH_3COO^-] + k_2[S] \qquad \ldots (5)$$

Substituting $[CH_3COO^-] = K_a[CH_3COOH]/[H^+]$ we get

$$k_{obs} = \left\{\frac{K_a k_1[CH_3COOH]}{[H^+]} + k_2\right\}[S] \qquad \ldots (6)$$

Rate law (6) envisages that the plot of k_{obs} versus [S] should be linear with almost no intercept on the ordinate. This is actually found to be the case (figure not shown). Further, as already pointed out, plots of k_{obs} versus $[CH_3COO^-]$ and k_{obs} versus $1/[H^+]$ are also linear with intercepts on the ordinate (Fig. 2). Values of the constants k_1 and k_2 have been calculated from the slopes and intercepts of the above plots respectively. These constants are used to predict the rate constants at varying $[S]_0$. Predicted values compare very well with the experimental rate constants (Table 4).

Table 5—Pseudo-first Order Rate Constants for Chlorination of Several Substituted Anilines by DCT in 1:1 (v/v) Aqueous Acetic Acid at 303 K

$10^4[DCT]_0 = 10^3[S]_0 = 5.0$ mol dm^{-3}; $\mu = 0.2$ mol dm^{-3} with NaOAc.

Aniline	$10^4 k_{obs}$ (s^{-1})	Aniline	$10^4 k_{obs}$ (s^{-1})
Unsubstituted	9.1	*m*-nitro	0.76
p-chloro	7.0	*o*-chloro	3.2
p-bromo	8.1	3,4-dichloro	4.0
p-iodo	8.9	N-methyl	18.0
p-methyl	10.1	N,N-dimethyl	6.0

The reaction between aniline and DCT via N-chloro intermediate is supported by the observation that there is no reaction between DCT and acetanilide (containing an electron-withdrawing N-acetyl group) under identical conditions and the introduction of NO_2 group in benzene ring decreases the rate by about 20 times. Further the rate of chlorination of *o*-chloroaniline is about one-third that for aniline (Table 5). While the substituent at the *para*-position decreases the rate by about 20%. Replacement of one of the hydrogens of $-NH_2$ group by methyl group increases the rate to almost double whereas replacement of both the hydrogen atoms decreases the rate. Electron-releasing substituents (such as Me) at the *para*- and *meta*-positions generally increase the rates while electron-withdrawing substituents decrease the rate (Table 5).

Large negative entropies of activation and high positive free energy of activation (Table 3) suggest the role of bond breaking in attaining the activated state.

The observed negative dielectric effect is in conformity with the Amis' concept[5] for dipolar molecule-dipolar molecule and dipolar molecule-negative ion interactions and the proposed mechanisms.

References

1 Gowda B T & Mahadevappa D S, *J chem Soc, Perkin Trans* 2, (1983) 323.

2 Gowda B T & Sherigara B S, *Oxidn Commn*, **9** (1986) 165; *Indian J Chem*, **25A** (1986) 960; **26A** (1987) 930 and *J Indian chem Soc*, **64** (1987) 158.

3 Gowda B T & (Mrs) Rao R V, *J chem Soc, Perkin Trans* 2, (1988) 355; *Oxidn Commun*, **10** (1987) 31; *Indian J Chem*, **24A** (1985) 1021; **25A** (1986) 578 and 908; **26A** (1988) 34, 39 and (d) *J Indian chem Soc*, **64** (1987) 403, 467 & 474.

4 Gowda B T & Bhat J I, *Tetrahedron*, **43** (1987) 2119; *React Kinet Catal Lett*, **31** (1986) 461; *Indian J Chem*, **25A** (1986) 1129 and 1149; **26A** (1987) 215 and *J Indian chem Soc*, **63** (1986) 665; **64** (1987) 150; **65** (1988) 159.

5 Amis E S, *Solvent effects on reaction rates and mechanisms* (Academic Press, New York) 1966.

Indian Journal of Chemistry
Vol. 28A, February 1989, pp. 124-128

Kinetics & Mechanism of Chlorination of Aniline by Trichloromelamine in Aqueous Acetic Acid—Perchloric Acid Medium: A Novel Dependence of Chlorinating Agent on Nature of Solvent System (Part 1)

P S RADHAKRISHNAMURTI* & J C PANIGRAHI
Department of Chemistry, Berhampur University, Berhampur 760 007

Received 23 October 1987; revised 16 February 1988; accepted 30 May 1988

Kinetics of chlorination of aniline by trichloromelamine (TCM) in aqueous acetic acid medium, over the temperature range 30°-45°C and solvent composition from 1% to 100% acetic acid have been reported. The orders of reaction in [substrate], [oxidant] and [acid], and the effect of neutral salts like KCl and melamine have been evaluated in 50%, 90% and 100% acetic acid. The results show a novel dependence of chlorinating agent on the nature of solvent system. Kendall's treatment has been applied to compute the acid-independent rate constants with respect to substrate. Plausible mechanisms are suggested.

Trichloromelamine (N^2,N^4,N^6-trichloro-2,4,6-triamino-1,3,5-triazine or TCM) an effective halogen carrier agent, is used in medicine and rubber industry. However, in comparison to other halogenating agents such as CAT, BAT, NBS, NCS etc. it has not been used so far as chlorinating agent in the study of kinetics and mechanism of chlorination of aromatic amines. This prompted us to undertake the title investigation.

Materials and Methods

The reagents used were of AR (BDH) grade and were recrystallised or redistilled before use. Trichloromelamine (Fluka), was used as such. The stock solution of TCM was prepared in 100% acetic acid in which it was highly stable and its concentration was determined iodometrically in acid medium in accordance with reaction (1)

$$\underset{\text{(TCM)}}{C_3N_6H_3Cl_3} + 6I^- + 3H^+ \leftrightharpoons \underset{\text{(Melamine)}}{C_3N_6H_6} + 3I_2 + 3Cl^- \quad \ldots (1)$$

The kinetics were monitored by estimating the disappearance of [TCM] at various time intervals by standard iodometric procedure. Rate constants were reproducible within ±5%. Self-decomposition of TCM was negligible under the conditions employed. The rate constants remained practically invariant in air or under O_2-free atmosphere. Only a representative set of average values of kinetic data at 35°C (±0.1)°C in different aqueous acetic acid-perchloric acid media are presented here. The product obtained was *p*-chloroaniline under the present experimental conditions.

Results and Discussion

The rate data at different [TCM], [substrate] and [$HClO_4$] and in the presence of added neutral salts like KCl, melamine and in solvent mixtures of different compositions, viz. 50%, 90% and 100% aq HOAc are recorded in Tables 1-3 respectively.

In 50% aq. acetic acid in the presence of perchloric acid the disappearance of TCM was followed for at least upto 60 to 75% of completion of reaction. The reaction in this medium followed pseudo-second order kinetics as seen from the linear plots of 1/titre versus time. But the observed rate constants decreased with increase in $[TCM]_0$. This may be due to the existence of many competing equilibria. The order in [substrate] was unity at $[HClO_4] = 0.01$ mol dm^{-3} and became fractional at $[HClO_4] = 0.1$ mol dm^{-3} possibly due to the formation of more unreactive protonated form of substrate. The reaction rates were apparently independent of $[H^+]$ in the range studied which might be due to the cancellation of direct dependence on $[H^+]$ involved in the hydrolysis of TCM and inverse dependence on $[H^+]$ for the protonation of aniline. The rates remained invariant by the addition of KCl and melamine.

In 90% aq. acetic acid in the presence of $HClO_4$, the disappearance of TCM was followed upto 75% completion of the reaction. In this medium the reaction followed pseudo-first order kinetics, as seen from the linearity of the plots of log (titre) versus time. Here again the rate constants increased with increase in $[TCM]_0$. The rate of reaction was independent of change in [substrate]

Table 1—Pseudo-second Order Rate Constants at Varying $[TCM]_0$, [Aniline] and $[HClO_4]$
Solvent = 50% (v/v) aq. HOAc. temp. = 35°C

10^4 [TCM] (mol dm^{-3})	10^4 [Aniline] (mol dm^{-3})	10^2 $[HClO_4]$ (mol dm^{-3})	$k_{2(obs)}$ (mol^{-1} dm^3 sec^{-1})	10^{-4} $k_{2(obs)}/[S]_{free}$ i.e. acid independent rate constants
1.68	50	1.0	4.95	
4.47	50	1.0 ($h_0 = 1.89$)	1.27	12.98
9.14	50	1.0	0.67	
18.98	50	1.0	0.287	
5.0	20	1.0	0.485	12.43
5.0	100	1.0	2.92	14.98
5.0	200	1.0 ($h_0 = 1.89$)	4.33	11.13
5.0	50	5.0 ($h_0 = 1.39$)	1.202	38.99
5.0	50	10.0 ($h_0 = 1.1$)	1.34	84.76
5.0	200	5.0 ($h_0 = 1.39$)	2.93	23.76
5.0	200	10.0 ($h_0 = 1.1$)	2.7	40.69
5.0	20	10.0	0.999	157.97
5.0	50	1.0	1.6^{a_1}	
5.0	50	1.0	1.51^{a_2}	
5.0	50	1.0	1.94^{a_3}	
5.0	50	1.0	1.17^{b_1}	
5.0	50	1.0	1.13^{b_2}	
5.0	50	1.0	0.95^{b_3}	
5.0	50	1.0	0.594^{c_1}	
5.0	50	1.0	1.27^{c_2}	
5.0	50	1.0	1.44^{c_3}	
5.0	50	1.0	2.01^{c_4}	

a_1,a_2,a_3—at [melamine] = 0.001, 0.002, 0.005 mol dm^{-3} respectively, b_1,b_2,b_3—at [KCl] = 0.001, 0.005, 0.01 mol dm^{-3} respectively, c_1,c_2,c_3,c_4—at 30°, 35°, 40°, 45°C respectively.

Table 2—Pseudo-first Order Rate Constants at Varying $[TCM]_0$, [Aniline] and $[HClO_4]$

Solvent = 90% (v/v) aq. HOAc, temp. = 35°C

10^4 [TCM] (mol dm^{-3})	10^4 [Aniline] (mol dm^{-3})	10^2 $[HClO_4]$ (mol dm^{-3})	10^4 k_{obs} (sec^{-1})	$10^{-4} \times k_{obs}/[S]_{free}$ (i.e. acid independent rate constants)
1.588	50	1.0	6.9	0.19512
4.77	50	1.0 ($h_0 = 0.69$)	12.0	
8.34	50	1.0	18.8	
5.0	20	1.0	13.57	0.55163
5.0	100	1.0	12.34	0.100325
5.0	200	1.0	13.26	0.0539024
5.0	20	10.0	37.6	13.0058
5.0	100	10.0	37.6	2.6021
5.0	50	0.4 ($h_0 = 0.83$)	14.9	0.175459
5.0	50	2.0 ($h_0 = 0.44$)	22.8	0.65915
5.0	50	5.0 ($h_0 = 0.06$)	31.8	2.22025
5.0	50	10.0 ($h_0 = -0.24$)	36.94	5.1107
5.0	50	1.0	6.43^{a_1}	
5.0	50	1.0	4.72^{a_2}	
5.0	50	1.0	4.13^{a_3}	
5.0	50	1.0	3.79^{b_1}	
5.0	50	1.0	3.45^{b_2}	
5.0	50	1.0	1.12^{b_3}	
5.0	50	1.0	7.1^{c_1}	
5.0	50	1.0	12.0^{c_2}	
5.0	50	1.0	15.73^{c_3}	

a_1,a_2,a_3—at [melamine] = 0.001, 0.002, 0.005 mol dm^{-3} respectively, b_1,b_2,b_3—at [KCl] = 0.001, 0.005, 0.01 mol dm^{-3} respectively, c_1,c_2,c_3—at 30°, 35°, 40°C respectively.

and the order in $[H^+]$ was fractional. The rate decreased by the addition of KCl and melamine.

In 100% acetic acid in the presence of $HClO_4$, the pseudo-first order rate constant marginally decreased with the increase in $[TCM]_0$. A unit slope of the plot of log k_{obs} versus log [S] indicated the order in [substrate] as unity. The order in $[H^+]$ was inverse fractional. The rate constant initially increased with the addition of melamine, then progressively decreased with further addition of melamine.

The cumulative effect due to solvent and acidity in the reaction of a basic substrate like aniline can be better understood by the application of Kendall's treatment[1], which envisages the computation of true acid-independent rate constants with respect to substrate.

Trichloromelamine undergoes hydrolysis in different ways in different HOAc-$HClO_4$ media as shown in Scheme 1.

After the application of Kendall's treatment, and with the acid-independent rate constants with respect to substrate, calculated within the limits of experimental errors, and within the limitations involved in employing the treatment, the rate data (Tables 1-3) show that:

(i) In 50% aq. acetic acid in the presence of $HClO_4$, the reaction is first order in [substrate] and

Table 3—Pseudo-first Order Rate Constants at Varying $[TCM]_0$, [Aniline] and $[HClO_4]$

Solvent = 100% HOAc, temp. = 35°C

10^4 [TCM] (mol dm^{-3})	10^4 [Aniline] (mol dm^{-3})	10^2 $[HClO_4]$ (mol dm^{-3})	10^4 k_{obs} (sec^{-1})	10^{-4} $k_{obs}/[S]_{free}$ (i.e. acid and independent rate constants)
1.515	50	1.0	13.06	5.372
3.782	50	1.0	12.0	
		($h_0 = -0.75$)		
7.89	50	1.0	10.45	
5.0	25	1.0	3.63	3.249
5.0	100	1.0	27.5	6.156
5.0	200	1.0	47.0	5.261
5.0	20	5.8	1.34	3.5662
5.0	100	5.8	6.15	3.2643
5.0	50	0.6	20.15	8.041
		($h_0 = -0.7$)		
5.0	50	5.8	3.55	6.545
		($h_0 = -1.25$)		
5.0	50	1.0	78.0[a1]	
5.0	50	1.0	12.8[a2]	
5.0	50	1.0	6.4[a3]	

a_1,a_2,a_3,—at [melamine] = 0.001, 0.002, 0.005 mol dm^{-3} respectively.

(A) 2R-NHCl $\underset{\text{DISPROPORTIONATION}}{\overset{K}{\rightleftharpoons}}$ R-NCl_2 + R-NH_2

R-NCl_2 + H_2O $\underset{\text{DECOMPOSITION}}{\overset{K_0}{\rightleftharpoons}}$ R-NHCl + HOCl

(B) R-NHCl + H_2O $\underset{\text{HYDROLYSIS}}{\overset{K_h}{\rightleftharpoons}}$ R-NH_2 + HOCl

(C) R-NHCl + $\overset{+}{H}$HOAc $\overset{K_2}{\rightleftharpoons}$ R-NH_2 + ClOAcH^+

Where, R = 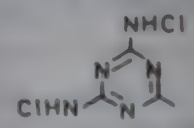

SCHEME-1

the unit slope obtained from the plot of log $k_{obs}/[S]_{free}$ versus h_0 (h_0 values for various percentages of aq. acetic acid have been taken from Wiberg[2]), indicates that $[H^+]$ is being used for the hydrolysis of TCM to afford active TCM species. The rate constants at different solvent compositions from 1 to 80% HOAc are reported in Table 4. The apparent invariance in rate is due to cumulative effect of acidity function towards protonation-deprotonation equilibrium and to the formation of positive species (ClOAcH^+) in the presence of more HOAc i.e. in low dielectric constant of the

Table 4—Pseudo-second Order/First Order Rate Constants at Varying HOAc (v/v)

[Aniline] = 50.0×10^{-4} mol dm^{-3}, $[TCM]_0 = 5.0 \times 10^{-4}$ mol dm^{-3}, $[HClO_4] = 1.0 \times 10^{-2}$ mol dm^{-3} and temp. = 35°C

% HOAc (v/v)		$k_{2(obs)}$ (mol^{-1} dm^3 sec^{-1})	10^{-4} $k_{2(obs)}/[S]_{free}$ (i.e. acid independent rate constants)
1	($h_0 = 1.6$)	1.91	38.82
6	($h_0 = 1.75$)	1.57	22.0
10	($h_0 = 1.83$)	1.7	20.0
20	($h_0 = 1.89$)	1.99	20.0
30	($h_0 = 1.88$)	0.976	10.0
50	($h_0 = 1.89$)	1.27	13.0
60	($h_0 = 1.75$)	1.16	16.0
70	($h_0 = 1.4$)	1.024	32.0
79.5	($h_0 = 1.08$)	1.634	108.0
		10^4 $k_{1(obs)}$ (s^{-1})	
84.5		6.17	
89.5		15.05	
94.5		43.6	
97.0		82.25	
99.5	(i.e. pure HOAc)	12.0	

medium (equilibrium C, Scheme 1). Such a species has also been reported in CAT reactions[3,4] in solvent media containing high percentages of AcOH. The data in Table 4 show that $k_{obs}/[S]_{free}$ values, first decrease for solvent media containing 1 to 30% HOAc, and then increase with the further increase in HOAc content of the reaction medium. Hence, at lower percentages of HOAc (i.e. 1 to 30% and even upto 80%) the reaction is of dipole-dipole type which tends to positive ion-dipole type by the accumulation of ClOAcH^+ at higher percentages of HOAc, resulting in a change in order from second to first order above 80% HOAc with respect to oxidant.

(ii) In 90% aq. HOAc in the presence of $HClO_4$ the plot of $k_{obs}/[S]_{free}$ versus h_0 is linear with a slope of more than unity. This increase in order in $[H^+]$ in comparison to that in 1-80% HOAc can be traced to the main equilibrium which leads to the formation of ClOAcH^+ (equilibrium C, Scheme 1) followed by another equilibrium (equilibrium B, Scheme 1) leading to the formation of H_2OCl^+ to a certain extent. The large enhancement of rates with increase in HOAc from 80% to 97% is due to the competing effects of both acidity function (h_0) and the dielectric constant of the medium.

(iii) In 100% HOAc-$HClO_4$ system, the rate again falls. The reason is due to change of effective TCM species as a result of change in solvent

system and also due to change in dielectric constant of the medium. The observed constancy in values of $k_{obs}/[S]_{free}$ at different $[S_0]$, clearly indicates that the order in [substrate] is unity and the constant values of $k_{obs}/[S]_{free}$ at different $[HClO_4]$ or h_0 confirms that RNHCl itself is the effective species in pure HOAc-$HClO_4$ system and that it does not undergo hydrolysis in 100% acetic acid.

Mechanism and rate law

Before postulating a mechanism and the rate law it is pertinent to keep the following results in view:

(i) Dependence on TCM is solvent-dependent (second order dependence on TCM changes to first order in solvent media containing higher percentages of acetic acid).

(ii) Dependence on [substrate] is also solvent-dependent (unity below 80% HOAc, zero order in 90% HOAc and first order in 100% HOAc).

(iii) First order dependence in $[H^+]$ in 1-80% aq. HOAc and independent of $[H^+]$ in pure acetic acid after acidity corrections.

Under present experimental conditions chlorination by molecular chlorine is ruled out, as the rates remain unaffected in the presence of halides, i.e. KCl. N-Chlorination of aniline under the conditions used is unlikely, since N-halo intermediates are favoured only at very low temperatures and also if it were the case, the smooth kinetics could not have been followed by iodometry.

Hence as postulated earlier in the chlorination of amines by CAT and NCS[5,6], the results obtained in the present study indicate that the reactions occur by direct halogen transfer from the active species of TCM present at different solvent compositions to the aromatic system.

Consistent with the observed results the most suitable mechanism in 50% and in 90% and 100% HOAc are presented in Schemes 2 and 3 respectively.

$$S + H^+ \overset{K_1}{\rightleftharpoons} SH^+$$

$$S + [TCM]_T \xrightarrow[\text{slow}]{k} \text{Products}$$

Scheme 2

In 50% aq. acetic acid-$HClO_4$ system and for activated type of substrates which are highly reactive, K_h and K_D (equilibria A and B of Scheme 1) being very slow steps compared to K and K_2 (equilibria A and C of Scheme 1), $R-NCl_2$ and $ClOAcH^+$ are the active species present, which compete with each other in their reactions with the substrate in slow steps.

$$S + RNCl_2 \xrightarrow[\text{slow}]{k'} \text{Products}$$

$$S + ClOAcH^+ \xrightarrow[\text{slow}]{k''} \text{Products}$$

Scheme 2 leads to rate law (2)

$$\text{Rate} = -\frac{d[TCM]_T}{dt} = k[S][TCM]_T \qquad \ldots (2)$$

$$\text{or } k'[S][RNCl_2] + k''[S][ClOAcH^+]$$

$$= k'K[S][RNHCl]^2 + k''K_2[S][RNHCl][H^+][HOAc]$$

$$= [S][RNHCl]^2\left\{Kk' + \frac{K_2K''[H^+][HOAc]}{[RNHCl]}\right\}$$

$$\text{But } [S]_T = [S] + [SH^+] = [S] + K_1[S][H^+] = [S]\{1 + K_1[H^+]\}$$

$$\text{or } [S] = \frac{[S]_T}{1 + K_1[H^+]}$$

$$\text{Rate} = \frac{[S]_T[RNHCl]^2}{1 + K_1[H^+]}\left\{Kk' + \frac{K_2k''[H^+][HOAc]}{[RNHCl]}\right\}$$

$$\text{or } \frac{\text{Rate}}{[RNHCl]^2} = \frac{-d[TCM]_T/dt}{[RNHCl]^2} = k_{obs}$$

$$= \frac{[S]_T}{1 + K_1[H^+]}\left\{Kk' + \frac{K_2k''[H^+][HOAc]}{[RNHCl]}\right\}$$

$$S + H^+ \overset{K}{\rightleftharpoons} SH^+$$

$$RNHCl + H^+ + HOAc \overset{K_2}{\underset{\text{slow}}{\rightleftharpoons}} RNH_2 + ClOAcH^+$$

$$S + ClOAcH^+ \xrightarrow{\text{fast}} \text{Products}$$

$$S + RNHCl \xrightarrow[\text{slow}]{k'''} \text{Products}$$

Scheme 3

Scheme 3 leads to rate law (3)

$$\text{Rate} = -\frac{d[\text{TCM}]_T}{dt} = \frac{K_2[\text{RNHCl}][\text{H}^+][\text{HOAc}]}{[\text{RNH}_2]} + \frac{k''[\text{S}]_T[\text{RNHCl}]}{(1+K_h[\text{RNHCl}])(1+K_1[\text{H}^+])}$$

$$\text{or } k_{obs} = \frac{\text{Rate}}{[\text{RNHCl}]} = \frac{K_2[\text{H}^+][\text{HOAc}]}{[\text{RNH}]_2} + \frac{k''[\text{S}]_T}{(1+K_1[\text{H}^+])(1+K_h[\text{RNHCl}])} \quad \ldots(3)$$

In 90% HOAc-$HClO_4$ system, $ClOAcH^+$ species is more predominant over RNHCl species and in 100% HOAc-$HClO_4$ system RNHCl species is more predominant. The rate law (3) therefore reduces to Eqs (4) and (5).

$$k_{obs} = \frac{K_2[\text{H}^+][\text{HOAc}]}{[\text{RNH}_2]} \quad \text{(in 90\% aq. HOAc} - HClO_4 \text{ system)} \quad \ldots(4)$$

$$\text{and } k_{obs} = \frac{k''[\text{S}]_T}{(1+K_1[\text{H}^+])(1+K_h[\text{RNHCl}])}$$

(in 100% HOAc − $HClO_4$ system) ... (5)

The rate laws derived from Schemes 2 and 3 explain all the kinetic orders observed.

Acknowledgement

One of the authors (JCP) is grateful to the UGC, New Delhi for the award of a junior research fellowship.

References

1 Ikchoon L & Kendall F H, *J Am chem Soc*, 88 (1966) 3813.
2 Wiberg K B & Evans R J, *J Am chem Soc*, 80 (1958) 3019.
3 De La Mare P B D, Hilton I C & Vernon C A, *J Am chem Soc*, 82 (1960) 4039.
4 Thiagarajan V & Natarajan M M, *J chem Soc, Perkin II* (1975) 1590.
5 Radhakrishnamurti P S & Rao M D P, *Indian J Chem*, 14(A) (1976) 485.
6 Radhakrishnamurti P S & Sahu S N, *Indian J Chem*, 14(B) (1976) 898.

Indian Journal of Chemistry
Vol. 28A, February 1989, pp. 129-131

Metal Complexes of S-Acetyl(β-N-acetyl)dithiocarbazate

M T H TARAFDER
Department of Chemistry, University of Rajshahi, Rajshahi, Bangladesh

Received 30 *December* 1987; *revised* 15 *March* 1988; *accepted* 20 *May* 1988

The new ligand, S-acetyl(β-N-acetyl)dithiocarbazate ($CH_3CONHNHCSSCOCH_3$) reacts with metal ions only in alkaline medium as a bidentate uni-negative (N,S^-) donor ligand giving complexes of type $[M(NS^-)_2]$[M = Ni(II) and Zn(II)], $[M'(NS^-)_2X_2]$ [M' = Zr(IV) and Th(IV); X = NO_3^- and NCS^-], $[Cr(NS^-)_2X\cdot H_2O]$ and $[UO(NS^-)_2X_2]$. Analytical, conductivity and magnetic measurements, and spectral data of the complexes are consistent with four-coordination of Ni(II) and Zn(II) ions while zirconium, thorium and chromium analogues are six-coordinate. The uranium complexes are seven-coordinate.

Coordination properties of a number of novel N,O or N,O,S donor ligands have been reported from our laboratory[1-7]. As a part of our general study of N,S ligands, we report herein the synthesis and charcterization of new complexes of Ni(II), Zn(II), Zr(IV), Th(IV), Cr(III) and U(VI) with a bidentate, S-acetyl (β-N-acetyl)dithiocarbazate.

Materials and Methods

Infrared spectra were recorded in KBr on a Pye-Unicam SP3-300 infrared spectrophotometer, electronic spectra on a LKB-Ultrospec K4053 spectrophotometer, PMR spectra in $CDCl_3$ on a Varian XL-300 spectrophotometer using TMS as an internal standard and mass spectra on a Hitachi RMU-6D instrument operating at 70 eV. Conductivities of 10^{-3} *M* solutions of the complexes were measured at ~25°C in dimethyl sulfoxide (DMSO) using a WPA CM35 conductivity meter fitted with a dip-cell and platinized electrodes. Magnetic susceptibilities were measured at room temperature by the Faraday method. Diamagnetic corrections for the constituent elements were obtained using Pascal's constants[8].

Preparation of S-acetyl(β-N-acetyl)dithiocarbazate (SADTC)

To a solution of potassium hydroxide (11.4 g) in 90% ethanol (70 ml) was added hydrazine hydrate (10 g) and the mixture was cooled to 0°C. Carbon disulfide (15.2 g) was added dropwise to the above mixture with constant stirring during 1 hr, the light brown layer was separated, dissolved in cold 40% ethanol (60 ml), kept in an ice-bath and acetyl chloride (25 g) was added to it dropwise with vigorous stirring. A white product which separated out was filtered, washed with water, dried, recrystallized from ethanol and dried over P_4O_{10}; yield 10.5 g (Found: C, 31.1; H, 4.2; S, 33.0. $C_5H_8N_2S_2O_2$ requires C, 31.2; H, 4.2; S, 33.3%); IR: 3310 (νNH), 1620 (νC=O), 1090 (νC=S) cm^{-1}; PMR: δ 3.35 (3H, CH_3), 7.3 (ArH), 10.2 (NH); MS: *m/z* 192, 160, 149, 128, 77, 64, 57, 43, 32.

(a) Preparation of [M(NS)$_2$][M = Ni(II)] (complexes **1** *and* **2**), *[M'(NS)$_2$(NO$_3$)$_2$] [M' = Zr(IV) and Th(IV)] (complexes* **3** *and* **5**), *[Cr(NS)$_2$NO$_3$·H$_2$O] (complex* **7**) *and [UO(NS)$_2$(NO$_3$)$_2$] (complex* **9**); *[NS = deprotonated form of SADTC]*

SADTC (0.008 mol) was added to aq. potassium hydroxide (0.008 mol in 30 ml water), stirred for 5 min, filtered, and to the filtrate was added, with stirring, a solution of a metal nitrate (0.004 mol) in water (20 ml) and heated on a water-bath for 20 min. The resulting precipitate was filtered, washed with water and ethanol and dried *in vacuo* over P_4O_{10}.

(b) Preparation of [M'(NS)$_2$(NCS)$_2$] [M' = Zr(IV) and Th(IV)] (complexes **4** *and* **6**), *[Cr(NS)$_2$(SCN)H$_2$O] (complex* **8**) *and [UO(NS)$_2$(NCS)$_2$] (complex* **10**)

To a solution of hydrated metal nitrate (0.004 mol) in anhydrous methanol (30 ml) was added a solution of potassium thiocyanate (0.016 mol) in the same solvent (25 ml). The precipitated potassium nitrate was filtered, the filtrate added to an aqueous solution (30 ml) of SADTC (0.004 mol) containing potassium hydroxide (0.008 mol). The precipitate obtained was filtered, washed with water and ethanol and dried *in vacuo* over P_4O_{10}.

Results and Discussion

The analytical data of the complexes are given in Table 1. The electrical conductivities of 10^{-3} *M*

Table 1—Characterization Data of Complexes[a]

Compd	Colour	Found (Calc) %		
		M[a]	C	H
$[Ni(CH_3CONHNCSSCOCH_3)_2]$ (**1**)	Buff	13.2(13.3)	27.2(27.2)	3.1(3.2)
$[Zn(CH_3CONHNCSSCOCH_3)_2]$ (**2**)	Colourless	14.6(14.6)	26.6(26.8)	3.1(3.1)
$[Zr(CH_3CONHNCSSCOCH_3)_2(NO_3)_2]$ (**3**)	-Do-	15.2(15.3)	19.8(20.1)	2.3(2.3)
$[Zr(CH_3CONHNCSSCOCH_3)_2(NCS)_2]$ (**4**)	-Do-	15.2(15.5)	24.2(24.4)	2.3(2.4)
$[Th(CH_3CONHNCSSCOCH_3)_2(NO_3)_2]$ (**5**)	-Do-	31.2(31.4)	16.0(16.3)	1.9(1.9)
$[Th(CH_3CONHNCSSCOCH_3)_2(NCS)_2]$ (**6**)	-Do-	31.4(31.8)	19.6(19.7)	1.9(1.9)
$[Cr(CH_3CONHNCSSCOCH_3)_2(NO_3)H_2O]$ (**7**)	Blue	10.0(10.1)	23.1(23.3)	3.1(3.1)
$[Cr(CH_3CONHNCSSCOCH_3)_2(SCN)H_2O]$ (**8**)	-Do-	10.0(10.2)	25.8(25.9)	3.0(3.1)
$[UO(CH_3CONHNCSCOCH_3)_2(NO_3)_2]$ (**9**)	Yellow	31.0(31.3)	15.5(15.8)	1.8(1.8)
$[UO(CH_3CONHNCSSCOCH_3)_2(NCS)_2]$ (**10**)	-Do-	31.5(31.7)	19.0(19.1)	1.8(1.9)

[a]Ni(II) and Zn(II) were determined gravimetrically (as dimethylglyoximato complex) and complexometrically (with EDTA) respectively[23]. Zr(IV)[13], Th(IV)[12] and U(VI)[11] were determined gravimetrically as oxides after complete ignition of the complexes.

solutions in DMSO indicated that the complexes were non-electrolytes suggesting that the anions were coordinated in all the complexes.

The ligand SADTC is a potential bidentate ligand and sterically favourable three types of coordinations (**1a**, **2a** and **3a**) are possible.

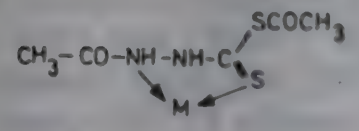

(1a)

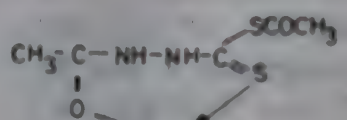

(2a)

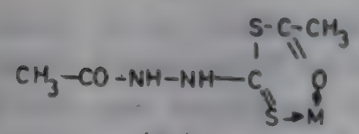

(3a)

In the IR spectra of the complexes the ν(CO) mode of the free ligand remains unchanged excluding structures (**2a**) and (**3a**). SADTC reacts with metal ions only in alkaline medium. Attempts to prepare complexes from a neutral medium were unsuccessful. This suggests that nucleophilicity of the ligand is greatly enhanced in alkaline medium probably due to creation of an anionic site *in situ*[1,3,4,6]. Presumably, the ligand exists in thione and thiolo tautomeric forms (**1b**) and (**1c**) although the PMR spectrum does not show any SH proton indicating that **1b** is the predominant form. However, the non-electrolytic and diamagnetic nature of $[Ni(NS^-)_2]$ (**1**) provide strong evidence that in alkaline medium the ligand is deprotonated and bonding occurs through the thiolate anion, generated from thiol (**1c**), causing spin-pairing in the complex[9]. Similar observations were made for complexes of S-benzoyl (β-N-benzoyl)dithiocarbazate, $(C_6H_5CONHNHCSSCOC_6H_5)$[10]. Besides, the IR spectra of **1-10** indicate shift of ν(C=S) mode of the free ligand and a sharp band at 1570-1550 cm^{-1}, attributable to ν(C=N) mode. The β-nitrogen coordination is evident from the shift of ν(NH) of the free ligand appearing at 3310 cm^{-1} to lower wavenumbers (3080-3250 cm^{-1}) in **1-10**. The far IR spectra of the complexes exhibit bands in the region 460-275 and 350-230 cm^{-1} which are tentatively attributed to ν(M−N) and ν(M−S) modes [M = Ni(II), Zn(II),Zr(IV), Th(IV), Cr(III) and U(VI)], respectively[1,4,5,11-16]. The IR spectra of **3**, **5**, **7** and **9** exhibit bands at about 1490, 1285, 1010 and 810 cm^{-1} characteristic of unidentate nitrate group[5,15]. The complexes **4**, **6**, **9** and **10** exhibit intense band in the region 2000-2050 cm^{-1} assignable to ν(C≡N) mode. This suggests that thiocyanate is coordinated through the nitrogen indicating that Zr(IV),Th(IV) and U(VI) behave as class A acceptors[17,18]. The complex **8**, however, shows ν(C≡N) at 2115 cm^{-1} arising from S-coordinated thiocyanato moiety[17,18]. Unexpectedly it indicates that Cr(III) is a softer acid than Zr(IV) and Th(IV). This is attributed to the higher ionization potentials[19] of Zr(IV) and Th(IV) compared to that of Cr(III) making the former ions more acidic than the latter. The uranium complexes **9** and **10** display band at 915 cm^{-1} due to ν(U=O) mode[10]. Complexes **7** and **8** show broad band around 3380 cm^{-1} arising from coordinated water molecule[11-13].

All of the complexes, except those of chromium, are diamagnetic. The chromium complexes **7** and **8** have magnetic moments of 3.99 and 4.02 B.M., respectively corresponding to three unpaired electrons. The electronic spectra of zinc, zirconium, thorium and uranium complexes exhibit a single band in the region 280-350 nm due to charge transfer transition. The electronic spectrum of the nickel complex **1** is consistent with a square-planar geometry[20,21]. The ob-

served absorptions at 520, 395 and 320 nm correspond to $^1A_{1g} \rightarrow {}^1A_{2g}$, $^1A_{1g} \rightarrow {}^1B_{1g}$ and $^1A_{1g} \rightarrow {}^1E_g$ transitions in D_{4h} symmetry, respectively. The chromium complexes **7** and **8** exhibit three bands at around 550, 430 and 380 nm corresponding to $^4A_{2g} \rightarrow {}^4T_{2g}$, $^4A_{2g} \rightarrow {}^4T_{1g}$ and $^4A_{2g} \rightarrow {}^4T_{1g}(P)$ transitions in O_h symmetry, respectively[20,22].

Acknowledgement

We express our grateful thanks to Prof A D Westland, Department of Chemistry, University of Ottawa, Canada for the PMR and mass spectra and to Prof M A Raqib for help in procuring microanalyses from Germany.

References

1 Ali M A & Tarafder M T H, *J inorg nucl Chem*, **39** (1977) 1785.
2 Ali M A & Bose R, *J inorg nucl Chem*, **39** (1977) 265.
3 Tarafder M T H & Ali M A, *Can J Chem*, **56** (1978) 2000.
4 Tarafder M T H, Miah M A J, Bose R N & Ali M A, *J inorg nucl Chem*, **43** (1981) 3151.
5 Ali M A, Uddin M, Uddin M N, Chowdhury D A & Tarafder M T H, *Indian J Chem*, **25A** (1986) 238.
6 Tarafder M T H, Begum M & Rahman M L, *Indian J Chem*, **25A** (1986) 377.
7 Ali M A, Hossain SM G, Majumder S M M H, Uddin M N & Tarafder M T H, *Polyhedron*, **6** (1987) 1653.
8 Figgis B N & Lewis J, *Modern coordination chemistry*, edited by J Lewis & R G Wilkins (Interscience, New York) 1959; Selwood P W, *Magnetochemistry* (Interscience, New York) 1956.
9 Livingstone S E, *Quart Rev*, **19** (1965) 386.
10 Tarafder M T H & Roy S, *Indian J Chem*, (In press).
11 Westland A D & Tarafder M T H, *Inorg Chem*, **20** (1981) 3992.
12 Westland A D & Tarafder M T H, *Inorg Chem*, **21** (1982) 3228.
13 Tarafder M T H & Miah M A L, *Inorg Chem*, **25** (1986) 2265.
14 Tarafder M T H & Ahmed A, *Indian J Chem*, **25A** (1986) 729.
15 Nakamoto K, *Infrared spectra of inorganic & coordination compounds* (John Wiley, New York) 1963.
16 Adams D M, *Metal-ligand & related vibrations* (Arnold, London) 1967.
17 Basolo F, Baddley W H & Burmeister J L, *Inorg Chem*, **3** (1964) 1202.
18 Destefano N J & Burmeister J L, *Inorg Chem*, **10** (1971) 998.
19 Samsonov G V, *Handbook of the physicochemical properties of the elements* (Plenum Press, New York) 1968.
20 Lever A B P, *Inorganic electronic spectroscopy* (Elsevier, Amsterdam), 1968, Chap. 9.
21 Gray H B & Ballhausen C J, *J Am chem Soc*, **85** (1963) 260.
22 Figgis B N, *Introduction to ligand fields* (Interscience, New York) 1967.
23 Vogel A I, *A text book of inorganic quantitative analysis* (Longmans, London) 1962.

Indian Journal of Chemistry
Vol. 28A, February 1989, pp. 132-134

Derivatives of Cobalt(III) & Nickel(II) Dithiophosphinates with Polydentate Nitrogen Donors

R N MUKHERJEE*, B B S SHASTRI, S SHANKAR & D L MASCARENHAS
Department of Chemistry, Indian Institute of Technology, Bombay 400 076

Received 15 *December* 1987; *revised and accepted* 16 *May* 1988

Octahedral, mixed ligand complexes of cobalt(III) and nickel(II) containing dithiophosphinates and polydentate nitrogen donors have been prepared. Magnetic and spectral data have been utilised in the characterisation of the complexes.

Dithio ligands such as xanthates, dithiocarbamates, dithiophosphates and dithiocarboxylates form, in general, complexes with cobalt(III) with octahedral stereochemistry. In contrast, Co(II) forms tetrahedral complexes with dithiophosphinates[1]. Such Co(II) complexes interact with unidentate heterocyclic nitrogen donors such as pyridine to form penta- or hexa-coordinate adducts with the retention of +2 oxidation state of the metal[2]. Further, it is also known that polydentate nitrogen donors such as ethylenediamine (en), propanediamine (pn), diethylenetriamine (dien), triethylenetetramine (trien) and dimethylglyoxime (DMGH) form stable octahedral complexes with Co(III). In view of this it was of interest to synthesise mixed ligand cobalt complexes containing both polydentate nitrogen donors and dithiophosphinates [di(2,4-dimethylphenyl)dithiophosphinate or diphenyldithiophosphinate, see structure I] to see if there is any change in the oxidation state of cobalt in the resulting system. Complexes of a few nickel dithiophosphinates containing these ligands are also reported.

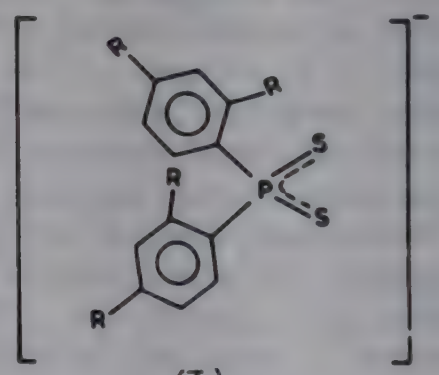

(I)

X^- (R=H or Me)

Materials and Methods

All the chemicals used were of AR grade. Dithiophosphinic acids were synthesized by the method described before[3].

Preparation of complexes: (i) $[Co(X)_2(DMG)]$

$CoCl_2 \cdot 6H_2O$ (2 g) was dissolved in methanol (30 ml) and 2% methanolic solution of DMGH was added dropwise till the colour changed from pink to light brown. Air was bubbled through this solution for 4 hr. To the resulting dark brown solution methanol (50 ml) was added followed by the methanolic solution of sodium salt of the ligand (5.6 g in 30 ml) with constant stirring. The brown crystalline complex was washed with methanol and dried *in vacuo*.

$[Co(X)_2(L)](X)$ [L = en or dien]

To an aqueous solution (30 ml) of $CoCl_2.6H_2O$ (2 g) a slight excess of the amine (~3 ml) was added till the colour changed from pink to light brown. Air was bubbled through this solution for 1 hr. The addition of the methanolic solutions of NaX (~7 g in 30 ml) with constant stirring yielded a brown compound which was filtered, washed with H_2O-MeOH and dried.

$[Co(X)_2(L)](X)$ [L = 1,2-pn] and $[Co(X)(L)](X)_2$ [L = trien]

Methanolic solution (10 ml) of the amine (~3ml) was added to $CoCl_2 \cdot 6H_2O$ (2 g) in MeOH (30 ml). The colour of the solution turned from pink to light brown and air was bubbled through this mixture for 2 hr. Addition of NaX in MeOH (~7 g in 30 ml)gave a brown product which was washed with methanol and dried.

$[Ni(X)_2(DMGH)]$

To a chloroform solution (10 ml) of $Ni(X)_2$ (2 g) a 1% solution of DMGH in EtOH was added until the solution turned green. It was filtered and the green filtrate on slow evaporation gave a green solid, which was collected and then washed with ethanol.

Table 1—Colour, Analytical, Magnetic & Electronic Spectral Data of the Complexes

Complex (Colour)	R[a]	Found (calc) %			μ_{eff} (B.M.)	Band maxima (cm^{-1})
		M	S	N		
$[Co(X)_2(DMG)]$ (Brown)	Me	7.38 (7.50)	16.05 (16.32)	3.21 (3.57)	Diamagnetic	14850, 27000
$[Co(X)_2(en)](X)$ (Brown)	Me	5.43 (5.69)	18.26 (18.58)	2.43 (2.70)	-Do-	17850, 27750
$[Co(X)_2(en)](X)$ (Brown)	H	6.74 (6.81)	21.93 (22.10)	3.15 (3.23)	-Do-	17800, 27700
$[Co(X)_2(1,2\text{-pn})](X)$ (Brown)	Me	5.66 (5.62)	18.12 (18.37)	2.45 (2.67)	-Do-	28600
$[Co(X)_2(1,2\text{-pn})](X)$ (Brown)	H	6.42 (6.70)	21.56 (21.81)	2.85 (3.18)	-Do-	28550
$[Co(X)_2(dien)](X)$ (Brown)	Me	5.20 (5.40)	17.57 (17.84)	3.55 (3.89)	-Do-	21700, 28550
$[Co(X)_2(dien)](X)$ (Brown)	H	6.38 (6.50)	20.96 (21.22)	4.34 (4.62)	-Do-	17900, 28400
$[Co(X)(trien)](X)_2$ (Brown)	Me	5.04 (5.26)	17.06 (17.15)	4.65 (5.00)	-Do-	20000, 28250
$[Co(X)(trien)](X)_2$ (Brown)	H	6.08 (6.19)	20.08 (20.16)	5.71 (5.88)	-Do-	20800, 28200
$[Ni(X)_2(DMGH)]$ (Green)	Me	7.23 (7.47)	16.09 (16.30)	3.27 (3.56)	2.90	14750, 23600
$[Ni(en)_3](X)_2$ (Pale pink)	Me	6.90 (6.91)	14.95 (15.09)	9.55 (9.89)	3.05	11780, 18770
$[Ni(1,2\text{-pn})_3](X)_2$ (Pale pink)	Me	6.50 (6.58)	14.20 (14.38)	9.21 (9.42)	3.06	11630, 18800
$[Ni(1,3\text{-pn})_3](X)_2$ (Pale pink)	Me	6.42 (6.58)	14.18 (14.38)	9.32 (9.42)	2.98	11630, 18030
$[Ni(dien)_2](X)_2$ (Pale pink)	Me	6.55 (6.70)	14.40 (14.64)	9.40 (9.60)	2.94	11630, 19140

(a) See structure (I)

$[Ni(L)_3](X)_2$ [L= en, 1,2-pn or 1,3-pn] and $[Ni(dien)_2](X)_2$

The aliphatic amine (~3 ml) was added dropwise to a chloroform solution (10 ml) of $Ni(X)_2$ (2 g) until it turned pink. A pale pink complex precipitated almost immediately, which was collected and washed with methanol and dried.

Physical measurements

IR spectra of the samples were recorded in KBr on a Pye-Unicam SP 2000 spectrophotometer and UV-visible spectra were recorded on a Shimadzu UV 260 spectrophotometer. Magnetic susceptibilities at room temperature were determined using a Gouy balance with $Hg[Co(SCN)_4]$ as the standard.

Results and Discussion

The colour, analytical, magnetic and electronic spectral data of the complexes are given in Table 1.

Cobalt complexes

In a preliminary experiment addition of methanolic solution of DMGH to a solution of cobalt(II) chloride in the same solvent followed by the addition of the sodium salt of dithio ligand (NaX) gave a brown complex which exhibited magnetic moment much lower than that expected for a six-coordinate cobalt(II) system and it varied for products independently prepared. This was indicative of partial oxidation of Co(II) to Co(III) and therefore the synthesis was modified by bubbling air through the reaction mixture for 4 hr before adding NaX. This yielded a brown diamagnetic complex which analysed for $Co(X)_2$ (DMG), showing coordination of both dithiophosphinate and dimethylglyoximate ligands around Co(III) central metal ion. The complex was stable in air and soluble in common organic solvents. IR spectrum of the compound in KBr displayed bands at 1050 and 1240 cm^{-1} which may be attributed to $\nu N-O$ modes[4]. However, the appearance of $\nu C=N$ at a

lower frequency (1530 cm^{-1}) than that observed for other dimethylglyoximate complexes of trivalent metal is not properly understood. In its electronic spectrum in chloroform a weak shoulder at 14850 and a strong band at 27000 cm^{-1} were observed.

The diamagnetic octahedral cobalt(III) complexes obtained with dithiophosphinate and polydentate nitrogen donors are insoluble in water but slightly soluble in chloroform as observed for other ionic compounds containing sulphur donors[5]. Electronic spectral bands (Table 1) are in agreement with hexacoordinate geometry[6-9]. The appearance of ν_{as} P−S and ν_sP−S at 650 and 590 cm^{-1}, respectively is in agreement with the presence of bidentate dithiophosphinates in the molecule. An additional band observed at 670 cm^{-1} is due to the uncoordinated dithiophosphinate group. The lowering of the free amine band from 3300 cm^{-1} to ~3100 cm^{-1} on complexation indicates the coordination of all the nitrogen atoms of the bases. In the ethylenediamine (en) and 1,2-diaminopropane(1,2-pn)complexes, the amine and two dithiophosphinates provide a hexacoordinate S_4N_2 core around Co(III) with one dithiophosphinate anion outside the coordination sphere. In the presence of tetradentate triethylenetetramine (trien), two dithiophosphinates are expected to be uncoordinated and a complex with CoS_2N_4 core is obtained. Complexes in which dithiophosphinates are present both as unidentate and bidentate ligands have been reported earlier[10-12]. In view of this $[Co(X)_2$ (dien)](X) may be considered as a plausible formulation for the derivative obtained with diethylenetriamine (dien). Octahedral geometry for cobalt(III) is achieved in this complex through coordination of tridentate dien together with bidentate and unidentate dithiophosphinates.

Nickel complexes

The green adduct $Ni(X)_2$ (DMGH) belongs to a rare class of compounds in which dimethylglyoxime (DMGH) acts as a neutral donor. Thermogravimetric studies show that the DMGH molecule is lost at 192°C and the chelate decomposes subsequently. Room temperature μ_{eff} value of 2.90 B.M. and the appearance of electronic absorption bands at 14750 cm^{-1} [$^3A_{2g} \rightarrow {}^3T_{1g}(F)$] and 23600 cm^{-1} [$^3A_{2g} \rightarrow {}^3T_{1g}(P)$] in its reflectance spectrum are consistent with octahedral stereochemistry.

Nickel dithiophosphinate forms only 1:3 pale pink complexes with en, 1,2-pn, and 1,3-pn and 1:2 complex with dien. Attempts to synthesize 1:1 and 1:2 adducts were unsuccessful in the case of bidentate amines. These complexes are insoluble in common organic solvents. Their solid state reflectance spectra exhibit a band around 11600 and a shoulder around 18800 cm^{-1} (Table 1). The band positions are in agreement[13] with those reported for $[NiN_6]^{2+}$ chromophore and may be assigned to $^3A_{2g} \rightarrow {}^3T_{2g}(F)$ and $^3A_{2g} \rightarrow {}^3T_{1g}(F)$ transitions respectively. This octahedral stereochemistry is supported by room temperature μ_{eff} values in the range of 2.94-3.06 B.M. The sulphur ligands therefore appear to take no part in coordination. This is also supported by the appearance of a single P-S vibration around 670 cm^{-1}. The coordination of all the nitrogen atoms is supported by the lowering of νN−H from 3300 to ~3100 cm^{-1} in these complexes.

References

1 Mukherjee R N & Shankar S, *Indian J Chem* **24A** (1985) 939.
2 Mukherjee R N, Shankar S & Mascarenhas D L, *Bull chem Soc Japan*, **59** (1986) 3239.
3 Higgins W A, Vogel P W & Craig W G, *J Am chem Soc*, **77** (1955) 1864.
4 Berger K, Ruff I & Ruff F, *J inorg nucl Chem*, **27** (1965) 179.
5 Critchlow P B & Robinson S D, *J chem Soc Dalton Trans*, (1975) 1367.
6 Atoh M, Kashiwabara K, Ito H, Ito T & Fujita J, *Bull chem Soc Japan*, **57** (1984) 3139.
7 Kojima M & Fujita J, *Bull chem Soc Japan*, **56** (1983) 139.
8 Gillard R D & Wilkinson G, *J chem Soc*, (1963) 3193.
9 Crayton P H & Mattern J A, *J inorg nucl Chem*, **13** (1960) 248.
10 Alison J M C, Stephenson T A & Gould R O, *J chem Soc (A)*, (1971) 3690.
11 Alison J M C & Stephenson J A, *J chem Soc Dalton Trans* (1973) 254.
12 Tebbe T N & Muetterties E L, *Inorg Chem*, **9** (1970) 629.
13 Biagini S & Cannas M, *J chem Soc (A)*, (1970) 2398.

Indian Journal of Chemistry
Vol. 28A, February 1989, pp. 135-139

Coordination Compounds of Rare Earth Cyanoacetates

(Kum) M A VAIDYA & S C JAIN*
Chemistry Division, Bhabha Atomic Research Centre, Trombay, Bombay 400 085

Received 15 *February* 1988; *revised and accepted* 25 *April* 1988

Coordination compounds of rare earth cyanoacetates, $[Ln(NCCH_2COO)_3.L\text{-}L]$, where Ln = La, Pr, Nd, Eu, Gd, Tb, Dy, Yb, Lu or Y and L-L = 2,2′-bipyridyl (Bipy) or 1,10 phenanthroline (Phen), have been synthesised and characterised by elemental analysis, infrared spectroscopy (4000-200 cm^{-1}), thermogravimetric analysis, molar conductance measurements and X-ray diffraction powder patterns. Comparative donor behaviour of Bipy and Phen towards lanthanide cyanoacetates in terms of the thermal stabilities of the complexes and the polarizing power (e/r^2) of Ln^{3+} ion has been discussed.

In continuation of our work[1] on the synthesis and characterization of hydrated lanthanide cyanoacetates, $[Ln(NCCH_2COO)_3.2H_2O]$, we thought it of interest to study whether the chelating ligands Bipy and Phen could replace strongly bonded water molecules. It was also of interest to study as to how a potential chelating ligand with fixed molecular geometry would modify the coordination behaviour of the cyanoacetate ion. It was also considered worthwhile to compare the ligating behaviour of Bipy and Phen towards lanthanides with increasing polarizing power of Ln^{3+} ions.

Materials and Methods

Hydrated tris-cyanoacetates of lanthanides were prepared by dissolving the respective carbonates in aqueous cyanoacetic acid[1]. The 1:1 Phen or Bipy adducts of the lanthanide cyanoacetates were prepared by direct interaction of the reactants in 50% (v/v) methanol solution. The products were crystallized out from the solution by partial evaporation on a water bath. The products were filtered out, washed with methanol and dried in an oven at 105-110°C for several hr.

The metal contents of the compounds were determined by firing the complexes to the stable metal oxides. Microanalysis of carbon, hydrogen and nitrogen was carried out at the Analytical Chemistry Division of our research centre. Analytical results are summarized in Tables 1 and 2.

The infrared spectra were recorded in nujol and fluorolube mulls on a Perkin Elmer grating spectrophotometer, model 577, using cesium iodide optics. X-ray diffraction powder patterns were obtained by using CuK_α radiation. A thin layer of the sample was spread evenly on a glass slide using colloidion in amyl acetate and the diffraction pattern was recorded on a chart. Interplanar *d*-spacings and the diffraction line intensities were determined from the chart recordings.

Thermogravimetric measurements of the representative compounds were carried out (~200 mg) in air at a heating rate of 4 K min^{-1} using a Stanton thermobalance. Stable intermediate phases, as indicated by the thermograms, were isolated separately and identified by infrared spectra.

Magnetic susceptibility measurements at room temperature, were carried out by Gouy method using $CuSO_4.5H_2O$ as the reference material. Sus-

Table 1 — Analytical Data of $[Ln(NCCH_2COO)_3.Bipy]$ Compounds

Compound, Colour	Calc. (Found), %			
	C	H	N	Metal
$[La(cyac)_3.(2,2'Bipy)]$ White	41.69 (39.65)	2.58 (2.55)	12.80 (12.15)	25.40 (25.45)
$[Pr(cyac)_3.(2,2'Bipy)]$ Green	41.53 (39.62)	2.91 (2.76)	12.75 (12.14)	25.68 (25.43)
$[Nd(cyac)_3.(2,2'Bipy)]$ Violet	41.29 (39.09)	2.89 (2.67)	12.68 (12.07)	26.12 (25.77)
$[Eu(cyac)_3.(2,2'Bipy)]$ White	40.70 (38.77)	2.5 (2.68)	12.50 (12.83)	27.13 (26.76)
$[Gd(cyac)_3.(2,2'Bipy)]$ White	40.32 (39.72)	2.48 (2.67)	12.38 (11.99)	27.82 (26.97)
$[Tb(cyac)_3.(2,2'\text{-}Bipy)]$ White	40.20 (38.77)	2.47 (2.57)	12.34 (11.81)	28.02 (28.12)
$[Dy(cyac)_3.(2,2'\text{-}Bipy)]$ White	39.95 (39.22)	2.45 (2.69)	12.27 (11.94)	28.47 (27.91)
$[Yb(cyac)_3.(2,2'Bipy)]$ White	39.23 (38.45)	2.41 (2.56)	12.04 (11.81)	29.77 (29.31)
$[Lu(cyac)_3.(2,2'Bipy)]$ White	39.10 (38.21)	2.40 (2.50)	12.00 (12.04)	30.00 —
$[Y(cyac)_3.(2,2'Bipy)]$ White	45.87 (44.62)	2.82 (3.03)	14.08 (13.60)	17.88 (17.50)

(cyac) = $(NCCH_2COO)$

Table 2—Analytical Data of [Ln(NCCH$_2$COO)$_3$.Phen] Compounds

Compound, Colour	Calc. (Found), %			
	C	H	N	Metal
[La(cyac)$_3$.(1,10 Phen)] White	44.14 (43.66)	2.46 (2.19)	12.26 (11.83)	24.33 (24.34)
[Pr(cyac)$_3$.(1,10 Phen)] Green	43.98 (43.07)	2.44 (2.32)	12.22 (12.06)	24.61 (24.71)
[Nd(cyac)$_3$.(1,10 Phen)] Violet	43.73 (43.00)	2.43 (2.19)	12.15 (12.17)	25.03 (24.84)
[Eu(cyac)$_3$.(1,10 Phen)] White	43.15 (42.33)	2.40 (2.25)	11.99 (13.14)	26.03 (26.00)
[Gd(cyac)$_3$.(1,10 Phen)] White	42.76 (42.38)	2.38 (2.23)	11.88 (11.97)	26.69 (26.25)
[Tb(cyac)$_3$.(1,10 Phen)] White	42.64 (42.40)	2.37 (2.03)	11.85 (11.65)	26.90 (27.70)
[Dy(cyac)$_3$.(1,10 Phen)] White	42.39 (42.00)	2.36 (2.59)	11.78 (12.00)	27.33 (27.00)
[Yb(cyac)$_3$.(1,10 Phen)] White	41.65 (41.83)	2.31 (2.13)	11.57 (11.60)	28.59 (28.45)
[Y(cyac)$_3$.(1,10 Phen)] White	48.38 (47.76)	2.69 (2.40)	13.44 (13.37)	17.07 (17.14)

(cyac) = (NCCH$_2$COO)

ceptibility was corrected for the presence of diamagnetic components.

Results and Discussion

Although derived from the hydrated parent tris-cyanoacetates, [Ln(NCCH$_2$COO)$_3$.2H$_2$O], the present complexes do not retain any water molecules. An attempt to obtain adducts with monodentate ligands such as C_5H_5N, $(C_2H_5)_2NH$, $(CH_3)_2SO$ or $(C_6H_5)_3PO$ was unsuccessful; instead, the original hydrated tris-cyanoacetate was obtained in each case. This strongly suggests that chelation plays an important role in the replacement of the two coordinated water molecules. It is interesting to note that only 1:1 adduct with Bipy could be formed. An attempt to obtain 1:2 adduct of Bipy from [Tb(NCCH$_2$COO)$_3$.2H$_2$O] was unsuccessful.

Similar to the hydrated parent compounds, these chelates also do not melt but decompose on heating to ~200°C. The non-volatility and insoluble nature of the compounds in organic solvents such as acetone, methanol, acetonitrile, tetrahydrofuran, benzene, chloroform, etc., indicate that in the solid state they are probably polymeric in nature.

The compounds are soluble in water in which they behave as non-electrolytes. An attempt to determine molecular weight by cryoscopic method in water suggested strong dissociation of the compound into non-ionic species.

Infrared spectra of all the present compounds display $\nu(C\equiv N)$ bands at 2300 cm^{-1} as compared to the band reported at 2254 cm^{-1} for sodium cyanoacetate[3]. A positive shift of the order of 46 cm^{-1} confirms coordination of C≡N group through nitrogen[2,4]. Further support[5] of the cyano-nitrogen bonding to metal atom is reflected by an increase in the $\delta(C\text{-}C\equiv N)$ from 394 to 420 cm^{-1}.

The magnitude of separation of the ν_{as} COO and ν_sCOO modes of the carboxylate group ($\Delta\nu$ COO) is a sensitive indicator of its mode of coordination[6,7]. It is very high for unidentate and significantly lower for bidentate bonding as compared to that for ionic (COO). The ν_{as}(COO) bands in the Bipy adducts lie in the range 1665 to 1700 cm^{-1}. It is interesting to note that there is a gradual increase in the ν_{as}(COO) as one moves from La to Lu in the series but the ν_s(COO) remains almost unaltered at 1420 cm^{-1}. Such a behaviour of the two ν(COO) bands parallels that of the (COO) groups of CF_3COO^- which are reported to unsymmetrically bridge two metal atoms[6]. A plot of ν_{as}(COO) vs polarizing power (e/r^2) of Ln^{3+} ion gives a curve which gradually rises from La to Lu and attains a maxima at Gd. Such a behaviour is not surprising if one takes into consideration the enhanced stability of Gd^{3+} due to its half filled 4*f* shell. In the case of yttrium, which belongs to *d*-block elements, the ν_{as}(COO) appears at 1700 cm^{-1}. This value is comparable to that of the higher members of the lanthanide family.

When Bipy and Phen form complexes with metal ions their infrared spectra undergo changes[8-11], particularly in the regions 1400-1650 cm^{-1} (C=C and C=N ring stretching vibrations), 950-1050 cm^{-1} (breathing modes) and 750-850 cm^{-1} (C-H out-of-plane deformation). In the case of Bipy complexes the ligand bands at 1590, 1570 and 1550 cm^{-1} show a gradual positive shift to the region 1630-1565 cm^{-1} as a result of complex formation. Also the strong band at 755 cm^{-1} of the free ligand splits into medium strong bands at about 740 and 800 cm^{-1} (ref.12). The split does not seem to be sensitive to the nature of the central metal ions present in the complex. The medium peak at 995 cm^{-1} in Bipy is assigned to ring breathing mode. On chelation, it shifts to 1020-1035 cm^{-1} region and appears as a strong band. There is a general tendency of this band to shift to higher wave number as one goes from La to Lu in the series. This shift to higher

frequency is expected in view of the higher polarizing power (e/r^2) with increase in atomic number in the series.

In Phen complexes, the infrared bands in the region 1400-900 cm^{-1} do not show any change on coordination but bands in the 900-700 cm^{-1} region show marked changes. Two strong bands at 735 and 850 cm^{-1} for free Phen (associated with the out-of-plane hydrogen deformation) split as a result of coordination. Coordination also causes a general upward shift of the bands in the 1600-1400 cm^{-1} region which are attributed to ring vibrations[12]. The 620 cm^{-1} band in uncomplexed Phen appears to be shifted to higher frequency and intensified on chelation[9,13].

New bands in the region 500-550 cm^{-1} for Bipy and Phen complexes are assigned to Ln-O stretching mode[14]. Also, bands at 410 cm^{-1} for Bipy and at 405 cm^{-1} for Phen are shifted to higher wave numbers and intensified on chelation[12,13].

It is interesting to note that the νLn-O (carboxylate) bands in the 500-600 cm^{-1} region occur at higher frequencies as one proceeds from La to Lu, indicating stronger bonding as the polarizing power (e/r^2) of the cation increases. The abrupt change at gadolinium has been attributed to the added stabilization caused by half filled $4f$ shell. A similar trend was observed by us in the case of hydrated triscyanoacetates[1]. This indicates that several factors, besides polarizing power are operating to determine the position of ν(Ln-O).

The νLn-N bands in the case of lanthanide chloride and nitrate complexes with Bipy or Phen are reported in the region 250-200 cm^{-1} (ref.13). In the present study the infrared spectra in the 300-200 cm^{-1} region are complicated because of the presence of two types of ν(Ln-N) bands, one due to Ln-N (cyano) and the other due to Ln-N (Bipy or Phen). In our earlier work with $[Ln(NCCH_2COO)_3.2H_2O]$, bands nears 280 cm^{-1} were assigned to νLn-N(cyano)[1]. Next lower band, therefore, can be assigned to νLn-N(ligand) band. It is noteworthy that there is a tendency for the νLn-Nband to shift to higher frequency with increasing atomic number of the metal atom. Similar to the ν(Ln-O) bands, ν(Ln-N) (ligands) bands also show an abrupt shift to higher wave number at gadolinium. The ν(Y-N) bands are comparable to ν(Lu-N) bands probably due to identical ionic radii.

The infrared studies strongly suggest that the nitrogen of the cyano group and both the oxygens of the carboxylate group are involved in coordination. Also the ligands Bipy and Phen form chelates under such conditions; therfore, the structure of $[Ln(NCCH_2COO)_3.L\text{-}L]$ is rather unlikely to be a monomer. More likely structure is a polymeric network with bridging carboxylate and cyano groups (where $NCCH_2COO^-$ ion acts in a tridentate manner and the ligand forms a chelate). Such a coordination polyhedron, with central metal atom having a coordination number of eleven, can be viewed either as a pentacapped trigonal antiprism or monocapped pentagonal antiprism. But in the absence of single crystal X-ray data, definite structures cannot be assigned. Trivalent rare earth ions with multidentate ligands are known to form complexes having coordination number from ten to twelve[15,16]. Such polyhedra usually possess low symmetry because of non-directional bonding of the Ln^{3+} ions. X-ray diffraction powder pattern data (Table 3) suggest the compounds to be isostructural.

TGA and DTA of some of the compounds were carried out in air. Decomposition of the Bipy adducts, in general, started at lower temperatures as compared to that of the Phen adducts of the same metal cyanoacetate. While the parent compound $[Pr(NCCH_2COO)_3.2H_2O)]$ started de-

Table 3—X-ray Data of the Rare Earth Cyanoaceate Complexes

$[La(cyac)_3.(2,2'Bipy)]$		$[Gd(cyac)_3.(2,2'Bipy)]$		$[Lu(cyac)_3.(2,2'Bipy)]$		$[Pr(cyac)_3.(1,10\ Phen)]$		$[Tb(cyac)_3.(1,10\ Phen)]$	
[d]Cukα	$I/I_o \times 100$	[d]CuKα	$I/I_o \times 100$	[d]CuKα	$I/I_o \times 100$	[d]CuKα	$I/I_o \times 100$	[d]CuKα	$I/I_o \times 100$
10.048	100	9.9579	100	9.7390	81.2	11.632	15.5	11.787	11.5
8.2143	29	8.1539	31.5	9.2510	100	9.1650	100	9.1650	100
7.5122	31.1	7.4995	64.1	8.5384	93.5	8.3456	22.6	8.3456	16.7
5.1434	10.6	5.0819	18.9	7.3872	66.7	6.1720	10.4	6.1892	12.07
4.9911	12.1	4.9415	14.8	6.2130	59.4	4.3744	10.1	4.6177	6.3
3.7760	12.1	3.8338	34.1	4.0042	39.1	4.0583	14.3	4.0257	12.6
3.6627	20.6	3.6627	21.5	3.8617	36.2	4.0221	13.7	3.9724	9.2
3.5758	11.8	3.5339	15.9	3.6479	31.2			3.6043	6.3

(cyac) = $(NCCH_2COO)$

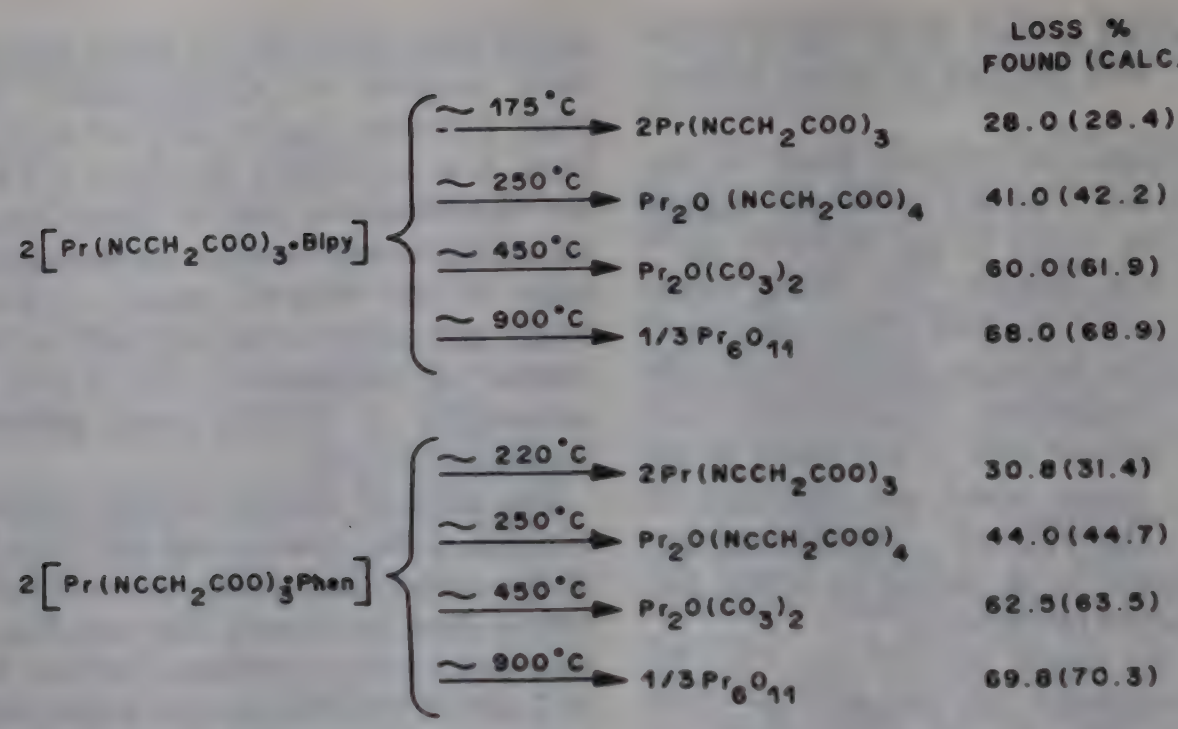

composing at 180°C, its Bipy and Phen adduts, $[Pr(NCCH_2COO)_3.Bipy]$ and $[Pr(NCCH_2COO)_3.Phen]$, showed steep decomposition at 145°C and 200°C respectively in their TGA curves. In the DTA curve the first endothermic peak for the Bipy adduct appeared at 146°C as compared to 240°C for the corresponding Phen adduct. This shows that Bipy is a weaker ligand than Phen. Highly conjugated Phen is expected to form a stronger complex than Bipy. TG studies further show that the decomposition pattern consists of four steps. The stable intermediates, as observed in thermograms, were separately isolated for $[Pr(NCCH_2COO)_3.Bipy]$ and $[Pr(NCCH_2COO)_3.Phen]$ adducts by independently heating small amounts of compounds in a furnace at various temperatures. In each case mass loss (%) and infrared spectra were studied to identify the probable phases. On the basis of studies carried out, the above mode of decomposition can tentatively be proposed for the compounds.

The end product in both cases, when the compounds are heated at 800-900°C, comes out to be the most stable oxide phase Pr_6O_{11} as confirmed by X-ray diffraction powder patterns.

Magnetic moments of $[Tb(NCCH_2COO)_3.Phen]$ (9.55 B.M.) and $[Tb(NCCH_2COO)_3.Bipy]$ (9.50 B.M.) were determined at room temperature and compared with that of the parent hydrated compound $[Tb(NCCH_2COO)_3.2H_2O]$ (9.6 B.M.). The obtained values are quite comparable with that of the Tb^{3+} ion reported in literature[1]. This indicates that the $4f$ electrons do not participate in bond formation, as expected.

In conclusion it can be stated that the strongly coordinated water molecules in $[Ln(NCCH_2COO)_3.2H_2O]$ can be displaced by chelating ligands like Bipy and Phen; like the parent compounds, these chelated adducts are also polymeric in solid states where cyano- and carboxylate groups form bridges between metal atoms. The Phen adducts are thermally more stasble than the corresponding Bipy adducts and the compounds decompose through the formation of oxycarbonates as the intermediate phase.

Acknowledgement

The authors express their gratitude to Dr J P Mittal, Head, Chemistry Division and Dr A J Singh, Head, Inorganic Chemistry and Pure Materials Section for their continued interest in the work. Thanks are also due to Dr C S P Iyer, Analytical Chemistry Division and Dr A B Phadnis, Water Chemistry Division for carrying out micro-analysis and thermo-gravimetric analysis respectively.

References

1 Vaidya M A, Desphande S G, Jain V K & Jain S C, *Inorg chim Acta*, **143** (1988) 123.
2 Jain S C & Rivest R, *Can J Chem*, **41** (1963) 2130.
3 Sinha D & Katon J E, *Appl Spectros*, **26** (1972) 599.
4 Jain S C & Rivest R, *Inorg Chem*, **6** (1967) 467.
5 Cartwright M, Edwards D A & Potts J M, *Inorg chim Acta*, **34** (1979) 211.
6 Bismondo A, Casellato U, Sitran S & Graziani R, *Inorg chim Acta*, **110** (1985) 175.
7 Graner C D & Hughes B, *Adv Inorgchem & Radiochem*, **17** (1975) 1.
8 Crawford N P & Melson G A, *J chem Soc (A)*, (1969) 427.
9 Schilt A A & Taylor R C, *J inorg nucl Chem*, **9** (1959) 211.

10 Sinha S P, *Spectrochim Acta*, **20** (1964) 879.
11 Hart F A & Laming F P, *J inorg nucl Chem*, **27** (1965) 1825.
12 Jain S C & Rivest R, *Inorg chim Acta*, **4** (1970) 291.
13 Ferraro J R, Basile L J & Kovacic D L, *Inorg Chem*, **5** (1966) 391.
14 Mehta P C & Tondon S P, *Proc of the 9th rare earth research conf*, Blacksburg, Virginia, Oct 10-14, 1971, Vol.1, p.64.
15 Bünzli J C G & Klein B, *The RE in modern science & technology* (Plenum, New York), Vol.3, 1981, p.97.
16 Bünzli J C G, Klein B, Wessner D, Schenk K J, Chapuis G, Bombien G & Peoli G de, *Inorg chim Acta*, **54** (1981) L43.

Indian Journal of Chemistry
Vol. 28A, February 1989, pp. 140-144

Synthesis & Characterisation of Co(II), Ni(II), Cu(II), Zn(II), Ru(II), Pd(II) & Pt(II) Complexes with Substituted Quinazoline (3H)-4-ones

B PRABHAKAR, K LAXMA REDDY† & P LINGAIAH*
Department of Chemistry, Kakatiya University, Warangal 506 009

Received 18 *January* 1988; *revised* 4 *April* 1988; *accepted* 2 *May* 1988

Complexes of Co(II), Ni(II), Cu(II), Zn(II), Ru(II), Pd(II) and Pt(II) with 2-methyl-3-acetaminoquinazoline-(3H)-4-one (MAQ) and 2-phenyl-3-acetaminoquinazoline-(3H)-4-one (PAQ) have been synthesized and characterised by analytical, conductivity, magnetic moment and infrared, electronic and ESR spectral data. Analytical data show that the complexes are of the thype ML_2X_2 [where M = Co(II), Ni(II) and Cu(II), L = MAQ/PAQ and X = acetate ion], Zn L $(CH_3COO)_2$ and $M'L_2Cl_2$, [M' = Ru(II), Pd(II) and Pt(II)]. All the complexes, except Pd(II) and Pt(II) complexes, are neutral in DMF. However, Pd(II) and Pt(II) complexes are found to be 1:2 electrolytes. Infrared spectral data indicate that MAQ and PAQ act as neutral bidentate ligands coordinating through carbonyl oxygen and imino nitrogen. Co(II), Ni(II) and Ru(II) complexes have been found to be octahedral, Cu(II) tetragonal and Pd(II) and Pt(II) complexes square-planar, whereas Zn(II) complexes are tetrahedral. Various ligand field parameters of Co(II) and Ni(II) complexes and ESR parameters of Cu(II) complexes have been calculated.

In continuation of our earlier work[1,2], we report here the synthesis and characterisation of Co(II), Ni(II), Cu(II), Zn(II), Ru(II), Pd(II) and Pt(II) complexes with 2-methyl-3-acetamino quinazoline (3H)-4-one (MAQ) and 2-phenyl-3-acetamino quinazoline (3H)-4-one (PAQ).

Materials & Methods

Anthranilic acid, hydrazine hydrate, acetic anhydride and other solvents used in this work were BDH reagents of AR grade. Ruthenium(III) chloride, palladium(II) chloride and platinum(II) chloride were obtained from Johnson Matthey Chemicals, London. Rest of the metal salts were obtained from Chempure Chemicals Limited, Bombay. MAQ and PAQ were prepared as reported in literature[3,4] and their purities checked by TLC and melting point data. The complex $RuCl_2(DMSO)_4$ was prepared by the literature method[5].

Preparation of the complexes

In the preparation of Co(II), Ni(II), Cu(II) and Zn(II) complexes the following general procedure was adopted. The metal salt solution (30 ml) in methanol was added dropwise to the ligand solution in methanol (50 ml) with constant stirring. In all the cases, the ligand concentration was in excess over that required by 1:3 (metal:ligand) ratio. The reaction mixture was refluxed on a water bath for 60-120 min and cooled. The solid thus obtained was filtered and washed several times with hot water and methanol and dried *in vacuo* over fused calcium chloride.

Ru(II) complexes

The complex, (dichloro) tetrakis (dimethyl sulphoxide) ruthenium(II), $[RuCl_2(DMSO)_4]$, is a convenient source for the preparation of a variety of mixed ligand ruthenium(II) complexes. The complex $[RuCl_2(DMSO)_4]$, was prepared by the method of Wilkinson *et al.*[5]. The complex, $[RuCl_2(DMSO)_4]$ (0.2 g) was suspended in toluene (30 ml) and refluxed for 1 hr with the appropriate ligand in acetone (30 ml). In each case 1:3 (metal:ligand) ratio was maintained. The whole suspension dissolved under reflux resulting in a clear solution. It was then evaporated under reduced pressure to remove the excess of solvent. The residue was treated with diethyl ether when the solid complex precipitated. This was filtered off, washed several times with diethyl ether, recrystallized from methanol-ether and dried *in vacuo*.

Palladium(II) and platinum(II) complexes

To a solution of metal(II) chloride (0.1 mol) in 0.1 *N* HCl was added a methanolic solution of the ligand (0.3 mol). The reaction mixture was refluxed on a water bath for 30-40 min. The complex precipitated out in neutral medium on cooling. It was filtered, washed several times with hot methanol and dried *in vacuo* over fused calcium chloride.

The analytical data (C, H, N) for the ligands and their metal complexes were obtained from the micro-analytical laboratory, Calcutta University, Cal-

†Present address: Department of Chemistry, Regional Engineering College, Warangal 506 004

Table 1—Analytical Data of the Complexes

Complex	Colour (m.p., °C)	Analysis Found (Calc.), %			
		M	C	N	H
$[Co(MAQ)_2(CH_3COO)_2]$	Brown (298)	9.64 (9.60)	51.06 (51.01)	13.74 (13.68)	4.58 (4.52)
$[Co(PAQ)_2(CH_3COO)_2]$	Brick red (296)	8.01 (7.95)	58.78 (58.65)	11.42 (11.39)	4.35 (4.30)
$[Ni(MAQ)_2(CH_3COO)_2]$	Brown (310)	9.61 (9.53)	51.08 (51.00)	13.75 (13.68)	4.58 (4.49)
$[Ni(PAQ)_2(CH_3COO)_2]$	Dark brown (305)	7.98 (7.79)	58.79 (58.52)	11.43 (11.33)	4.35 (4.30)
$[Cu(MAQ)_2(CH_3COO)_2]$	Green (300)	10.32 (10.22)	50.68 (50.51)	13.64 (13.58)	4.54 (4.49)
$[Cu(PAQ)_2(CH_3COO)_2]$	Dark green (310)	8.59 (8.48)	58.41 (58.38)	11.35 (11.28)	4.32 (4.29)
$[Zn(MAQ)(CH_3COO)_2]$	Colourless (315)	16.32 (16.25)	44.95 (44.88)	10.49 (10.38)	4.24 (4.18)
$[Zn(PAQ)(CH_3COO)_2]$	Colourless (310)	14.19 (14.08)	52.13 (52.07)	9.12 (9.06)	4.12 (4.08)
$[Ru(MAQ)_2Cl_2]$	Snuff (296)	16.67 (16.59)	43.56 (43.49)	13.86 (13.79)	3.63 (3.59)
$[Ru(PAQ)_2Cl_2]$	Snuff (320)	13.84 (13.79)	53.60 (52.56)	11.50 (11.45)	3.56 (3.49)
$[Pd(MAQ)_2]Cl_2$	Yellow (318)	17.40 (17.32)	43.18 (43.09)	13.74 (13.69)	3.59 (3.45)
$[Pd(PAQ)_2]Cl_2$	Dark yellow (312)	14.46 (14.32)	52.21 (52.09)	11.42 (11.38)	3.53 (3.44)
$[Pt(MAQ)_2]Cl_2$	Snuff (302)	27.87 (27.78)	37.71 (37.65)	12.00 (11.92)	3.14 (3.05)
$[Pt(PAQ)_2]Cl_2$	Snuff (305)	23.67 (23.58)	46.60 (46.51)	10.19 (10.10)	3.15 (3.07)

[a]All the complexes decomposes above the temp. cited.

cutta. The metal contents in the complexes were determined after heating the complexes to decomposition followed by titration with EDTA, using xylenol orange indicator in the case of cobalt and eriochrome black-T for zinc. Copper was estimated by iodometry and nickel by gravimetry using dimethyl glyoxime reagent using standard prcedures. Molar conductivities of the complexes in DMF were measured using a Digisun digital conductivity meter, model DI-909. Magnetic susceptibilities were measured at room temperature by Gouy method using $Hg[Co(SCN)_4]$ as the calibrant. Diamagnetic corrections were applied using Pascal's constants. Infrared spectra in the region 4000-200 cm^{-1} were recorded in KBr and nujol on a Perkin-Elmer infrared spectrophotometer model-283. Electronic spectra of the complexes were recorded in DMF on a Shimadzu multipurpose recording spectrophotometer model MPS-5000. The ESR spectra of Cu(II) complexes in solid state and in DMF solutions at room temperature were recorded on a Varian E-4, X-band spectrometer.

Results and Discussion

All the complexes are stable at room temperature and are non-hygroscopic. They decompose at higher temperatures (> 230°C). The complexes are insoluble in water and many of the common organic solvents, but are slightly soluble in acetone and appreciably in DMF. The analytical data of the complexes (Table 1) indicate their compositions as $CoL_2(CH_3COO)_2$, $NiL_2(CH_3COO)_2$, $CuL_2(CH_3COO)_2$, $ZnL(CH_3COO)_2$, $Ru\,L_2Cl_2$, $Pd\,L_2$ and $Pt\,L_2$, where L = MAQ or PAQ. The molar conductances in DMF at 1×10^{-3} *M* concentrations of all the complexes except Pd(II) and Pt(II) complexes are found to be in the range 10-20 $ohm^{-1}\,cm^2\,mol^{-1}$ indicating their non-ionic nature[6]. However, complexes of Pd(II) and Pt(II) show Λ_M in the range 100-120 $ohm^{-1}\,cm^2\,mol^{-1}$ indicating that they are 1:2 electrolytes[6].

Infrared spectra

In the infrared spectra of the ligands 2-methyl-3-acetamino quinazolin-(3H)-4-one and 2-phenyl-3-

acetamino quinazolin-(3H)-4-one, two types of carbonyl groups are observed, one due to quinazolone ring (>C=O) and the other due to (>C=O) of acetamino group. A strong band corresponding to ν(C=O) of the quinazolone ring is observed at 1690 cm^{-1}. This band is shifted to lower wavenumbers by 40-50 cm^{-1} in the IR spectra of all the complexes indicating that the quinazolone ring carbonyl oxygen is invariably coordinated to all the metal ions[7]. The ligands show another strong band at 1640 cm^{-1} assignable to the carbonyl of acetamino group, which remains unchanged in the spectra of all the complexes suggesting non-involvement of oxygen of this group on coordination[4,8]. A sharp band ~3300 cm^{-1} present in the ligands, may be assigned to stretching vibration of the amino N−H group[9]. A shift of this band by 30-50 cm^{-1} towards lower wave numbers in all the complexes indicates the participation of N−H group in the metal-ligand bond formation. The participation of nitrogen of amido group in coordination also supports the non-involvement of oxygen of carbonyl group of acetamino group because in that case a seven-membered ring would result. However, the nitrogen may be involved in coordination to form the stable five-membered ring chelate[10].

In addition, the infrared spectra of the complexes of Co(II), Ni(II), Cu(II) and Zn(II) show bands around 1510, 1450, 1340 and 710 cm^{-1} which can be assigned to ν_{as}(COO), ν_s(COO), δ(CH_3)− and δ(OCO) vibrations respectively indicating the presence of acetate ion in the coordination sphere[11]. Both the ligands are neutral and also form neutral complexes with all the metals except Pd(II) and Pt(II). The ionic type of Pd(II) and Pt(II) complexes (confirmed from the conductivity data) indicates that anions are present outside the coordination sphere.

The $RuCl_2(DMSO)_4$ complex shows a strong band in the region 1050-1100 cm^{-1} corresponding to the νS=O mode of S-bonded DMSO ligands[12]. Absence of this band in the complexes of Ru(II) indicates the replacement of DMSO by the MAQ and PAQ ligands. However, a new strong band appears in the far IR spectra of complexes of Ru(II) at 300 cm^{-1} indicating that chloride ion is present in coordination sphere. The participation of oxygen and nitrogen in coordination in all the complexes is further supported by the appearance of ν(M−O) and ν(M−N) bands at 400 and 500 cm^{-1} respectively in their far infrared spectra[13,14].

Electronic spectra & magnetic moments

The electronic spectra of Co(II) complexes exhibit three bands at 8100, 16900 and 19800 cm^{-1} which may be ascribed to the transitions $^4T_{1g}(F) \rightarrow {}^4T_{2g}(F)$ (ν_1), $^4T_{1g}(F) \rightarrow {}^4A_{2g}(F)$($\nu_2$) and $^4T_{1g}(F) \rightarrow {}^4T_{1g}(P)$($\nu_3$) respectively characteristic of octahedral geometry[10]. The Ni(II) complexes show bands at 9200, 14000 and 25300 cm^{-1} due to the $^3A_{2g}(F) \rightarrow {}^3T_{2g}(F)$ (ν_1), $^3A_{2g}(F) \rightarrow {}^3T_{1g}(F)$($\nu_2$) and $^3A_{2g}(F) \rightarrow {}^3T_{1g}(P)$($\nu_3$) transitions respectively in an octahedral field[15]. The octahedral geometry of Co(II) and Ni(II) complexes is further supported by the ratio of ν_2/ν_1 which lies around 2.0 and 1.60 respectively[16]. Various spectral parameters have been calculated according to the equations of Lever[17]. The calculated 10 *Dq* values of Co(II) and Ni(II) complexes suggest for these ligand a place between water and ammonia in the spectrochemical series. The *B*-values for the complexes are lower than those for free ion values which is an indication of orbital overlap and delocalization of *d*-orbitals. The present *B*-values are less than unity, suggesting considerable covalent character of the metal-ligand bonds. From the values of 10*Dq* and *B* thus obtained, the transition bands ν_1, ν_2 and ν_3 have also been calculated[17]. The experimental values are seen to be in good agreement with the calculated ones. The magnetic moments of the Co(II) and Ni(II) complexes are in the ranges expected for octahedral geometry[18,19].

Tetragonal Cu(II) complexes involve three transitions, viz. $^2B_{1g} \rightarrow {}^2B_{2g}$, $^2B_{1g} \rightarrow {}^2E_g$ and $^2B_{1g} \rightarrow {}^2A_{1g}$ but bands due to these transitions usually overlap to give one broad absorption band[20]. Both the present Cu(II) complexes under investigation show one such broad band in the region 15000-16000 cm^{-1} suggesting that these complexes are of tetragonal type. All the Cu(II) complexes are found to be paramagnetic and possess magnetic moment values corresponding to one unpaired electron (1.82 B.M.). The

Table 2—ESR Spectral Data of Cu(II) Complexes

Special Parameter	Complex	
	$[Cu(MAQ)_2(CH_3COO)_2]$	$[Cu(PAQ)_2(CH_3COO)_2]$
$g_\parallel$	2.23	2.22
$g_\perp$	2.05	2.04
$\lvert g \rvert$	2.11	2.10
α^2	0.52	0.47
β^2	1.05	1.11
γ^2	0.88	0.77
$r_\parallel^2$	0.54	0.52
$r_\perp^2$	0.45	0.36
$A_\parallel \times 10^5$ (cm^{-1})	13.3	13.5
$A_\perp \times 10^5$ (cm^{-1})	8.2	8.1
$\lvert A \rvert \times 10^5$ (cm^{-1})	11.6	11.7
G	4.77	5.77
λ	460	440

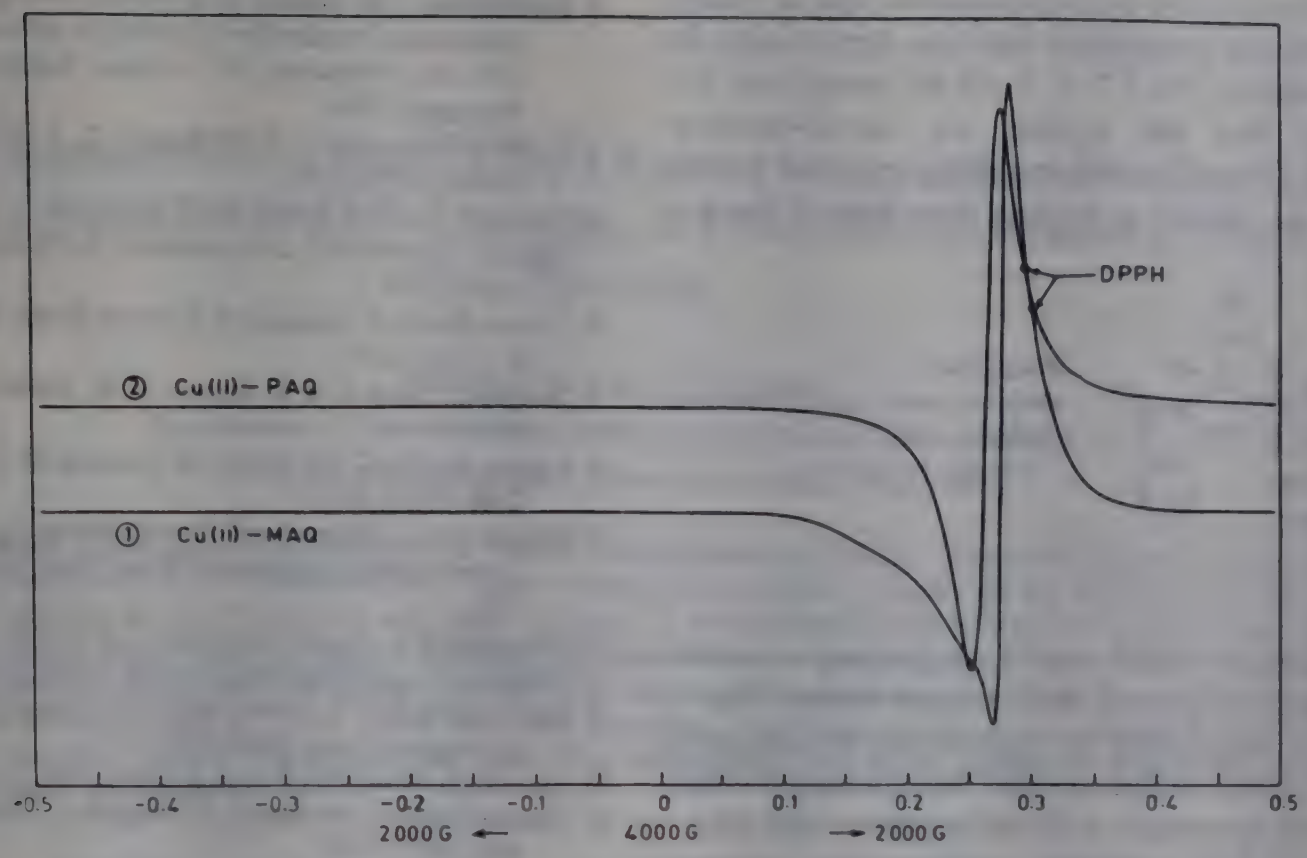

Fig. 1—ESR spectra of Cu(II) complexes

two spin-allowed $d-d$ transitions are observed in the Ru(II) complexes at 19000 and 24000 cm^{-1} corresponding to the $^1A_{1g} \rightarrow {}^1T_{1g}$ and $^1A_{1g} \rightarrow {}^1T_{2g}$ transitions respectively in the octahedral field[21]. The absence of splitting of lower energy band in the electronic spectra of Ru(II) complexes indicates, that there is no tetragonal distortion.

Pd(II) complexes exhibit two bands at 15000 and 20000 cm^{-1}, which may be due to $^1A_{1g} \rightarrow {}^1A_{2g}$ and $^1A_{1g} \rightarrow {}^1E_g$ transitions respectively characteristics of square-planar geometry[22]. The Pt(II) complexes show two bands at 20000 and 25000 cm^{-1} which may be assigned to $^1A_{1g} \rightarrow {}^1E_g$ and $^1A_{1g} \rightarrow {}^1A_{2g}$ transitions respectively characteristic of square-planar geometry[23]. All the Ru(II), Pd(II), Pt(II) and Zn(II) complexes are diamagnetic in nature.

ESR spectra

A representative one-line ESR spectra of Cu(II) complexes with 2-methyl-3-acetamino quinazoline(3H)-4-one and 2-phenyl-3-acetamino quinazoline(3H)-4-one are given in Fig. 1 and the ESR parameters are listed in Table 2.

The ESR spectra of polycrystalline samples of both the Cu(II) complexes exhibit two g values (Table 2) indicating the overall symmetry to be tetragonal around the copper(II) ion. No bands corresponds to $M_s = \pm 2$ transitions are observed in the spectrum ruling out any Cu-Cu interaction. The solid state spectra of Cu(II) complexes are similar to those obtained in solution at room temperature. Kivelson and Neiman[24] have demonstrated that for covalent environment $g_\parallel$ is less than 2.3 and for ionic environment, this is usually 2.3. Thus, the metal-ligand bonding in these complexes is regarded as covalent. The evaluation of ESR covalency parameters also supports this observation. From the observed 'g' value it is evident that the unpaired electron lies predominantly in the $d_{x^2-y^2}$ orbital. The complexes also show anisotropic ESR spectra with $g_\parallel > g_\perp$ characteristic of a tetragonal geometry. It may be noted that for the complexes with $d_{x^2-y^2}$ ground state, strong interaction along 'Z' axis is accompanied by increase in the value of $g_\parallel$. Strong axial bonding leads to an increase in the length of the bond in $X-Y$ plane which results in a decrease in both in-plane covalency and the energy of $d_{x^2-y^2}$ transition[25]. Both these effects tend to increase the value of $g_\parallel$. The ESR spectrum does not show any hyperfine splitting. However, $A_\parallel$ and $A_\perp$ values are calculated[26], by taking one third of the line widths at half maximum and A_0 as 1/3 $(A_\parallel + 2A_\perp)$.

The axial symmetry parameter G defined as $g_\parallel - 2.0023/g_\perp - 2.0023$ is shown to be a measure of the exchange interaction between copper centers in the polycrystalline solids. The present 'G' values indicate that there is no exchange interaction in solid state between the two copper centers[27].

Further, orbital reduction parameters viz, α^2, β^2,

γ^2, $r_\parallel^2$, $r_\perp^2$ and λ have been calculated. The α^2 values for the present complexes indicate appreciable in-plane covalency. As $r_\parallel^2 > r_\perp^2$ in all the complexes, it is concluded that the ligands are out-of-plane-π-bonded[28]. The spin-orbit coupling constant for the complexes is found to be less than that of the free

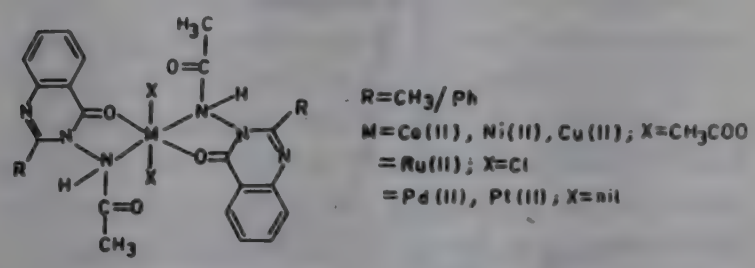

(I)

metal ion ($\lambda_0 = -828$ cm^{-1}), suggesting considerable mixing of ground and excited terms. The g-values are also useful for calculating the magnetic moments of the complexes and the calculated values are in good agreement with the experimental ones.

Based on their analytical, conductance, magnetic and infrared, electronic and ESR spectral data, the complexes have been assigned the structure (I).

Acknowledgement

One of the authors (BP) is grateful to the CSIR, New Delhi for the award of a senior research fellowship.

References

1 Laxma Reddy K, Sri hari S & Lingaiah P, *Indian J Chem*, **24A** (1985) 318.
2 Prabhakar B, Laxma Reddy K & Lingaiah P, *Indian J Chem*, **27A** (1988) 217.
3 Taylor Bogert Marston & Ross A Gortner, *J Am chem Soc*, **31** (1909) 943.
4 Ravishankar Ch, *Studies in synthesis, biological and pharmacological evaluation of some* 6,8-*dibromoquinazolin*-(3*H*)-*one derivatives*, Ph.D. thesis, Kakatiya University, Warangal, 1984.
5 Evans I P, Spender A & Wilkinson G, *J chem Soc* (*Dalton Trans*), (1973) 204.
6 Geasy W J, *Coord Chem Rev*, 7 (1971) 81.
7 Sahai R, Agarwal R S & Kushwaha S S, *J Indian chem Soc*, 7 (1982) 853.
8 Laxma Reddy K, Lingaiah P & Veera Reddy K, *Polyhedron*, 5 (1986) 1519.
9 Sengupta, Sahni S K & Kapoor R N, *Indian J Chem*, **20A** (1981) 692.
10 Laxma Reddy K, Sri Hari S & Lingaiah P, *Indian J Chem*, **23A** (1984) 172.
11 Nakamoto K, *Infrared and Raman spectra of inorganic and coordination compounds* (Wiley, New York) 1978, 229, 231.
12 Reynolds W L, *Progr Inorg Chem*, **12** (1970) 1.
13 Mishra N C, *J Indian chem Soc*, **55** (1978) 839.
14 Seetharama Rao T, Laxma Reddy K, Swamy S J & Lingaiah P, *Indian J Chem*, **24A** (1985) 942.
15 Sacconi L, *Trans Met Chem*, **4** (1968) 199.
16 Laxma Reddy K, Sri Hari S & Lingaiah P, *J Indian chem Soc*, **60** (1983) 1020.
17 Lever A B P, *J chem Educ*, **45** (1966) 711.
18 Figgis B N, *Introduction to ligand fields* (Wiley Eastern, New Delhi), 1966, 339.
19 Khulbe R C, Bhoon Y K & Singh R P, *J Indian chem Soc*, **9** (1981) 940.
20 Nishida Y & Kida S, *Coord Chem Rev*, **27** (1979) 275.
21 Preti C, Tosi G & Zannihi P, *J inorg nucl Chem*, **41** (1979) 485.
22 Gray H B & Ballhausen C J, *J Am chem Soc*, **85** (1963) 260.
23 Seetharama Rao T, Laxma Reddy K & Lingaiah P, *Indian J Chem*, (in press).
24 Kivelson D K & Naiman R, *J chem Phys*, **35** (1961) 149.
25 Smith D W, *J chem Soc, A* (1970) 3108.
26 Zacharias P S, Mary Elizabathe & Ramchandraiah A, *Indian J Chem*, **23A** (1984) 26.
27 Procter I M, Hathaway B J & Nicholis P, *J chem Soc, A* (1968) 1678.
28 Hathaway B J, *Struct Bonding* (*Berlin*), **14** (1973) 60.

Indian Journal of Chemistry
Vol. 28A, February 1989, pp. 145-149

Trace Determination of Iron(III) by a Kinetic Method Based onCatalase like Activity of $[(trien)Fe(OH)_2]^+$ Complex on Decomposition Rate of Hydrogen Peroxide

NISHI GUPTA & P C NIGAM*

Department of Chemistry, Indian Institute of Technology, Kanpur 208 016

Received 15 *December* 1987; *revised and accepted* 27 *May* 1988

A sensitive kinetic method is developed for the trace determination of Fe(III). The method is based on the catalase-like catalytic activity of $[(trien)Fe(OH)_2]^+$ (trien = triethylenetetraamine) complex on the decomposition rate of hydrogen peroxide at *p*H = 10.0 ± 0.02 and temp. = 25 ± 0.1°C. At moderately high concentration of hydrogen peroxide, the initial rate is linearly related to [catalyst]. A fixed-time procedure is used to obtain a linear calibration curve between the initial rate and [catalyst] in the ferric ion concentration range of 1.0×10^{-8} to 4.9×10^{-6} mol dm^{-3}. The detection limit is 1×10^{-8} mol dm^{-3} and maximum percentage error is 12.5 in the lower limit. The method is sensitive, accurate, inexpensive and rapid. The interferences from a large number of cations with the exception of Mn^{2+} are negligible.

In recent years, there have been reports that many complexes of transition metals are more effective catalysts than their aquo metal ions in catalysing the decomposition of H_2O_2. The discovery by Wang[1] that the trien complex of Fe(III) possesses a catalase-like activity, though of a lesser order (catalase has four active sites while this complex has two) for the decomposition of H_2O_2 prompted us to investigate the analytical possibilities of this reaction for trace determination of Fe(III). One observation of considerable analytical interest to us is that, barring Mn(II), the presence of many cations does not affect the rate of decomposition reaction materially. Hence trace determinationof Fe(III) in the presence of a large number of cations has been investigated.

Materials and Methods

Hydrogen peroxide (30% v/v, AR, BDH) was purified by distillation under reduced pressure (60 mm Hg) after removing any Fe(III) and other cations by percolation through a column of acid-regenerated Dowex 50X-8 resin (50-100 mesh). The concentration of H_2O_2 in the distillate was determined by titration against standard potassium permanganate. Stock solutions of ferric perchlorate and trien were prepared in doubly distilled water. The trien complex of ferric ions was prepared by mixing ferric perchlorate with trien taken in 1000-fold excess. Sodium hydroxide (AR, BDH) or perchloric acid 70% (AR, BDH) were used for adjusting the *p*H at any desired value. To avoid complications, buffers were not used. The effect of ionic strength was negligible as tested by earlier workers[1] as well as by us. Scrupulous cleaning of apparatus was very necessary for obtaining consistent results. All glassware were rinsed with a solution of 10^{-2} *M* NaCN at *p*H 9, washed with water, treated with 10^{-2} *M* EDTA at *p*H 9, and again rinsed many times with triply distilled water. This could ensure removal of any trace metal impurities held on the glass surfaces. Finally the apparatus was steamed before use.

Procedure

The reactant solutions were equilibrated at 25 ± 0.1°C for 30 min. The reaction was regarded as starting when a solution of $[(trien)Fe(OH)_2]^+$ was quickly poured into a reaction vessel containing a solution of H_2O_2. Aliquots of the reaction mixture were drawn at regular time intervals and poured into excess standard ceric sulphate solution. Ceric sulphate remaining unconsumed at any time, which also corresponded to the amount of H_2O_2 remaining undecomposed, was determined by titration with standard ferrous ammonium sulphate using *o*-phenanthroline as an indicator.

In order to correct for traces of Fe(III) that may be present in the reagents or in glassware as an impurity, a blank determination was performed for each kinetic run with trien and H_2O_2 but without Fe(III). The initial rates corresponding to each [Fe(III)] were determined by the plane mirror method[2]. For drawing calibration curves, the concentration changes of H_2O_2 for a fixed-time interval were plotted against concentration of the

$[(trien)Fe(OH)_2]^+$ complex. This is often referred to as the fixed-time procedure for determining initial rate.

Results

Effect of varying hydrogen peroxide and $[(trien)Fe(OH)_2]^+$ *concentrations*

The plots showing the effect of varying $[H_2O_2]$ on the initial rate of the decomposition at three different concentrations of $[(trien)Fe(OH)_2]^+$ complex are Michaelis-Menten type saturation curves (Fig. 1). The values of initial rates (or turnover numbers) are higher than those reported by Wang[1]. If any inhibitor were present in the system the initial rates (or turnover numbers) were bound to be lower. As mentioned in the experimental section, our samples of H_2O_2 had been scrupulously purified while Wang[1] made no mention about the purity of H_2O_2 employed. Under specified conditions, the initial rate is linearly related to $[(trien)Fe(OH)_2]^+$ concentration in the lower concentration range, attains a maximum value and then decreases (Fig. 2). This decrease can be explained if it is assumed that the given complex dimerises giving, perhaps, oxygen-bridged dimeric species which is non-catalytic. The change in catalytic character can be understood if the mechanism proposed by Wang[1] is assumed to hold good.

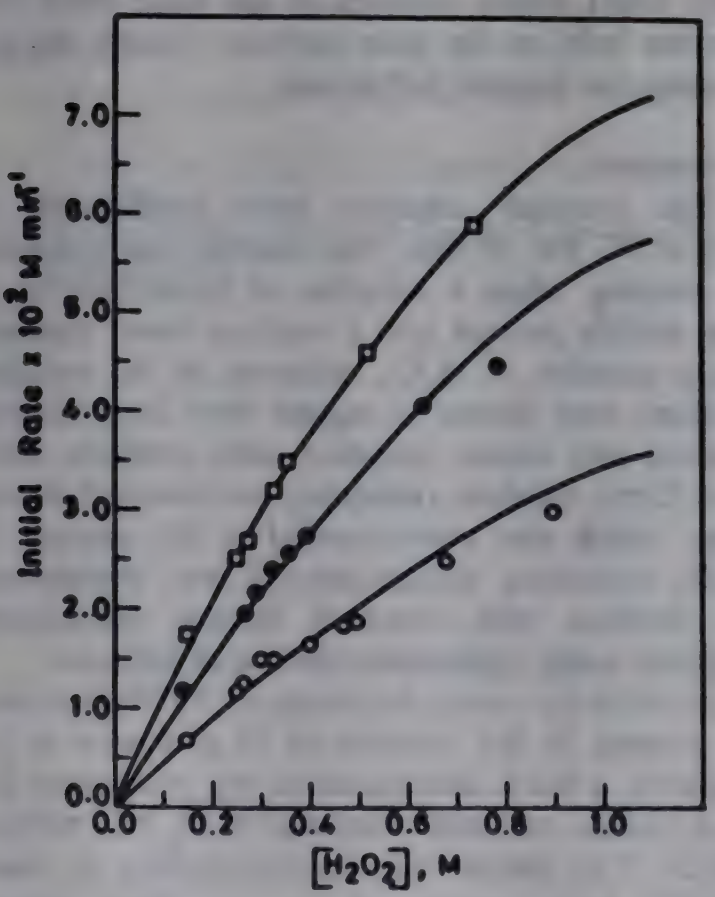

Fig. 1—Hydrogen peroxide decomposition rate as a function of $[H_2O_2]$ at $pH = 10.0 \pm 0.1$, temp. $= 25 \pm 0.1°C$ and $[(trien)Fe(OH)_2]^+ = 6.3 \times 10^{-7}$ mol dm^{-3} (□); 4.7×10^{-7} mol dm^{-3} (●); and 3.15×10^{-7} mol dm^{-3} (○)

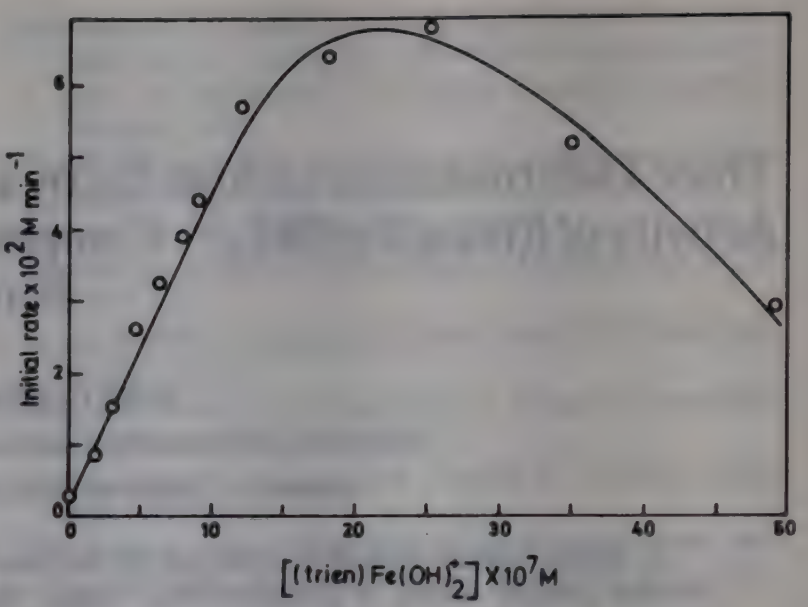

Fig. 2—Hydrogen peroxide decomposition rate as a function of $[(trien)Fe(OH)_2]^+$ at $pH = 10.0 \pm 0.1$ and temp. $= 25 \pm 0.1°C$

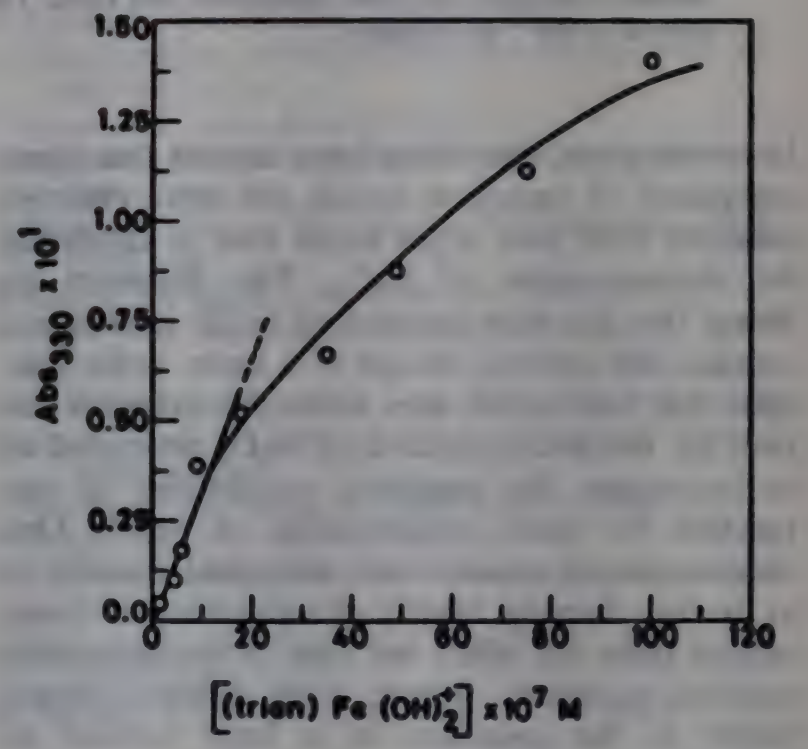

Fig. 3—Absorbance of $[(trien)Fe(OH)_2]^+$ at 330 nm as a function of concentration

Table 1—Effect of Various Interfering Ions

$[H_2O_2] = 0.35$ mol dm^{-3}, $[Fe^{3+}] = 6.3 \times 10^{-7}$ mol dm^{-3}, $[trien] = 4.8 \times 10^{-3}$ mol dm^{-3}, $pH = 10.0 \pm 0.02$, temp. $= 25° \pm 0.1°C$

Ion	Concentration (10^6 mol dm^{-3})	$[Fe^{3+}]$ found (10^7 mol dm^{-3})	Error %
Ni^{2+}	6.3	5.75	8.7
Pb^{2+}	6.3	5.76	8.6
Cu^{2+}	6.3	5.56	11.8
Ag^{+}	6.3	5.83	7.5
Mn^{2+}	6.3	5.76	8.6
Co^{2+}	6.3	5.76	8.6
Al^{3+}	6.3	6.20	1.6

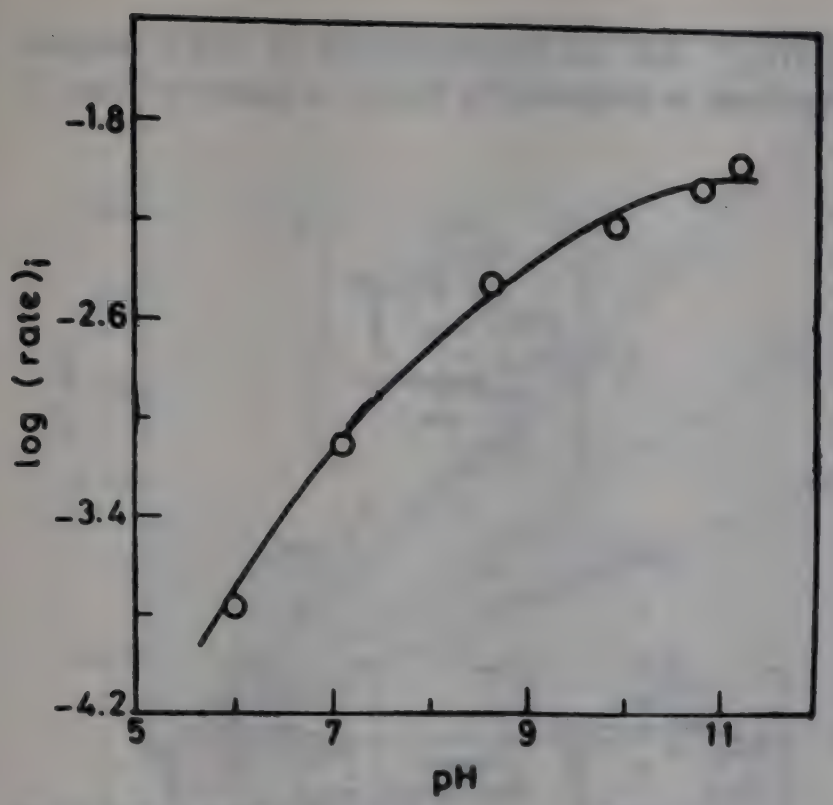

Fig. 4—Effect of *p*H on decomposition rate of hydrogen peroxide, $[Fe^{3+}] = 6.3 \times 10^{-7}$ mol dm^{-3}, [trien] $= 4.8 \times 10^{-3}$ mol dm^{-3}, temp. = 25°C

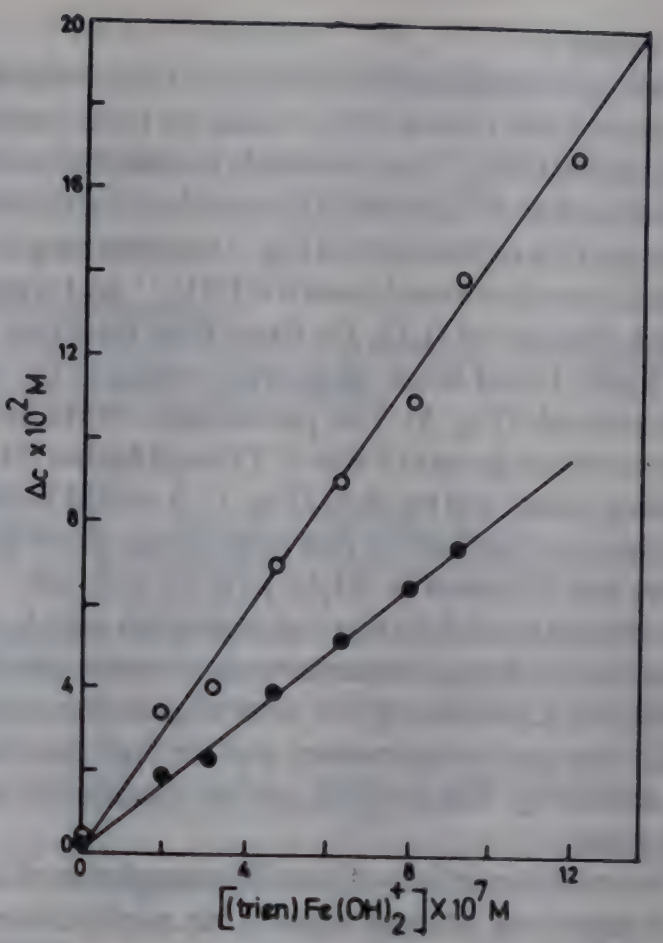

Fig. 5—Calibration curves between $[(trien)Fe(OH)_2]^+$ and initial rate [(○) Concentration changes in 5 min (ΔC_5); and (●) concentration changes in 2 min (ΔC_2)]

An evidence for dimerization can be provided by considering the spectral changes of $[(trien)Fe(OH)_2]^+$ at different concentrations. Of the two peaks observed at 310 and 330 nm the height of the first relative to the second enhances as the concentration of the complex increases from 9.7×10^{-7} to 7.5×10^{-6} mol dm^{-3}. If the first peak is assigned to the dimer and the second to the monomer, the ratio (A_{310}/A^2_{330}) gives a measure of the equilibrium constant for the transformation: $2\,\text{monomer} \overset{K}{\rightleftharpoons} \text{dimer}$. The ratio was found to be reasonably constant (12.7 ± 1.6) in this concentration range confirming the existence of monomer ⇌ dimer equilibrium.

It is also interesting to note that the expected Beer's law relationship between [complex] and absorbance at 330 nm begins to deviate from linearity (Fig. 3) above the concentration level where the catalytic activity also starts decreasing (Fig. 2). Thus our postulate about loss of catalytic power of the complex $[(trien)Fe(OH)_2]^+$ because of dimer formation at higher concentration is reasonable. Similar dimerization is known also for some other complexes of Fe(III), the most well known examples being formation of $[Fe_2(CN)_{10}]^{4-}$ from $[Fe(CN)_5H_2O]^{3-}$ and of $[Fe_2L_2O]$ from [FeL(OH)], where L = EDTA, HEDTA and CYDTA[4] (EDTA = ethylenediaminetetraacetic acid; HEDTA = N-hydroxyethylethylenediaminetriacetic acid and CYDTA = 1,2-cyclohexanediaminetetraacetic acid).

Effect of pH

The effect of varying *p*H on the rate of decomposition of H_2O_2 is shown in Fig. 4. The rate increases linearly and then levels off. This is not unexpected and is due to a progressive increase in the relative concentration of the reactive species, viz. $[(trien)Fe(OH)_2]^+$ complex as *p*H changes from seven to ten. Above *p*H 10 the formation of $[(trien)Fe(OH)_2]^+$ is complete and hence the rate attains a limiting value.

Table 2—Concentration Change of H_2O_2 at Fixed Time (ΔC_t) as a Function of [Iron(III)]

$[H_2O_2] = 0.35$ mol dm^{-3}, *p*H = 10.0 ± 0.02, temp. = 25°C ± 0.1°C

$[Fe^{3+}] \times 10^7$ (mol dm^{-3})	$\Delta C_2 \times 10^2$ (mol dm^{-3})	Error (%)	$\Delta C_5 \times 10^2$ (mol dm^{-3})	Error (%)
0.1	0.4	12.2	0.5	10.0
2.0	2.25	8.2	3.4	12.5
3.15	1.9	6.1	4.0	9.5
4.7	4.0	5.1	7.0	4.4
6.3	5.2	1.9	9.0	3.3
8.0	6.5	0.8	11.0	6.2
9.2	7.45	1.35	14.0	2.9
12.0	—	—	17.0	2.9

ΔC_2 and ΔC_5 indicate the concentration changes within 2 and 5 minutes respectively

Effect of interfering cations

The effect of a large number of cations when present in ten-fold excess over $[Fe^{3+}]$ has been investigated and the results are given in Table 1.

Discussion

Having investigated the conditions under which the decomposition rate of H_2O_2 would be most sensitive to $[(trien)Fe(OH)_2]^+$ and relatively insensitive to other factors such as *p*H and $[H_2O_2]$, we rechecked the initial linear portion of the curve of Fig. 2 for obtaining a calibration curve between $[(trien)Fe(OH)_2]^+$ and concentration changes of H_2O_2 for fixed-time intervals of 2 and 5 min. Good linear plots were obtained for both time intervals (Fig. 5). The percentage errors for the two curves are given in Table 2. Though higher $[H_2O_2]$ (limiting value) will be ideal (Fig. 1), it would become an expensive method in that case. Since good linear curves are obtained at $[H_2O_2] = 0.35$ mol dm^{-3} we have chosen to stick to this concentration which gives a reasonable change in concentration under specified conditions. Considering low level of concentration of Fe(III) that can be determined and the high specificity and sensitivity, this method can be considered to be very good.

The catalytic activity of iron(III) complexes of some other negatively charged ligands, viz. nitrilotriacetate ion (NTA), ethylenediaminediacetate ion (EDDA) and ethylenediaminetetraacetate ion (EDTA) has been investigated before[1]. Though these ligands produced chelates of somewhat similar structure, they possessed negligible catalytic activity compared to the trien complex. This lack of reactivity has been attributed to an increase in ionic character of the Fe – O bond in these chelates. A recent investigation by Oakes and coworkers[5] demonstrated, however, that the chelate $[Fe(EDTA)(OH_2)]^{2-}$ is also a good catalyst though not as good as $[(trien)Fe(OH)_2]^+$ (this work).

Wang[1] also tested the catalytic activity of quite a few cations in the presence of trien and came to the conclusion that only $[(trien)Fe(OH)_2]^+$ and to a much lesser extent $[(trien)Mn(OH)]^+$ show remarkable catalytic activity. According to him chelates of many other cations, however, showed negligible catalytic activity compared to chelates of Fe(III) and Mn(II). These included Mg(II), Al(III), Ca(II), Cr(III), Co(III), Ni(II), Cu(II), Zn(II), Sr(II), Ag(I), Cd(II), Ba(II), Tl(I) and Pd(II). The high degree of specificity of Fe(III) and Mn(II) is not easy to explain because many ions listed above possess same charges and comparable ionic radii. The comparative catalytic activities of both $[(trien)Fe(OH)_2]^+$ and $[(trien)Mn(OH)]^+$ are, perhaps, understandable because they are isoelectronic. The presence of a large number of cations in about ten-fold excess causes a maximum error of 12.5%. Even Mn(II) causes an interference comparable to other ions listed in Table 1 at this low concentration though it may cause more serious interference if present in higher concentration.

The mechanism of catalytic activity of $[(trien)Fe(OH)_2]^+$ for the decomposition of H_2O_2 in basic medium, as proposed by Wang[1], is shown in Chart 1.

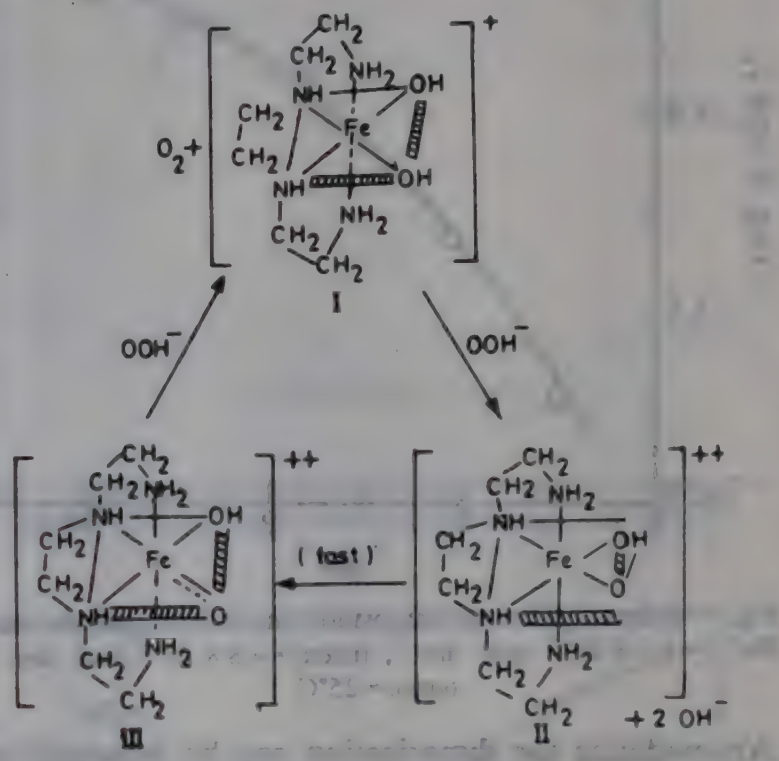

Chart 1—Mechanism of catalytic action of $[(trien)Fe(OH)_2]^+$ for the decomposition of hydrogen peroxide

Trien forms a quadridentate chelate with ferric ion. Steric considerations favour structure(I) where one primary nitrogen atom is above and the other below the square plane and two OH groups occupy two adjacent d^2sp^3 coordination sites. In the presence of H_2O_2 both the OH substituents can be displaced by OOH^- ion, the latter being capable of forming two coordinate links with Fe(III) through oxygen atoms. The resulting chelate(II) is unstable because the original O – O bond length of 1.3 Å in peroxide ion tends to stretch until the second activated complex (III) is formed. The activation energy of about 17 kcal mol^{-1} for cleavage of O – O bond in hydrogen peroxide is considerably lowered to 7 kcal mol^{-1} in the presence of $[(trien)Fe(OH)_2]^+$ complex[6] because of compensation in energy provided by the simultaneous formation of a stable Fe – O bond as shown in compound (III). This compound can readily react with a second OOH^- to yield oxygen and regenerate compound (I). Wang[1] also provided supporting evidence for the mechanism proposed by him.

The loss of catalytic activity with increase in concentration of $[(trien)Fe(OH)_2]^+$ in our study becomes understandable because dimerization, possibly to give oxygen-bridged dimeric species, takes away the two adjacent OH sites where the splitting mechanism is initiated. It has been shown[1] that replacement of quadridentate trien by pentadentate tetren, gives a complex of practically no catalytic activity. This is due

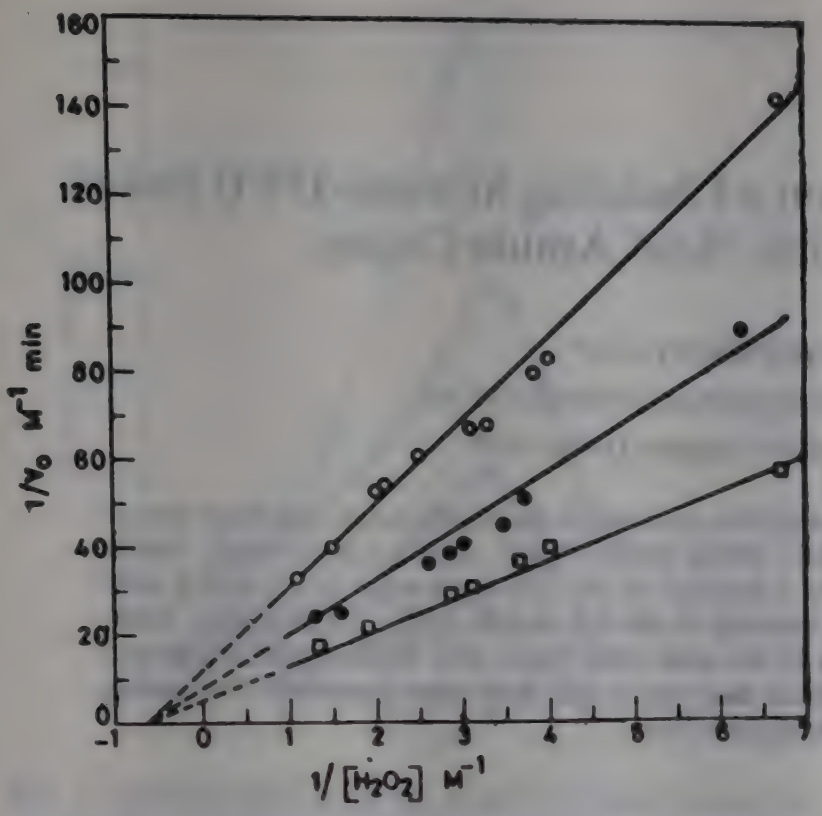

Fig. 6—Lineweaver-Burk plots for estimating K_M

to loss of one of the OH groups necessary for the operation of the splitting mechanism discussed above. The Lineweaver-Burk plots between $1/v_0$ (reciprocal of initial rate) and $1/[H_2O_2]$ at three different [catalyst] are given in Fig. 6 and their extrapolation to abscissa intercept, enables one to estimate the value of $K_m = 1.56 \pm 0.2$ mol dm^{-3}†. K_m is a rough measure of the affinity of the catalyst for the substrate, i.e. H_2O_2. A higher value of K_m would imply that the catalyst $[(trien)Fe(OH)_2]^+$ requires a relatively high concentration of H_2O_2 to attain its half maximal rate of catalysis.

Acknowledgement

The authors thank Dr R M Naik, for valuable help rendered from time to time.

References

1 Wang J H, *J Am chem Soc*, 77 (1955) 4715.
2 Frost A R & Pearson R G, *Kinetics & mechanism* (John Wiley, New York) (1970).
3 Espenson J H & Walenuk S G, *J inorg Chem*, 11 (1972) 2035.
4 Wilkins R G & Yelin R E, *Inorg Chem*, 8 (1969) 1470.
5 Francis K C, Cummins D & Oakes J, *J chem Soc Dalton Trans*, (1985) 493.
6 Tinoco I (Jr), Sauer K & Wang J C, *Physical chemistry*, (Prentice Hall, New Jersey) 1978, pp. 328.
7 Lehninger A L, *Principles of biochemistry* (CBS Publishers Delhi) 1984, pp. 216.

† This value is higher compared to that ot catalase ($K_M = 0.025$ mol dm^{-3}) and some other catalytic species[7] and comparable to the values obtained by us from the data of Wang[1].

Indian Journal of Chemistry
Vol. 28A, February 1989, pp. 150-153

Selective Separation of Uranium(VI) on a Chelating Styrene-DVB Based Resin Containing Quinaldinic Acid Amide Group

(Miss) NIYATI DAS & JYOTIRMOY DAS*

Department of Chemistry, University of Burdwan, Burdwan 713 104

Received 21 *January* 1988; *revised and accepted* 11 *May* 1988

A new chelating styrene-DVB based resin containing quinaldinic acid amide functional group, has been synthesised and characterised. The sorption patterns of Na(I), K(I), Be(II), Ca(II), Mg(II), Zn(II), Cd(II), Cu(II), Pb(II), Ni(II), Bi(III), Fe(III), Ti(IV) and U(VI) have been studied as a function of *p*H. The resin sorbs U(VI) over a wide range of *p*H (1.0 to 4.0) with a maximum sorption of 0.32 mmol/g at *p*H 3.5 to 4.0. Zn(II), Cd(II), Cu(II), Ni(II), Pb(II), Fe(III) and Ti(IV) are also sorbed to different extents by the resin while Na(I), K(I), Be(II), Ca(II), Mg(II) and Bi(III) are not sorbed. Conditions for separation of U(VI) from these metal ions have been identified. The eluting agent used for U(VI) is 3 *N* HNO_3 and the recovery recorded is about 99.9%.

Very few chelating ion exchangers[1-3] have been used for the separation and preconcentration of U(VI), among which N-phenyl and N-methyl substituted hydroxamic acid resins[4] are worth special mention. The aim of the present investigation was to develop a chelating ion-exchanger for the selective and rapid separation of the trace amounts of U(VI) from other metal ions. In this work a new styrene-DVB (8%) based chelating resin containing quinaldinic acid amide as a functional group has been synthesised and used for the preconcentration and separation of U(VI) from various metal ions.

The resin reported in this work has a much higher sorption capacity for uranyl ion compared with those of the other resins developed so far, exhibits a smooth peak of sorbance and does not require any gradient elution.

Materials and Methods

An atomic absorption spectrophotometer (Shimadzu AA-646) and a double beam UV-visible spectrophotometer (Shimadzu Acculab 20) were used for measurement of the concentrations of the metal ions. A digital *p*H meter (Sambros-335) was used for adjustment of *p*H. Infrared spectrum was recorded in KBr matrix on a Beckmann Acculab-10 IR spectrophotometer. Nitrogen was determined by a standard Micro-Duma's apparatus. A gravity-flow column with an appropriate reservoir was used as holder of the ion exchange resin.

Uranium solution was prepared from uranyl nitrate (E. Merck) and the metal content was determined by the standard method[5]. The stock solutions of various metal ions were prepared from their salts or oxides and estimated following standard methods.

Buffer solutions were prepared by mixing different proportions of standard solutions of sodium chloride and hydrochloric acid (*p*H 0.5 to 3.5), acetic acid and sodium acetate (*p*H 3.5 to 5.9) and Na_2HPO_4 and KH_2PO_4 (*p*H 5.9 to 8.0). During studies on separation from lead, HNO_3 and NaOH were used to control the *p*H.

Synthesis of the resin

Styrene-DVB polymer beads (80-100 mesh size) containing 8% DVB (Thermax Private Ltd., Poona, India) was nitrated using a mixture of H_2SO_4 and HNO_3. After washing the nitrated product with water, it was reduced to aminopolystyrene by tin (E. Merck) and conc. hydrochloric acid. The aminated product was then condensed with quinaldinyl chloride[6] by refluxing the mixture in toluene medium on a waterbath for 24 hr. A schematic diagram of the synthesis of the resin is given below:

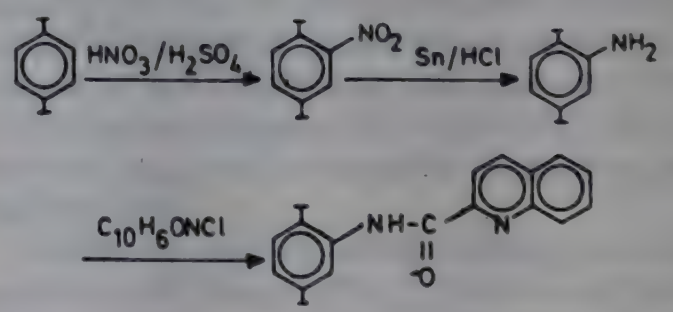

Schematic Diagram

Determination of sorption capacity of the resin for U(VI) and other metal ions

The sorption capacity of the resin for different metal ions was determined by batch and column

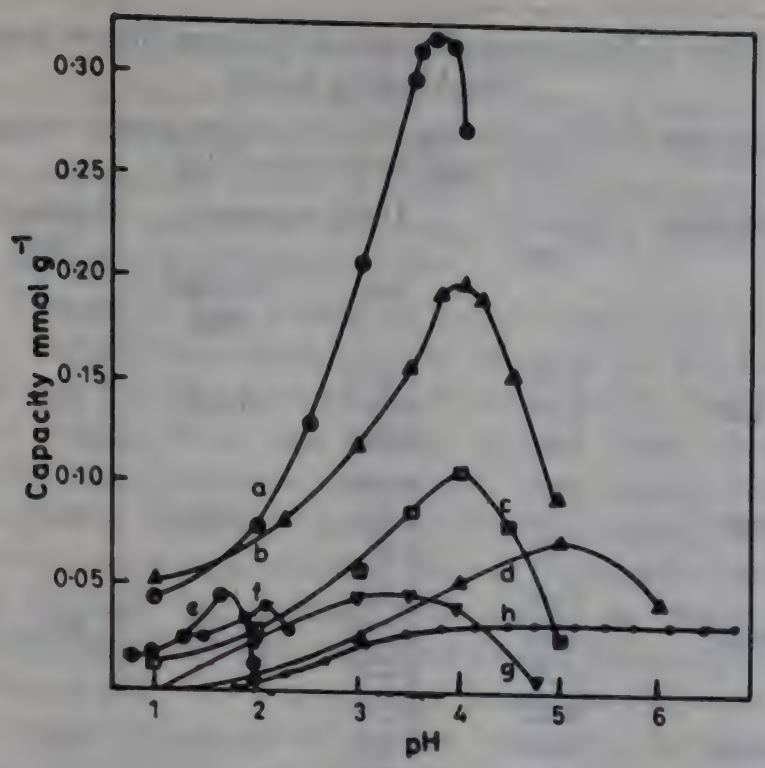

Fig. 1—Sorption capacity of the resin for different metal ions as a function of *p*H [(a) U(VI), (b) Pb(II), (c) Cu(II), (d) Cd(II), (e) Fe(III), (f) Ti(IV), (g) Ni(II) and (h) Zn(II)]

opeations. In batch operation, ~0.5 g of the air-dried resin was stirred on a magnetic stirrer for 24 hr with an excess of the desired metal ion solution of known strength (0.1 *M*) and volume (10 ml); the *p*H was controlled by a suitable buffer. The sorbed metal ions were eluted by using appropriate eluting agents [2*N* H_2SO_4 for Na(I), K(I),Ca(II), Mg(II),Zn(II), Cd(II), Cu(II), Ni(II) and Fe(III); 4*N* H_2SO_4 for Ti(IV); 3*N* HNO_3 for Be(II), Pb(II), Bi(III) and U(VI)]. The whole process was repeated for different *p*H values. The eluted metal ions and also the metal ions left in the wash solution were determined following standard methods. The sorption capacity of each of these metal ions against *p*H has been shown in Fig. 1.

In column operation, a glass column (1 cm i.d., 30 cm length) was packed with ~22 g resin. The resin was initially swollen with 2*N* HCl and then washed with deionised water. The packed column was washed with appropriate buffer. The flow rate was adjusted at 0.5-1.5 ml/min. Calculated excess amount of the desired metal ion (150 ml, 0.1 *M*), at desired *p*H, was passed through the column, washed with appropriate buffer and eluted with suitable eluting agents as stated earlier. The sorption capacity in column operation was slightly lower than the capacity in batch operation. Concentrations of different metal ions left in the washings and after elution from the resin were determined by an appropriate method, e.g., for Ca(II), and Mg(II) by titration with EDTA, for Na(I), K(I), Zn(II), Cd(II), Cu(II), Ni(II), and Fe(III) by atomic absorption/flame emission spectrometry and for

Table 1—Sorption Capacity of Uranium(VI) on Quinaldinic Acid Amide Resin

Batch Method*			Column Method†		
*p*H	Amount of resin (g)	Capacity (mmol g^{-1})	*p*H	Amount of resin (g)	Capacity (mmol g^{-1})
1.0	0.59385	0.05	1.0	22	0.03
2.0	0.61391	0.08			
2.5	0.55329	0.13	2.5	22	0.1
3.0	0.65732	0.21	3.0	22	0.17
3.5	0.53714	0.30			
3.7	0.56233	0.32	3.7	22	0.28
4.0	0.57127	0.28	4.0	22	0.26

*U(VI) taken = 10 ml of 0.1 *M* solution; †U(VI) taken = 150 ml of 0.1 *M* solution

Be(II)[7], Pb(II), Bi(III) and U(VI)[8] by colorimetry using standard organic reagents. The results of the determination of maximum sorption capacities of uranium(VI) studied by both batch and column operations are given in Table 1.

Separation and determination of uranium in uraninite ore

A weighed amount of the ore (200-400 mg) was treated first with dil. HNO_3 and then with 5 ml of conc. H_2SO_4 following a standard procedure[9]. Finally, the volume was made upto 250 ml. The solution was adjusted to *p*H ~ 1.0, and 10 ml EDTA (~1 *M*) was added. The *p*H of the solution was raised to ~4.0. Excess of EDTA did not affect the sorption capacity of U(VI) around *p*H ~ 4.0 but suppressed the exchange of other metal ions present in the solution and also prevented precipitation due to hydrolysis. The solution was then percolated through the resin column and uranium was eluted with 3*N* HNO_3, as described earlier.

Results and Discussion

Characterisation of the resin

The resin being a new one, was characterised by its water regain value, infrared spectrum, its stability towards acids and alkali, elemental analysis and metal exchange capacity.

Water regain value was observed to be 0.37 g/g, indicating appreciable sorption capacity of the resin[10]. Infrared spectrum of the resin showed a band at 1500 cm^{-1} indicating the presence of −CONH− grouping. In addition to this sharp band, the IR spectrum exhibited medium bands at 1615, 1600 and 1438 cm^{-1} which are very close to the ring breathing bands[11] of quinaldinic acid.

Table 2—Separation of Uranium(VI) from Diverse Ions

[Amount of uranium(VI) = 0.23 mg; *p*H = 3.7 (or 1 for*) column: glass; 1 cm i.d.; 30 cm height; resin taken = 22g]

Metal ions	Amount (mg)	U(VI) recovered (mg)	U(VI) recovered average (mg)	Recovery (%)
Na(I)	0.50	0.23	0.23	100
	1.00	0.23		
	1.50	0.23		
K(I)	1.0	0.23	0.23	100
	2.0	0.23		
	3.0	0.23		
Be(II)	0.116	0.23	0.229	99.8
	0.232	0.23		
	0.348	0.229		
Ca(II)	0.60	0.23	0.23	100
	1.20	0.23		
	1.80	0.23		
Mg(II)	1.0	0.23	0.23	100
	1.5	0.23		
	2.0	0.23		
Zn(II)*	0.151	0.228	0.228	99.1
	1.51	0.228		
	3.02	0.227		
Cd(II)*	1.20	0.228	0.229	99.8
	2.40	0.229		
	3.60	0.229		

Table 3—Separation of Uranium(VI) from Diverse Ions Using Masking Agents

[Amount of U(VI) = 0.23 mg; *p*H = 3.7; column: glass; 1 cm i.d.; 30 cm height; resin taken = 22 g]

Metal ions	Amount (mg)	U(VI) recovered (mg)	U(VI) recovered average (mg)	Recovery (%)
Cu(II)[a]	0.65	0.227	0.228	99.1
	1.30	0.227		
	1.95	0.229		
Pb(II)[a]	0.60	0.228	0.229	99.7
	1.20	0.23		
	1.80	0.23		
Bi(III)[b]	1.45	0.227	0.228	99.1
	2.90	0.229		
	4.34	0.229		
Fe(III)[a]	0.222	0.227	0.228	99.1
	0.444	0.229		
	0.666	0.229		
Ti(IV)[c]	0.75	0.229	0.229	99.7
	1.50	0.229		
	2.25	0.228		

In presence of (a) EDTA (b) thiourea (c) fluoride

The resin was found to be stable for at least 7 days in 4 *N* H_2SO_4, 4 *N* HNO_3, 4 *N* HCl, 4 *N* $HClO_4$ and 2 *N* NaOH because no appreciable changes in nitrogen content and sorption capacity were found after treatment with the above mentioned reagents.

The thermogravimetric analysis (TGA) showed that the dried resin started decomposing at 260°C and loss in weight (20.2%) was attributed to the loss of quinaldinic acid group.

The resin was also found to be quite stable to γ-radiation. There was no loss of activity on exposure to a 3.12 or 9.36 M. rad source for 24-72 hr. However, on exposure to 18.72 M. rad source for 144 hr, the activity decreased by 12%. The activity of the resin was measured by the sorption capacity of U(VI) before and after exposing the resin to radiation.

The nitrogen content of the nitrated polymer was found to be 11.31%. After reduction, the resin contained 11.46% nitrogen. Amino group was estimated by titration in nonaqueous medium[12] which indicated about 68% conversion of nitro-resin to amino-resin. The nitrogen content of the final chelating resin was found to be 9.22%. The conversion of amino group to quinaldinic acid amide group was calculated as 85%. Thus, the final resin contained about 21.5% of quinaldinic acid amide group and this value agrees with TGA result which is slightly lower as the TGA experiment was carried out in presence of air. The metal exchange capacity of both nitrated and aminated polymer was found to be negligible; hence, the free amino and nitro groups present in the final resin are not the active sites of the resin.

Metal absorption capacity and separation

Conditions for separation of U(VI) from the metal ions Na(I), K(I), Be(II), Ca(II), Mg(II), Zn(II), Cd(II), Cu(II), Pb(II), Ni(II), Bi(III), Fe(III) and Ti(IV) were studied.

Among the above metal ions, Cd(II), Ni(II) and Zn(II) showed different sorption patterns in the *p*H region ~2.0-5.0, but at *p*H ~ 1.0 they were not sorbed by the resin and instead U(VI) was sorbed by the resin in the *p*H region ~1.0 to 4.0. So, for the separation of U(VI) from these metal ions the mixture was maintained at *p*H ~ 1.0, the resin column was washed with the same buffer and the mixture was passed through the column when only U(VI) was sorbed by the resin.

Separation of Zn(II), Cd(II) and Ni(II) from U(VI) was also achieved between *p*H 3.5 and 4.0. But, as the resin sorbs Zn(II), Cd(II) and Ni(II) in small amounts, EDTA was used to suppress the chelation of these metal ions. At *p*H ~ 1.0 sorption capacity of U(VI) is small. Hence, when urani-

um(VI) was present in small amounts and other metals in larger amounts the first method was followed but when U(VI) was present in larger amount and the others in smaller quantities, separation was performed following the latter method at *p*H 3.5 to 4.0 (Table 2).

Copper(II) was sorbed in the *p*H range 1.0-4.0. So, before separation, it was marked by EDTA (10 ml, 1.0 *M* solution). Na(I), K(I), Be(II), Ca(II) and Mg(II) were not sorbed by the resin. But Bi(III) was hydrolysed above *p*H ~ 1.0. Hence, thiourea was added to keep Bi(III) in solution, the mixture was maintained at *p*H ~ 3.5 and percolated through the column and eluted as before. Fe(III) and Ti(IV) are also hydrolysed above *p*H ~ 2.0 and *p*H ~ 2.5 respectively; below the *p*H mentioned they are sorbed by the resin to some extent. So EDTA and F^- were used as masking agents for Fe(III) and Ti(IV) respectively. When separation of U(VI) and Ti(IV) was studied, polythene containers were used.

Pb(II) showed absorption pattern similar to that of U(VI). Hence, EDTA was used as masking agent during the separation of U(VI) from Pb(II). Alternatively, both of these ions could be sorbed on the resin and Pb(II) eluted first with EDTA though this process was more time consuming (Table 3).

In each case, amount of uranium(VI) taken was 0.23 mg. Each separation was carried out three times; in the first instance the amount of foreign ion taken was close to that of U(VI), followed by experiments with larger amounts. In each case the recovery of uranium was over 99%.

When uranium present in uraninite ore was separated and determined using this resin, uranium found was 0.157% against the reported value of 0.16%.

A few other separations, e.g., Fe(III) from Cu(II), Zn(II) or Cd(II) can also be effected using this resin. However, these separations are not reported as they are of limited practical utility due to low sorption capacities of the metal ions.

Acknowledgement

The authors are indebted to the UGC, New Delhi, for the financial support and to Thermax Private Ltd., Poona, India for the gift sample of styrene-DVB polymer beads.

References

1 Vernon F & Kyffin T W, *Anal chim Acta*, **94** (1977) 317.
2 Orf G M & Fritz J S, *Analyt chem*, **50** (1978) 1328.
3 Ghosh J P & Das H R, *Talanta*, **28** (1981) 274.
4 Phillips R J & Fritz J S, *Anal chim Acta*, **139** (1982) 237.
5 Vogel A I, *Quantitative inorganic analysis*, 4th Edn (ELBS & Longman, London) 1978, 487.
6 Hammick D L & Dickinson W P, *J chem Soc*, I (1929) 214.
7 Chaudhuri N K, *Organic reagents in inorganic analysis, uses of some β-Ketoanilides* (PhD thesis, Burdwan University) 1972, p. 77.
8 Sandell E B, *Colorimetric determination of traces of metals* (Interscience, New York) 1959, pp. 331, 570, 916.
9 Kodama K, *Quantitative inorganic analysis* (Interscience, New York) 1963, 298.
10 Inczedy J, *Analytical applications of ion-exchangers* (Pergamon, Oxford) 1966, 29.
11 Bellamy L J, *The infrared spectra of complex molecules* Vol. 2 (Chapman & Hall, London) 1975, 310.
12 Ficken G E & Lane E S, *Anal chim Acta*, **16** (1957) 207.

Indian Journal of Chemistry
Vol. 28A, February 1989, pp. 154-156

Notes

Stabilities of Quinarene Hydrocarbons

DILIP K DEB

Department of Physics, Panskura Banamali College, Panskura 721 139

PRATIP R RAY

Department of Chemistry, Dinabandhu Andrews College, Calcutta 700 084

and

NIRAD G MUKHERJEE*

Department of Chemistry, University College of Science, Calcutta 700 009

Received 27 *November* 1987; *revised* 4 *May* 1988; *accepted* 6 *June* 1988

The stabilities of quinarene hydrocarbons (**1-9**) have been studied in the light of their homodesmotic and isodesmic energies. The data point to extreme instability of these compounds.

All attempts to prepare the parent quinarene hydrocarbons, viz, 1-cyclopropenylidino-4-methylenocyclohexa-$\Delta^{2,5}$-diene (**1**); 1-cyclopentadienylidino-4-methylenenocyclohexa-$\Delta^{2,5}$-diene (**2**); 1-cycloheptatrienylidino-4-methylenocyclohexa-$\Delta^{2,5}$-diene (**3**); 1,4-*bis*-cyclopropenylidino cyclohexa-$\Delta^{2,5}$-diene (**4**); 1-cyclopentadienylidino-4-cyclopropenylidino cyclohexa-$\Delta^{2,5}$-diene (**5**); 1-cycloheptatrienylidino-4-cyclopropenylidino cyclohexa-$\Delta^{2,5}$-diene (**6**); 1,4-bis(cyclopentadienylidino)cyclohexa-$\Delta^{2,5}$-diene (**7**); 1-cycloheptatrienylidino-4-cyclopentadienylidinocyclohexa-$\Delta^{2,5}$-diene (**8**); and 1,4-bis(cycloheptatrienylidino)cyclohexa-$\Delta^{2,5}$-diene (**9**) have so far failed though the preparation of some of their derivatives[1-8] have been reported. Formation, especially of 9,9-diphenyl derivative of **3** and 11,11-diphenyl derivative of **8**, has still remained questionable[9]. The inability to obtain these in the laboratory attracted the attention of the theoretical chemists to estimate their stabilities. These attempts involved semiempirical SCFMO calculations with[9] or without[10] CI within various levels of approximation, and a comparison of resonance energy per bond or per π-electron of these compounds with those of benzenoids, and semi-benzenoids. In an earlier paper[11] we have shown that the isodesmic energy (IMOSE) and homodesmotic energy (HMOSE) per bond are better criteria for this purpose as these exclude the contributions of extraneous factors not directly linked with stability. In a subsequent paper[12], we have shown that these can act as very good reactive indices for predicting the reactivities of polynuclear hydrocarbon undergoing Diels-Alder reaction. In this note we present the results of calculation of the IMOSE and HMOSE values per C−C bond of compounds **1-9** and to see whether the values can throw any light on their stabilities.

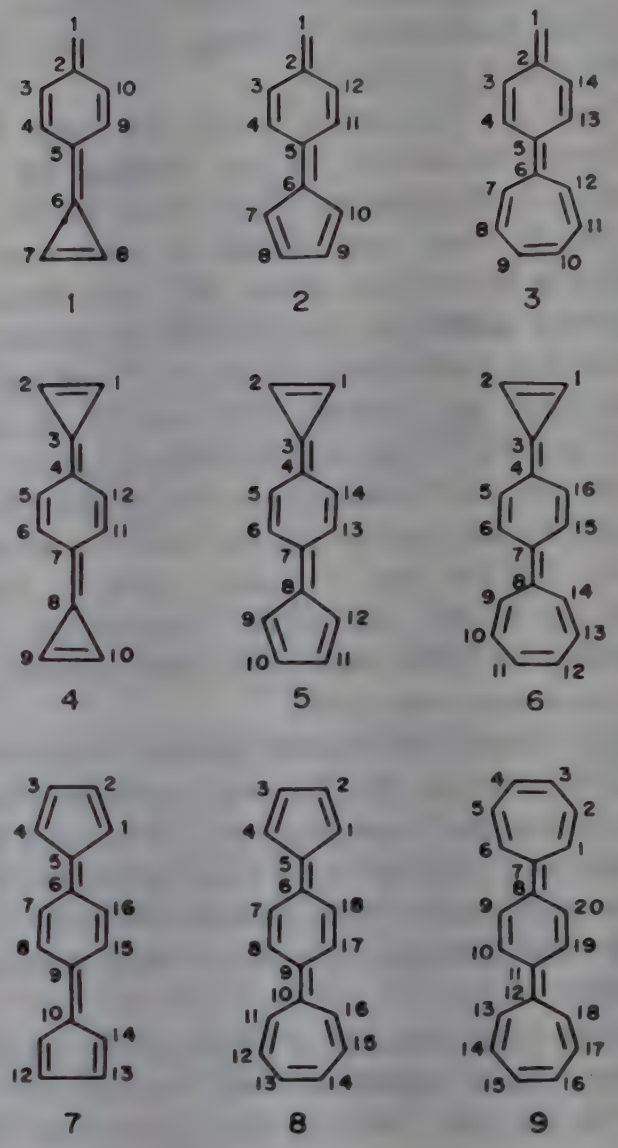

Fig. 1. Molecules studied.

IMOSE and HMOSE values of **1-9** were calculated using the method given earlier[11]. In the case of completely cyclic compounds (**4-9**) the following formulae were used[11,12].

$$\text{HMOSE: } (a-b)\,\text{DVE} + \left(\frac{3b-2a}{2}\right) C_4H_6 \rightarrow C_aH_b + \left(\frac{a}{2}\right) C_2H_4$$

$$\text{IMOSE: } \frac{2a-b}{2} C_4H_6 \rightarrow C_aH_b + \left(\frac{3a-2b}{2}\right) C_2H_4$$

Table 1—Isodesmic (IMOSE) and Homodesmotic (HMOSE) Energies and Resonance Energy (RE) C – C Bond for Compounds **1-9**

Molecule	IMOSE/C – C (eV)	HMOSE/C – C (eV)	RE/C – C (eV)*			RE/electron (eV)
			a	b	c	
1	0.05398	0.07464	0.1500	0.1443	0.00002	0.0206
2	0.04876	0.06624	0.1594	0.1524	0.0007	0.0132
3	0.04822	0.06337	0.1557	0.1477	0.0046	0.0111
4	0.01696	0.03761	0.1567	0.1560	—	—
5	0.1012	0.12014	—	—	—	—
6	0.04107	0.05791	0.1671	0.1631	0.0058	0.0004
7	0.03506	0.05189	0.1852	0.1716	0.0120	—
8	0.08637	0.10152	—	—	—	—
9	0.04584	0.05861	0.1710	0.1650	0.0090	0.0021

*Resonance energies have been taken from ref. 10.

For compounds (**1-3**) with a side bond in the benzene ring the following modified formula for HMOSE was used.

$$\text{HMOSE: } (a-b+1)\text{DVE} + \left(\frac{3b-2a-4}{2}\right)C_4H_6 = C_aH_b + \left(\frac{a-2}{2}\right)C_2H_4$$

where C_aH_b is the compound considered and DVE is divinylethylene.

For reasons given in the earlier paper[11] a Hückel method was employed with the values of the resonance integral as equal to 1.751×10^5 kJ/mol. A test SC Hückel calculation on **9** using a method described elsewhere[13] did not show any great improvement and hence the idea of using any other SCF method was dropped. Since, like resonance energy, IMOSE and HMOSE values also increased with increase in the number of electrons, the total energy failed to provide information on the stability or aromaticity of these compounds. It was envisaged that energy per C – C bond may be a good parameter for the purpose. In Table 1, are given the HMOSE/C – C and IMOSE/C – C for **1-9** along with various resonance energy values calculated by Banerjee and Dasgupta[10]; all the energy values being given in electron volts.

As the compounds contain odd-membered cycloenyl rings attached to the benzene ring, one should expect them to behave as semibenzenoids. But Banerjee and Dasgupta[10] found that the resonance energy per C – C bond or per C atom (for Hess and Schaad method) for all the compounds were far below the minimum limits prescribed for semibenzenoids. In Dewar and de LLoano method (not included in Table 1) resonance energy per C – C bon ' came out negative for all the compounds indicating their high instability. Banerjee and Dasgupta, however, failed to get any convergence for compounds **5** and **8** and hence any comment on the relative stability of these compounds was not possible. This situation does not arise in our case.

It is seen from Table 1 that the IMOSE/C – C and HMOSE/C – C values of **1-4**, **6**, **7** and **9** not only are well below the prescribed limits (vide ref. 11) of semibenzenoids (<0.08 and <0.10 respectively) but also below the limit for the nonbenzenoids (<0.06 and <0.07 respectively). Thus all the resonance energy calculations or the IMOSE and HMOSE calculations point towards extreme unstability of **1-9**. This is not surprising as each of these compounds has only one Kekule structure and therefore MORT[14] (molecular orbital resonance theory) involving these structures is nil. Table 1 shows that **5** and **8** have the maximum stability within the group. Unfortunately resonance energy data are not available for these compounds as the SCF interactions did not converge in the calculation of Banerjee and Dasgupta[10].

References

1 Kende A S, *J Am chem Soc*, **85** (1963) 1882.

2 Von Heldon R, Ter Borg A P & Bickel A F, *Recl Trav Chim Pays Bas Belg*, **81** (1962) 599.

3 Jutz C & Voithenleitner F, *Chem Ber*, **97** (1964) 29.

4 Nozoe T, *Chem Abstr*, **62** (1965) 5234.

5 Bladon P, Pauson P L, Proctor G P & Rodger W J, *J chem Soc, C* (1966) 926.

6 Takahashi K, *Tetrahedron Lett*, (1970) 1235.

7 Takahashi K, Takenaka S & Nozoe T, *Tetrahedron*, **30** (1974) 2194.

8 Takahashi K, Takenaka S & Nozoe T, *Bull chem Soc Japan*, **47** (1974) 2272.

9 Yamguchi H & Nakajima T, *Bull chem Soc Japan*, **48** (1975) 1325.

10 Banerjee P & Dasgupta N K, *Indian J Chem*, **19A** (1980) 1115.

11 Ray P R & Mukherjee N G, *Indian J Chem*, **16A** (1978) 371.

12 Ray P R & Mukherjee N G, *Indian J Chem*, **24A** (1985) 330.

13 Mukhopadhyay A & Mukherjee N G, *Int J Quantum Chem*, **19** (1981) 515.

14 Zivkovic T, *Theoret Chim Acta (Berl)*, **61** (1982) 363.

Indian Journal of Chemistry
Vol. 28A, February 1989, pp. 157-158

Characterization of Tin Oxide Supported Vanadia & Molybdena Catalysts by Low Temperature Oxygen Chemisorption Technique

K NARSIMHA, Ch SIVARAJ,
B MAHIPAL REDDY & P KANTA RAO*
Catalysis Section,
Regional Research Laboratory, Hyderabad 500007

Received 3 *March* 1988; *accepted* 9 *May* 1988

Two series of SnO_2 supported V_2O_5 and MoO_3 catalysts prepared have been characterized by means of low temperature oxygen chemisorption and X-ray diffraction techniques. Oxygen uptake as a function of loading of V_2O_5 on $V_2O_5-SnO_2$ catalysts increases linearly upto 3.2 wt. % V_2O_5 and then decreases, whereas on MoO_3-SnO_2 catalysts also oxygen uptake increases and reaches a maximum at 3 wt. % MoO_3 and thereafter remains constant. These results have been interpreted in terms of patchy monolayer models of V- and Mo-oxide phases.

Selective chemisorption of oxygen at low temperatures on supported molybdena and vanadia catalysts has generated interest in recent years[1-4]. Chemisorption of oxygen can provide quantitative information about the dispersion of vanadium and molybdenum oxide phases on different supports. In pursuant to the earlier systematic investigations from this laboratory on $MoO_3-Al_2O_3$ (ref. 5), MoO_3-ZrO_2 (ref. 6), MoO_3-TiO_2 (ref. 7), $V_2O_5-Al_2O_3$ (ref. 8) and $V_2O_5-SiO_2$ (ref. 3) catalysts a comparative study has been made on V_2O_5-SnO_2 and MoO_3-SnO_2 catalyst systems by low temperature oxygen chemisorption (LTOC) technique.

SnO_2 supported catalysts containing 0.5 to 5.5 wt. % V_2O_5 or MoO_3 were prepared by wet impregnation technique using required amounts of aqueous ammonium metavanadate or ammonium heptamolybdate solution. The impregnated samples were dried at 120°C for 12 hr and calcined at 500°C for 6 hr. Pure SnO_2 support was prepared by precipitating stannic hydroxide from stannic chloride with dilute ammonia solution. The precipitates were dried at 120°C for 16 hr and calcined at 600°C for 6 hr in air. LTOC measurements were performed at −78°C on the catalysts, prereduced in a flow of hydrogen at 500°C for 6 hr (see ref. 8). The X-ray diffractograms were recorded on a Philips PW 1051 diffractometer using Ni-filtered CuK_α radiation.

Oxygen uptake values as a function of catalyst composition are shown in Fig. 1. Oxygen uptake per gram of catalyst on $V_2O_5-SnO_2$ catalysts increases linearly as a function of vanadia loading upto about 3.2 wt % and then decreases rapidly with further increase in loading. In the case of MoO_3-SnO_2 catalysts oxygen uptake also increases linearly with increase in molybdena loading again upto about 3 wt. % and thereafter it remains constant with further loading. This saturation loading represents the completion of monolayer coverage of the active support surface by the active component. Similar observations were made earlier on Al_2O_3, SiO_2, ZrO_2 and TiO_2 supported systems at different V_2O_5 and MoO_3 loadings respectively[3,5-8]. An interesting observation to be noted from Fig. 1 is that the optimum catalyst composition for both the systems appears to be the same, though oxygen chemisorption capacities are very different. The present study as well as the earlier report[3] testify to the fact that the specific surface area of the support mainly determines monolayer concentration of the active component and the strength of interaction between the support and the active component governs the dispersion and hence oxygen uptake capacity.

BET surface areas, surface coverages and dispersions on various catalysts are given in Table 1.

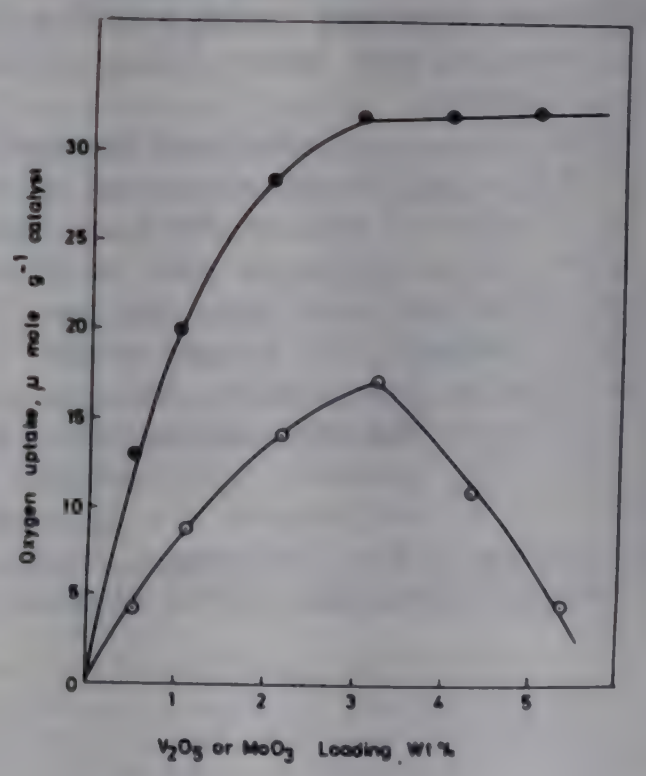

Fig. 1-Oxygen uptake at −78°C plotted as a function of catalyst composition [⊙, $V_2O_5-SnO_2$; and ●MoO_3-SnO_2 catalysts]

Table 1 – Composition, Oxygen Chemisorption and BET Surface Areas of Various Catalysts

Catalyst	Composition (wt. %)		Oxygen uptake (μ mol g^{-1} cat)	BET surface area (m^2/g)	Surface coverage[a]	% Dispersion[b]
	V_2O_5	MoO_3				
VSn-1	0.5	—	4.1	29.0	4.2	15.0
VSn-2	1.1	—	8.9	28.0	9.5	14.8
VSn-3	2.2	—	14.0	25.9	16.0	11.7
VSn-4	3.2	—	17.4	28.7	17.9	10.0
VSn-5	4.3	—	10.8	28.0	11.4	4.6
VSn-6	5.4	—	4.5	25.2	5.3	1.5
MoSn-1	—	0.5	13.1	29.1	13.7	75.4
MoSn-2	—	1.0	20.0	28.5	21.4	57.6
MoSn-3	—	2.0	28.6	27.2	32.1	41.2
MoSn-4	—	3.0	31.9	26.8	36.3	30.6
MoSn-5	—	4.0	32.2	25.6	38.3	23.2
MoSn-6	—	5.0	32.6	24.4	40.7	18.8

[a] Defined as: 100 (active surface area/BET surface area). active surface areas are calculated according to refs. 7 and 8.
[b] It is the ratio of number of chemisorbed O atoms to the total number of V or Mo atoms multiplied by 100.

A small decline in the BET surface area from lower loading to higher loading can be seen for both the catalyst systems. Similarly, dispersion also decreases with increase in the concentration of the active component. A comparison of dispersion values on both the systems clearly show that molybdena is dispersed much better than vanadia at all the loading levels. The surface coverages, like oxygen uptake, also increase as a function of loading upto the monolayer loading and then decreases or levels off with further V_2O_5 or MoO_3 contents respectively.

The initial increase and subsequent decrease or levelling off in oxygen uptake capacity of the catalysts as a function of V_2O_5 or MoO_3 on different supports are interpreted in terms of 'patchy monolayer' model[9] of V- or Mo-oxide phase on the support surface[2,3]. The present results also once again confirm these concepts. Based on that model, it was shown that the coordinatively unsaturated sites (CUS), generated upon reduction in hydrogen, were the exact locations for dissociative O_2 chemisorption at low temperatures. As the V or Mo loading increases the number of these reduced V- or Mo-oxide patches increases with attendant increase in the number of CUS upto the monolayer level. Hence, oxygen uptake increases linearly with loading upto this level. Beyond monolayer level, further addition of Mo leads to the formation of another Mo oxide layer on top of the first monolayer[2]. This growth in size of small patches rather in number is expected not to add new CUS per unit of Mo with further addition of MoO_3. Hence, oxygen uptake levels off beyond this loading. However, in the case of V_2O_5 catalysts an additional amount of vanadia beyond the monolayer loading neither covers the free support surface nor forms multilayer patches, but it gets deposited as nonreducible three-dimensional V_2O_5 crystallites on top of the first monolayer phase[3]. Hence, oxygen uptake declines beyond monolayer loading due to blockage of already existing CUS. No characteristic XRD peaks due to V_2O_5 or MoO_3 phase were observed even upto the highest loadings. It is quite possible since, the crystallites formed may be less than 4 nm, beyond the detection capability of the technique. In conclusion, it is worth mentioning once again that the LTOC technique can precisely determine the V or Mo levels where the formation of monolayer completes.

We thank the CSIR, New Delhi for the award of research fellowships to KN and CHS.

References

1 Weller S W, *Acc chem Res*, **16** (1983) 101.
2 Nag N K, *J Catal*, **92** (1985) 432, and references therein.
3 Nag N K, Chary K V R, Rao B R & Subrahmanyam V S, *Appl Catal*, **31** (1987) 73.
4 Reddy B M, Chary K V R, Subrahmanyam V S & Nag N K, *J chem Soc Faraday Trans* 1, (1985) 1655.
5 Reddy B M & Subrahmanyam V S, *Appl Catal*, **27** (1986) 1.
6 Reddy B M, Chary K V R, Rao B R, Subrahmanyam V S, Sunandana C S & Nag N K, *Polyhedron*, **5** (1986) 191.
7 Reddy B M & Subrahmanyam V S, *React Kinet Catal Lett*, **31** (1986) 429.
8 Nag N K, Chary K V R, Reddy B M, Rao B R & Subrahmanyam V S, *Appl Catal*, **9** (1984) 225.
9 Hall W K, *in Proceedings 4th Climax International Conference on the chemistry and uses of molybdenum*, edited by H F Barry & P C H Mitchel (Climax Molybdenum Co, Michigan) 1982, pp. 224.

Indian Journal of Chemistry
Vol. 28A, February 1989, p. 159

Photolysis of Alkali Hexa(formato)ferrates(III) in Solution

A S BRAR*, S BRAR & S SANDHU†
Chemistry Department, Indian Institute of Technology, New Delhi 110016

Received 3 *October* 1987; *revised* 26 *February* 1988; *accepted* 29 *April* 1988

Photolysis of alkali hexa(formato)ferrates(III) in solution and solid phase has been investigated. The formation of iron(II) species has been detected by UV spectroscopy. Solid state photolysis does not show the formation of Fe(II) species.

Photochemical reduction of iron(III) in formic acid has been shown to occur by intermolecular electron transfer from formate ion to metal and the formation of 1:1 complex has been observed[1]. The radical formed in the primary process reduces the ground state complex leading to the formation of final product. The mechanism has been supported by the fact that photolysis of ferric citrate system induces the polymerization of vinyl monomers[2,3]. During liquid state photolysis of potassium tris(oxalato)ferrate(III) formation of $[Fe(ox)_2]^{2-}$ has been reported[4-6]. A literature survey reveals that no work has been done on the photolysis of alkali hexa(formato)ferrate(III) and hence the title investigation.

The methods of preparation and chemical analysis of alkali hexa(formato)ferrates(III) (Li^+, Na^+, K^+, Cs^+, NH_4^+) have already been reported[8]. The experimental procedure for solution photolysis in acidic medium has also been published earlier[9].

Absorption spectra of alkali hexa(formato)ferrates(III) exhibit only strong CT bands (from ligand to metal) in the region of 400 to 300 nm. No bands corresponding to the forbidden *d-d* transitions are observed. These observations show that iron atom is in high spin state (d^5) and so all the crystal field transitions are Laporte-forbidden.

A 0.2 *M* solution of alkali metal hexa(formato)ferrate(III) was prepared in 0.1 *M* sulphuric acid solution and subjected to photolysis by irradiating it with radiations from a mercury lamp having an intensity of 1.1×10^{17} quanta/s. An aliquot (5 ml) of this solution was withdrawn at different time intervals, 1,10-phenanthroline added to it and the absorbance noted at 510 nm. The photochemical reduction was studied at 25°C.

†Chemistry Department, G.N.D. University, Amritsar 143005.

The rate of formation of Fe(II) species is the highest in the case of sodium hexa(formato)ferrate(III) and the lowest in the case of caesium hexa(formato)ferrate(III). The values of quantum yield for the formation of Fe(II) species, are 1.1×10^{-3}, 2.0×10^{-3}, 1.8×10^{-3} and 0.288×10^{-3} in the case of lithium, sodium, potassium and caesium hexa(formato)ferrates, respectively. These values indicate that physical deactivation is the predominant process. The order of quantum yield is less that that in the photochemical reduction of Fe(III) species in the presence of formic acid[1]. On the basis of quantum yield the photo induced decomposition mechanism shown in Scheme 1, can be proposed.

$$[Fe^{3+}(HCOO)_6^-]^{3-} \xrightarrow{h\nu} [Fe^{3+}(HCOO)_6^-]^{3-*} \quad \ldots (1)$$

$$[Fe^{3+}(HCOO)_6^-]^{3-*} \rightarrow [Fe^{3+}(HCOO)_6^-]^{3-} + h\nu' \quad \ldots (2)$$

$$[Fe^{3+}(HCOO)_6^-]^{3-*} \rightarrow Fe^{2+} + 5HCOO^- + HCOO \quad \ldots (3)$$

Scheme 1

The values of quantum yields are too small ($\approx 10^{-3}$) and the possibility of reaction (3) is also small in acidic medium.

Solid state photolysis was also investigated by exposing these complexes to 250 watt mercury lamp for 400 hr. The Mössbauer spectrum of irradiated samples did not show any observable change. This indicates that there is no reduction to Fe(II) species in the solid state photolysis. It has been observed that the liquid state photolysis products on long standing in air are reoxidized, showing thereby that the ferrous species formed during photolysis is unstable.

Quantum yield values for the formation of iron(II) species follow the order: Na− > K− > Li− > Cs-complex. It is possible that size of the cation and charge density play an important role in the photochemical reduction of ferric species in this reaction.

References

1 Bendale J H & Bridge N K, *J phys chem*, **69** (1955) 783.
2 Subramanium R V & Santappa M, *Makromol Chem*, **22** (1957) 147.
3 Avans M G & Uri N, *Nature*, **164** (1949) 404.
4 Allmand A J & Young K W, *J chem Soc*, (1931) 3079.
5 Bisikatwa N A, *Ukrain Khim Zhur*, **17** (1950) 807.
6 Calvert J G & Pitts J N, *Photochemistry*, (Academic Press, New York) 1976, p. 784.
7 Frahn J L, *Aust J Chem*, **11** (1958) 399.
8 Brar A S, Brar S & Sandhu S S, *Ratiochem Radio Anal Lett*, **49** (1981) 207.
9 Brar A S & Randhawa B S, *Polyhedron*, **3** (1984) 169.

Indian Journal of Chemistry
Vol. 28A, February 1989, pp. 160-161

Excess viscosities of binary mixtures of water with tetrahydrofuran & dioxane at 303.15 K

R Venkateswarlu, Pallagolla Rajasekhar & K S Reddy*

Department of Chemistry, Sri Venkateswara University, Tirupati 517 502

Received 25 *April* 1988; *revised* 10 *June* 1988; *accepted* 1 *July* 1988

Excess viscosities and partial molar excess viscosities of binary mixtures of water with tetrahydrofuran and dioxane have been computed from the viscosities and the densities of pure components and mixtures over the complete range of mol fraction. Excess properties are positive and their significance is discussed in terms of the molecular interactions in the mixtures.

Molecular interactions in the mixtures of tetrahydrofuran (THF) and dioxane with water have been thoroughly investigated in terms of excess thermodynamic properties[1-8], except in terms of excess viscosities. We report herein excess viscosities and partial molar excess viscosities for the title binary mixtures at 303.15 K.

Water, dioxane (E Merck) and THF (Reidel) were purified by literature methods. The purity of the samples was ascertained by comparing their densities and boiling points with the literature values[9]. Viscosities were measured with an Ostwald viscometer and the values were accurate to ±0.5%, while densities were measured using a bicapillary pycnometer with an accuracy of $\pm 5 \times 10^{-5}$ g cm^{-3}. All the mixtures were prepared by weight.

Excess viscosities were calculated using Eq (1) and the values are given in Table 1.

$$\ln \eta^E = \ln \eta - [x_1 \ln \eta_1 + (1 - x_1) \ln \eta_2] \quad \ldots (1)$$

Excess viscosities are represented with a polynomial equation[10] of the form (2)

$$\ln \eta^E = \frac{x_1(1 - x_1)[a_1 + a_2(1 - 2x_1) + a_3(1 - 2x_1)^2]}{[1 + a_0(1 - 2x_1)]} \quad \ldots (2)$$

where a_0 is skewing constant and is calculated using Eq. (3)

$$a_0 = -2(1 - 2x_{1,ext})/[1 + (1 - 2x_{1,ext})^2] \quad \ldots (3)$$

In Eq. (3), $x_{1,ext}$ is the mol fraction corresponding to maximum $\ln \eta^E$. The parameters a_1, a_2 and a_3 are obtained by the method of least squares and are given in Table 2 along with standard deviation (σ). Partial molar excess viscosities for components 1 and 2 were calculated[11] and the results are included in Table 1.

The results presented in Table 1 reveal that the excess viscosities are positive over the whole range

Table 1—Mole fraction (x_1), density (ρ), viscosity (η), excess viscosity ($\ln \eta^E$) and partial molar excess viscosities of components 1 and 2 ($\ln \bar{\eta}_1^E$ & $\ln \bar{\eta}_2^E$) at 303.15 K

x_1	ρ g·cm^{-3}	η cp	$\ln \eta^E$	$\ln \bar{\eta}_1^E$	$\ln \bar{\eta}_2^E$
Tetrahydrofuran (1) + Water (2)					
0.0000	0.99561	0.793	—	—	—
0.0485	0.98717	1.217	0.455	15.055	−0.372
0.1010	0.97709	1.381	0.608	9.567	−0.406
0.1479	0.96663	1.425	0.664	6.648	−0.331
0.2006	0.95508	1.366	0.649	4.484	−0.252
0.3276	0.93338	1.098	0.505	1.576	−0.011
0.4903	0.91347	0.853	0.330	0.439	0.239
0.6398	0.89921	0.674	0.174	0.041	0.401
0.7728	0.88973	0.565	0.067	−0.038	0.393
0.9015	0.88144	0.500	0.012	−0.014	0.239
0.9491	0.87912	0.484	0.003	−0.004	0.136
1.0000	0.87652	0.469	—	—	—
Dioxane (1) + Water (2)					
0.0000	0.99561	0.793	—	—	—
0.0495	1.01324	1.122	0.335	11.815	−0.337
0.1010	1.02333	1.361	0.516	9.096	−0.446
0.1464	1.02913	1.505	0.605	7.177	−0.489
0.1964	1.03201	1.602	0.655	5.523	−0.478
0.3401	1.03402	1.579	0.606	2.383	−0.301
0.4812	1.03053	1.405	0.454	0.832	0.054
0.6535	1.02712	1.221	0.272	0.116	0.566
0.8065	1.02432	1.071	0.102	−0.034	0.680
0.9033	1.02303	1.017	0.027	−0.020	0.469
0.9495	1.02260	1.008	0.007	−0.007	0.270
1.000	1.02190	1.014	—	—	—

Table 2—Skewing constant (a_0), least square parameters (a_1, a_2, a_3) and standard deviation ($\sigma \ln \eta^E$) at 303.15 K for the binary mixtures of water with THF and dioxane

a_0	a_1	a_2	a_3	$\sigma(\ln \eta^E)$
Tetrahydrofuran + Water				
−0.9415	0.8922	−0.4251	1.2517	0.037
Dioxane + Water				
−0.9396	0.5325	−1.3441	1.8387	0.027

of mol fraction for the two systems. The plot of ln η^E versus mol fraction is highly unsymmetrical and skewed towards water-rich region with maximum in ln η^E at about $x_1 = 0.15$ and $x_1 = 0.2$ for the systems THF + water and dioxane + water respectively. This typical behaviour in water-rich region may be interpreted on the basis of enhancement of water-water interactions of hydrophobic nature and the presence of weak H-bonding between unlike molecules[12]. At higher values of x_1, the H-bonding in water may be broken and intercomponent H-bonding may become predominant. Further, the large values of ln $\bar{\eta}_1^E$, in water-rich mixtures also support the above interpretation.

One of the authors (KSR) is grateful to the UGC, New Delhi for financial assistance.

References

1 Malcolm G N & Rowlinson J S, *Trans Faraday Soc*, 53 (1957) 921.

2 Scott H, *J chem engng Data*, 6 (1961) 19.

3 Morcom K W & Smith R W, *Trans Faraday Soc*, 66 (1970) 1073.

4 Nakayama H & Shinoda K, *J chem Thermody*, 3 (1971) 401.

5 Glew G N & Watts H, *Can J Chem*, 51 (1973) 1933.

6 Kiyohara O & Benson G C, *Can J Chem*, 55 (1977) 1354.

7 Kiyohara O, Arcy P J D & Benson G C, *Can J Chem*, 57 (1979) 1006.

8 Inglese A, Ferino H, Marongiu B, Solinas V & Torazza S, *Thermochim Acta*, 65 (1983) 169.

9 Riddick J A & Bunger W S, *Organic solvents, Techniques of chemistry*, Vol. II (Wiley-Interscience, New York) 1970.

10 Handa Y P & Benson G C, *Fluid Phase Equilibria*, 3 (1979) 185.

11 Goates J R, Ott J B & Moellmer J F, *J chem Thermody*, 9 (1977) 249.

12 Franks F, *Water—A comprehensive treatise*, Vol. II (Plenum Press, New York) 1973.

Indian Journal of Chemistry
Vol. 28A, February 1989, pp. 162-163

Kinetics of Oxidation of Lactic, Mandelic & Glycollic Acids by Diperiodatonickelate(IV) in Alkaline Media

U CHANDRAIAH, C P MURTHY† & SUSHAMA KANDLIKAR*
Department of Chemistry, Nizam College, Hyderabad 500 001

Received 6 *November* 1987; *revised* 6 *April* 1988; *accepted* 6 *June* 1988

The title reactions show first order dependence in [Ni(IV)] and [substrate]. The rate of oxidation increases with increase in [OH^-] and decreases with increase in [periodate]. A probable mechanism involving an adduct formation between substrate and Ni(IV) and its slow decomposition in slow step is proposed.

The earlier work[1] from our laboratory dealt with kinetics and mechanism of oxidation of aliphatic amines by diperiodatonickelate(IV) (DPN). As an extension, the present note describes the results of oxidation of lactic, mandelic and glycollic acids by DPN.

Potassium salt of mandelic acid (puriss, Fluka), and glycollic and lactic acids (both Reidel) were prepared and used as substrates. Other chemicals used were of (AR, BDH) grade. Diperiodatonickelate(IV) was prepared as reported by Ray[2] and standardized by method reported earlier[1]. The progress of the reaction was followed by measuring the disappearance of Ni(IV) at 410 nm employing UV-vis double beam spectrophotometer (Shimadzu, Japan). Stoichiometric studies showed that one mol of oxidant reacts with one mol of substrate. Under kinetic conditions the oxidation products were identified as the corresponding keto acids by their characteristic spot tests[3].

Under the conditions [Ni(IV)] ≪ [substrate] the plot of log (absorbance) versus time were linear ($r = 0.98$) indicating the order in [Ni(IV)] to be unity. From the slopes of such plots the pseudo-first order rate constants (k') were evaluated. The plots of log k' versus log [substrate] were also linear ($r = 0.97$) with a unit slope in each case indicating order in [substrate] to be unity.

The rate of reaction was found to increase with increase in [OH^-] and showed an inverse dependence on [periodate]. For instance, in the reaction with lactic acid, at fixed [Ni(IV)], [lactic acid] and temperature (300 K) the rate constant (k') increased from 5.02×10^{-4} s^{-1} to 13.1×10^{-4} s^{-1} when [OH^-] was increased from 1.5×10^{-3} mol dm^{-3} to 1.0×10^{-2} mol dm^{-3}. For the same reaction at constant [Ni(IV)], [lactic acid], [OH^-] and temperature (300 K) the rate constant, 10^4 k', decreased from 8.34 s^{-1} to 3.75 s^{-1} as 10^6 [periodate] was increased from 1.30 mol dm^{-3} to 8.00 mol dm^{-3}.

The rate of oxidation was not affected by added salts. Polymerisation or reduction in rate was also not observed by addition of acrylamide indicating absence of radical formation.

In aqueous solution diperiodatonickelate(IV) gets hydrated[4,5] and under the present experimental conditions the complex is assumed to exist as $[Ni(OH)_2(H_3IO_6)_2]^{2-}$ as discussed earlier[1]. (For simplicity $[Ni(OH)_2(H_3IO_6)_2]^{2-}$ is represented as $[Ni(OH)_2(HL)_2]$, $H_3IO_6^{2-}$ as HL and $H_2IO_6^{3-}$ as L). The fact that the rate increases with increase in [OH^-] indicates an equilibrium between a deprotonated reactive species and a protonated unreactive species.

$$Ni(OH)_2(HL)_2 + OH^- \overset{K_1}{\rightleftharpoons} Ni(OH)_2L(HL) + H_2O \quad \ldots (1)$$

The inverse dependence of rate on [periodate] indicates the probable existence of a dissociative equilibria in which the Ni(IV) moiety loses a periodate ligand forming monoperiodatonickelate(IV) (Eq. 2)

$$Ni(OH)_2L(HL) \overset{K_2}{\rightleftharpoons} Ni(OH)_2L + HL \quad \ldots (2)$$

Thus monoperiodatonickelate(IV), $Ni(OH)_2L$, is assumed to be the reactive species and its concentration is expected to be much less than that of diperiodatonickelate(IV).

As Ni(IV) has already been reported[1,6] to behave as a two electron oxidant, we assume here a two electron transfer from the alcoholic function to Ni(IV) species in the rate-determining step.

The possibility of involvement of alkoxide ion does not appear probable as effect of added salts on rate of reaction was negligible. The rates of reaction followed the order: mandelic acid > glycollic acid > lactic acid indicating that electron withdrawing substituents at the α-position increased the rate of oxidation. Hence the reaction is assumed to proceed through an adduct formation which decomposes in the slow step with the removal of α-hydrogen probably as proton. This assumption re-

†Department of Chemistry, Osmania University, Hyderabad 500 007.

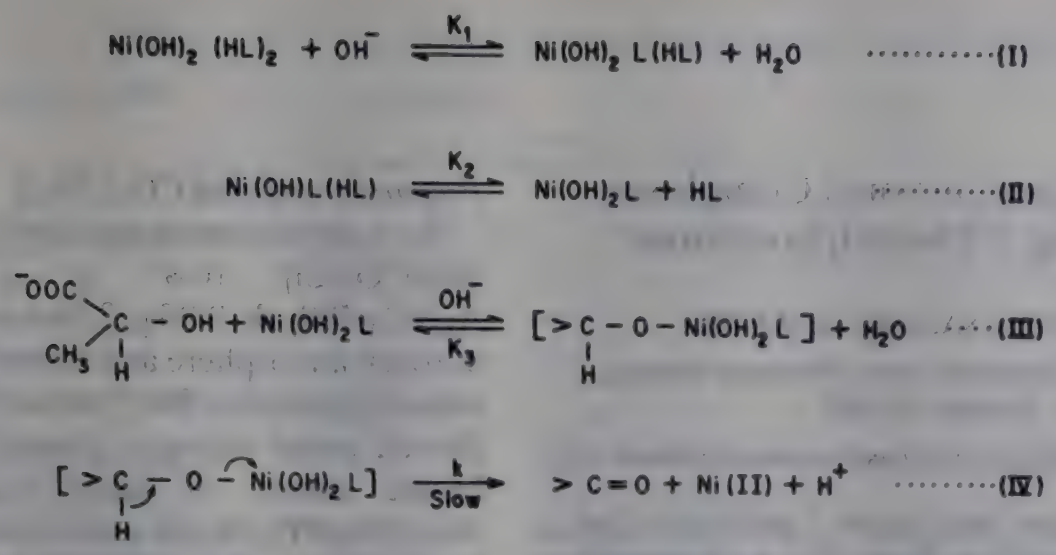

Scheme 1

ceives support from the absence of any reaction between Ni(IV) and *t*-butanol.

A plausible mechanism based on above discussion can be written as shown in Scheme 1.

The rate law derived from Scheme 1 is given by Eq. (3)

$$-\frac{d[\mathrm{Ni(IV)}]_t}{dt} = \frac{kK_1K_2K_3[\mathrm{Ni(IV)}]_t[\mathrm{S}][\mathrm{OH}^-]}{K_1K_2[\mathrm{OH}^-]+\{K_1[\mathrm{OH}^-]+1\}\mathrm{HL}} \quad \ldots (3)$$

or

$$-\frac{d\ln[\mathrm{Ni(IV)}]_t}{dt} = \frac{kK_1K_2K_3[\mathrm{S}][\mathrm{OH}^-]}{K_1K_2[\mathrm{OH}^-]+\{K_1[\mathrm{OH}^-]+1\}\mathrm{HL}} \quad \ldots (4)$$

where $[\mathrm{Ni(IV)}]_t$ represents the total [Ni(IV)] which is taken as the sum of $[\mathrm{Ni(OH)_2(HL)_2}]$, $[\mathrm{Ni(OH)_2L(HL)}]$ and $[\mathrm{Ni(OH)_2L}]$. The above rate law explains all experimental observations. Equation (4) envisages a linear plot between $1/k'$ versus $1/[\mathrm{OH}^-]$. This was found to be true for all the substrates, thus supporting the proposed mechanism.

Since electron-withdrawing groups facilitate the abstraction of proton in the slow step the rate of oxidation increases in their presence.

Activation parameters and second order rate constants (k'') for all substrates studied are listed in Table 1. The positive entropy of activation suggests that the transition state is less rigid than the reactant which is evident from the slow step in the mechanism wherein a rigid complex gets decomposed into products. The constancy in $\Delta G^{\ddagger}$ values suggests similar mechanism to be operative in all substrates.

Table 1—Second Order Rate Constants (k'') and Activation Parameters at 300 K

Substrate	$k'' \times 10^2$ (dm³ mol⁻¹ s⁻¹)	E_a	$\Delta H^{\ddagger}$	$\Delta G^{\ddagger}$	$\Delta S^{\ddagger}$
		(kJ mol)			(J K⁻¹ mol⁻¹)
Lactic acid	4.17	110.3	107.8	81.3	88.2
Glycollic acid	20.9	102.3	99.8	77.3	75.0
Mandelic acid	68.4	93.9	91.5	74.4	57.6

The authors express their thanks to Prof. T. Navaneeth Rao, and Prof. B. Sethuram, for their constant encouragement and useful discussions. One of the authors (UC) is thankful to the CSIR, New Delhi for the award of a senior research fellowship.

References

1 Chandraiah U, Jafferali Khan, Murthy C P & Sushama Kandlikar, *Indian J Chem*, **26A** (1987) 475.
2 Ray P, *Inorganic synthesis*, Vol. V, Edited by Therald Moellar (McGraw-Hill, New York) 1957, p. 201.
3 Feigl F, *Spot tests in organic analysis* (Elsevier, Amsterdam), 1966, p. 482.
4 Crouthamel C E, Meek H V, Martin D S & Banks C V, *J Am Chem Soc*, **71** (1949) 3631.
5 Crouthamel C E, Meeks H V & Martin D S, *J Am chem Soc*, **73** (1951) 82.
6 Murthy C P, Sethuram B & Navaneeth Rao T, *Z phys Chem*, (in Press).

Indian Journal of Chemistry
Vol. 28A, February 1989, pp. 164-166

Molybdenum Carbonyl Complexes Containing 2-Thienylphosphines

V K JAIN*, V S SAGORIA & M S GILL

Bhabha Atomic Research Centre, Chemistry Division, Bombay 400 085

Received 25 *January* 1988; *revised and accepted* 25 *March* 1988

Complexes of the type $[Mo(CO)_5(PR_3)]$ and $[Mo(CO)_4(PR_3)_2]$ (PR_3 = $PMeth_2$, $PEtth_2$, PPh_2th, $PPhth_2$, Pth_3; th = 2-thienyl) have been prepared and characterized by elemental analyses and IR and $^{31}P\{^1H\}$NMR data. The $[Mo(CO)_4(PR_3)_2]$ complexes exist in *cis*-configuration. Oxidative addition of bromine to $[Mo(CO)_4(PR_3)_2]$ yields $[Mo(CO)_3Br_2(PR_3)_2]$.

The coordination chemistry of tertiary phosphine ligands derived from 2-thienyl group has received only a little attention[1,2]. In view of considerable recent interest in molybdenum phosphine complexes[3-5], presently we have prepared a few molybdenum carbonyl complexes with some 2-thienylphosphines, viz. tri-(2-thienyl)phosphine (Pth_3), phenyl-di-(2-thienyl)phosphine ($PPhth_2$), methyl-di-(2-thienyl)phosphine ($PMeth_2$), diphenyl-2-thienylphosphine (PPh_2th) and ethyl-di-(2-thienyl)-phosphine ($PEtth_2$).

Preparation of $[Mo(CO_5)(PR_3)]$

To a dichloromethane solution (20 ml) of $[Et_4N][Mo(CO)_5Cl]$[6] (0.89 g; 2.21 mmol), solid $AgNO_3 \cdot PPh_2th$ (0.95 g; 2.16 mmol) was added under nitrogen atmosphere and stirred for 2 hr. To this was added anhydrous ether (5 ml) and the reaction mixture filtered under nitrogen atmosphere. To the yellow filtrate excess of ether was added to give $[Mo(CO)_5(PPh_2th)]$ as a pale yellow solid; yield 40%. Similarly other $[Mo(CO)_5(PR_3)]$ complexes were prepared.

Preparation of cis-$[Mo(CO)_4(PR_3)_2]$

Dichloromethane solution (25 ml) of *cis*-$[Mo(CO)_4(piperidine)_2]$[7] (1.43 g; 3.77 mmol) was treated with a solution of $PPhth_2$ (2.05 g; 7.46 mmol) under nitrogen atmosphere and the mixture refluxed with stirring for 30 min. The reaction mixture was concentrated to 10 ml under reduced pressure and MeOH (20 ml) added. On cooling pale yellow crystals of $[Mo(CO)_4(PPhth_2)_2]$ separated out which were filtered off, washed with hexane and dried *in vacuo*; yield 1.89 g (66%). Identical method was employed for the preparation of other complexes of the type $[Mo(CO)_4(PR_3)_2]$.

Table 1—Physical and Analytical Data for Molybdenumcarbonyl Complexes of Tertiary 2-Thienylphosphines

Sl No*	Complex	m.p. °C	Found (Calc) %		
			C	H	Mo
1	$[Mo(CO)_5(PMeth_2)]$	—	38.7 (37.5)	4.7 (2.0)	— —
2	$[Mo(CO)_5(PPh_2th)]$	220(d)	49.8 (50.0)	4.3 (2.6)	— —
3	$[Mo(CO)_5(PPhth_2)]$	135-8(d)	44.2 (44.7)	2.8 (2.2)	— —
4	$[Mo(CO)_5(Pth_3)]$	75(d)	38.7 (39.5)	2.2 (1.8)	— —
5	$[Mo(CO)_4(PMeth_2)_2]$	85-7	41.6 (41.8)	2.6 (2.9)	— —
6	$[Mo(CO)_4(PEtth_2)_2]$	123-5	41.8 (43.6)	5.0 (3.4)	14.3 (14.5)
7	$[Mo(CO)_4(PPh_2th)_2]$	246(d)	57.9 (58.1)	4.4 (3.5)	13.2 (12.9)
8	$[Mo(CO)_4(PPhth_2)_2]$	240-5(d)	50.7 (50.8)	2.7 (2.9)	12.9 (12.7)
9	$[Mo(CO)_4(Pth_3)_2]$	205-10(d)	43.3 (43.7)	2.2 (2.4)	12.3 (12.5)
10	$[MoBr_2(CO)_3(PPhth_2)_2]$	82-100(d)†	— —	— —	10.9 (10.8)
11	$[MoBr_2(CO)_3(Pth_3)_2]$	115-30(d)†	— —	— —	10.8 (10.7)

*Complexes 1-9 were recrystallised from CH_2Cl_2-ether and 10,11 from carbon tetrachloride-hexane
†Complexes decomposed with gas evolution

Table 2—$^{31}P\{^1H\}$ NMR and νCO Data for Molybdenum Complexes Containing 2-Thienylphosphines

Ligand/Complex	^{31}P NMR data			νCO† (cm^{-1})
	Solvent	δ(ppm)*	Δδ† (ppm)	
$PMeth_2$	$CDCl_3$	−50.2[a]		
$PEtth_2$	$CDCl_3$	−37.2[a]		
PPh_3	$CDCl_3$	−4.7[a]		
PPh_2th	$CDCl_3$	−20.1[a]		
$PPhth_2$	$CDCl_3$	−33.7[a]		
Pth_3	$CDCl_3$	−45.8[b]		
$[Mo(CO)_5(PMeth_2)]$	$CDCl_3$	−0.5	49.7	2030, 1940,1900, 1865
$[Mo(CO)_5(PPh_3)]$	—	37.5[c]	42.2	
$[Mo(CO)_5(PPh_2th)]$	CH_2Cl_2	26.15[d]	46.25	2010, 1900, 1880
$[Mo(CO)_5(PPhth_2)]$	CH_2Cl_2	15.0[d]	48.7	2020, 1945, 1905, 1885
$[Mo(CO)_5(Pth_3)]$	CH_2Cl_2	6.6[d]	52.4	2020,1945, 1910, 1890
$[Mo(CO)_4(PMeth_2)_2]$	$CDCl_3$	−5.7	44.5	2020, 1935, 1895, 1860
$[Mo(CO)_4(PEtth_2)_2]$	$CDCl_3$	8.9	46.1	2020, 1925, 1895, 1860
$[Mo(CO)_4(PPh_3)_2]$	$CDCl_3$	38.3	43.0	
$[Mo(CO)_4(PPh_2th)_2]$	$CDCl_3$	26.7	46.8	2010, 1900, 1880
$[Mo(CO)_4(PPhth_2)_2]$	$CDCl_3$	15.6	49.3	2010, 1905, 1885
$[Mo(CO)_4(Pth_3)_2]$	$CDCl_3$	7.3	53.1	2010, 1905, 1885
$[MoBr_2(CO)_3(PPhth_2)_2]$	—	—	—	2020, 1945, 1900
$[MoBr_2(CO)_3(Pth_3)_2]$	—	—	—	2020, 1955,1910

*85% H_3PO_4 as external reference
† Δδ is the coordination shift from free ligand in $CDCl_3$
‡ In nujol mull
(a) From ref. 2; (b) from ref. 1; (c) from ref. 8; and (d) spectra recorded in external lock mode and shifts are corrected for internal lock.

Preparation of $[MoBr_2(CO)_3(Pth_3)_2$

A solution of bromine (0.04 ml) in carbon tetrachloride was added dropwise with stirring to a solution of $[Mo(CO)_4(Pth_3)_2]$ (0.65 g; 0.84 mmol) in the same solvent (15 ml) during which brown suspension was formed. To this hexane (10 ml) was added. Precipitated complex was filtered off, washed with hexane and dried *in vacuo*; yield 70%. Similarly $[MoBr_2(CO)_3(Pth_2Ph)_2]$ was obtained.

Analytical data of these complexes are given in Table 1.

Reaction of $[Et_4N][Mo(CO)_5Cl]$ with silver nitrate adduct of 2-thienylphosphine yields pentacarbonyl complex, $[Mo(CO)_5(PR_3)]$. Tetracarbonyl complexes, *cis*-$[Mo(CO)_4(PR_3)_2]$ are conveniently obtained by displacement of piperidine from *cis*-$[Mo(CO)_4(piperidine)_2]$ by 2-thienylphosphines. Bromine oxidatively adds to $[Mo(CO)_4(PR_3)_2]$ (PR_3 = $PPhth_2$, Pth_3) to give $[MoBr_2(CO)_3(PR_3)_2]$.

The carbonyl region in the IR spectra of $[Mo(CO)_5(PR_3)]$ is compatible with other pentacarbonylmolybdenum(0) phosphine complexes[5,8,9]. The IR spectra of $[Mo(CO)_4(PR_3)_2]$ displayed mainly three bands (Table 2) for νCO modes. This indicates *cis*-geometry for these complexes. The *trans*-isomer would display only one νCO band in this region. Darensbourg and Kump[7] have shown that *cis*-$[Mo(CO)_4(PR_3)_2]$ complexes are often contaminated with *trans*-isomer as the νCO bands for both the isomers appear in the same region. Appearance of only one signal in the $^{31}P\{^1H\}$NMR spectra (Table 2) indicates that the present complexes exist exclusively in *cis*-configuration. The dibromides, $[MoBr_2(CO)_3(PR_3)_2]$ displayed three νCO bands[3,5,10].

The $^{31}P\{H\}$NMR spectra of Mo(0) carbonyl complexes displayed single resonance (Table 2) which is deshielded considerably from the resonance in the respective ligand. The following order of coordination shifts, and also the shielding, has been observed: $PPh_3 > PPh_2th > PPhth_2 > Pth_3$. It is evident that progressive replacement of the phenyl groups in PPh_3 by 2-thienyl groups causes coordination shift to increase or phosphorus to shield. This appears to be due to stronger electron-withdrawing nature of 2-thienyl group than that of phenyl. The observed trend has been reported for platinum(II) complexes[1,2].

Thanks are due to Dr J P Mittal for his interest and Analytical Chemistry Division, BARC for microanalyses.

References

1 Allen D W & Ashford D F, *J inorg nucl chem*, **38** (1976) 1953; Allen D W & Taylor B F, *J chem Soc Dalton Trans*, (1982) 51.

2 Clark H C & Jain V K, unpublished results.
3 Baker P K & Fraser S G, *Inorg chim Acta*, **116** (1986) L 1; Bencze L, Kraut-Vass A & Prokai L, *Chem Commun*, (1985) 911.
4 Brower D C, Winston P B, Tonker T L & Templeton J L, *Inorg Chem*, **25** (1986) 2883; Alyea E C & Somogyvari A, *Mag Res Chem*, **24** (1986) 357.
5 Cotton F A & Poli R, *Inorg Chem*, **26** (1987) 3228.
6 Abel E W, Butler I S & Reid J G, *J chem Soc*, (1963) 2068.
7 Darensbourg D J & Kump R L, *Inorg Chem*, **17** (1978) 2680.
8 Grim S O, Wheatland D A & McFarlane W, *J Am chem Soc*, **89** (1967) 5573.
9 Magee T A, Mathews C N, Wang T S & Wotiz J W, *J Am chem Soc*, **83** (1961) 3200.
10 Colton R & Tomkins I B, *Aust J Chem*, **19** (1966) 1143; **19** (1966) 1519.

Indian Journal of Chemistry
Vol. 28A, February 1989, pp. 167-168

Synthesis & Characterization of a Ten-coordinated Uranium(VI) Complex

I S AHUJA*, G L YADAVA† & SHAILENDRA TRIPATHI
Chemistry Department, Banaras Hindu University, Varanasi 221 005

Received 15 *February* 1988; *revised and accepted* 13 *May* 1988

A 1 : 2 complex of uranyl nitrate with bis-(2-pyridyl N-oxide)disulphide, a potentially tetradentate ligand, has been prepared and characterized on the basis of elemental analysis, molar conductance, electronic and IR spectral measurements down to 200 cm^{-1}. It is shown that the ligand acts only as bidentate chelating one bonding via N-oxide oxygen atoms leading to 9-membered ring formation. The nitrate groups also act as bidentate chelating ligands. The complex is tentatively assigned a ten-coordinated structure in the solid state.

Uranium(VI) in uranyl compounds has a pyramidal geometry as the two oxygens of the $[UO_2]^{2+}$ group always form the apical bonds and the other donor atoms form an equatorial polygon around the linear OUO group. So far, six is the maximum equatorial coordination number reported for the $[UO_2]^{2+}$ ion with an overall coordination number eight around uranium(VI)[1-8]. We now report the isolation of a 1 : 2 uranyl nitrate complex with bis-(2-pyridyl N-oxide)disulphide—a potentially tetradentate ligand—which is shown to have an overall coordination number ten around uranium(VI) in the solid state.

The 1 : 2 uranyl nitrate complex with bis-(2-pyridyl N-oxide)disulphide (obtained from M/s Ega Chemie, West Germany and used as such) was prepared by mixing together hot ethanolic solutions of the two reactants in the 1 : 2 molar ratio. The complex which formed was suction-filtered, washed with ethanol and dried in an air oven at ~ 80°C. Stoichiometry of the isolated complex was established by uranium and nitrate estimations gravimetrically. C, H and N were determined by microanalysis [Found: U, 26.5; NO_3, 14.0; C, 27.0; H, 1.75; N, 9.31. $UO_2B_2(NO_3)_2$ requires: U, 26.5; NO_3, 13.8; C, 26.7; H, 1.78; N, 9.35%]. The complex is soluble in DMF and behaves as a 1 : 2 electrolyte[9] ($\Lambda_M = 170\ \Omega^{-1}\ cm^2\ mol^{-1}$). Electronic spectrum of the complex was recorded in nujol in the range 200-600 nm on a Cary 14 recording spectrophotometer. IR spectra of the uncoordinated ligand and the complex were recorded in nujol on a Perkin-Elmer spectrophotometer Model 783 equipped with caesium iodide optics.

Bis-(2-pyridyl N-oxide)disulphide possesses four potential donor sites—(i) two sulphur atoms in-between the two pyridyl rings, and (ii) two N-oxide oxygen atoms. Rock salt region IR spectrum of the uranyl nitrate complex indicates clearly that the ligand coordinates via the N-oxide oxygen atoms. Normal modes of bis-(2-pyridyl N-oxide)disulphide that are likely to be affected the most on N-oxide coordination are the νNO and δNO. The νNO, which appears as a doublet at 1248 and 1232 cm^{-1} in the uncoordinated ligand, suffers a significant negative shift and occurs at 1210 and 1205 cm^{-1} in this complex. This decrease in the frequency of νNO modes is attributed to a decrease in the π-bond character of the NO bond as a result of oxygen-to-metal coordination. The δ NO, appearing as a strong band at 836 cm^{-1} in the uncoordinated ligand, is observed with almost similar intensity and frequency in the IR spectrum of this complex. These observations are consistent with those for N,N′-dioxide complexes with uranyl salts reported earlier[10,11]. The two N-oxide oxygen atoms may coordinate either (i) to two different metal atoms (bidentate bridging) giving rise to polymeric structures, or (ii) to the same metal ion (bidentate chelating) resulting in the formation of 9-membered rings. The bridging form, being more symmetrical, gives rise to fewer absorptions in the IR while the unsymmetrical chelating form gives rise to a multiplicity of bands. IR spectrum of the 1 : 2 uranyl nitrate complex with bis-(2-pyridyl N-oxide)disulphide shows multiplicity of bands, thereby indicating that both the oxygen atoms of the organic ligand are bonded to a single uranium atom resulting in the formation of 9-membered rings.

In addition to the ligand bands, IR spectrum of this complex shows absorption bands at 925 and 257 cm^{-1} due to ν_3 and ν_2 modes, respectively, of the uranyl group. Absence of a band at ~ 850 cm^{-1} due to ν_1 mode of the uranyl group, IR-forbidden in the free linear $[UO_2]^{2+}$ ion, implies that the linearity of the OUO group is maintained in this complex.

The symmetrical stretching mode ν_3 at ~ 1360 cm^{-1} in ionic nitrates (D_{3h} symmetry) splits up into its components which occur at 1520 cm^{-1} (ν_1) and 1280 cm^{-1} (ν_4), masking the ligand bands in this region in the present compound. The doubly degenerate in-plane bending mode of the ionic nitrates at ~ 720 cm^{-1} also splits up into its components at 746

†Chemistry Department, Kamla Nehru Institute of Physical & Social Sciences, Sultanpur 228 118.

cm^{-1} (ν_3) and 704 cm^{-1} (ν_5). In addition to these, the symmetric stretching mode ν_1 (IR-inactive in ionic nitrates) becomes IR-active because of lowered symmetry upon coordination (D_{3h} to C_{2v}) and the frequency of ν_2 (~ 1045 cm^{-1} in ionic nitrates) is lowered (1032 cm^{-1}) in this compound. Moreover, two weak bands at 1775 and 1733 cm^{-1} are also observed in the nitrato combination mode region (1800-1700 cm^{-1}), which is more diagnostic of the mode of metal-nitrate coordination[12-17]. The observed magnitude of separation (240 cm^{-1})[12] of ν_1 (1520 cm^{-1}) and ν_4 (1280 cm^{-1}) modes and of the nitrato combination modes[10-16] (42 cm^{-1}) indicates the exclusive presence of bidentate chelating nitrato ligands[12-17]. Considering that (i) the nitrato groups act as bidentate chelating ligands for the uranyl group, and (ii) the organic ligand coordinates in a bidentate chelating manner (*vide supra*), the 1 : 2 uranyl nitrate complex with bis-(2-pyridyl N-oxide)disulphide is tentatively assigned a structure with ten-coordinated uranium(VI). Other possible structures involving the presence of both mono- and bi-dentate nitrato groups together are ruled out as these would require four bands (two sets corresponding to each type of coordination[12-14]) in the 1800-1700 cm^{-1} region. Moreover, absence of a band in the region 1800-1790 cm^{-1} clearly eliminates the possibility of structures involving monodentate[12,18] $M-O(NO_2)-M$ and/or bidentate[12,19] $M-ON(O)-O-M$ bridging nitrato groups.

The electronic spectrum of this complex exhibits three absorption bands[20] at 485, 435 and 365 nm and is consistent with the vibronic structure of the triatomic entity of the uranyl group. The band at 485 nm corresponds to the transition from apical oxygen to *f* orbital of the uranyl group. The other two bands are the consequences of the transitions $\pi \rightarrow f$ orbitals of the uranyl ion.

We thank the CSIR, New Delhi, for the award of a SRF to one of us (ST).

References

1 Cattalini L, Croatto U, Degatto S & Tondello E, *Inorg chim Acta Rev*, **5** (1971) 19.

2 Eller P G & Penneman R A, *Inorg Chem*, **15** (1976) 2439.

3 Forchioni A, Librando V & Poppalrado G C, *J chem Soc, Dalton*, (1977) 638.

4 Haeglel R & Boeyens J C A, *J chem Soc, Dalton*, (1977) 648.

5 Alcock N W & Esperas S, *J chem Soc, Dalton*, (1977) 893.

6 Manhas B S, Trikha A K & Singh Mangal, *Indian J Chem*, **16A** (1978) 431.

7 McCabe D J, Rusell R R, Karthikeyan S, Paine R T, Ryan R R & Smith B, *Inorg Chem*, **26** (1987) 230.

8 Pennington M & Alcock N W, *Inorg chim Acta*, **139** (1987) 49.

9 Geary W J, *Coord chem Rev*, **7** (1971) 81.

10 Ahuja I S & Singh Rajindar, *Spectrochim Acta*, **29A** (1973) 1879.

11 Ahuja I S, Singh Raghuvir & Sriramulu R, *J inorg nucl Chem*, **42** (1980) 627.

12 Curtis N F & Curtis Y M, *Inorg Chem*, **4** (1965) 804.

13 Lever A B P, Mantovani E & Ramaswamy B S, *Can J Chem*, **49** (1971) 1957.

14 Karayannis N M, Mikulski C M, Pytlewski L L & Labes M M, *J inorg nucl Chem*, **34** (1972) 3139; *Inorg Chem*, **13** (1974) 1146.

15 Ahuja I S, Singh Raghuvir & Singh Rajindar, *Spectrochim Acta*, **32A** (1976) 547.

16 Ahuja I S, Singh Raghuvir & Rai C P, *J molec Struct*, **49** (1978) 201.

17 Bullock J I, *J inorg nucl chem*, **29** (1967) 2255.

18 Wallwork S C & Addison W E, *J chem Soc*, (1965) 2925.

19 Camerson A F, Forrest K P, Taylor D W & Nuttall R H, *J chem Soc, A* (1971) 2492.

20 Bong-Il Kim, Kiyako G & Imoto S, *J inorg nucl chem*, **37** (1975) 763.

Indian Journal of Chemistry
Vol. 28A, February 1989, pp. 169-171

Stability Constants of the Binary Complexes of Co(II), Ni(II), Cu(II) & Zn(II) with Thiamine & Ternary Complexes with Thiamine as Primary Ligand & Thymine or Uracil as Secondary Ligand

S SATYANARAYANA* & K VENUGOPAL REDDY
Department of Chemistry, Nizam College (Osmania University)
Hyderabad 500 001

Received 9 *November* 1987; *revised and accepted* 2 *June* 1988

Stability constants of the 1 : 1 and 1 : 2 metal-thiamine (vitamin B_1) complexes and 1 : 1 : 1 metal-thiamine-thymine/uracil mixed ligand complexes have been determined in aqueous medium by potentiometric method at 35° ± 0.1°C and $\mu = 0.10$ *M* (KNO_3). The $\Delta \log K$ values for 1 : 2 metal-thiamine systems are positive whereas values for 1 : 1 : 1 metal-thiamine-thymine or -uracil systems are negative. So the $\Delta \log K$ values reveal that mixed ligand complexes are less stable than the binary (1 : 1) complexes.

Thiamine is present in all living organisms and is essential to life. Co-carboxylase, which is widely used in medicine, is a diphosphoric acid ester of thiamine. Co-carboxylase appears as a component of the metalloenzymes which catalyze the decarboxylation of α-ketoacids and some other biochemical reactions. In order to understand and simulate these vital processes, it is very important to study the complexing properties of thiamine. Fridman *et al.*[1-3] and Grinberg *et al.*[4] have studied the complexing properties of thiamine with some divalent metal ions. In the present investigation stability constnats of binary metal-thiamine complexes and ternary metal-thiamine-thymine/uracil complexes have been determined potentiometrically.

The experimental techniques employed for potentiometric study were similar to those reported in our earlier paper[5].

A Shimadzu double beam spectrophotometer with matched 1 cm quartz cell was used to recorded the spectra. All the solutions were equilibrated at 35°C, the ionic strength being maintained at 0.10 *M* using KNO_3; *p*H was maintained at 4.90 by adding NaOH. The compositions of the complexes were determined using mole ratio method[6]. The formation constants were evaluated using Leden's[7] method. The degree of formation is defined as the ratio of overall concentration of metal ion (C_M) to the equilibrium concentration of free metal ion [M],

$$\phi = \frac{C_M}{[M]} = 1 + k_1[L] + k_1k_2[L]^2$$

The coefficients k_1, k_2 of the variable [L] were obtained by constructing suitable auxiliary functions (ψ_1, ψ_2) and extrapolating these to zero value of the variable.

Thymine and uracil were obtained from M/s Sigma Chemicals, USA. Thiamine hydrochloride was an E. Merck reagent. The metal salt solutions were standardized by titration with disodium salt of EDTA[8]. Carbonate-free NaOH was prepared and standardized by titration with pure potassium hydrogen phthalate.

Calculations

The acid dissociation constants of the ligands were calculated by a direct algebraic method[9], using a combination of suitable material balanced equations. The following general expression was derived to calculate the dissociation constants of the ligands.

$$K_{na} = \frac{[H^+]\{(a-n+1)T_L + [H^+] - [OH^-]\}}{T_L - \{(a-n+1)T_L + [H^+] - [OH^-]\}} \quad \ldots (1)$$

where a = mol of base added per mol of ligand and T_L = total concentration of the ligand species.

For the calculation of stability constants of 1 : 1 and 1 : 2 metal-thiamine complexes, Eqs (2) and (3) respectively were used.

$$M^{2+} + H^+A \rightleftharpoons [MA]^{2+} + [H^+]$$

$$K_{MA}^{M} = \frac{[MA]^{2+}}{[M]^{2+}[A]} \quad \ldots (2)$$

$$MA^{2+} + H^+A \rightleftharpoons [MA_2]^{2+} + [H^+]$$

$$K_{MA_2}^{MA} = \frac{[MA_2]^{2+}}{[MA]^{2+}[A]} \quad \ldots (3)$$

For the calculation of stability constants of 1 : 1 : 1 ternary complexes (metal-thiamine hydrochloride-L), Eq. (4) was used.

$$K_{MAL}^{MA} = \frac{[MAL]^+}{[MA]^{2+}[L]^-} \quad \ldots (4)$$

where H^+A = thiamine hydrochloride and HL = thymine or uracil.

Metal-thiamine hydrochloride (1 : 1) *systems*

The titration curve of M(II)-thiamine hydrochloride [M(II) = Cu(II), Zn(II), Ni(II) and Co(II)]

showed a sharp inflection at $a = 1$. The formation of a 1 : 1 complex was assumed before the inflection point and the corresponding formation constants were calculated in the region of titration curve with $a = 0.3$ to 0.7. The stabilities of metal-thiamine hydrochloride were found to decrease in the order: Cu(II) > Ni(II) > Co(II) > Zn(II). The results are presented in Table 1.

Metal-thiamine hydrochloride (1 : 2) *systems*

For all the metal ions studied, viz., Cu(II), Zn(II), Ni(II) and Co(II), inflection was obtained at $m = 2$ (mol of base added per mole of metal ion). The stability constants $K^{MA}_{MA_2}$ were, however, calculated before $m = 2$ and the results are presented in Table 2.

Metal-thiamine hydrochloride-thymine or uracil (1 : 1 : 1) *systems*

The titration curves fo Cu(II)-thiamine hydrochloride-thymine or uracil systems showed a sharp inflection at $m = 1$. Similar titration curves were obtained for other metal ions, Zn(II), Ni(II) and Co(II). The titration curves indicate the stepwise complex formation of thiamine and thymine or thiamine and uracil. Complex formation of thiamine (vit. B_1) takes place before the inflection point and with thymine or uracil it takes place after the inflection point. The stability constants K^{MA}_{MAL} have been calculated in the buffer region with $m = 1.3$ to 1.7. The results are presented in Table 2.

Thiamine hydrochloride ($pK_a = 4.97$) binds with metal ion through N^1 of the pyrimidine ring[10-13]. The NMR spectra showed a large downfield shift of C_6-H, which is adjacent to N^1 of the pyrimidine ring supporting the involvement of N^1 in coordination[14]. The stabilities of the (1 : 1) metal-thiamine hydrochloride complexes are in the order: Cu(II) > Ni(II) > Co(II) > Zn(II). The 1 : 2 metal-thiamine hydrochloride systems are more stable than the corresponding 1 : 1 systems contrary to statistical considerations. The higher stabilities of the ternary systems as compared with those of the binary ones may be due to the stacking interaction of the ligands. The stacking is more pronounced at lower *p*H values than the neutral *p*H[15]. That is why the $\Delta \log K$ values for 1 : 2 metal-thiamine hydrochloride systems and metal-adenine-cytosine systems[16] are positive whereas for the metal-thymine or uracil (1 : 2) systems[5,17] the $\Delta \log K$ values are negative (Table 3).

The stability constants for 1 : 1 : 1 system of metal-thiamine hydrochloride-thymine or uracil decrease in the order: Cu(II) > Zn(II) > Ni(II) > Co(II). For the two ternary 1 : 1 : 1 systems the $\Delta \log K$ values are negative indicating that these systems are less stable than the binary 1 : 1 systems. This is in accordance with the statistical considerations. If the secondary ligand is negatively charged aromatic ligand like pyrocatechol[18], the ternary systems are more stable than the binary ones. In contrast, the stability constants of the mixed ligand complexes containing neutral donors [thymine ($pK_a = 9.51$) or uracil ($pK_a = 9.29$)] as the secondary ligands are in accord with the statistical considerations[5,17,19] where the statistical steric and electrostatic factors lead to lower stability constants for the 1 : 1 : 1 metal-ligand complexes as compared with those for the binary systems. A similar trend was observed in metal-bipyridyl-cytosine or thymine or uracil and metal-*o*-phenanthroline-cytosine or thymine or uracil[5,16,17] systems.

Table 1—Stability Constants of (1 : 1) Metal-Ligand Systems

[Temp. 35° ± 1°C; $\mu = 0.10\ M\ (KNO_3)$]

Metal ion	Metal-thiamine hydrochloride (1 : 1)	Metal-thymine (1 : 1)	Metal-uracil (1 : 1)
Cu(II)	2.69 (2.78)	6.61	6.04
Zn(II)	2.30	5.23	4.98
Ni(II)	2.52	4.24	3.89
Co(II)	2.36 (2.31)	4.10	3.83

Values are accurate upto ± 0.04; values in the parentheses are calculated spectrophotometrically.

Table 2—Stability Constants of (1 : 1 : 1) System

[Temp. 35° ± 1°C; $\mu = 0.10\ M\ (KNO_3)$]

Metal ion	Metal-thiamine hydrochloride (1 : 2)	Metal-T. HCl thymine (1 : 1 : 1)	Metal- T. HCl uracil (1 : 1 : 1)
Cu(II)	4.30 (4.39)	6.21	5.67
Zn(II)	4.10	4.97	4.35
Ni(II)	4.22	3.75	3.28
Co(II)	4.19 (4.10)	3.68	3.17

Values are accurate upto ± 0.05; values in the parentheses are calculated spectrophotometrically.

Table 3—Δ log *K* Values of Various Systems

Metal ion	M(II)-thiamine HCL (1 : 2)	M(II)-thiamine HCl-thymine (1 : 1 : 1)	M(II)-thiamine HCl-Uracil (1 : 1 : 1)
Cu(II)	+1.61	−0.40	−0.37
Zn(II)	+1.8	−0.26	−0.63
Ni(II)	+1.7	−0.49	−0.61
Co(II)	+1.83	−0.42	−0.66

References

1 Fridman Ya D, Levina M G, Sarbae D S, Tsoi E P & Moldogazieva A V, *Chem Abstr*, **88** (1978) 15256d.

2 Fridman Ya D & Gorokhov S D, *Chem Abstr*, **95** (1981) 128194v.

3 Fridman Ya D, Gorokhov S D & Zainutdinova A, *Chem Abstr*, **95** (1981) 214274c.

4 Grinberg A A & Khakinov Kh Kh, *Chem Abstr*, **6** (1961) 71.

5 Taqui Khan M M & Satyanarayana S, *Indian J Chem*, **21A** (1982) 913.

6 Yoe J H & Jones A L, *Indian Engng Chem Analyt Edn*, **16** (1944) 111.

7 Leden I, *Z phys Chem*, **A188** (1941) 160.

8 Schwarzenbach G, *Complexometric titrations* (Interscience, New York) 1957, 77.

9 Taqui Khan M M & Martell A E, *J phys Chem*, **66** (1962) 10.

10 Taqui Khan M M & Amarababu M, *J inorg nucl Chem*, **103** (1981) 76.

11 Gallo A A, Hansen I L, Sable H Z & Swift T J, *J biol chem*, **241** (1972) 247.

12 Kartz H B & Kustin K, *Biochim Biophys Acta*, **313** (1973) 235.

13 Gary J & Adeyemo A, *Inorg chim Acta*, **55** (1981) 93.

14 Hadjiliadis I N, Markopoulos J, Pneumtikakis G, KJatakis D & Theophanides T, *Inorg chim Acta*, **25** (1977) 21.

15 Gilligan T J & Schwarz G, *Biophys Chem*, **4** (1976) 55.

16 Taqui Khan M M & Jyothi M S, *J inorg nucl chem*, **40** (1978) 1731.

17 Taqui Khan M M & Satyanarayana S, *Indian J Chem*, **21A** (1982) 913.

18 Heurex G A L & Martell A E, *J inorg nucl Chem*, **28** (1966) 481.

19 Sigel H, *Metal ions in biological systems*, Vol 2, (Marcel Decker, New York) 1973.

Indian Journal of Chemistry
Vol. 28A, February 1989, pp. 172-173

Formation of Binary & Ternary Chelates of Calmagite with Lanthanides in Presence of Some Amino Polycarboxylic Acids

B SATYANARAYANA,
K L OMPRAKASH, M L N REDDY & A V CHANDRA PAL*
Department of Chemistry,
Osmania University, Hyderabad 500007

Received 30 *December* 1987; *revised* 29 *February* 1988;
accepted 11 *April* 1988

The formation constants of 1:1 and 1:2 binary Ln(III)-calmagite (CLM) and 1:1:1 ternary [Ln(III) – CLM – A] chelates [where Ln(III) = La, Pr, Nd, Gd, Dy and Y; A = iminodiacetic acid (IMDA), hydroxyethyliminodiacetic acid (HIMDA) and nitrilotriacetic acid (NTA)] have been determined *p*H-metrically in 50% (v/v) aq. methanol medium at 30°C and $I = 0.1$ *M* ($NaClO_4$). The ligand calmagite coordinates as a secondary ligand in presence of IMDA, HIMDA and NTA with all the metal ions. The order of formation constants of binary as well as ternary chelates is found to be: La < Pr < Nd < Gd < Dy > Y.

Calmagite [1-(2-hydroxy-5-methylphenylazo)-2-naphthol-4-sulphonic acid] (CLM) has been widely used as a metallo-chromic indicator in the complexometric titrations[1,2]. Calmagite offers an advantage in that its aqueous solution is more stable than that of Eriochrome Black-T. Recently, studies have been made on the ternary complex formation of Eriochrome Black-T chelates with lanthanides in presence of HIMDA, NTA, EDTA and CDTA[3]. A survey of literature reveals that little work has been done with the ligand calmagite. Therefore, it was though worthwhile to investigate the complexation reactions of calmagite with Ln(III) ions in the presence of aminopolycarboxylic acids.

We report here the potentiometric determination of formation constants of 1:1 and 1:2 binary chelates of calmagite with La(III), Pr(III), Nd(III), Gd(III), Dy(III) and Y(III) ions and formation of mixed ligand complexes of lanthanides with calmagite and aminopolycarboxylic acids, viz., iminodiacetic acid (IMDA), hydroxyethyliminodiacetic acid (HIMDA), nitrilotriacetic acid (NTA), cyclohexanediaminetetraacetic acid (CDTA), diethylenetriaminepentaacetic acid (DTPA), hydroxyethyl ethylenediaminetriacetic acid (HEDTA) and ethylenediaminetetraacetic acid (EDTA) in 50% (v/v) aq. methanol at 30°C and $I = 0.1$ *M* ($NaClO_4$).

Calmagite was purified by the method of Lindstrom *et al*[4]. The other reagents $NaClO_4$ (E Merck), EDTA (BDH), NTA (Sigma), CDTA (E Merck), DTPA (BDH), IMDA (Sigma), HIMDA (Fluka), HEDTA (Fluka) of AR/GR grade were used without further purification. Proton-ligand formation constants of calmagite and the metal-ligand formation constants of its lanthanide chelates were determined *p*H-metrically by Irving-Rossotti titration technique[5]. The formation constants of ternary systems were determined by the method of Ramamoorthy and Santappa[6]. *p*H meter readings (B) in 50% (v/v) methanol-water were corrected by the method of Van Uitert and Haas[7].

The *pK* values of calmagite, determined *p*H-metrically, were found to be 8.20 and 11.83. They correspond to the dissociation of hydroxyl groups in the molecule. The $-SO_3H$ group present in the molecule dissociates at much lower *p*H (*p*H < 2.0) and therefore its dissociation constant could not be determined. The values obtained in the present study are in good agreement with the values (8.14 and 12.35) reported earlier by Lindstrom and Diehl[1], which were determined spectrophotometrically in aqueous medium at 25°C.

The $\bar{n}$ (degree of formation) values ($0.1 < \bar{n} < 1.9$) obtained for Ln(III)-CLM system indicate the formation of 1:1 and 1:2 complexes. The ligand CLM starts coordinating with lanthanide ions at *p*H 5.5, 4.8, 4.7, 4.0, 4.0 and 4.2 for La(III), Pr(III), Nd(III), Gd(III), Dy(III) and Y(III) respectively. Formation of 1:2 chelates with Ln(III) ions may be explained in the light of their large size and high positive charge coupled with their tendency to attain higher coordination numbers.

In the ternary system the ratio of concentration of Ln(III), calmagite and aminopolycarboxylic acid (A) was maintained at 1:1:1, the concentration of each being kept at 0.001 *M*. In the ternary systemns studied, the mixed ligand curves closely follow the 1:1 Ln(III)-A (where A = IMDA, HIMDA and NTA) binary curves in the lower *p*H (< 4.0) region, until the protons of aminopolycarboxylic acid are neutralized, indicating that the binary Ln(III)-A complexes predominate in this region. Above this region the divergence of the ternary curve from those of the binary Ln(III)-A systems reveals the formation of ternary complexes of the type [Ln – A – CLM]. Here, calmagite acts as a

Table 1 – Equilibrium Constants of Binary and Ternary Metal Chelates of Some Lanthanides with Calmagite (L) and Iminodiacetic Acid, Hydroxyethyliminodiacetic Acid, Nitrilotriacetic Acid in 50% (v/v) Aq. Methanol

[I = 0.1 M($NaClO_4$); temp. = 30°C]

Constant*	La(III)	Pr(III)	Nd(III)	Gd(III)	Dy(III)	Y(III)
$\log K^{M}_{ML}$	10.78	12.13	12.38	13.18	13.48	13.08
$\log K^{ML}_{ML_2}$	7.44	8.97	9.42	9.87	10.09	9.70
$\log K^{MA}_{MAL}$						
			A = IMDA			
	9.35	10.34	10.65	11.32	11.58	11.34
			A = HIMDA			
	8.68	9.57	9.88	10.57	10.79	10.59
			A = NTA			
	8.20	8.81	9.01	9.89	10.27	9.82
$\Delta \log K$						
			A = IMDA			
	−1.43	−1.79	−1.73	−1.86	−1.90	−1.74
			A = HIMDA			
	−2.10	−2.56	−2.50	−2.61	−2.69	−2.49
			A = NTA			
	−2.58	−3.32	−3.37	−3.29	−3.21	−3.26

*Standard deviations are within ±0.05 log K units.

secondary ligand. The formation of ternary complexes is further supported by (i) intensification of colour and (ii) non-superimposable nature of the theoretical composite curve in the region of mixed-ligand complex formation[8].

However, in the case of HEDTA, EDTA, CDTA and DTPA the superimposable nature of theoretical composite curve with the experimental tittration curves indicates that calmagite does not coordinate with the primary [Ln – A] complex. This may be due to the hexadentate nature of CDTA, EDTA and HEDTA or octadentate nature of DTPA. This is further supported by the formation of blue colour (due to free CLM ion) in the pH range above 7.0 when Ln(III) ions are titrated with CDTA, EDTA, HEDTA or DTPA in presence of CLM. Hence these titrants replace $[CLM]^{2-}$ from [Ln – CLM] complexes at pH > 7.0,

$$[Ln-CLM] + A \rightarrow [Ln-A] + [CLM]^{2-} \quad \ldots (1)$$
red blue

where A = EDTA, HEDTA or DTPA.

The relative order of stabilities in all the metal-ligand systems [La(III) < Pr(III) < Nd(III) < Gd(III) < Dy(III) > Y(III)] is almost in accordance with increasing charge/radius ratio of the metal ions. The linear plots between log K_1 and Z^2/r (r is the radius of the metal ion) for various Ln(III) ions show that metal-CLM bond is primarily ionic in character[9].

The extent of favoured formation of the ternary complexes can be inferred from $\Delta \log K$ values[10]. The negative $\Delta \log K$ values (Table 1) reveal that the formation of ternary complexes is not favoured over that of binary complexes. This may be due to the availability of lesser number of coordinating sites for calmagite on primary complex [Ln – A] than on the free $Ln(aq)^{3+}$ ions[11].

The order of stabilities with respect to primary ligands is IMDA > HIMDA > NTA. This is due to the charge neutralization in the formation of the mixed chelates[10] as well as denticity of the ligands. In the case of IMDA and HIMDA, coordination of $[CLM]^-$ occurs with mono positive $[Ln-IMDA]^+$ or $[Ln-HIMDA]^+$ primary complex whereas in the case of NTA, it is between $[CLM]^-$ and a neutral primary complex [Ln – NTA]. Therefore, more electrostatic attraction is expected between $[CLM]^-$ and $[Ln-IMDA/HIMDA]^+$ than that between $[CLM]^-$ and [Ln – NTA] complex. A perusal of $\Delta \log K$ values also confirms the above trend.

Thanks are due to the CSIR, New Delhi for the award of a senior research fellowship to B S N.

References

1 Lindstrom F & Diehl H, *Analyt Chem*, **32** (1960) 1123.
2 Diehl H & Ellingboe J, *Analyt Chem*, **32** (1960) 1120.
3 Satyanarayana B, Omprakash K L, Chandrapal A V & Reddy M L N, *Indian J Chem*, **26A** (1987) 710.
4 Lindstrom F & Issac R, *Talanta*, **13** (1966) 1003.
5 Irving H & Rossotti H S, *J chem Soc*, 3397 (1953); 2904 (1954).
6 Ramamoorthy S & Santappa M, (a) *J inorg nucl Chem*, **32** (1970) 1623; (b) *Indian J Chem*, **9** (1971) 38.
7 Van Uitert L G & Haas G, *J Am chem Soc*, **75** (1953) 451.
8 Carey G H & Martell A E, *J Am chem Soc*, **89** (1976) 2859.
9 Ingle D B & Khanolkar D D, *J Indian chem Soc*, **50** (1973) 190.
10 Sigel H, *Angew Chem Int Edn*, **14** (1975) 394.
11 Thompson C & Loraas J A, *Inorg Chem*, **2** (1963) 89.

Indian Journal of Chemistry
Vol. 28A, February 1989, pp. 174-175

Formation constants of binary & ternary chelates of Ln(III) with maltol & kojic acid in presence of aminocarboxylic acids

M Narasimha Rao, K L Omprakash, A V Chandra Pal* & M L N Reddy

Department of Chemistry, Osmania University, Hyderabad 500 007

Received 7 March 1988; revised and accepted 6 June 1988

The formation constants of binary and ternary systems involving 3-hydroxy-2-methyl-4-pyrone (HMP) (maltol) and 5-hydroxy-2-hydroxymethyl-4-pyrone (HOMP) (kojic acid), with lanthanide metal ions [La(III), Pr(III), Nd(III), Gd(III), Dy(III) and Y(III)] in the presence of iminodiacetic acid (IMDA), hydroxyethyliminodiacetic acid (HIMDA) and nitrilotriacetic acid (NTA) have been determined in aqueous medium at 30°C and $\mu = 0.1$ *M* ($NaClO_4$). The order of stabilities of ternary systems is: HMP > HOMP and IMDA > HIMDA > NTA. These are explained in the light of the basicities of the ligands and charge neutralisation.

In continuation of our earlier studies[1] we report herein the formation constants of binary and ternary systems involving 3-hydroxy-2-methyl-4-pyrone (HMP, maltol) and 5-hydroxy-2-hydroxymethyl-4-pyrone (HOMP, kojic acid), with lanthanide metal ions [La(III), Pr(III), Nd(III), Gd(III), Dy(III) and Y(III)] in the presence of iminodiacetic acid (IMDA), nitrilotriacetic acid (NTA) and hydroxyethyliminodiacetic acid (HIMDA).

Maltol and kojic acid (Fluka), $NaClO_4$ (E. Merck), NTA and IMDA (Sigma) and HIMDA (Fluka) of AR grade were used as received. The proton-ligand formation constants of the ligands and the metal-ligand formation constants were determined *p*H-metrically using the Irving-Rossotti titration technique[2]. The formation constants of ternary systems have been evaluated by the method of Ramamoorthy and Santappa[3] in aqueous medium at 30°C and 0.1 *M* $NaClO_4$.

In binary systems the $\bar{n}$ values (0.1 to 1.9) indicate the formation of both 1:1 and 1:2 Ln(III)-L complexes (where L = HMP/HOMP). The metal-ligand formation constants evaluated by various computational techniques like half-integral, linear plots, pointwise calculations and method of least squares[4,5] are presented in Table 1. The stability order: La(III) < Pr(III) < Nd(III) < Gd(III) < Dy(III) > Y(III) is almost in accordance with the increasing charge/radius ratio of the metal ions[6].

The ternary complex formation is inferred from the non-superimposability of theoretical composite curve on the experimental curve in the region of mixed-ligand complex formation[5]. The ternary formation curve of Ln(III)-L-A coincides with Ln(III)-A curve (where A = HIMDA or NTA and L = HMP or HOMP] in the lower *p*H region and its divergence at higher *p*H region indicates the stepwise formation of the ternary complex. The ligand 'A' acts as primary ligand and the ligand 'L' as secondary ligand [equilibria (1) and (2)]

$$Ln^{3+} + A^{n-} \rightleftharpoons [Ln - A]^{(3-n)} \quad \ldots (1)$$

$$[Ln - A]^{(3-n)} + L^{-} \rightleftharpoons [Ln - A - L]^{(2-n)} \quad \ldots (2)$$

(where A = HIMDA or NTA and $n = 2$ for HIMDA and 3 for NTA).

In the case of ternary systems involving IMDA the ternary curve deviates from the beginning indicating the formation of the ternary complex in a simultaneous fashion [Eq. (3)]

$$Ln^{3+} + L^{-} + A^{2-} \rightleftharpoons [Ln - L - A] \quad \ldots (3)$$

The ternary formation constants are listed in Table 1. The ternary complexes [Ln − A − L] (where A = HIMDA/NTA and L = HMP/HOMP) formed in stepwise manner are less stable while those formed simultaneously [Ln − IMDA − HMP/HOMP] are more stable as compared to the binary complexes as revealed by $\Delta \log K$ values[7] (Table 1). The relative order of stabilities [La(III) < Pr(III) < Nd(III) < Gd(III) < Dy(III) > Y(III)] is the same as that found for binary systems.

The stability order of ternary systems of HMP and HOMP follows the order of the basicities of these ligands, e.g. HMP > HOMP. The order of stability with respect to primary ligands is IMDA > HIMDA > NTA. This could be due to charge neutralisation in forming ternary complexes[7]. In the case of IMDA, coordination occurs with Ln^{3+} to form a neutral metal complex [Eq. (3)]; with HIMDA the coordination of $[HMP]^-$/$[HOMP]^-$ occurs with monopositive $[Ln - HIMDA]^+$ primary complex to form neutral complex whereas in the case of NTA, coordination between $[HMP]^-$/$[HOMP]^-$ and neutral primary complex [Ln − NTA] occurs to form a negatively charged complex [Eq. (2)]. Therefore greater electrostatic attraction may be expected (i) between Ln^{3+}, [(HMP)/(HOMP)] and $[IMDA]^{2-}$; and (ii) between $[Ln - HIMDA]^+$ and L^- than between L^- and [Ln − NTA] complex.

Table 1—Binary and ternary formation constants* of maltol (L) and kojic acid (L') with aminocarboxylic acids [A^1 = IMDA; A^2 = HIMDA; A^3 = NTA] in aqueous medium

[I = 0.1 *M* $NaClO_4$; temp = 30°C]

log *K*	La(III)	Pr(III)	Nd(III)	Gd(III)	Dy(III)	Y(III)
$\log K^{M}_{ML}$	5.22	5.59	5.79	6.01	6.42	5.96
$\log K^{ML}_{ML_2}$	4.09	4.47	4.82	5.20	5.45	5.14
$\log K^{M}_{MA^1L}$	11.74	12.26	12.5	13.43	13.91	13.37
$\log K^{MA^1}_{MA^1L}$	(5.86)	(5.82)	(6.0)	(6.55)	(7.03)	(6.43)
$\Delta\log K$	0.64	0.23	0.21	0.74	0.61	0.67
$\log K^{MA^2}_{MA^2L}$	4.95	5.24	5.26	5.73	5.91	5.62
$\Delta\log K$	−0.27	−0.35	−0.53	−0.28	−0.51	−0.34
$\log K^{MA^3}_{MA^3L}$	4.08	4.36	4.69	5.15	5.30	4.85
$\Delta\log K$	−1.14	−0.96	−0.91	−0.61	−0.71	−0.78
$\log K^{M}_{ML'}$	5.03	5.15	5.23	5.38	5.72	5.32
$\log K^{ML'}_{ML'_2}$	3.98	4.5	4.61	4.96	5.13	5.01
$\log K^{M}_{MA^1L'}$	11.5	11.91	12.06	12.70	12.96	12.51
$\log K^{MA^1}_{MA^1L'}$	(5.61)	(5.47)	(5.56)	(5.74)	(6.23)	(5.83)
$\Delta\log K$	0.59	0.32	0.33	0.36	0.51	0.54
$\log K^{MA^2}_{MA^2L'}$	4.26	4.56	4.77	5.28	5.75	5.21
$\Delta\log K$	−0.77	−0.59	−0.46	−0.10	−0.07	−0.09
$\log K^{MA^3}_{MA^3L'}$	3.8	4.19	4.32	4.77	5.01	4.54
$\Delta\log K$	−1.14	−0.96	−0.91	−0.61	−0.71	−0.78

The values presented in parentheses are the stepwise formation constants evaluated from the simultaneous constants using Sigel's method[7].

*The deviations are within ± 0.03 log *K* units.

The distribution of metal among the various metal-ligand species was calculated using the computer program BEST[8]. The maximum percentage of mixed ligand complexes formed are 97%, 80% and 68% for La−HMP−IMDA, La−HMP−HIMDA and La−HMP−NTA species respectively and this is in accordance with the stabilities of mixed ligand complexes.

The authors are grateful to the CSIR, New Delhi for the award of a senior research fellowship to M N R.

References

1 Narasimha Rao M, Omprakash K L, Jagannadha Charyulu K, Chandra Pal A V & Reddy M L N, *Acta ciencia Indica*, 12 (1986) 31.

2 Irving H & Rossotti H S, *J chem Soc*, (a) (1953) 3397; (b) (1954) 2904.

3 Ramamoorthy S & Santappa M, (a) *J inorg nucl Chem*, (1970) 1623; (b) *Indian J Chem*, 9 (1971) 38.

4 Omprakash K L, Chandra Pal A V & Reddy M L N, *Indian J Chem*, (a) 21A (1982) 322; (b) 22A (1983) 546.

5 Carey G H & Martell A E, *J Am chem Soc*, 89 (1976) 2859.

6 Ingle D B & Khanolkar D D, *J Indian chem Soc*, 50 (1973) 190.

7 Sigel H, *Angew chem int Edn*, 14 (1975) 394.

8 Moitekaitis R J & Martell A E, *Can J Chem*, 60 (1982) 2403.

Indian Journal of Chemistry
Vol. 28A, February 1989, p. 176

A novel precipitate-based manganese(II) sensor

Naheed Faizan & M C Chattopadhyaya*
Department of Chemistry, University of Allahabad, Allahabad 211 002

Received 15 February 1988; revised 26 May 1988; accepted 13 June 1988

A new heterogeneous precipitate-based Mn(II) selective electrode has been prepared. The electrode is selective for Mn(II) ions in the presence of Zn(II), Cu(II), Mg(II), Fe(II), Ca(II), Ba(II), Al(III), NH_4(I). It gives a linear response in the concentration range of 1×10^{-1} to 5×10^{-6} mol dm^{-3} and can be used as an indicator electrode in the precipitation titration of Mn(II) against phosphate ion.

Koryta[1] has reviewed the sensitivity of a number of electrodes towards Mn(II) ions. In a recent paper Midgley and Mulcahy[2] described a Mn(IV) oxide electrode as an Mn(II) sensor and also reported the selectivity coefficient of this electrode towards Fe(III) and Pb(II) ions. In this note a new heterogeneous precipitate-based Mn(II) ion selective electrode is described.

Preparation of electrode

Manganisum sulphate (200 mg, Sarabhai-Merck) was dissolved in a minimum amount of 10% acetic acid solution. The solution of 8-hydroxyquinoline (450 mg) (BDH) was prepared in hot ethyl alcohol. When these two solutions were mixed a yellowish precipitate of $Mn(C_9H_6ON)_2$ was obtained which was filtered off, washed with distilled water and dried in air for 24 hr. This compound (100 mg) was mixed with epoxy resin (400 mg) (Araldite, Ciba-Giegy Ltd) on a Whatman filter paper No. 42. The paste dispersed on filter paper uniformly to produce layer of about 0.1 mm in thickness which was dried to form a membrane. This membrane was dipped in a solution of 0.1 mol dm^{-3} $MnSO_4$ for 24 hr to remove the adhering filter paper.

A small piece of membrane was fixed to one end of a glass tube of about 15 cm in length with the help of Araldite and dried. The tube was filled with 0.1 mol dm^{-3} solution of $MnSO_4$ and kept immersed in a solution of 0.01 mol dm^{-3} $MnSO_4$ for a week. A saturated calomel electrode (SCE) was immersed through the open end of the tube for electrical contact.

The emf values (versus SCE) were measured at $30° \pm 1°$ with a Philips *p*H meter (model-PR 9405 M). Solutions were stirred with magnetic stirrer.

A series of standard solutions of $MnSO_4$ in the concentration range of 1×10^{-1} to 5×10^{-6} mol dm^{-3} was prepared and the *p*H of each adjusted to 4 by adding acetate buffer in the ratio of 20:1. The potential of each solution (vs SCE) was measured with the help of the electrode prepared. A linear response was obtained in this concentration range and the slope was 20 mV per decade change in the concentration in first week; in second week the slope was 25 mV per decade change in concentration.

The response time of the electrode was obtained by noting the response, when the concentration of $MnSO_4$ was suddenly changed from 0.01 to 0.001 mol dm^{-3}. Within 30 sec 75% of total potential was reached when concentration was changed. After 40 sec potential was stabilised and remained constant thereafter. The electrode potential remained unchanged in the *p*H range of 3-13.

The selectivity coefficients were determined[3] as 0.1 for divalent Zn, Mg, Cu, Ca and Ba ions and as 0.5, 0.04 and 0.2 for Fe(II), Al(III) and NH_4(I) ions, respectively.

To examine the applicability of the electrode for the determination of Mn(II) ion, the precipitation titration of Mn(II) against $Na(NH_4)_2PO_4$ was performed using the prepared electrode as an indicator electrode and SCE as the reference electrode. For this purpose $MnSO_4$ solution (10 ml, 0.1 mol dm^{-3}) was taken in a beaker, diluted with distilled water and titrated against 0.1 mol dm^{-3} $Na(NH_4)_2PO_4$ solution. After each addition of titrant, the potential was measured. A break in titration curve was observed at the equivalence point.

The authors thank the UGC, New Delhi for the award of a junior research fellowship to one of them (NF).

References

1 Koryta J, *Anal Chim Acta*, 61 (1972) 329.
2 Midgley Derek & Mulcahy Dennis E, *Talanta*, 32 (1985) 7.
3 Moody G J & Thomas J D R, *Selective ion sensitive electrodes* (Merrow, London) 1971; *Talanta*, 18 (1971) 1251.

Indian Journal of Chemistry
Vol. 28A, February 1989, pp. 177-178

Electrochemical & Thermodynamic Behaviour of Palladium-Palladium Sulphide Electrode in Presence of Sulphide Ions

PRAVIN CHANDRA KATIYAR & MUKHTAR SINGH*
Department of Chemistry, Agra College, Agra 282002

Received 22 *February* 1988;
revised 29 *April* 1988; *accepted* 19 *May* 1988

The Pd-PdS electrode is reversible in respect of S^{2-} in aqueous, aquo-alcoholic and alkaline media. The plot of $E_{Pd\text{-}PdS}$ versus $\log[S^{2-}]$ is linear showing that the electrode can be successfully used in the quantitative determination of S^{2-} in aqueous, aquo-alcoholic and alkaline media. The values of E°, $(\partial E^\circ/\partial T)_P$ and thermodynamic functions; viz. ΔG°, ΔH° and ΔS° for the electrode reaction: $Pd_{(s)} + S^{2-}{}_{(aq.)} \rightleftharpoons PdS_{(s)} + 2e$, and the solubility product have been determined.

Herein we report the preparation, evaluation and application of hitherto not investigated Pd-PdS electrode.

All the chemicals used were of AR grade. The Pd-PdS electrode was prepared by the method described in an earlier publication[1]. The potential of the electrode in solutions containing S^{2-} was measured under different experimental conditions by setting up a cell of the type (A)

$$\text{Pd-PdS}/S^{2-}\,\|\,\text{(saturated) KCl}/Hg_2Cl_2, \text{Hg} \qquad \text{(A)}$$

The electrode was kept immersed in doubly distilled water after use.

The potential of Pd-PdS electrode was measured in well-stirred solutions of Na_2S of varying concentrations (1.0×10^{-5} to 1.0×10^{-2} *M*) at 25 ± 0.1°C. The electrode attained equilibrium potential within 3 min thereby showing that the response of the electrode towards S^{2-} is fairly rapid. The potential of the electrode remained steady upto eight months, indicating that the electrode is highly stable. The reproducibility of the electrode potential was ascertained by preparing the electrode six times using the same method and each time measuring its potential as a function of $[S^{2-}]$. It was found that the variation in the electrode potential was within the limits of standard deviation (1.2×10^{-3}).

The plot of $E_{Pd\text{-}PdS}$ versus $\log[S^{2-}]$ with SCE as a reference electrode is linear from which E° of Pd-PdS electrode works out to be -0.815 V at 25 ± 0.1°C. The experimental slope value is 0.030 V which is very close to the theoretical (Nernstian) value of 0.0296 V (at 25°C). From the experimental slope it is inferred that two electrons per mole of S^{2-} are involved in the electrode reaction.

The potential of the electrode in 1.2×10^{-4} *M* Na_2S did not vary much in the presence of increasing concentrations (from 1×10^{-6} to 1×10^{-3} *M*) of some foreign ions, viz. F^-, Cl^-, Br^-, I^-, HCO_3^- and CO_3^{2-}. However, in the presence of $S_2O_3^{2-}$, SO_4^{2-} and NO_3^- some change in the potential of the electrode occurred. It is thus clear that Pd-PdS electrode is highly specific to S^{2-} and that it can be successfully used in the quantitative determination of S^{2-} in the presence of impurities such as F^-, Cl^-, Br^-, I^-, HCO_3^- and CO_3^{2-} ions.

The potential of the electrode (vs SCE) was measured as a function of $[S^{2-}]$ (from 1.0×10^{-5} to 1.0×10^{-2} *M*) in 25%, 50% and 75% (v/v) water-ethanol mixtures. In all the cases, the plots of $E_{Pd\text{-}PdS}$ versus $\log[S^{2-}]$ were linear thereby showing that this electrode can be successfully used in the quantitative determination of $[S^{2-}]$ in aq. ethanol medium. The values of E° of the electrode in 25%, 50% and 75% (v/v) water-ethanol mixtures are: -0.792, -0.826 and -0.876 V respectively and the experimental slope values are 0.029, 0.031 and 0.030 V respectively. From these slope values it is evident that the response of the electrode to $[S^{2-}]$ in aquo-alcohol is Nernstian.

A series of Na_2S solutions of varying concentrations were prepapred in BR buffers (*p*H 7.96 to 11.98), and the potential of the electrode was measured as function of $[S^{2-}]$ at fixed (controlled) *p*H values in the range of 7.96 to 11.98. Plots of $E_{Pd\text{-}PdS}$ versus $\log[S^{2-}]$ at different *p*H values are linear (Fig. 1). At *p*H 7.96, 8.95, 9.91, 10.38 and 11.98, the experimental slope values are 0.033, 0.030, 0.029, 0.033 and 0.030 V respectively. From these it appears that the electrode shows a fairly Nernstian response to $[S^{2-}]$. Therefore, this electrode can be successfully used in the quantitative determination of S^{2-} in the *p*H range of 7.96-11.98.

The response of Pd-PdS electrode to *p*H in the presence of Na_2S solution has also been studied. It is seen that the plots of $E_{Pd\text{-}PdS}$ versus *p*H are linear (Fig. 2) and their slopes are Nernstian. Thus Pd-PdS electrode can be used for the deter-

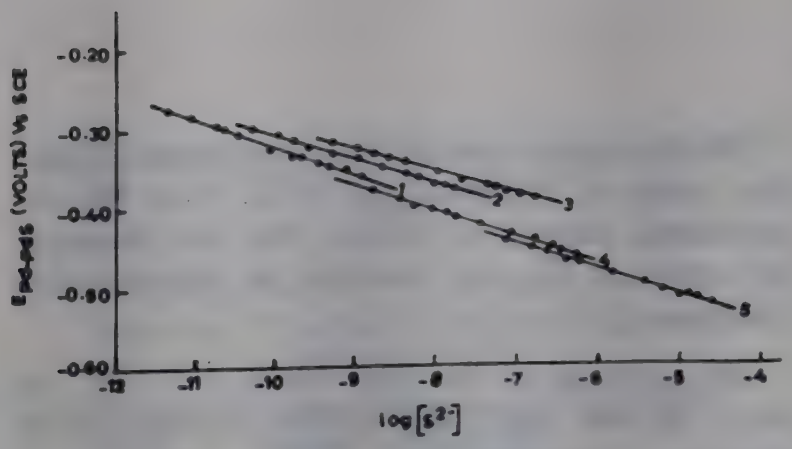

Fig. 1-Plots of $E_{Pd\text{-}PdS}$ versus $\log[S^{2-}]$ at different (controlled) *p*H values (7.96 to 11.98) at 25 ± 0.1°C [(1) *p*H 7.96, (2) *p*H 8.95, (3) *p*H 9.91, (4) *p*H 10.38 and (5) *p*H 11.98]

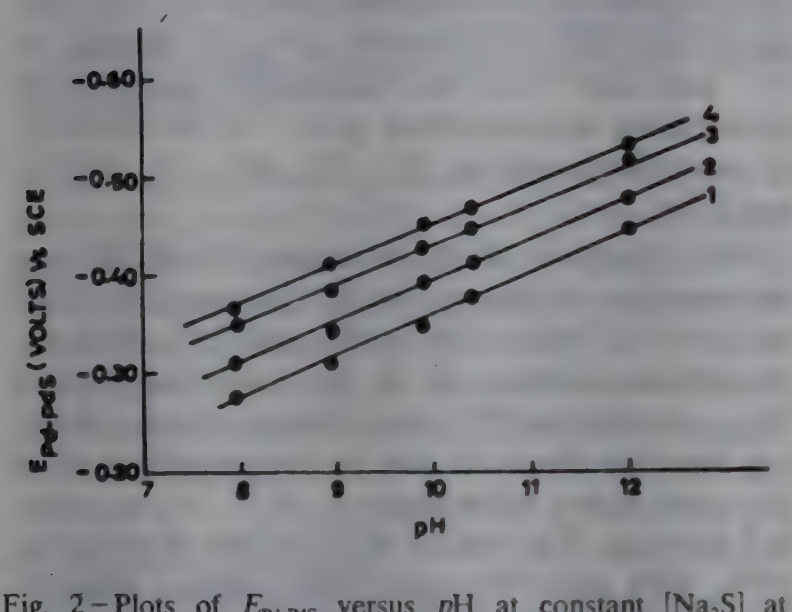

Fig. 2 – Plots of $E_{Pd\text{-}PdS}$ versus *p*H at constant [Na_2S] at 25 ± 0.1°C [(1) 4.4×10^{-5} *M*, (2) 3.5×10^{-4} *M*, (3) 5.3×10^{-3} *M* and (4) 1.3×10^{-2} *M*]

mination of *p*H in the range of 7.96 to 11.98 in the presence of S^{2-}.

The potentials of the electrode have been measured as a function of $[S^{2-}]$ at different temperatures ranging from 5-25°C, using three different concentrations (4.4×10^{-5}, 3.5×10^{-4} and 5.3×10^{-3} *M*) of Na_2S in aqueous, aquo-alcoholic (50% v/v) and alkaline media. The values of E° of Pd-PdS electrode obtained in different media at different temperatures are listed in Table 1. The temperature coefficient, $(\partial E°/\partial T)_p$ has been determined from the linear plots of E° versus T(°K) and the values are presented in Table 1. The thermodynamic functions $\Delta G°$, $\Delta H°$ and $\Delta S°$ for Pd-PdS electrode, in different media containing S^{2-}, have been calculated[2] at 25 ± 0.1°C and the values are listed in Table 2. From these data, the standard free energy of formation, $\Delta G_f°$ of PdS has been calculated following the method of Goates *et al.*[3,4] This works out to be −68.1 kJ mol^{-1} which is in close agreement with the literature[5] values of −66.9 kJ mol^{-1}.

Table 1 – E° Values and Temperature Coefficients of Pd-PdS Electrode in Aqueous, Water-Ethanol (50% v/v) and Alkaline (*p*H 7.96-11.98) Solutions of S^{2-}

	E° (V)					Temp. coeff.
	278 K	283	288	293	298	$\times 10^3$ (V/K)
Aqueous medium						
	−0.786	−0.791	−0.798	−0.804	−0.815	−1.42
Aquo-alcoholic (50% v/v) medium						
	−0.795	−0.799	−0.810	−0.815	−0.826	−1.53
Alkaline medium						
(*p*H)						
7.96	−0.751	−0.760	−0.765	−0.771	−0.782	−1.41
8.95	−0.766	−0.770	−0.779	−0.785	−0.796	−1.51
9.91	−0.791	−0.795	−0.805	−0.811	−0.821	−1.50
10.38	−0.815	−0.821	−0.830	−0.836	−0.845	−1.40
11.98	−0.829	−0.834	−0.846	−0.849	−0.859	−1.66

Table 2 – Values of $\Delta G°$, $\Delta H°$ and $\Delta S°$ of Pd-PdS Electrode in Aqueous, Aquo-alcoholic (50% v/v) and Alkaline media at 25 ± 0.1°C

Medium	$\Delta G°$ kJ mol^{-1}	$\Delta H°$ kJ mol^{-1}	$\Delta S°$ J mol^{-1}
Aqueous	153.9	74.9	−274.0
Aquo-alcoholic (50% v/v)	156.0	71.1	−296.6
Alkaline (*p*H)			
7.96	147.2	69.0	−271.9
8.95	150.2	66.5	−291.2
9.91	154.2	71.9	−289.1
10.38	159.8	82.0	−269.8
11.98	162.7	70.4	−320.0

Solubility product (K_{sp}) of PdS has been calculated from the standard free energy change of the reaction: $PdS(s) \rightleftharpoons Pd^{2+}(aq) + S^{2-}(aq)$ by means of the expression: $\ln K_{sp} = -\Delta G°/RT$. Since the value of $\Delta G_f°$ of PdS has already been calculated as −68.1 kJ mol^{-1} and using the literature values[5] of $\Delta G_f°$ for $S^{2-}_{(aq)}$ and $Pd^{2+}_{(aq)}$ as 85.77 kJ mol^{-1} and 176.5 kJ mol^{-1} respectively the value of K_{sp} works out to be 1.16×10^{-58} at 25 ± 0.1°C.

References

1 Sharma P & Singh M, *Indian J Chem*, **21A** (1982) 259, 847.

2 Daniels F & Alberty R A, *Physical chemistry*, (John Wiley, New York) 1966, p. 247.

3 Goates J R, Cole A G, Gray E L & Faux N D, *J Am chem Soc*, 73 (1951) 707.

4 Goates J R, Cole A G & Gray E L, *J Am chem Soc*, 73 (1951) 3596.

5 Lange's *Hand book of chemistry*, edited by John, A Dean (McGraw-Hill, New York) 1979.

Indian Journal of Chemistry
Vol. 28A, February 1989, pp. 179-180

Rapid Spectrophotometric Determination of Thallium with Mepazine Hydrochloride

H SANKE GOWDA* & G K REKHA
Department of Chemistry,
Central College, Bangalore University, Bangalore 560001

Received 8 *February* 1988; *revised and accepted* 26 *May* 1988

Mepazine hydrochloride reacts with thallium(III) at room temperature in phosphoric acid medium to give an orange-red species with an absorption maximum at 512 nm. The reaction obeys Beer's law over the concentration range 0.1-13.0 μg/ml of thallium(III) with an effective spectrophotometric range of 1.8-11.0 μg/ml. The molar absorptivity is 1.60×10^4 dm^3 mol^{-1} cm^{-1}. The efficacy of the method is shown by the successful determination of thallium in synthetic thallium alloys.

Determination of microgram amounts of thallium is of great importance because of its toxic nature and its increasing industrial applications[1]. Most of the reagents proposed for the spectrophotometric determination of thallium are extraction-photometric reagents. During the course of our investigations on the analytical applications of N-alkyl derivatives of phenothiazines, it was found that 10-[(1-methyl-3-piperidyl)methyl] phenothiazine hydrochloride or mepazine hydrochloride [MH] forms an orange-red species with thallium(III) in acid solution at room temperature. This colour reaction has been used for the rapid spectrophotometric determination of thallium(III). The proposed method offers the advantages of simplicity, rapidity, reasonable selectivity and sensitivity and wider range of determination without the need for extraction or heating.

A stock solution of thallium(III) was prepared by adding bromine water to requisite quantity of thallium(I) sulphate dissolved in doubly distilled water until a faint yellow colour persisted and heating the solution carefully to remove the excess of bromine. The solution was cooled, diluted to 100 ml and standardised volumetrically[2]. The stock solution was further diluted to give a standard solution containing 100 μg/ml of thallium(III). The reagent solution (0.2% wt/v) was prepared in doubly distilled water and stored in an amber glass bottle in a refrigerator. Solutions of foreign ions of suitable concentrations were prepared using AR grade reagents. A Hitachi 150-20 spectrophotometer with matched 1 cm quartz cells was used for absorbance measurements.

Procedure

To an aliquot of the sample solution containing 45-275 μg of thallium(III), 10 *M* phosphoric acid (8 ml) and 0.2% MH solution (8 ml) were added. The mixture was diluted to 25 ml with doubly distilled water and the absorbance was measured at 512 nm against a reagent blank. The thallium(III) content was determined from the standard calibration graph.

Mepazine hydrochloride reacts with thallium(III) instantaneously at room temperature (26 ± 2°C) in sulphuric or phosphoric acid medium to form an orange-red species believed to be a radical cation[3]. The sensitivity of the reaction and the stability of the orange-red species are almost the same in both sulphuric and phosphoric acid media. Thallium(III) can be determined spectrophotometrically in sulphuric acid medium, but many common ions such as Fe(III), Cu(II), Se(IV), Hg(II) and Pb(II) interfere in the determination. Hence, phosphoric acid (3*M*) is recommended as the maximum absorbance is observed instantaneously in 2-5*M* phosphoric acid medium. The absorbance decreases below this acidity range and slightly increases above this range.

The orange-red species exhibits maximum absorbance at 512 nm. The absorbance of thallium(III) solution and the reagent blank is negligible at this wave length. A 31-fold molar excess of the reagent was found necessary for maximum colour intensity. The absorbance remained constant for at least 1 h. The temperature had no effect on the absorbance over the range 5-45°C. The absorbance remained unchanged within the limit of experimental error when the order of addition of reactants was varied.

The system obeys Beer's law in the range 0.1-13.0 μg/ml of Tl(III). The optimum concentration range for the effective spectrophotometric determination of thallium as evaluated by Ringbom's method is 1.8-11.0 μg/ml of Tl(III). According to Sandell's expression, the sensitivity of the reaction is 12.2 ng cm^{-2} and the molar absorptivity is 1.60×10^4 dm^3 mol^{-1} cm^{-1}. The standard deviation calculated from five determinations in a solution containing 4 μg/ml of Tl(III) is 0.03 and the relative error is less than ± 2%.

The extent of interference by foreign ions associated with thallium in its alloys and minerals was determined by measuring the absorbance of a so-

Table 1 – Determination of Thallium in Its Alloys

Alloy	Composition	Tl taken (ppm)	Tl* found (ppm)	Rel. error (%)	St. deviation (ppm)
Antrification alloy	2% Tl, 98% Cu	2.00	2.02	+1.00	0.03
		4.00	4.00	—	0.00
		6.00	6.05	+0.83	0.02
Low melting alloy	8.9% Tl, 44.2% Bi, 35.8% Pb, 11.1% Cd	8.90	8.86	−0.45	0.01
		10.00	9.92	−0.80	0.03
		10.80	10.85	+0.46	0.05
Low melting alloy	7% Tl, 52% Bi, 34% Pb, 7% Cd	3.50	3.48	−0.57	0.02
		7.00	7.03	+0.43	0.01
		5.50	5.54	+0.73	0.02

* Average of five determinations.

lution containing 4 μg/ml of thallium(III) and varying amounts of diverse ions. The following amouts (μg/ml) of the ions were found to give an error below ±2%. Fe(III), 400; Cu(II), 1500; Ni(II), 800; Zn(II), 900; Mn(II), 100; W(VI), 60; Pb(II), 60; Ag(I), 20; Bi(III), 5; Hg(II), 400; Cd(II), 800; Se(IV), 200; Au(III), 0.5; Co(II), 30; Mo(VI), 4000; As(III), 30; Al(III), 400; Sb(III), 400; citrate, 200; tartrate, 200; acetate, 800; oxalate, 100; fluoride, 300; iodide, 10; chloride, 30; nitrate, 30; thiocyanate, 1.0; EDTA, 300; thiosulphate, 0.2; carbonate, 2000. The tolerance limit of Bi(III) and Au(III) could be increased to 60 and 6 μg/ml respectively by using 250 μg/ml EDTA and 1.0 μg/ml thiocyanate respectively.

Determination of thallium in alloys

The method was applied to the determination of thallium in Tl–Cu alloy (antrification alloy) and Tl–Bi–Pb–Cd alloys (low melting alloys). As analysed samples of these alloys were not available, synthetic mixtures corresponding to the compositions of these alloys were prepared and thallium content was determined following the standard procedure described earlier. The results are presented in Table 1. The results show that thallium can be determined in presence of other metal ions.

The authors thank the UGC, New Delhi, for financial assistance and Prof. K M Shivanandaiah and Prof. P S Veerabhadrappa for facilities.

References

1 Korenman I M, *Analytical chemistry of thallium* (Ann Arbor-Humphrey, London), 1969, pp. 2 and 3.

2 Sanke Gowda H, Shakunthala R & Subrahmanya U, *Indian J Chem*, **20A** (1981) 68.

3 Dwivedi P C, Gurudath Rao S N, Bhat S N & Rao C N R, *Spectrochim Acta, Part-A*, **31** (1975) 129.

Indian Journal of Chemistry
Vol. 28A, February 1989, pp. 181-182

Extractive Spectrophotometric Determination of Palladium(II) Using Mixed Ligand Complex Formation with Pyridine/α-Picoline/β-Picoline/γ-Picoline/2, 4, 6-Collidine & Iodide

T K THOKDAR, A SARKAR, P K PARIA* & S K MAJUMDAR

Department of Chemistry, North Bengal University, Darjeeling 734 430

Received 11 *September* 1987; *revised and accepted* 3 *March* 1988

Palladium(II) forms complexes with pyridine/α-picoline/β-picoline/γ-picoline/2,4,6-collidine in presence of potassium iodide. These are extractable into chloroform and absorb at 354-360 nm. The molar absorptivities of the complexes are in the range $1.6\text{-}1.9 \times 10^4$ l mol^{-1}cm^{-1}. The formation of these complexes has been utilized to propose an extractive spectrophotometric method of determination of palladium. The notable metal interference is due to mercury. Use of other common organic solvents provides no special advantages.

There are reports on extraction of iodide complexes of platinum metals with tributylphosphate in hexane as the coordinating solvent, and using this method the platinum metals have been separated from each other[1,2]. It has been noted that palladium(II) iodide forms complexes with pyridine or its methyl substituted derivatives in aqueous solution. These mixed ligand complexes are extractable into chloroform. These systems have been studied now to develop a simple spectrophotometric method for the determination of palladium. Apart from pyridine, other bases used are α-picoline, β-picoline, γ-picoline and 2, 4, 6-collidine.

Absorbance measurements were made with a Shimadzu PR1 model spectrophotometer with stoppered quartz cells of 10 mm optical path length. An ECL 5651 digital *p*H meter was used to measure the acidities of the aqueous solutions.

Palladium(II) chloride (Johnson & Matthey) (1g) was dissolved in 1 ml hot conc. HCl and diluted to 250 ml with distilled water followed by standardisation by dimethylglyoxime[3]. A working solution (41.75 ppm Pd) was prepared by dilution.

Chloroform (E. Merck), pyridine (BDH), α-picoline (Reidel), β-picoline (BDH), γ-picoline (Fluka) and 2, 4, 6-collidine (BDH) were distilled before use. Potassium iodide (BDH) and all the other reagents used were of analytical reagent grade. Stock solutions of desired diverse ions were prepared from their nitrates, chlorides or sulphates by dissolving pure samples in dilute acid or pure water. Sodium/ammonium salts were used in the case of anions. The metal contents were determined by standard methods[3].

General procedure

To an aliquot containing 10-100 μg of palladium was added 1 ml of 0.015 *M* aqueous potassium iodide and 0.02 ml of pyridine/α-picoline/β-picoline/γ-picoline/2, 4, 6-collidine followed by addition of adequate amount of distilled water to make up the volume upto 10 ml. The mixture thus obtained was equilibrated with 10 ml of chloroform for 30 sec. The two layers were allowed to settle for 1 min. The separated organic layer was shaken with anhydrous sodium sulphate to remove any retained water droplets. *p*H of the aqueous solution, after extraction, was measured. Finally the absorbance of the chloroform extract was measured at the λ_{max} of the complex against a reagent blank. Amount of palladium(II) was determined from a previously prepared calibration curve.

The absorption spectra of palladium(II) complexes in chloroform, extracted as above, exhibit maxima as indicated in Table 1. The reagent blanks show insignificant absorbances from 300 nm onwards. Beer's law is obeyed at the respective absorption maxima. All the absorption measurements were carried out against respective reagent blanks. The systems are stable for at least 48 hr.

The liquid-liquid extraction behaviour of Pd(II)-complexes was investigated in the *p*H range 0-14.0. After extraction, *p*H of the aqueous solution was measured in each case. In presence of pyridine bases, quantitative extraction of palladium(II) was found to be achieved in the *p*H range 3.5-10.0. From the graph $pH_{1/2}$ values were evaluated to be 1.6 & 10.7.

The optimum reagent concentrations were found to be 1 ml of 0.015 *M* KI and 0.02 ml of pyridine/α-picoline/β-picoline/γ-picoline/2, 4, 6-collidine for quantitative extraction of 41.75 μg of palladium. Higher concentrations of the reagents (upto 4 ml of 0.015 *M* KI and 0.1 ml of pyridine bases) had no adverse effects on the extraction behaviour.

Apart from chloroform, other common organic solvents such as carbon tetrachloride, benzene and ethyl acetate were tested as extracting solvents. The molar absorptivities of the palladium(II) complexes (on the basis of Pd content) at the respective absorption maxima in various solvents are shown in Table 1. It has been found that use of other organic solvents of-

Table 1—Details of Extractive Methods

Parameter	Base employed				
	Pyridine	α-Picoline	β-Picoline	γ-Picoline	2,4,6-Collidine
λ_{max}(nm)	359[a]	355[a]	356[a]	356[a]	354[a]
	366[b]	360[b]	365[b]	363[b]	360[b]
	365[c]	360[c]	362[c]	361[c]	360[c]
	355[d]	355[d]	356[d]	356[d]	359[d]
Molar absorptivity* ($mol^{-1}cm^{-1}$)	1.68×10^{4}[a]	1.79×10^{4}[a]	1.70×10^{4}[a]	1.75×10^{4}[a]	1.98×10^{4}[a]
	1.63×10^{4}[b]	1.94×10^{4}[b]	1.78×10^{4}[b]	1.88×10^{4}[b]	1.78×10^{4}[b]
	1.78×10^{4}[c]	2.19×10^{4}[c]	1.73×10^{4}[c]	1.98×10^{4}[c]	1.83×10^{4}[c]
	1.78×10^{4}[d]	2.04×10^{4}[d]	2.08×10^{4}[d]	1.88×10^{4}[d]	1.83×10^{4}[e]

Extracting solvents: a-chloroform, b-carbon tetrachloride, c-benzene & d-ethyl acetate
* Measured at corresponding absorption maxima

fers no special advantages. Chloroform was used as the extracting solvent in the present investigation.

Different amounts of palladium were extracted by the general procedure and the absorbance of the chloroform extracts was measured at the respective absorption maxima. In all the cases Beer's law was found to be valid over the concentration range 1-10 μg Pd/ml.

Effect of diverse ions—In order to study the effect of diverse ions on the extraction behaviour, a definite amount of palladium(II) was extracted and determined according to the general procedure in presence of the respective foreign ions. All the bases i.e., pyridine, α-picoline, β-picoline, γ-picoline and 2, 4, 6-collidine showed similar behaviour towards the extraction of palladium. In each case an average of three determinations was taken. An ion was considered to interfere if the recovery of Pd(II) differed by more than ± 3% from the actual amount taken.

It was found that 41.75 μg of palladium could easily be determined without any interference in presence of the following cations and anions, the amounts (mg) taken being mentioned in parentheses: Co(II) (5.1), Ni(II) (5.3), Cd(II) (4.9), Zn(II) (6.7), V(V) (5.2), Rh(III) (2.4), Zr(IV) (1.2), U(VI) (5.1), Mn(II) (3.9), Cr(III) (4.8), La(III) (4.2), Al(III) (3.9), Th(IV) (4.1), Be(II) (6.9), Pb(II) (1.3) and Bi(III) (1.1). Iron(III) (1.2) and Cu(II) (0.2) were kept in the aqueous phase by masking them with ammonium hydrogen fluoride and citrate respectively. All attempts to remove the interference due to Hg(II) failed. Pt(IV) interfered in all cases except in the 2, 4, 6-collidine system where the interference was avoided by extracting Pd at *p*H 10.0. Among the anions tested the following (10 mg each) did not interfere: EDTA, borate, phosphate, tartrate, citrate, fluoride, bromide, ascorbate, phthalate. However, thiocyanate and thiosulphate, even in trace amounts interfered seriously.

Table 2—Reproducibility of the Method Using 2,4,6-Collidine

Palladium taken (μg)	Palladium found (μg)	Relative mean deviation (%)
10.44	10.5	3.8
20.88	20.7	1.7
41.75	41.9	1.2
62.62	62.1	0.77
83.50	83.3	0.91

Among the based used, 2, 4, 6-collidine is found to be most sensitive. With this reagent the precision and accuracy of the method were tested (Table 2) by analysing solutions containing a known amount of Pd following the recommended procedure. Average of six determinations was taken in each case.

References

1 Faye G H & Inman W R, *Analyt Chem*, **35** (1963) 985.
2 Berg E W & Lau E Y, *Analyt chim Acta*, **27** (1962) 248.
3 Vogel A I, *A textbook of quantitative inorganic analysis* (ELBS, London), 1962.

Indian Journal of Chemistry
Vol. 28A, February 1989, pp. 183-184

BOOK REVIEWS

Secondary Ion Mass Spectroscopy of Solid Surfaces by V T Cherepin (VNU Science Press BV, Utrecht, The Netherlands), 1987, pp. viii + 141, Price 121 DM.

The results obtained by modern surface analytical techniques can be interpreted with increased confidence limits only when the acquisition is carried out simultaneously using a variety of compatible techniques. This is particularly true of secondary ion mass spectroscopy (SIMS) as has been stressed by the author of this book that 'the data generated using SIMS would be more useful if this technique is combined with AES, XPS, ISS and TDMS'. In fact in two tables (Tables 5.1 and 5.2 on pages 132 and 133) the author has compared the energy flux, surface damage mechanism and analytical capabilities of each of these techniques, which are appropriate to comprehend the advantages and limitations of SIMS.

The book is divided into five chapters. Chapters 1 and 2 deal with the physical background, the method of data collection for specific requirements and the details of instrumental features. Chapters 3-5 summarise the results obtained by the application of this technique to problems in adsorption, catalysis, oxidation, corrosion, adhesion, implant profiles, identification of surface compounds and many other important fields. In an exclusive chapter, the author has attempted to erase the apprehension that SIMS could be more useful for identification of the constituents alone and has detailed how one can generate quantitative data for structural and composition analysis. In Chapter 4, the details of in-depth analysis, which is one of the inherent features of this method has been outlined.

This book, as it is stated, seems to have two objectives, namely (i) to meet the interests of those well versed in this area and (ii) as a guide to beginners. Though it has definitely achieved fully the second objective, the fulfillment of the first objective could only be evaluated from the citation profile of this book in the subsequent publications. As is mostly true of any translation, this monograph translated from the original Russian text, has also incorporated a few misspelt words, some of them even distracting a smooth reading. This is especially true when ammonia synthesis and decomposition on iron surfaces is referred to as ammonium synthesis and decomposition.

On the whole, this book will be a welcome addition to the book-shelf containing volumes dealing with the various surface analytical techniques.

B. Viswanathan
Department of Chemistry
Indian Institute of Technology
Madras 600 036

Future Directions in Polymer Colloids, edited by M.S. El-Aasser and R.M. Fitch (Martinus Nijhoff Publishers, Dordrecht, Boston, Lancaster), 1987. pp. X + 402, Price $ 110.

This book, published in cooperation with NATO Scientific Affairs Division, forms the proceedings of NATO advanced research workshop on 'Future Directions in Polymer Colloids' held in Racine, Wisconsin, USA during June 30-July 4, 1986. This book has been published in memory of Alan Rembaum (1916-86), a great scientist and an inventor, who died of cancer prior to this conference. But for his untimely death, he would have contributed in great measure to the discussions and published proceedings.

Since the discovery of first synthetic latex in mid 1930's, the field of polymer colloids has been growing rapidly not only encompassing the applied aspects but also the basic and engineering aspects. The NATO advanced research workshop brought together 63 scientists and engineers from both academia and industry on a single platform. The main objective of the workshop was to develop position papers outlining the future directions of research in five selected areas of polymer colloids, viz. (i) emulsion copolymerisation and particle morphology, (ii) rheology of latex systems and concentrated dispersion, (iii) polymer-stabilised latexes, (iv) new techniques for the characterisation of polymer colloids and (v) polymer colloids in biomedical field. Each position paper was followed by invited papers.

In the first position paper, 'Emulsion Copolymerisation and Particle Morphology' the state of the art, mechanism of emulsion polymerisation, applications, goals for the next decade, characterisation, particle morphology, physical and colloidal properties, mathematical models, on-line measurement and control of reaction were covered.

The discussion on second position paper, 'Rheology of Latex Systems and Concentrated Dispersions' centred round the following topics: viscoelastic properties, deformation other than shear, effects of external fields, time-dependent thixotrophic and viscoeleastic effects, interaction of radiation with flowing systems, dielectric spectroscopy and experimental characterization of certain dispersions, electroviscous effects, characterization of suspensions in non-Newtonian fluids, wall effects (width and geometry of the flow channel), theoretical studies such as microscopic theories, ordering in sheared suspensions, flocculated systems and computer simulation. It was the considered view that increasing capability of computers to solve complex equations and to simulate rheological experiments will greatly enhance our understanding of the rheology of polymer colloids in future.

In the third position paper 'Polymer Stabilised Latex', the following aspects were covered: Stability, interparticle forces, structure of adsorbed and depleted polymer layers at interfaces and preparation of model colloids. It was concluded that much work, both theoretical and experimental, has to be carried out on polymer-stabilised latex systems. The future directions of research activity in each of these areas were also highlighted in depth.

In the position paper, 'New Techniques in Characterisation of Colloids', particle size distribution (light scattering, X-rays, small angle neutron scattering and other methods), the nature of surface groups, morphology and characterisation of latices by adsorption studies, surface potential and cross-linking frequency by various methods were covered. Techniques needing further development were also outlined.

There were two position papers in the area of 'Polymer Colloids in Biomedical Field'. The first one covered the following five applications of polymer colloids in the biomedical field: (i) bone marrow transplantation; (ii) solid-phase immunoassays; (iii) drug delivery systems; (iv) extracorporeal and hemoperfusion systems; and (v) identification and enumeration of lymphocyte populations. In the second position paper 'Future Directions in Latex Agglutination Assays' the use of the latex particles in diagnostic immunoassays was discussed. It was indicated that the recent development of improved polymer particles, and emerging innovations in the development of particles with defined properties, will facilitate a broad range of basic and applied uses of polymers in biomedical field in future.

Scientists and technologists who participated in this conference have made commendable efforts to provide an update state of art and have also focussed the future directions of research in the area of polymer colloids. This book should serve as a good reference material for researchers both in universities and industry. This book is a welcome addition to the library. The Editors M.S. El.Aasser and R.M. Fitch deserve compliments for their effort in bringing out this excellent volume.

Asit Baran Mandal & K S V Srinivasan*
Central Leather Research Institute
Adyar, Madras 600 020

Indian Journal of Chemistry
Vol. 28A, February 1989, pp. 185-186

ANNOUNCEMENTS

IUPAC Recommendations on Atmospheric Chemistry Terms

The *Glossary* contains definitions of over 600 scientific terms in common use in atmospheric chemistry. The diversified nature of the scientists involved in research in atmospheric chemistry, chemists, meteorologists, physicists, biologists, engineers, health scientists, and others, points to the very special need for a definition of the common terms employed by each specialist. The *Glossary* was prepared to provide unambiguous definitions of terms and units employed by the international research community in atmospheric chemistry to help achieve reliable communications between all parties. Where alternative terms are in common use to describe a given process, piece of equipment, feature, or quantity used in atmospheric chemistry, recommended choices are given. The range of terms includes those encountered in describing the properties and composition of the atmosphere, clouds, solar radiation, chemical and physical changes in atmospheric components instrumentation employed in analysis of the atmospheric components and in air quality control, and in effects of certain trace gases on materials, plants, and animals.

Comments on the glossary should be sent by 31 October 1989 to the Chairman of the Commission on Atmospheric Chemistry: Prof J G Calvert, National Center for Atmospheric Research, Atmospheric Chemistry and Aeronomic Division, POB 3000, Boulder, Colorado 80307-3000, USA.

IUPAC Recommendations on Classification of Analysers in Clinical Chemistry

The classification scheme suggested should be helpful in making understandable the various concepts of mechanized and automated analytical systems. It should be used as a guide for teaching automation in clinical chemistry, and as a base for describing new instrumentation by manufacturers and professionals.

A mechanized analytical system comprises an analyser and the reagents required to perform a specified analysis. The term analyser is a measuring system which is defined as a complete set of measuring instruments and other equipment assembled to carry out a specified measurement task.

Usually analytical systems are classified accoding to the principle of their transport system, e.g., discrete and flow procedures. In the document a further subdivision is achieved by considering methodology, number of tests, sampling and processing procedures or test selection. Common examples are included into the scheme presented.

IUPAC Recommendations on the Description and Measurement of Analytical Carry-over Effects

This document makes recommendations concerning the terminology of carry-over and its classification. The conceptual aspects of specimen-dependent and specimen-independent carry-over are outlined, and both the experimental determination and calculation of carry-over effects are described in detail.

The term carry-over is commonly used to describe a process by which extraneous materials are carried into a reaction mixture. These materials can be either parts of a specimen, or reagents including the diluent or wash solution. In such cases, carry-over means the transfer of material (specimen or reagents) from one container, or from one reaction mixture, to another one. It can be either unidirectional or bidirectional in a series of specimens or assays.

Carry-over effects should be expressed in units (e.g. in mol L^{-1} or U L^{-1}) which are used to present the results rather than as quantity fractions. This concept of presenting carry-over effects as a difference of two results or its corresponding percentage value has two advantages: it is applicable to all conditions which at present are encountered in practice, and it directly informs on how much a particular result deviates from the correct value which is obtained in the absence of carry-over effects.

Those desirous of having the full texts of the above documents may write to the Executive Secretary, Indian National Science Academy, Bahadur Shah Zafar Marg, New Delhi 110 002.

National Symposium on Structure and Bonding in Inorganic Materials

A symposium on structure and bonding in inorganic materials will be held at the Shivaji University, Kolhapur from 23 to 25 May 1989. The aim of the symposium is to bring together chemists and physicists interested in the structure and bonding of inorganic materials in general and high temperature super-conductors, ferrites or catalysts in particular. The main themes of the symposium will be:

(i) Synthesis, analysis and structure of ceramic bulk superconducting materials and related compositions

(ii) Techniques of solid state physics and chemistry

(iii) Oxygenation, fluxional chemistry, mixed valence, geochemistry of oxide minerals and characterisation of mixed oxides

(iv) Ferrites, catalysts and semiconducting materials of oxidic compositions

(v) Novel coordination compounds in solid state studies

(vi) Teaching of theoretical and experimental aspects of superconductivity

Further information may be obtained from the convener of the symposium, Dr C K Bhaskare, Chemistry Department, Shivaji University, Kolhapur 416 004.

वैज्ञानिक तथा अनुसंधान पुस्तकालय
SCIENTIFIC & RESEARCH LIBRARY
Accession No .....
17 JUL 1989
सी.एफ.टी.आर.आई. क्षेत्रीय केन्द्र
C.F.T.R.I. REGIONAL CENTRE, LUDHIANA

THE WEALTH OF INDIA

An Encyclopaedia of Indian Raw Materials and Industrial Products, published in two series :
(i) Raw Materials, and **(ii) Industrial Products.**

RAW MATERIALS

The articles deal with Animal Products, Dyes & Tans, Essential Oils, Fats & Oils, Fibres & Pulps, Foods & Fodders, Drugs, Minerals, Spices & Flavourings, and Timbers and other Forest products. Names in Indian languages, and trade names are provided.

For important crops, their origin, distribution, evolution of cultivated types and methods of cultivation, harvesting and storage are mentioned in detail. Data regarding area and yield and import and export are provided. Regarding minerals, their occurrence and distribution in the country and modes of exploitation and utilization are given. The articles are well illustrated. Adequate literature references are provided.

Eleven volumes of the series covering letters A–Z have been published.

Vol. I : A (Revised) Rs. 300.00; Vol. I (A-B) Rs. 120.00; Vol. II (C) Rs. 143.00; Vol. III (D-E) with index to Vols. I-III Rs. 158.00; Vol. IV (F-G) Rs. 150.00; Vol. IV Suppl. Fish & Fisheries Rs. 84.00; Vol. V (H-K) Rs. 171.00; Vol. VI (L-M) Rs. 135.00; Vol. VI : Suppl. on Livestock including poultry Rs. 153.00; Vol. VII (N-Pe) Rs. 150.00; Vol. VIII (Ph-Re) Rs. 129.00; Vol. IX (Rh-Sc) Rs. 200.00; Vol. X (Sp-W) Rs. 338.00; Vol. XI (X-Z) with Cumulative Index to Vols. I-XI Rs. 223.00.

INDUSTRIAL PRODUCTS

Includes articles giving a comprehensive account of various large, medium and small scale industries. Some of the major industries included are : Acids, Carriages, Diesel Engines, Fertilizers, Insecticides & Pesticides, Iron & Steel, Paints & Varnishes, Petroleum Refining, Pharmaceuticals, Plastics, Ship & Boatbuilding, Rubber, Silk, etc.

The articles include an account of the raw materials and their availability, manufacturing processes, and uses of products, and industrial potentialities. Specifications of raw materials as well as finished products and statistical data regarding production, demand, exports, imports, prices, etc. are provided. The articles are suitably illustrated. References to the sources of information are provided.

Nine volumes of the series covering letters A–Z have been published.

Part I (A-B) Rs. 87.00; Part II (C) Rs. 111.00; Part III (D-E) with Index to Parts I-III Rs. 150.00; Part IV (F-H) Rs. 189.00; Part V (I-L) Rs. 135.00; Part VI (M-Pi) Rs. 42.00; Part VII (Pl-Sh) Rs. 90.00; Part VIII (Sl-Tl) Rs. 99.00; Part IX (To-Z) with Index to Parts I-IX Rs. 120.00.

HINDI EDITION : BHARAT KI SAMPADA—PRAKRITIK PADARTH

Vols. I to VII and two supplements of Wealth of India—Raw Materials series in Hindi already published.

Published Volumes :

Vol. I (अ-औ) Rs. 57.00; Vol. II (क) Rs. 54.00; Vol. III (ख-न) Rs. 54.00; Vol. IV (प) Rs. 125.00; Vol. V (फ-मेरो) Rs. 90.00; Vol. VI (मेल-स) Rs. 120.00; Vol. VII (रे-वाटा) Rs. 203.00; Vol. VIII (वाय-सीसे) Rs. 300.00.

Supplements :

Fish & Fisheries (Matsya & Matsyaki) Rs. 74.00;
Livestock (Pashudhan aur Kukkut Palan) Rs. 51.00

Vols. IX to XI under publication.

Please contact :

SENIOR SALES AND DISTRIBUTION OFFICER

PUBLICATIONS & INFORMATION DIRECTORATE, CSIR
Hillside Road, New Delhi 110 012

RN 7090/63

CSIR PUBLICATIONS

WEALTH OF INDIA

An encyclopaedia of the economic products and Industrial resources of India issued in two series

RAW MATERIALS SERIES – Contains articles on plant, animal and mineral resources.

	Rs.	$	£
Vol. I(A) (Revised)	300.00	94.00	74.00
Vol. I (A-B)	120.00	60.00	26.00
Vol. II (C)	143.00	66.00	34.00
Vol. III (D-E)	158.00	64.00	40.00
Vol. IV (F-G)	98.00	54.00	24.00
Supplement (Fish & Fisheries)	84.00	32.00	21.00
Vol. V (H-K)	171.00	68.00	42.00
Vol. VI (L-M)	135.00	68.00	30.00
Supplement (Livestock including Poultry)	153.00	68.00	39.00
Vol. VII (N-Pe)	150.00	60.00	38.00
Vol. VIII (Ph-Re)	129.00	64.00	28.00
Vol. IX (Rh-Se)	156.00	70.00	38.00
Vol. X (Sp-W)	338.00	150.00	85.00
Vol. XI (X-Z)	223.00	77.00	44.00

INDUSTRIAL PRODUCTS SERIES – Deals with major, Small-Scale and Cottage Industries

Part I (A-B)	87.00	40.00	22.00
Part II (C)	111.00	48.00	28.00
Part III (D-E)	150.00	67.00	39.00
Part IV (F-H)	189.00	84.00	48.00
Part V (I-L)	135.00	46.00	34.00
Part VI (M-Pi)	42.00	16.00	5.60
Part VII (Pl-Sh)	90.00	36.00	12.00
Part VIII (Si-Ti)	99.00	54.00	20.00
Part IX (To-Z)	120.00	68.00	24.00

BHARAT KI SAMPADA (Hindi Edition of Wealth of India, Raw Materials):

Vol. I (अ-औ)	57.00	32.00	13.00
Vol. II (क)	54.00	30.00	12.00
Vol. III (ख-न)	54.00	30.00	12.00
Vol. IV (प)	125.00	68.00	32.00
Vol. V (फ-मेरे)	90.00	44.00	20.00
Vol. VI (मेल-रू)	120.00	54.00	26.00
Vol. VII (रे-वाटा)	203.00	80.00	50.00
Vol. VIII (वाय-सीसे)	300.00	80.00	50.00
Livestock (Kukkut Palan)	51.00	30.00	12.00
Fish & Fisheries (Matsya aur Matsyaki)	74.00	42.00	10.00
A Dictionary of Generic & Specific Names of Plants & Animals Useful to Man	45.00	22.00	10.00

Please Contact :

SENIOR SALES & DISTRIBUTION OFFICER
PUBLICATIONS & INFORMATION
DIRECTORATE, CSIR
HILLSIDE ROAD, NEW DELHI - 110012

OTHER PUBLICATIONS

	Rs.	$	£
The Useful Plants of India	192.00	64.00	48.00
A Dictionary of the Flowering Plants in India by H. Santapau & A.N. Henry	63.00	28.00	16.00
Glossary of Indian Medicinal plants by R.N. Chopra, S.L. Nayar & I.C. Chopra	93.00	32.00	20.00
Supplement to Glossary of Indian Medicinal Plants by R.N. Chopra, I.C. Chopra & B.S. Verma	51.00	18.00	12.00
The Flora of Delhi by J.K. Maheshwari	42.00	16.00	5.50
Illustrations to the Flora of Delhi by J.K. Maheshwari	105.00	44.00	26.00
Herbaceous Flora of Dehra Dun by C.R. Babu	216.00	120.00	44.00
Gnetum by P. Maheshwari & Vimla Vasil	30.00	12.00	4.00
Marsilea by K.M. Gupta	62.00	27.00	16.00
Aquatic Angiosperms	30.00	12.00	4.00
Indian Fossil Pteridophytes by K.R. Surange	99.00	44.00	25.00
Cedrus by P. Maheshwari & Chhaya Biswas	63.00	28.00	16.00
Proteaceae by C. Venkata Rao	108.00	48.00	27.00
Pinus by P. Maheshwari & R.N. Konar	45.00	22.00	16.00
Loranthaceae by B.M. Johri & S.P. Bhatnagar	83.00	37.00	21.00
Abies & Picea by K.A. Chowdhury	21.00	12.00	4.20
Indian Thysanoptera by T.N. Ananthakrishnan	39.00	16.00	5.20
The Millipede Thyropygus by G. Krishnan	18.00	7.00	2.40
Indian Sardines by R.V. Nair	33.00	14.00	4.40
Drug Addiction with special Reference to India by R.N. Chopra & I.C. Chopra	19.00	7.00	2.40
Diosgenin & other Steroid Drug Precursors by L.V. Asolkar & Y.R. Chandha	54.00	26.00	12.00
Cholera Bacteriophages by Dr. Sachimohan Mukerjee	45.00	20.00	12.00
Cottonseed Chemistry & Technology by K.S. Murti & K.T. Achaya	116.00	64.00	26.00
Corrosion Map of India	27.00		3.60
Rural Development and Technology: A Status Report-cum-Bibliography by PR Bose and V.N. Vashist	150.00	76.00	34.00
Termite Problems in India	14.00	6.00	1.80
Research & Development Management	38.00	20.00	
Proceedings of the Seminar on Primary Communications in Science & Technology in India by R.N. Sharma & S. Seetharama	78.00	35.00	68.00

Packing and Postage Extra

Printed & Published by Shri S.S. Saksena, Editor, Publications & Information Directorate (PID)
Hillside Road, New Delhi 110012, at PID Photocomposition-cum-Printing Unit

Regd No. D(C)-1018